

**THE ISOLATION AND CHARACTERISATION OF *PROTEUS*
MIRABILIS BACTERIOPHAGES AND THEIR EFFECT ON
THE COLONISATION AND BLOCKAGE OF URINARY
CATHETERS**

RICHARD W THOMPSON BSc.

A thesis submitted in partial fulfilment of the requirements of the University of the
West of England, Bristol for the degree of Doctor of Philosophy

This research programme was carried out in collaboration with the Bristol
Urological Institute, Bristol

Department of Applied Sciences, University of the West of England, Bristol

June 2018

Authors Declaration

This copy has been supplied on the understanding that it is copyright material and no quotation from the thesis may be published without proper acknowledgement.

Abstract

Catheter associated urinary tract infection seriously complicates the care of an already vulnerable patient set and has been estimated to cost the UK National Health Service in excess of one billion pounds per annum. Approximately 50 % of patients catheterised for more than 28 days will experience catheter blockage due to the formation of crystalline biofilm on the eye holes, balloon and lumen of the catheter (Getliffe, 1994) as a result of colonisation by *Proteus mirabilis*. Blockage can lead to significant complications such as pyelonephritis and septicaemia.

To date, strategies to reduce or prevent these infections from occurring have met with limited success. One potential approach to prevent catheter colonisation and blockage is the application of bacteriophages as a catheter coating. Natural parasites of bacteria, bacteriophages offer several advantages over conventional antimicrobial treatment including replication at the site of infection, specificity and, in some cases, biofilm degrading ability.

Three novel bacteriophages vB_PmiS_NSM6, vB_PmiP_#3 and vB_PmiM_D3 were isolated from environmental sources and characterised phenotypically and genetically utilising electron microscopy, host range analysis and, for phages vB_PmiS_NSM6 and vB_PmiP_#3, genome sequencing via hybrid assembly. The isolated phages belong to the *Caudovirales* order and sequence data analysis indicated that they are lysogenic. They possess the characteristic modular architecture of their dsDNA genomes that are densely packed with coding sequence. Both phages displayed terminal redundancy which is indicative of a headful packaging strategy and both appear to be circularly permuted. Putative function was obtained for 63 % of the coding sequences for phage vB_PmiS_NSM6 and 52 % of genes identified in phage vB_PmiP_#3.

The effect of these phages, either individually or as a cocktail, on *P. mirabilis* colonisation of urinary catheters in an *in vitro* bladder model was investigated. Models were run for 24 h and adhered bacteria used as an indicator of phage activity verses untreated control. A reduction of greater than 3 log₁₀ was observed for phage vB_PmiS_NSM6 treated catheters in comparison to untreated controls across all three sections of catheter analysed. Phage vB_PmiP_#3 reduced bacterial adherence by 1 log₁₀ across all sections and a similar reduction was observed with phage vB_PmiM_D3 of greater than 1 log₁₀. These data were confirmed with scanning electron microscopy (SEM) which showed a significant reduction in crystalline deposits on the phage treated catheters. The time taken for the mineralised biofilm to occlude the catheter lumen in the presence of bacteriophages was also investigated. Time to blockage was extended from 36.2 h to 58.47 h (an increase of 61.49 %) for phage vB_PmiS_NSM6, from 41.17 h to 51.73 h (an increase of 25.67 %) for phage vB_PmiP_#3 and from 40.97 h to 62.40 h (an increase of 52.31 %) for phage vB_PmiM_D3.

Phages vB_PmiS_NSM6 and vB_PmiM_D3 displayed activity against each other's isolating strain. This enabled the assessment of a two phage cocktail. The cocktail increased time to blockage by approximately 7 % compared to single phage treatment for both bacterial isolates. These data provide some evidence of efficacy of bacteriophage pre-treatment of urinary catheters in an *in vitro* model of *P. mirabilis* infection of the catheterised bladder, despite the lysogenic nature of the phages investigated. As such, this suggests phage treatment of catheters warrants further investigation.

Acknowledgements

Firstly, I would like to thank Adele Long, the former director of the Bristol Urological Institute (BUI), for being instrumental in securing the funding for this project and believing in me and my idea. Thanks also to Karen Evely at the BUI for the additional administrative and organisational support required to allow me to undertake this study part-time.

Next I would like to thank my original supervisor Professor Viv Salisbury for agreeing to take me on as a student and undertaking a project in an area of research that she had little prior experience of. Without her the project would never have gotten off the ground. Special thanks also to my current supervisor Dr Shona Nelson, for agreeing to take me on as a student upon Viv's retirement and for all the help and support she has given me over the duration of the project. The last couple of years have been a particularly challenging time for me personally, Shona has not only supported me as my PhD supervisor but also as a friend and confidant. I am forever grateful for all the guidance she has given me, and also for all the parenting wisdom and clothes she provided for my daughter since her birth! Thanks also to my other supervisors, Dr Roy Pemberton who covered Shona's maternity leave and Dr Nicola Morris for allowing me to undertake these studies, being flexible with working arrangements and providing much advice and support over the years. Thanks also to Dr Dann Turner for all the help and support he has given me from his time as a fellow PhD student throughout his post-Doctoral study and now as a lecturer. Dann was instrumental in the planning and execution of the sequencing work conducted, his expertise in this field has been invaluable. I feel very lucky to have been surrounded by such interesting and accomplished individuals throughout the project, without their endless help and encouragement it simply wouldn't have been possible.

Thanks also to the laboratory technical team at the University of the West of England for their support and advice, especially Dr Gill Smith, Dr Lee Graham, Dave Corry, and Dr Dave Patton for his assistance with electron microscopy.

I would like to extend my thanks to the microbiology department at Southmead hospital for supplying me with *Proteus mirabilis* isolates, and to Wessex Water for providing me with activated sludge and raw sewage, specifically Alex Jones for his willingness to facilitate my research, and Reuben Hardy for collecting and delivering the samples.

Thanks also to Professor Eshwar Mahenthiralingam for his support and assistance with the analysis of PFGE gels at the University of Cardiff.

Finally, I would like to thank my wife for her love and encouragement, and for being my best friend. Without her none of this would have been possible.

Table of Contents

| | |
|---|-----|
| Authors Declaration | i |
| Abstract | ii |
| Acknowledgements..... | iii |
| List of Figures | ix |
| List of Tables..... | xi |
| Abbreviations | xii |
| Chapter 1 Introduction..... | 1 |
| 1.1 Overview..... | 1 |
| 1.2 Urinary incontinence | 1 |
| 1.3 Urinary catheters..... | 3 |
| 1.4 Catheter associated urinary tract infection (CAUTI) | 5 |
| 1.4.1 Biofilms | 7 |
| 1.4.2 Catheter associated mineralised biofilms | 10 |
| 1.5 <i>Proteus mirabilis</i> | 11 |
| 1.6 Attempts at preventing catheter-associated urinary tract infection..... | 17 |
| 1.6.1 Antimicrobial coatings | 18 |
| 1.6.2 Modification of surface properties..... | 19 |
| 1.6.3 Dietary modification | 21 |
| 1.6.4 Plant-based antimicrobials | 21 |
| 1.6.5 Iontophoresis | 22 |
| 1.6.6 Enzyme inhibitors | 22 |
| 1.6.7 Quorum sensing inhibitors | 23 |
| 1.6.8 Bacterial interference | 23 |
| 1.7 Bacteriophages..... | 24 |
| 1.7.1 Bacteriophage morphology | 27 |
| 1.7.2 Bacteriophage life cycles | 29 |

| | |
|--|----|
| 1.7.3 Phage therapy | 34 |
| 1.7.4 Advantages over traditional antimicrobial agents | 34 |
| 1.7.5 Requirements for phage therapy | 37 |
| 1.7.6 Regulatory issues surrounding phage therapy | 38 |
| 1.7.7 Phage treatment of uropathogens | 39 |
| 1.7.8 Foreign language literature | 41 |
| 1.8 Study aims | 42 |
| Chapter 2 Materials and Methods | 43 |
| 2.1 Bacterial strains and growth media | 43 |
| 2.2 Determination of bacterial numbers..... | 45 |
| 2.2.1 Drop plate method | 45 |
| 2.2.2 Spread plate method | 45 |
| 2.2.3 Spiral plating device..... | 45 |
| 2.3 Pulsed-Field Gel Electrophoresis (PFGE) on bacterial isolates..... | 46 |
| 2.4 Determination of bacteriophage titres | 48 |
| 2.5 Isolation of bacteriophages..... | 48 |
| 2.6 Propagation and purification of bacteriophages | 49 |
| 2.7 Transmission electron microscopy..... | 51 |
| 2.8 Host range | 51 |
| 2.9 Adsorption rate constant | 52 |
| 2.10 One step growth..... | 53 |
| 2.11 Extraction of bacteriophage genomic DNA..... | 54 |
| 2.11.1 Concentration and yield of DNA..... | 55 |
| 2.12 Genome size estimation by pulsed field gel electrophoresis..... | 55 |
| 2.13 Restriction digest of genomic DNA..... | 56 |
| 2.14 Genomic termini elucidation..... | 56 |
| 2.14.1 Cohesive ends..... | 56 |

| | |
|--|----|
| 2.14.2 Terminal specificity | 57 |
| 2.15 Genome sequencing and annotation | 57 |
| 2.16 Structural proteins..... | 59 |
| 2.16.1 Bradford assay | 59 |
| 2.16.2 SDS-PAGE | 59 |
| 2.17 Adherence of bacteriophages to catheter surfaces..... | 59 |
| 2.18 Assessment of removal of viable adherent organisms from catheters | 60 |
| 2.19 Sectioned-catheter suspension tests | 60 |
| 2.20 <i>In vitro</i> bladder model experiment | 61 |
| 2.21 24 h in vitro bladder model experiment | 63 |
| 2.22 Assessment of time to catheter blockage..... | 64 |
| 2.23 Scanning electron microscopy of catheter sections | 64 |
| Chapter 3 Characterisation of the isolated Bacteriophages..... | 66 |
| 3.1 Introduction..... | 66 |
| 3.2 Results | 68 |
| 3.2.1 Isolating Bacteriophages..... | 68 |
| 3.2.2 Restriction analysis and genome size estimation of phages vB_PmiS_NSM6 and vB_PmiP_#3 | 72 |
| 3.2.3 Transmission electron microscopy of the isolated phages | 75 |
| 3.2.4 Host range analysis and host library assessment | 75 |
| 3.2.5 Adsorption rate determination and one step growth..... | 83 |
| 3.2.6 Genomic sequencing and analysis phage vB_PmiS_NSM6 | 87 |
| 3.2.7 Genes involved in genome packaging, virion structure and morphogenesis | 89 |
| 3.2.8 Genes involved in Lysogeny..... | 92 |
| 3.2.9 Nin-like gene cassette..... | 94 |
| 3.2.10 Lysis Cassette | 95 |

| | |
|---|-----|
| 3.2.11 Regulatory Sequences: Promoters and Terminators | 96 |
| 3.2.12 Determination of physical genome ends/termini | 97 |
| 3.2.13 Genomic sequencing and analysis phage vB_PmiP_#3..... | 101 |
| 3.2.14 Structure and Morphogenesis Module | 104 |
| 3.2.15 Genes Involved in Lysogeny..... | 107 |
| 3.2.16 Nin-like Region..... | 108 |
| 3.2.17 Lysis Cassette | 109 |
| 3.2.18 Regulatory Sequences: Promoters and Terminators | 109 |
| 3.2.19 Packaging strategy | 110 |
| 3.3 Discussion | 112 |
| Chapter 4 Phage therapy in an <i>in vitro</i> model system..... | 118 |
| 4.1 Introduction..... | 118 |
| 4.2 Results | 119 |
| 4.2.1 Assessment of biofilm removal | 119 |
| 4.2.2 Catheter section suspension tests..... | 121 |
| 4.2.3 Quantification of phages adhered to catheters | 123 |
| 4.2.4 <i>In vitro</i> bladder models, 24 h experiment, <i>P. mirabilis</i> NSM 6..... | 124 |
| 4.2.5 <i>In vitro</i> bladder models, 24 h experiment, <i>P. mirabilis</i> #3 | 128 |
| 4.2.6 <i>In vitro</i> bladder models, 24 h experiment, <i>P. mirabilis</i> D3 | 132 |
| 4.2.7 <i>In vitro</i> bladder models: Time to blockage experiments..... | 136 |
| 4.2.8 24 hour <i>In vitro</i> bladder models utilising a two phage cocktail | 143 |
| 4.2.9 Time to blockage experiments for <i>In vitro</i> bladder models treated with a two phage cocktail..... | 151 |
| 4.3 Discussion | 155 |
| Chapter 5 Discussion | 165 |
| 5.2 Further work..... | 176 |
| References..... | 179 |

Appendix: Supplementary Material 209

List of Figures

| | |
|--|-----|
| FIGURE 1. FOLEY CATHETER..... | 3 |
| FIGURE 2. DIAGRAM SHOWING URETHRAL CATHETERISATION OF A MALE AND A FEMALE | 5 |
| FIGURE 3. <i>P. MIRABILIS</i> BIOFILM DEVELOPMENTAL SEQUENCE ON A URINARY CATHETER | 9 |
| FIGURE 4. SWARMING MORPHOLOGY OF <i>PROTEUS MIRABILIS</i> ON SOLID MEDIA | 12 |
| FIGURE 5. DIENES LINES | 15 |
| FIGURE 6. THE THREE FAMILIES OF THE ORDER <i>CAUDOVIRALES</i> | 28 |
| FIGURE 7. DIAGRAMMATIC REPRESENTATION OF THE LIFE CYCLE OF THE TAILED BACTERIOPHAGES | 30 |
| FIGURE 8. DIAGRAMMATIC REPRESENTATION OF THE MAINTENANCE AND EXIT FROM LYSOGENY | 33 |
| FIGURE 9. DIAGRAMMATIC REPRESENTATION OF PULSED FIELD GEL ELECTROPHORESIS | 47 |
| FIGURE 10. DIAGRAM DEPICTING SIDE PUNCTURE METHOD FOR COLLECTING BACTERIOPHAGES | 50 |
| FIGURE 11. ORGANISATION OF BACTERIOPHAGE DILUTIONS FOR HOST RANGE SPOT PLATE ASSAY | 52 |
| FIGURE 12. A DIAGRAMMATIC REPRESENTATION OF THE <i>IN VITRO</i> BLADDER MODEL | 62 |
| FIGURE 13. DIAGRAM DEPICTING THE SECTIONS OF FOLEY CATHETER EXCISED AND EXAMINED FOLLOWING THE 24 H EXPERIMENT | 63 |
| FIGURE 14. DIAGRAM DEPICTING THE SECTIONS I TO IV OF FOLEY CATHETER EXCISED AND EXAMINED BY SEM FOLLOWING 24 H EXPERIMENT | 65 |
| FIGURE 15. RESTRICTION ENDONUCLEASE DIGEST OF BACTERIOPHAGES VB_RMIS_3, VB_PMIS_5, VB_PMIS_7..... | 69 |
| FIGURE 16. RESTRICTION ENDONUCLEASE DIGEST OF BACTERIOPHAGES VB_PMIS_4 AND VB_PMIS_6..... | 69 |
| FIGURE 17. PFGE ON WHOLE DNA FROM THE FIVE ISOLATED BACTERIOPHAGES | 70 |
| FIGURE 18. PHOTOGRAPH'S OF PLAQUES..... | 72 |
| FIGURE 19. RESTRICTION ENDONUCLEASE DIGESTS OF BACTERIOPHAGE VB_PMIS_NSM6..... | 73 |
| FIGURE 20. RESTRICTION ENDONUCLEASE DIGESTS OF BACTERIOPHAGE VB_PMIP_#3. | 74 |
| FIGURE 21. PULSED FIELD GEL ELECTROPHORESIS OF BACTERIOPHAGES EXTRACTED GENOMIC DNA..... | 74 |
| FIGURE 22. TRANSMISSION ELECTRON MICROGRAPHS | 75 |
| FIGURE 23. PFGE PROFILES OF <i>P. MIRABILIS</i> ISOLATES DIGESTED WITH <i>NOTI</i> | 76 |
| FIGURE 24. PFGE PROFILES OF <i>P. MIRABILIS</i> ISOLATES DIGESTED WITH <i>NOTI</i> | 76 |
| FIGURE 25. PFGE PROFILES OF <i>P. MIRABILIS</i> ISOLATES DIGESTED WITH <i>NOTI</i> | 77 |
| FIGURE 26. PFGE PROFILES OF <i>P. MIRABILIS</i> ISOLATES DIGESTED WITH <i>NOTI</i> | 77 |
| FIGURE 27. PFGE PROFILES OF <i>P. MIRABILIS</i> ISOLATES DIGESTED WITH <i>NOTI</i> | 78 |
| FIGURE 28. DENDROGRAM | 80 |
| FIGURE 29. ADSORPTION RATE CONSTANT | 84 |
| FIGURE 30. ONE STEP GROWTH CURVE..... | 86 |
| FIGURE 31. GENOME MAP OF VB_PMIS_NSM6..... | 88 |
| FIGURE 32. VB_PMIS_NSM6 STRUCTURAL PROTEINS RESOLVED BY 1D SDS PAGE | 89 |
| FIGURE 33. ASSAY FOR THE DETERMINATION OF COHESIVE GENOME TERMINI PHAGE VB_PMIS_NSM6..... | 98 |
| FIGURE 34. TIME DEPENDANT DIGESTION OF GENOMIC DNA WITH EXONUCLEASE BAL-31 PHAGE VB_PMIS_NSM6 . | 99 |
| FIGURE 35. NEIGHBOUR-JOINING TREE OF LARGE TERMINASE SUB UNIT AMINO ACID SEQUENCES..... | 100 |

| | |
|--|-----|
| FIGURE 36. GENOME MAP OF VB_PMI _P _#3 | 102 |
| FIGURE 37. VB_PMI _P _#3 STRUCTURAL PROTEINS RESOLVED BY 1D SDS PAGE..... | 104 |
| FIGURE 38. ASSAY FOR THE DETERMINATION OF COHESIVE GENOME TERMINI PHAGE VB_PMI _P _#3 | 111 |
| FIGURE 39. TIME DEPENDANT DIGESTION OF GENOMIC DNA WITH EXONUCLEASE BAL-31 PHAGE VB_PMI _P _#3 | 112 |
| FIGURE 40. VIABLE RECOVERED BACTERIA..... | 120 |
| FIGURE 41. CATHETER SECTION SUSPENSION TESTS..... | 122 |
| FIGURE 42. ADHERED PHAGES..... | 123 |
| FIGURE 43. PHOTOGRAPH OF THE BLADDER MODEL..... | 124 |
| FIGURE 44. IMPACT OF PHAGE PRE-TREATMENT ON BACTERIAL BIOFILM FORMATION BY <i>P. MIRABILIS</i> NSM6 | 126 |
| FIGURE 45. SCANNING ELECTRON MICROGRAPHS OF UN-TREATED AND PHAGE TREATED CATHETERS REMOVED FROM THE <i>IN VITRO</i> BLADDER MODEL SYSTEM AFTER 24 H | 127 |
| FIGURE 46. IMPACT OF PHAGE PRE-TREATMENT ON BACTERIAL BIOFILM FORMATION BY <i>P. MIRABILIS</i> #3 | 130 |
| FIGURE 47. SCANNING ELECTRON MICROGRAPHS OF UN-TREATED AND PHAGE TREATED CATHETERS REMOVED FROM THE <i>IN VITRO</i> BLADDER MODEL SYSTEM AFTER 24 H | 131 |
| FIGURE 48. IMPACT OF PHAGE PRE-TREATMENT ON BACTERIAL BIOFILM FORMATION BY <i>P. MIRABILIS</i> D3..... | 134 |
| FIGURE 49. SCANNING ELECTRON MICROGRAPHS OF UN-TREATED AND PHAGE TREATED CATHETERS REMOVED FROM THE <i>IN VITRO</i> BLADDER MODEL SYSTEM AFTER 24 H | 135 |
| FIGURE 50. PHOTOGRAPH OF A BLOCKED CATHETER REMOVED FROM THE <i>IN VITRO</i> BLADDER MODEL SYSTEM | 136 |
| FIGURE 51. IMPACT OF PHAGE VB_PMI _S _NSM6 PRE-TREATMENT ON TIME TO BLOCKAGE BY <i>P. MIRABILIS</i> NSM6... .. | 138 |
| FIGURE 52. IMPACT OF PHAGE VB_PMI _P _#3 PRE-TREATMENT ON TIME TO BLOCKAGE BY <i>P. MIRABILIS</i> #3 | 140 |
| FIGURE 53. IMPACT OF PHAGE VB_PMI _P _D3 PRE-TREATMENT ON TIME TO BLOCKAGE BY <i>P. MIRABILIS</i> D3 | 142 |
| FIGURE 54. IMPACT OF PHAGE COCKTAIL PRE-TREATMENT ON BACTERIAL BIOFILM FORMATION BY <i>P. MIRABILIS</i> NSM6 | 144 |
| FIGURE 55. IMPACT OF PHAGE COCKTAIL PRE-TREATMENT ON BACTERIAL BIOFILM FORMATION BY <i>P. MIRABILIS</i> D3 ... | 146 |
| FIGURE 56. IMPACT OF VB_PMI _S _NSM6 PRE-TREATMENT ON BACTERIAL BIOFILM FORMATION BY <i>P. MIRABILIS</i> D3 | 148 |
| FIGURE 57. IMPACT OF VB_PMI _M _D3 PRE-TREATMENT ON BACTERIAL BIOFILM FORMATION BY <i>P. MIRABILIS</i> NSM6. | 150 |
| FIGURE 58. IMPACT OF PHAGE COCKTAIL PRE-TREATMENT ON TIME TO BLOCKAGE BY <i>P. MIRABILIS</i> NSM6 | 152 |
| FIGURE 59. IMPACT OF PHAGE COCKTAIL PRE-TREATMENT ON TIME TO BLOCKAGE BY <i>P. MIRABILIS</i> D3 | 154 |

List of Tables

| | |
|--|-----|
| TABLE 1. SUMMARY OF THE TYPES OF URINARY INCONTINENCE AND THE TREATMENT OPTIONS..... | 2 |
| TABLE 2. BACTERIAL ISOLATES USED IN THIS STUDY. | 43 |
| TABLE 3. BACTERIOPHAGES ISOLATED IN THE FIRST PHASE OF ENRICHMENTS | 68 |
| TABLE 4. BACTERIOPHAGES ISOLATED FROM THE SECOND PHASE OF ENRICHMENTS. | 71 |
| TABLE 5. HOST RANGE ANALYSIS. | 81 |
| TABLE 6. THE POSITION AND SEQUENCE OF THE PUTATIVE RHO INDEPENDENT TERMINATORS | 97 |
| TABLE 7. THE POSITION AND SEQUENCE OF THE PUTATIVE RHO INDEPENDENT TERMINATORS | 110 |
| TABLE 8. FUNCTIONAL ANNOTATION OF THE PREDICTED CODING SEQUENCES OF PHAGE VB_PMiS_NSM6 | 210 |
| TABLE 9. FUNCTIONAL ANNOTATION OF THE PREDICTED CODING SEQUENCES OF PHAGE VB_PMiP_#3..... | 215 |

Abbreviations

| | |
|-------------|---|
| μA | Microampere |
| μg | Microgram |
| μL | Microlitre |
| A | Adenosine |
| AHL | N-acyl homoserine lactones |
| AMR | Antimicrobial resistance |
| ATCC | American type culture collection |
| ATF | Ambient-temperature fimbriae |
| <i>attB</i> | Bacterial attachment site |
| <i>attP</i> | Phage attachment site |
| AU | Artificial urine |
| bp | Base pairs |
| BSA | Bovine serum albumen |
| C | Cytosine |
| CAUTI | Catheter associated urinary tract infection |
| CDC | Centres for disease control |
| CDS | Coding sequence |
| CECT | Spanish type culture collection |
| CFU | Colony-forming unit |
| Ch | French unit of measure, named after creator Charrière |
| cm | Centimetre |
| COS | Cohesive |
| CPSs | Capsule polysaccharides |
| DKP | Diketopiperazine |
| DNA | Deoxyribonucleic acid |
| dsDNA | Double stranded deoxyribonucleic acid |
| DTT | Dithiothreitol reducing agent |
| DUF | Domain of unknown function |
| eDNA | Extra cellular deoxyribonucleic acid |
| EDTA | Ethylenediaminetetraacetic acid |
| End | Endolysin |
| EPS | Extracellular polymeric substances |
| FDA | Food and drug administration |
| g | Gram |
| G | Gauge |
| G | Guanine |
| GMO | Genetically modified organism |
| GMP | Good manufacturing practice |
| gp | Gene product |
| GRAS | Generally regarded as safe |
| h | Hour |
| HF | High fidelity |
| Hol | Holin |
| HPA | Health protection agency |
| ICTV | International Committee on Taxonomy of Viruses |
| Ids | Identification of self (operon) |

| | |
|-----------------|--|
| Ig | Immunoglobulin |
| IHF | Integration host factor |
| Int | Integrase |
| IP | Intellectual property |
| kb | Kilo-base pair |
| kDa | Kilodalton |
| KV | Kilovolt |
| L | Litre |
| LB | Lennox Luria Broth |
| LDS | Lithium dodecyl sulphate buffer |
| LPS | Lipopolysaccharide |
| M | Molecular size marker |
| mg | Milligram |
| min | Minute |
| mL | Millilitre |
| mm | Millimetre |
| mmol | Millimolar |
| MOI | Multiplicity of infection |
| MRK | Mannose-resistant <i>Klebsiella</i> -like fimbriae |
| MTP | Major tail protein |
| MW | Molecular weight |
| NCIMB | National collections of industrial, marine and food bacteria |
| nm | Nanometre |
| OD | Optical density (wavelength) |
| ORF | Open reading frame |
| PBS | Phosphate-buffered saline |
| PCR | Polymerase chain reaction |
| PEG | Polyethylene glycol |
| PFGE-RFLP | Pulse field gel electrophoresis restriction fragment length polymorphism |
| PFU | Plaque-forming unit |
| pH | Pondus hydrogenii |
| pH _n | Nucleation pH |
| Ptl | Portal protein |
| PVC | Polyvinyl chloride |
| Pvp | Polyvinylpyrrolidone |
| QS | Quorum sensing |
| RBS | Ribosome-binding site |
| RNA | Ribonucleic acid |
| rpm | Rotations per minute |
| s | Seconds |
| SD | Standard deviation |
| SDS | Sodium dodecyl sulphate |
| SDS-PAGE | Sodium dodecyl sulphate polyacrylamide gel electrophoresis |
| SEM | Scanning electron microscopy |
| SM | Saline-magnesium buffer |
| SOP | Standard operating procedure |
| ssb | Single stranded DNA-binding proteins |
| STW | Sewage treatment works |

| | |
|------------|---|
| T | Thiamine |
| T_SS | Type (<u>number</u>) secretion system |
| TBE | Tris-borate EDTA buffer |
| TE | Tris-chlorine EDTA buffer |
| TEM | Transmission electron microscopy |
| TerL | Large terminase subunit |
| TerS | Small terminase subunit |
| TMP | Tape measure protein |
| tRNA | Transfer ribonucleic acid |
| TSB | Tryptone Soya Broth |
| Tsp | Tail spike protein |
| U | Units |
| UI | Urinary incontinence |
| UPGMA | Unweighted pair group method with arithmetic mean |
| UTI | Urinary tract infection |
| UV | Ultraviolet |
| V | Volts |
| v/v | Volume/volume |
| WGS | Whole genome sequencing |
| w/v | Weight/volume |
| <i>x g</i> | Gravitational force |
| Xis | Excisionase |
| ΔG | Gibbs free energy |

Chapter 1 Introduction

1.1 Overview

The human bladder is an attractive site for bacterial colonisation since it is maintained at 37°C, and is supplied by a near constant flow of nutritious liquid medium in the form of urine. Bacterial infections of the bladder can lead to fever, cystitis and urethritis, however, more severe conditions can manifest, such as acute pyelonephritis, calculus formation, renal scarring and bacteraemia. Left untreated these conditions can lead to urosepsis and death (Warren, 1997). The healthy bladder prevents infection with the cyclical filling and flushing that occurs through micturition, however, if this cycle is interrupted, such as through use of an indwelling urinary catheter, the likelihood of infection increases. Catheterised patients are susceptible to infection at a cumulative rate of 3-7 % per day (Hooton *et al.*, 2010) and catheter-associated urinary tract infections (CAUTI) are the most frequent nosocomial infections (Jacobsen *et al.*, 2008). The financial burden to health care providers is substantial and has been estimated to cost the UK National Health Service (NHS) between £1 and £2.5 billion per annum, due to delayed patient discharge, increased demand upon staff resources and extended antimicrobial treatment (Feneley, Hopley and Wells, 2015). No commercially available catheter resists infection (Morris, Stickler and Winters, 1997) and the continued increase of antimicrobial resistance is compounding and severely complicating the care and treatment of often vulnerable patients. Alternative solutions are needed to treat and prevent these infections. One candidate approach to address this issue is the use of bacteriophages. The bacteriophages are obligate viral parasites of bacteria. A virulent infection results in lysis and therefore the death of the bacterial cell. The current AMR crisis is currently driving research into phage therapy due to the real possibility of a post-antibiotic future.

1.2 Urinary incontinence

Urinary incontinence (UI) as defined by the International Continence Society is the “complaint of the involuntary loss of urine” (Haylen *et al.*, 2009). This condition can have a serious impact on the psychological health and the social interactions of the afflicted individual (Busby-Whitehead, and Johnson, 1999). UI is more frequent in

women than men and becomes more prevalent with age (Irwin *et al.*, 2006). There are different types of UI and the causes for their presentation are varied (Table 1).

Table 1. Summary of the types of urinary incontinence and the treatment options. Adapted from Abrams *et al.* (2002).

| Type | Description | Management |
|--|---|--|
| Stress | involuntary leakage on effort or exertion, for example coughing or sneezing. | absorbent products, behavioural therapy, catheterisation, occlusion devices, surgeries, pharmacologic. |
| Urge | involuntary leakage accompanied by or immediately preceded by urgency. | bladder training, anticholinergic drugs, Botox, surgery. |
| Mixed | involuntary leakage associated with urgency and also with exertion. | see urge and stress. |
| Enuresis/ Nocturnal enuresis | any involuntary loss of urine/ loss of urine occurring during sleep. | absorbent products. |
| Retention/overflow | incomplete emptying of the bladder caused by obstruction or detrusor underactivity. | absorbent products, intermittent catheterisation, indwelling catheterisation. |
| Continuous urinary incontinence | continuous leakage. | absorbent products, catheterisation. |

Urinary incontinence can arise from functional abnormalities as well as neurological disorders including multiple sclerosis, stroke or a spinal cord injury resulting in a diverse demographic of patients that undergo long-term bladder catheterisation.

1.3 Urinary catheters

Urinary catheters are predominantly used for the management of urinary incontinence. However, they are also used to accurately measure urine output either in post-operative or in critically ill patients, during surgical procedures to drain urine and to irrigate the bladder or to administer chemotherapy drugs (Feneley, Hopley and Wells, 2015). The modern indwelling Foley catheter (Figure 1) consists of a thin flexible tube with a rounded tip and two drainage holes. It is retained in the bladder by inflation of the retention balloon with sterile water. A funnel for connecting a drainage collection receptacle lies at the basal end of the device. This design has not changed significantly since its introduction in 1937 by Dr Frederic Foley and is itself an evolution of an idea which dates back 3,500 years according to the available records (Feneley, Hopley and Wells, 2015).

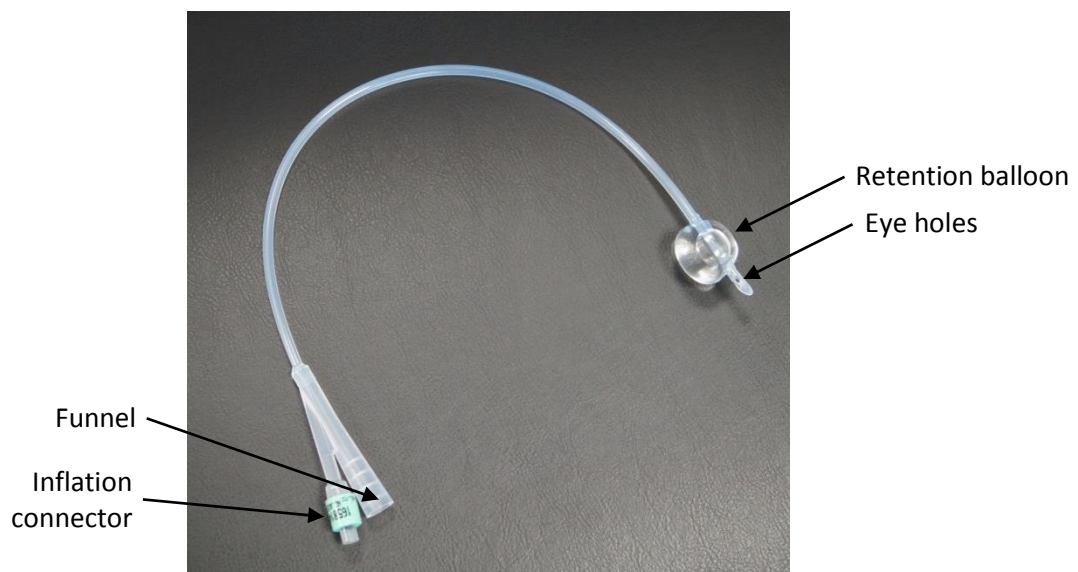


Figure 1. Foley catheter. Indicated are the main features; the eye holes through which urine drains, the retention balloon which retains the device in the bladder, the funnel through which urine drains and collection equipment is connected, and the inflation connector that receives a syringe that is used to inflate/deflate the retention balloon with sterile water.

These devices can be inserted through the urethra, or a passage is made between the lower abdominal wall and the bladder, a procedure termed suprapubic catheterisation. Suprapubic insertion is used when the urethra is damaged or blocked or for increased comfort and access for patients who are chair bound. Reitz *et al.* (2006) suggest that suprapubic catheterisation allows better patient quality of life and satisfaction when compared with urethral catheterisation, however, there is a risk of perforating the bowel upon insertion (Ahluwalia *et al.*, 2006).

Indwelling catheters can be made of rubber, plastic (PVC), silicone and latex. Due to allergic complications with latex catheters they are usually covered in a layer of silicone (Shenot *et al.*, 1994). The material affects the comfort of the end user and material properties also dictate the wall thickness and, therefore, the size of the lumen. A catheter made of silicone possesses a wider lumen when compared to latex (Feneley, Kunin and Stickler, 2012). A larger lumen is favourable, especially if blood clots may be passed. Catheters come in various sizes, measured in Charrière (ch) units. In order to balance function with patient comfort the smallest size is used that will still allow adequate drainage (McGill, 1982; Feneley, Hopley and Wells, 2015).

Unfortunately there are a number of flaws with the design and use of catheters that carry with them substantial co-morbidities. In men, when inserting a catheter uretherally, bends in the urethra and constriction caused by the prostate (Figure 2) can lead to damage occurring as the catheter is forced against the urethral wall (Willette and Coffield, 2012). Urethral trauma can also occur upon catheter removal. When deflated, the retention balloon does not return to the original size preceding inflation and forms a cuff. The cuff complicates removal, particularly in suprapubic catheterisations as the channel is not flexible (Parkin *et al.*, 2002). The retention balloon can occasionally burst and the pieces must be removed as they may block successive catheters or act as the seeds of bladder stones (Chrisp and Nacey, 1990). Damage to the bladder can occur when the catheter is in place, the tip and balloon can abrade the bladder lining. Damage can also occur as the catheter drains. Fluid flowing through the lumen causes suction that pulls the collapsing bladder into the drainage holes. Over time this can lead to the formation of pseudopolyps (Milles, 1965). Damage caused to the bladder lining compromises

this usually impermeable layer, allowing bacteria to adhere and invade, giving access to the bloodstream which could lead to septicaemia (Feneley, Kunin and Stickler, 2012).

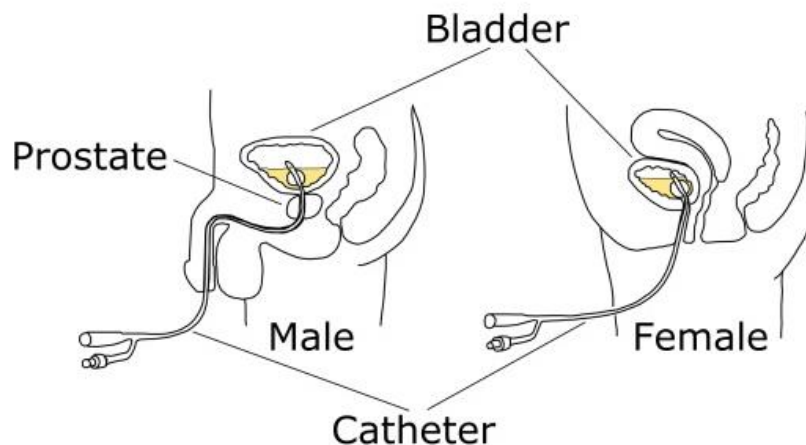


Figure 2. Diagram showing urethral catheterisation of a male and a female. Indicated is the prostate on the male where a bend in the urethra and constriction caused by the gland can lead to damage upon catheter insertion. Also depicted in both male and female is the sump of urine that remains in the bladder due to the position of the drainage holes above the retention balloon.

1.4 Catheter associated urinary tract infection (CAUTI)

A significant failing associated with the Foley catheter is that they are susceptible to bacterial colonisation. Catheters *in situ* for less or more than 28 days are considered short-term or long-term, respectively. The cumulative rate of infection is 3-7 % per day (Hooton *et al.*, 2010). At these levels infection becomes almost inevitable in those patients who are catheterised for greater than 4 weeks (Stickler, 2008; Choong *et al.*, 2001; Warren, 1997; Kunin, 1997). Most of these infections are asymptomatic (Tambyah and Maki, 2000) but approximately 10-25 % of patients will go on to develop symptomatic urinary tract infection. If these symptoms are not rapidly diagnosed and treated, urosepsis and death can occur (Niël-Weise *et al.*, 2012). Long-term catheterisation is also associated with encrustation and blockage in about 50 % of cases (Getliffe, 1994) and can lead to chronic infection, the formation of bladder stones, chronic renal inflammation, renal failure and in the

longer term, bladder cancer and death (Warren, 1997). Blockage events lead to painful distention of the bladder necessitating an emergency procedure to remove the offending device. Alternatively, bypassing of the catheter can occur which renders the patient incontinent causing distress.

Urinary catheters are subject to infection because they act as a bridge from the highly colonised periurethral region, to the bladder, which is warm, moist and rich in nutrients. The act of catheter insertion through the urethra can introduce bacteria into the bladder as the first few centimetres of the urethra in both men and women are colonised with bacteria (Jacobsen *et al.*, 2008). There are two other routes bacteria can take to infect the catheterised bladder. They can ascend extraluminally between the catheter and the urethral epithelial cells, assisted by hydrostatic forces as a mucoid film develops between the catheter and the urethra (Parida and Mishra, 2013), or alternatively, bacteria can gain access intraluminally via contamination of the drainage tap and transit to the bladder within the catheter lumen (Stamm, 1991; Tambyah, Halvorson and Maki, 1999). Most infections occur via the extraluminal route since the introduction of the closed drainage system in the 1960s. However, poor practice relating to the care of the closed drainage system or when emptying the bag can lead to contamination and intraluminal infection (Powers, 2016; Garibaldi *et al.*, 1974; Kunin and McCormack, 1966). The presence of a urinary catheter undermines the natural defence mechanism the body uses to prevent bacterial ascension to the bladder. In healthy individuals the periodic filling and flushing washes out any ascending bacteria and the complete emptying of the bladder also assists in preventing infection. Catheters prevent complete emptying of the bladder due to the position of the retention balloon beneath the drainage holes (Figure 2). The sump of urine that develops acts as a refuge for bacteria that enter the bladder (Hashmi *et al.*, 2003). The sump is constantly replenished with fresh urine at a rate between 0.55 and 1.38 ml per minute in healthy adults (Israni and Kasiske, 2011), and can be compared to a chemostat, a device used for the continuous culture of bacteria.

Some aspects of catheter construction also render it susceptible to bacterial colonisation. The surfaces of the lumen are rough and uneven when viewed with an electron microscope and present an opportunity for colonisation. Both Latex and

Silicone catheters possess uneven topology (Stickler *et al.*, 2003). Latex catheters can also possess diatom skeletons (Stickler and Morgan, 2008). Diatomaceous earth is used to assist in the removal of the device from the metal moulds, however, they offer an attractive site for microbial adherence. To accommodate the inflation tube, the lumen is crescent shaped and possesses constrictions at the crescent's tips that trap debris and initiate blockage (Stickler *et al.*, 2003; Cox, 1990). Furthermore, the manufacturing process that forms the drainage eye holes produces a very uneven topology that favours bacterial colonisation. Micro-colonies can more easily form in the deep valleys of this surface and from here can proceed to colonise the entirety of the catheter (Stickler *et al.*, 2003). It is notable that most blockage events occur at, or just beneath, the eye holes.

1.4.1 Biofilms

The bacterial populations that form on catheter surfaces utilise a strategy that is thought to be the preferred mode of growth for bacteria in nature; the biofilm. Evidence of this mode of growth exists in the fossil record as far back as 3.25 billion years (Westall *et al.*, 2001) but it was not until the 1980s that biofilms were associated with medical devices (Hall-Stoodley, Costerton and Stoodley, 2004). There are key benefits for bacteria when growing associated with a surface. Firstly, nutrients concentrate on surfaces in natural environments (Busscher and van der Mei, 2012). Secondly, the extracellular polymeric substances (EPS) that are exuded by the bacteria when growing on a surface serve to protect them from environmental stresses such as desiccation, ultraviolet radiation, antibiotics and host immune responses (Delcaru *et al.*, 2016). The EPS has been postulated to act as a "recycling centre" by retaining components from lysed cells, nutrients, enzymes and DNA which may serve as a pool for horizontal gene transfer (Flemming, 2016; Delcaru *et al.*, 2016). Biofilms are associated with indwelling medical devices and are a significant cause of chronic infections and device rejection (Donlan, 2001). Biofilms are significantly more refractory to antimicrobials than planktonic bacteria (Høiby *et al.*, 2010). In addition to providing a physical shield from environmental stresses, the EPS matrix can also bind and neutralise antimicrobials effectively reducing the agent to sub-lethal concentrations (Nichols *et al.*, 1988). Within biofilms different nutrient gradients produce zones of starved

or stationary phase microorganisms which are recalcitrant to antibiotics as these usually require an active metabolism to be effective (Hall-Stoodley, Costerton and Stoodley, 2004). Oxygen concentration gradients can also exist leading to anaerobic regions where, for example, aminoglycoside antibiotics would be less effective (Tack and Sabath, 1985). Similarly, gradients in pH, nutrients and bacterial waste products could all contribute to resistance mechanisms. Another mechanism of resistance is the presence of persister cells within the population of the biofilm. Persister cells represent a “transient phenotypic variant that is tolerant to antimicrobials” (Conlon, Rowe and Lewis, 2015). They are speculated to be low in cellular energy (ATP) and, therefore, metabolically inactive which imparts resistance (Waters *et al.*, 2016). Their presence contributes to the overall antimicrobial resistance of the biofilm, acting as a source for reinfection following a course of antibiotics (Stewart and William Costerton, 2001). When growing *in vivo*, various host components can also become incorporated into the biofilm. These components can act as a means of evading host immune response; for example in cardiac valves, platelets and fibrin encapsulate the biofilm and prevent recognition by leukocytes (Durack, 1975). In the case of urinary catheters, the presence of urease producing bacteria can lead to the precipitation of calcium and magnesium phosphates from urine which become incorporated into the biofilm and eventually lead to catheter blockage (Stickler and Feneley, 2010).

Understanding the process of biofilm formation (Figure 3) can lead to novel strategies in tackling these persistent communities. Initially a bacterial cell comes into contact with a surface, either through motility or from physical forces. These forces contribute collectively at different rates depending on the surface, medium, and bacterial properties. They include Van der Waal forces, electrostatic (attractive and repulsive), Brownian motion and hydrogen bonding (Donlan, 2002). The bacterium recognises its location via mechanotransduction. Mechanical forces are sensed by a mechanotransmitting structure, such as flagella, type IV pili or channels in the cell envelope. After the force is sensed a response is enacted, for example, biofilm formation (Persat, 2017).

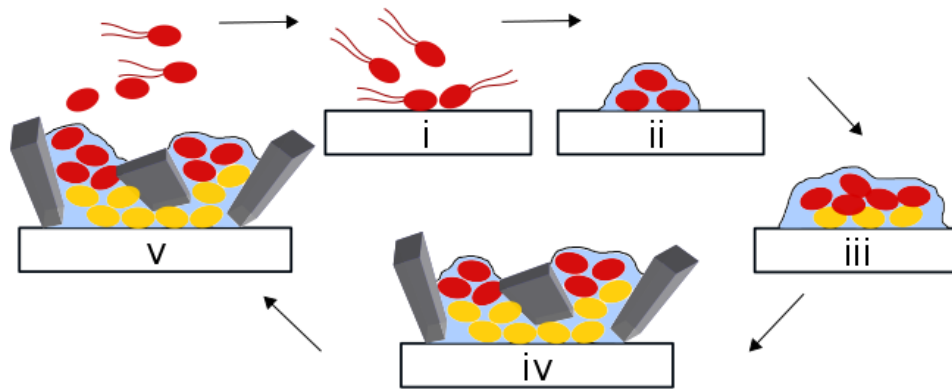


Figure 3. *P. mirabilis* biofilm developmental sequence on a urinary catheter. (i) Reversible attachment of planktonic bacteria. (ii) Irreversible attachment to surface. (iii) Secretion of EPS, yellow cells represent a less metabolically active state than the red cells. (iv) Calcium and magnesium phosphate crystals embed in developing biofilm. (v) Dispersal of daughter cells.

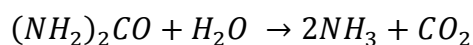
In the case of a urethral catheter, a conditioning film of host proteins forms on the surface facilitating attachment (Lo, Lange and Chew, 2014). Initially reversible attachment occurs. Bacterial flagella, fimbriae, and pili anchor the cell against hydrodynamic and repulsive forces and subsequently the appendages bond to the conditioning film resulting in irreversible attachment. The up- and down-regulation of genes was purported to occur to express a biofilm specific phenotype, however, it was more recently suggested that biofilm formation progresses by a sequence of successive adaptations to environmental and nutritional circumstances rather than a programmed mechanism (Bjarnsholt, 2013). Following attachment to a substratum, quorum sensing (QS) is thought to occur. QS is a density dependant coordination mechanism and can be used to coordinate various activities in biofilm and planktonic cultures. QS has been implicated in biofilm development in numerous uropathogens (Delcaru *et al.*, 2016). The proliferation of microcolonies in the biofilm occurs with a concomitant production of EPS. EPS is responsible for cohesion and adhesion and makes up 50 – 90 % of the organic carbon in the biofilm (Evans, 2000). The EPS consists of secreted polysaccharides, extracellular DNA (eDNA), proteins, surfactants, lipids, glycolipids and membrane vesicles but the composition varies according to the constituent bacterial species and environment (Bridier *et al.*, 2017). The presence of uronic acids and ketyl linked pyruvates

confers an anionic property which allows the association of divalent cations such as calcium and magnesium (Donlan, 2002) as seen for urinary catheters.

Biofilms develop a complex three dimensional structure but the maturation of the biofilm and the morphology is dependent on the fluid dynamics near the surface. A mature biofilm sheds some cells to disperse the community. Biofilms exhibit movement and should not be thought of as static entities. In high shear environments they show “creeping activity” and the formation of transitory waves and areas of greater detachment exist (Costerton *et al.*, 2003).

1.4.2 Catheter associated mineralised biofilms

The majority of the organisms that infect the catheterised urinary tract originate from the patient’s own microbiota. They tend to be of periurethral skin or faecal origin (Maki and Tambyah, 2001). The bacteria that are first to exploit this new niche include *Staphylococcus epidermidis*, *Escherichia coli* and *Enterococcus faecalis*. The relative ease at which infections occur means bacterial entry is recurrent and the composition changes over time (Liedl, 2001). The organisms that seem to persist in patients catheterised for the long term are *Pseudomonas aeruginosa*, *Proteus mirabilis*, *Providencia stuartii*, *Morganella morganii* and *Klebsiella pneumoniae*. Most infections are polymicrobial (Macleod and Stickler, 2007) which can complicate treatment. *Proteus* species, *P. aeruginosa*, some *Providencia* species, *M. morganii*, *K. pneumoniae*, *Staphylococcus aureus* and coagulase negative staphylococci all possess urease enzymes that catalyse the hydrolysis of urea to ammonia and carbon dioxide.



The increasing concentration of ammonia in the residual volume of urine in the bladder and on the catheter surface caused by urease activity raises the pH until a threshold, termed the nucleation pH, is reached and calcium phosphate (hydroxyapatite) and magnesium ammonium phosphate (struvite) precipitate and combine with the developing biofilm (Hedelin *et al.*, 1984). This will eventually lead to the mineralisation of the biofilm and blockage of the urinary catheter (Bruce *et al.*, 1974). Blockage can have serious repercussions, especially for patients in the community with limited access to healthcare professionals. A patient with a blocked

catheter might be rendered incontinent as the bladder fills and urine leaks extraluminally. Alternatively, the blockage can lead to painful distention of the bladder as it fills with urine until medical intervention occurs. If blockage goes unnoticed, infected urine can reflux to the kidneys where it can lead to the development of kidney stones, and other serious sequelae such as pyelonephritis, septicaemia and shock (Stickler and Zimakoff, 1994). The mineralised biofilm can break off during catheter removal and these fragments become the seeds of bladder stones and a source of bacteria that persist despite catheter changes resulting in chronic infections. Up to 50 % of all patients undergoing long-term catheterisation will be subject to catheter encrustation and blockage (Kunin, Chin and Chambers, 1987). *P. mirabilis* has been shown to have the most active urease enzyme (Jones and Mobley, 1987; Stickler *et al.*, 1998a) and is implicated in blockage events in the majority of cases (Mobley and Warren, 1987; Kunin, 1989; Stickler *et al.*, 1993).

1.5 *Proteus mirabilis*

First isolated from putrefied meat by Hauser in 1885, *P. mirabilis* is a gram-negative, motile, facultatively anaerobic bacillus of the family Enterobacteriaceae. It can be isolated from soil, stagnant water, the intestinal tract of mammals and, as a consequence, sewage (Wenner and Rettger, 1919). Named after Proteus from Homer's *Odyssey*, who was endowed with the "gift of endless transformation" to evade his pursuers, *P. mirabilis* is dimorphic, existing in two distinct morphologies and can evade the immune system. *P. mirabilis* possesses a number of key virulence factors that facilitate its infection of the catheterised urinary tract. One such factor is *P. mirabilis*'s ability to swarm, that is, flagella-mediated movement across a surface. When plated out onto solid media *P. mirabilis* differentiates into a distinct morphotype and forms concentric rings as it swarms and consolidates across a surface (Figure 4). Waves occur in concert producing the archetypical concentric rings exhibiting multicellular behaviour. The swarming morphotype is primarily concerned with flagellum-mediated motility, the consolidation phase, which was thought of as a resting phase, is actually a phase of intense activity during which the cell prepares for the subsequent round of swarming (Pearson *et al.*, 2010).

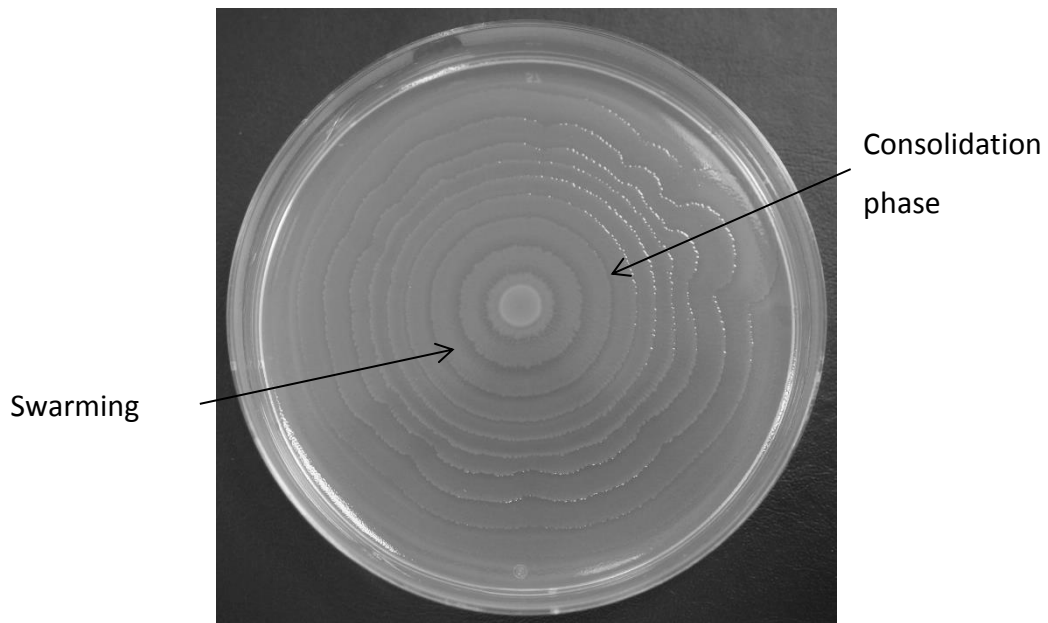


Figure 4. Swarming morphology of *Proteus mirabilis* on solid media. Photograph of *P. mirabilis* NSM6 swarming across the surface of a Tryptone soya agar plate. The concentric rings form as the bacterium swarms and consolidates before the next round of swarming.

The *P. mirabilis* swarming phenotype is considered a key virulence factor in urethral catheter infections as knock-out mutants that were unable to swarm were only able to migrate over catheters that were hydrogel coated (Jones *et al.*, 2004). Swarming therefore contributes to catheter infection by facilitating the migration of *P. mirabilis* from the catheter entry/exit site to the bladder. The swarming response is thought to be triggered by the inhibition of flagella rotation, surface contact and cell-cell signalling (Armbruster, Hodges and Mobley, 2013). The metabolic state of the cell and environmental conditions it experiences also play a role in swarming and the presence of specific amino acids, glutamine and histidine, which are highly concentrated in human urine (Tan and Gajra, 2006), seems necessary (Armbruster and Mobley, 2012). The differentiated swarmer cells elongate 20-50 fold, become multinucleated and can express thousands of flagella (Hoeniger, 1965). The swarmer cells align themselves with their flagella coiled together forming rafts (Jones *et al.*, 2004). Individual swarmer cells cannot move on their own and must be part of a raft, making swarming an obligatory multicellular behaviour (Kearns, 2010). The movement is facilitated by an extracellular slime that is thought to lubricate the movement of the cells (Stahl, Stewart and Williams, 1983). Swarming

bacteria are capable of migrating over large distances. Stickler and Hughes (1999) demonstrated that *P. mirabilis* can migrate distances of up to 10 cm in 24 h over catheter surfaces, although this rate alters dependent upon the catheter material. It has been suggested that *P. mirabilis* can carry other bacteria with them when swarming and thus facilitate ascension to the bladder. Stickler and Hughes, (1999) also noted a trail of vegetative cells left in the wake of the migratory swarm and postulated that these cells would go on to produce biofilms under appropriate conditions, leading to colonisation of the entire catheter. Furthermore, swarming cells have been observed emerging from biofilms and it was hypothesised that they may facilitate dispersal of the community (Jones *et al.*, 2007). Interestingly, it has been noted that swarming must be repressed to allow biofilm formation and to allow the continued attachment to surfaces (Liaw, Lai and Wang, 2004) so there must clearly be a switch back to the vegetative state to maintain an infection.

The infection and subsequent blockage of a urinary catheter by the production of crystalline deposits might be enhanced by swarming behaviour, as urease activity is increased 30-fold in swarmer cells (Allison, Lai and Hughes, 1992). Thus, swarming not only contributes to the initial infection of a catheter but also to colonisation and eventual blockage, highlighting why this phenotype is considered a key virulence factor in CAUTI. Various other factors central to the pathogenicity of *P. mirabilis* are also increased in the swarming morphotype, and the ability to invade cells is thought to be limited to swarmers (Allison, Lai and Hughes, 1992).

The capsular polysaccharides (CPS) of *P. mirabilis* have been shown to enhance crystal formation. The CPS of *P. mirabilis* are anionic, which enables the binding of metallic cations (Mg^{2+} , Ca^{2+}). Dumanski *et al.* (1994) showed that struvite formation occurred at lower pH in the presence of CPS and that a greater number of struvite crystals formed at pH 7.5-8.0 with CPS present compared to other experimental conditions. They speculated that the anionic nature of the CPS concentrates Mg^{2+} at the LPS, which is readily released to go on and form struvite crystals.

An interesting phenomenon occurs when two separate strains of swarming *P. mirabilis* meet. The leading edges of both swarms stop, and a clear line forms between them (Figure 5), termed a Dienes line (Dienes, 1946). In contrast, the

leading edge of colonies of the same strain do not form a clear boundary line and merge together. The bacteria are recognising self, versus non-self, and direct bacterial contact is required for this to occur (Budding *et al.*, 2009). The dominant Dienes type is thought to kill the submissive and the submissive type differentiates at the boundary into round cell types, although no precise mechanism has been suggested (Budding *et al.*, 2009). This competitive killing only occurs when swarming over surfaces, as when different Dienes types are grown in broth, no killing occurs. Various attempts have been made to explain the phenomenon and it seems it is a complex system with the involvement of multiple genes. One factor is the production and secretion of the bacteriocin proticine. Boundaries form between strains differing in proticine production and sensitivity, however, there are strains that do not produce proticines and still form boundaries even with other proticine deficient strains (Senior, 1977). Gibbs, Urbanowski and Greenberg (2008) identified a cluster of genes that have roles in self-recognition, calling them the *ids* (identification of self) operon, of which six genes were identified. As a swarm front comes into contact with another, a subset of cells express the *ids* genes and cross the boundary with the other swarm. This is sufficient to propagate the signal of self-versus non-self. Alteri *et al.* (2013) identified a type VI secretion system (T6SS) that plays a role in interspecies competition and killing. The authors constructed targeted mutants in the secretion system, demonstrating that Dienes line formation requires cell-cell contact and that killing is dependent upon the T6SS and associated primary effectors. Thus, it seems that the T6SS, *ids* and proticine all play a role in the recognition and killing of different strains during the Dienes phenomenon.

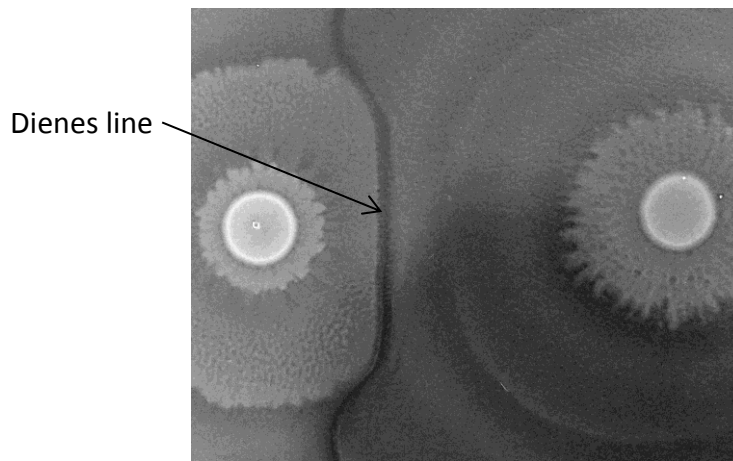


Figure 5. Dienes lines. The formation of a Dienes line occurs between the leading edges when the migratory swarms of two different Dienes types meet. Isolates plated on TSA and incubated at 37°C.

Once *P. mirabilis* gains access to the catheterised urinary tract it must be able to withstand the shear forces it might encounter in this new niche. It is able to attach itself to various mucosal surfaces, and inert materials, via the utilisation of fimbriae (Rocha, Pelayo and Elias, 2007). Fimbriae are thin flexible projections that have adhesins at their tips. The *P. mirabilis* genome contains 17 putative fimbrial operons, which is the most observed in any bacterial species (Pearson *et al.*, 2008). Five fimbrial types have been described, (Rocha, Pelayo and Elias, 2007) of which two have been implicated in adherence to catheters. These are mannose-resistant *Klebsiella*-like fimbriae (MRK) and ambient-temperature fimbriae (ATF). Although MRK fimbriae have not directly been observed in catheter attachment in *P. mirabilis*, they have been implicated in catheter attachment by *P. stuartii* (Mobley *et al.*, 1988) and *P. penneri* (Yakubu, Old and Senior, 1989) therefore it seems likely they carry out a similar function in *P. mirabilis*. ATF were so named as their expression is highest at 23°C. Their role in infecting mucosal surfaces in a mouse model of ascending urinary tract infection was ruled out by Zunino *et al.* (2000) as no loss of virulence was observed between ATF deficient mutants and wild type. It was suggested, therefore, that the ATF could play a role in the environment. Scavone *et al.* (2016) showed that the fimbriae play a role in biofilm formation, and also speculated that ATF might have a role in attachment to abiotic surfaces. More

work is required to determine what type of fimbriae play a role in attachment to catheter surfaces as its disruption could lead to possible prevention strategies.

After ascending the urinary tract, and colonising the bladder, *P. mirabilis* may ascend the ureters to the kidneys' proximal tubular epithelial cells that act as a barrier to the parenchyma. In order to infect the kidneys, damage is caused by a haemolysin and by urease to the single cell thick epithelium (Mobley *et al.*, 1991). Levels of haemolysin production have been shown to correlate to invasive ability in laboratory studies using green monkey kidney cells (Peerbooms, Verweij and Maclaren, 1984). However, mutants with defective haemolysin activity were still able to invade cells at a similar rate to the wild type (Mobley *et al.*, 1996). It appears that haemolysin production is not essential but plays a role in cellular invasion. Intracellular invasion represents a strategy by which *P. mirabilis* can avoid the immune response of the host. Mathoera *et al.* (2002) demonstrated that invasion offers protection from some antibiotic treatments, although crystals formed inside the cells and it was not clear if these crystals provided the protection from the antibiotic in a similar manner to how they do in the formation of stones, which is another approach *P. mirabilis* utilises to persist in the bladder or kidneys. *P. mirabilis* also possesses a serralyisin metalloproteinase, ZapA, which offers protection from the mucosal immune response by cleaving the secretory immunoglobulins A1, IgA2, and Ig3 as well as the antimicrobial peptides hBD1 and LL-37 (Belas, Manos and Suvanasuthi, 2004). ZapA has been shown to be a key virulence factor in the murine model of ascending UTI as significantly fewer ZapA deficient mutants were recovered from the urine and bladder compared to wild type (Walker *et al.*, 1999).

It is clear that *P. mirabilis* is well adapted to proliferating in the catheterised urinary tract and is implicated in almost all blockage events in the long-term catheterised patient (Mobley and Warren, 1987). The most important virulence factors are arguably the potent urease it possesses and its ability to swarm. These factors, combined with the failings of the Foley catheter can lead to significant morbidity (and mortality) for those catheterised for the long term. Understanding these issues might lead to improved catheter design or novel approaches to tackling these infections that have a serious effect on an already vulnerable patient group.

1.6 Attempts at preventing catheter-associated urinary tract infection

Several strategies have been pursued with the aim of preventing the colonisation of urethral catheters. Unfortunately, none so far have been successful at preventing *P. mirabilis* from causing encrustation and blockage. A study conducted by Dance *et al.* (1987), in which an extensive catheter care procedure was followed, highlights a major issue encountered when trying to inhibit bacteria with a single antimicrobial; the problem of resistance. Chlorhexidine solutions were used to clean the periurethral skin prior to catheter insertion and, once the catheter was inserted, the same solution was used daily to clean the catheter-meatal junction. An antiseptic lubricious gel was used for insertion to prevent bacterial infection upon entry. Further chlorhexidine was maintained in the drainage bags and a cream containing the antimicrobial was applied daily to the periurethral region. Despite the extensive attempt to block all entry points of bacteria, an outbreak of a chlorhexidine and multidrug resistant strain of *P. mirabilis* occurred, affecting more than 90 patients. The issue only abated once the policy was ceased. Indeed, using any single antimicrobial, especially with decreasing concentrations as in the form of a catheter coating, is risking resistance occurring and further complicating the care of patients and contributing to the global increase of antibiotic resistance.

There have been two commercially available “anti-infective” catheters available in the UK: a nitrofurazone-coated silicone catheter (Rochester Medical, Minnesota, USA) and a latex catheter that possesses a silver alloy coating and a hydrogel layer (C R Bard, New Jersey, USA). The nitrofurazone catheter is ineffective against *P. mirabilis*, as well as many other urinary pathogens such as *C. albicans*, *E. faecium*, *K. pneumoniae* and *P. aeruginosa* (Johnson, Johnston and Kuskowski, 2012) as they are inherently resistant to its mode of action. Nitrofurazone is reduced intracellularly to produce reactive intermediates which are thought to damage various intracellular targets, such as ribosomes (McOsker and Fitzpatrick, 1994). When compared to the silver catheter, nitrofurazone was more effective in preventing growth under the conditions tested (Johnson, Johnston and Kuskowski, 2012) however concerns about developing resistance are warranted (Siddiq and Darouiche, 2012). The antimicrobial properties of Silver have been recognised for many centuries although its mode of action has only relatively recently been

elucidated. Silver blocks the respiratory chain in the cytochrome oxidase and NADH-succinate-dehydrogenase region and therefore disrupts ion transportation and energy generation (Jansen *et al.*, 1994). There is also some evidence that it binds to DNA and causes denaturation (Feng *et al.*, 2000). It is the fact that it works on multiple processes within the cell that has generated interest amongst researchers, however, resistance to silver can still occur (Panáček *et al.*, 2018). Its use has been shown to be beneficial in short-term catheterisations (Schumm and Lam, 2008) however the cost needs to be carefully considered as short-term asymptomatic infections cause minimal harm and cease once the catheter is removed. Silver has demonstrated little effect in preventing infections caused by *P. mirabilis* or, indeed, for the long-term catheterised. A meta-analysis of the data revealed insufficient evidence for the recommendation of either silver or nitrofurazone for the long-term catheterised (Jahn, Beutner and Langer, 2012). In fact, the nitrofurazone catheter has now been withdrawn from the market (Fisher *et al.*, 2015). Morgan, Rigby and Stickler (2009) investigated encrusted silver catheters and were able to show that the antimicrobial effect of silver was masked by crystal formation and deposition on catheter surfaces which allowed *P. mirabilis* to encrust and block the catheters unabated. The amount of silver released from the catheters was also tested and none was detectable in the run off from the catheters, suggesting that if an antimicrobial treatment is to be successful it must elute from the surface at appropriate concentrations to prevent the bacterial population from elevating the urinary pH and, therefore, suppress crystal deposition.

1.6.1 Antimicrobial coatings

Further attempts at bacterial inhibition have been made using antimicrobial coatings. One such coating is Gendine; a mixture of gentian violet and chlorohexidine. Hachem *et al.* (2009) had success in using Gendine impregnated catheters in a rabbit model, finding it to be more efficacious than a silver-infused catheter. Complete eradication did not occur and no information was gathered for long-term use as catheters were only in place for four days so it remains to be seen if this strategy is appropriate for the longer term. Although the coating was well tolerated with no toxicity-related effects noted, resistance is still a concern with this approach. Similarly, a prospective, randomised, multi-centre clinical trial of a

catheter impregnated with rifampicin and minocycline found that these agents significantly reduced the rate of Gram positive bacteriuria but had no effect on Gram negative bacteria or yeasts (Darouiche *et al.*, 1999). Whilst this effect is partially beneficial, most persistent infections are by Gram negative organisms and they need to be tackled as a priority.

Triclosan has shown promise as a preventative for *P. mirabilis* infections and infections caused by *E. coli*, *K. pneumoniae*, *S. aureus* and, to a lesser extent, by *E. faecalis* and *P. stuartii*. It disrupts the cell walls of both Gram positive and Gram negative bacteria. When instilled in the inflation balloon of a silicone catheter at a concentration of 10 g/L Jones *et al.* (2006) could prevent catheter encrustation and blockage by *P. mirabilis* for 7 days. They also speculated that the concentration of Triclosan in the urine would be maintained for 12 weeks, which is the maximum duration a catheter can be maintained in place. The authors were not concerned about resistance to Triclosan occurring as at the time of writing, it had not been observed, however, resistance to Triclosan does occur and worryingly, confers resistance to other clinically important antimicrobials (Carey and McNamara, 2014; Carey *et al.*, 2016; McNamara and Levy, 2016). However, Triclosan is ineffective against *P. aeruginosa*, *S. marcescens* and *M. morgani* which while less commonly associated with CAUTI, are also urease producing. Lastly, Triclosan has some dangerous degradation products (Fiss, Rule and Vikesland, 2007) and contamination and accumulation in aquatic environments could lead to hormonal effects in humans and aquatic animals (Olaniyan, Mkwetshana and Okoh, 2016). Recently the FDA banned the use of Triclosan in soaps, although Triclosan is still permitted in medical products and toothpaste. The regulatory authorities in the UK were not willing to consider its use in catheters and the approach was not taken forward (personal communication with D. Stickler, 2010).

1.6.2 Modification of surface properties

Polyvinylpyrrolidone (pvp) is a nonionic water-soluble polymer that is similar to hydrogel, in that it increases the lubrication of the catheter making the device more comfortable for the patient. Tunney and Gorman (2002) suggested that bacterial adherence was less to pvp coated polyurethane than for an uncoated control and that crystal formation also decreased. Kazmierska *et al.* (2010) found that it was

ineffective in preventing encrustation and blockage in an *in vitro* bladder model and the addition of iodine had no long-term effect as bacteria and crystals still readily adhered. Patient comfort, however, is a significant factor in clinical decision making when selecting a catheter type (Vapnek, Maynard and Kim, 2003).

Heparin has been used in both catheter coatings and urethral stents to prevent bacterial adherence. Heparin is antithrombogenic and has strong electro-negative charge, thus repels cellular organisms. Tenke *et al.* (2004) showed a significant increase in time to blockage experiments using heparin-treated urethral catheters challenged with *P. mirabilis* in an *in vitro* model. However, the catheters did eventually block. Interestingly, on further analysis the catheters were free from encrustation and had blocked via a mucus-like plug. They also conducted a small, twenty patient trial in which heparin-coated stents had less encrustation compared to controls over 2-6 weeks (Tenke *et al.*, 2004). However, in another study heparin was shown not to reduce bacterial adherence in stents (Lange *et al.*, 2009). It seems that Heparin is most beneficial in vascular settings and that the interaction of components found in the urinary tract make it less effective.

The previous examples of surface modification have been in the form of coatings to enhance lubricity and prevent adherence. An alternative biomimetic approach is currently undergoing clinical trial (NCT02669342) in Canada using a catheter with a micro-patterned surface. The Sharklet catheter's surface is modified to mimic the dermal denticles of shark skin, which appear to be immune to marine fouling organisms. The creators speculate that the structure inhibits attachment and biofilm formation, although no precise mechanism is yet understood. Reddy *et al.* (2011) demonstrated a reduction in adherence by *E. coli* and noted smaller colonies when compared to a smooth control. Whether this approach will prevent crystalline deposits has not yet been determined.

Cranberry extract, a long-suggested preventative for UTIs, has also been investigated as a means to prevent adhesion of bacteria to surfaces. Proanthocyanidin trimers in extracts of the fruit act as anti-adhesion agents against uropathogenic *E. coli* (Foo *et al.*, 2000). The precise mode of action is unclear, although there is speculation that proanthocyanidin acts as a receptor analogue

and bind to the fimbrial tips, preventing adhesion to epithelial cells (Howell, 2007). Another suggested mode of action is via conformational changes in the fimbriae, reducing length and density (Liu *et al.*, 2006). Despite positive reports in the literature over the years, a Cochrane review (Jepson, Williams and Craig, 2012) concluded that the use of cranberry extract for preventing UTIs cannot be recommended.

1.6.3 Dietary modification

The long held recommendation of increasing fluid intake has been shown to be beneficial by diluting the urine, increasing the point at which precipitation of metal ions occurs, termed the nucleation pH (pH_n) (Suller *et al.*, 2005). A further increase in pH_n has been achieved by the addition of citrated drinks to the patients' fluid consumption. Citrate is a natural chelating agent of Mg^{2+} and Ca^{2+} . This approach has been shown to prevent the encrustation and blockage of urinary catheters by *P. mirabilis* (Stickler and Morgan, 2006). This approach is beneficial as it seems to have no negative effect on the patients, is active against a range of urease producing organisms, It does not, however, prevent bacterial infection, only the formation of crystalline deposits. Contrary to these findings, however, Bibby and Hukins, (1993) found that the acidification of urine was countered in the presence of urease, as further urea was hydrolysed raising the urinary pH. The authors suggested that acidic washouts could dissolve deposits but that the acidification of urine could not be recommended for preventing catheter encrustation. Therefore the consensus is not complete on this, compounded by the fact that it is quite difficult to change patient habits.

1.6.4 Plant-based antimicrobials

In searching for alternatives to traditional antimicrobials, increasing interest in plant-based antimicrobial extracts has arisen. These compounds often act on multiple sites and are, therefore, less prone to selecting for resistance. Malic *et al.* (2014) conducted preliminary trials to assess the ability of some of these extracts to reduce planktonic and biofilm populations of some common urease producing uropathogens. Cineole, eugenol, terpinen, and tea tree oil were trialled, with eugenol giving the best result against planktonic and biofilm populations. Biofilms proved much more resistant to the activity of the agents tested, presumably due to

the protective properties of biofilms as discussed previously (1.4.1). Sufficient effect was noted and the authors recommended further study to discern if eugenol could prevent CAUTI, either as a bladder washout or incorporated into a catheter coating.

1.6.5 Iontophoresis

Iontophoresis is a physical process by which ions flow diffusively in a medium driven by an electric field. Chakravarti *et al.* (2005) explored this process by passing silver wires through and next to the lumen of catheters and applied an electric potential of 9 V at a steady current of 150 μ A. The authors postulated that this caused the release of silver ions into the lumen, which prevented bacterial growth. Other suggested mechanisms of action have been put forward including the production of hypochlorous acid via electrolysis, superior repulsive forces between the microorganisms and the surfaces, oxidative stress and changes in pH (Voegelé *et al.*, 2015). A statistically significant increase in time to blockage was observed from 22 h to 156 h for the control and iontophoresis catheters, respectively (Chakravarti *et al.*, 2005). This method was unable to completely eradicate the bacteria and further studies *in vitro* and *in vivo* are warranted.

1.6.6 Enzyme inhibitors

The enzyme urease has become a target for manipulation as without the activity of this enzyme, catheter blockage would not occur. Morris and Stickler (1998) used the inhibitors acetohydroxamic acid and fluorofamide in an *in vitro* model of the catheterised urinary tract. They found that at concentrations of 1 μ g/ml both agents prevented the urinary pH from rising above pH 7.6 and levels of encrustation were reduced in the treated catheters. However, Acetohydroxamic acid is toxic and must not be systemically absorbed. Fluorofamide poses a reduced risk to health and was 1000-fold more effective in preventing encrustation. As expected, bacterial numbers were not affected with this intervention. This result has been repeated with other inhibitors that also possess bactericidal and bacteriostatic properties depending on concentration. These compounds are plant derived; for example the phenolic, vanillic acid (Torzewska and Rozalski, 2014), germa- γ -lactones (Amtul *et al.*, 2007), and plum juice (Zhu *et al.*, 2012).

1.6.7 Quorum sensing inhibitors

Quorum sensing is an attractive target for developing novel preventative strategies. Quorum sensing has been implicated in the formation and dispersal of biofilms in some species (Solano, Echeverz and Lasa, 2014), and it is this that has been the focus of the majority of attempts at disrupting quorum sensing to prevent catheter infections. N-acyl homoserine lactones (AHLs) have been shown to be produced by bacteria as they colonise the surface of catheters Stickler *et al.* (1998b) and Hentzer *et al.* (2003) were able to inhibit virulence factor expression by *P. aeruginosa* utilising a naturally inspired Furanone. Interestingly, the authors reported enhanced efficacy of antibiotic and dispersal via SDS treatment, which offers prospects of this therapy being used as an adjuvant to more traditional treatments. Unfortunately, due to toxicity, clinical use of Furanones is limited. Similar to the AHL system, diketopiperazines (DKPs) have been implicated in quorum sensing in *P. mirabilis*. Jones, Dang and Martinuzzi (2009) were able to show reduced bacterial numbers when using the antagonists tannic acid and *p*-nitrophenyl glycerol. Furthermore, the authors demonstrated a reduction in urease activity which resulted in lower pH and less crystal formation. Further work is required to determine a delivery method for this type of treatment and to discern if this approach is sufficient alone or if it is used in combination with antibiotics to enhance their efficacy. A major benefit of QS inhibitors is that as they are not involved in bacterial growth, therefore their inhibition should not apply strong selective pressures which usually result in resistance occurring.

1.6.8 Bacterial interference

Bacterial interference utilises benign bacteria to prevent the colonisation of the catheter by virulent pathogens, thereby exploiting antagonism between bacterial species and competition for resources. One study in which the bladder of patients with spinal cord injuries was inoculated with a strain of *E. coli* following targeted antibiotic treatment (Darouiche *et al.*, 2005) demonstrated the safety of this approach and showed a reduction in UTIs in the year following colonisation. However, this methodology was problematic as antibiotic treatment was ineffective in clearing the organisms infecting the bladder prior to installation and, as a result, the success rate of colonising with the benign strain was poor (Trautner, Hull and Darouiche, 2003). To counter this, catheters were colonised prior to the exposure

of urological pathogens *in vitro* (Trautner, Hull and Darouiche, 2003). The results showed a significant reduction in the uropathogens tested and the modified *E. coli* numbers remained stable, indicating this organism may persist. The success of this approach is in selecting an appropriate strain that is benign. The previous study utilised *E. coli* 83972, an isolate that caused persistent asymptomatic infection during a 3-year period of observation. It was then mutated by deleting a 800-base pair region in the *papG* gene which rendered it unable to make p fimbriae, which are implicated in the ability to cause pyelonephritis and bacteraemia. Subsequently the authors trialled this approach in a group of spinal cord injury patients and found the rate of symptomatic UTI decreased from 2.72 to 0.15 cases per 100 patient days. There are some problems with this approach. It could never be used on an immunocompromised patient and *P. mirabilis* tends to eliminate the benign strain (Trautner *et al.*, 2007; Prasad *et al.*, 2009) limiting effectiveness. In order to enhance the efficacy of this technique the bacterial interference was combined with bacteriophage therapy (Liao *et al.*, 2012). Bacteriophages are natural predators of bacteria and a virulent infection results in the killing of the host. The synergistic effect of combining the two treatment types produced the best reduction in *P. aeruginosa* biofilms under test conditions and represents a viable option for shifting the ecological balance in favour of the benign strain thus preventing the uropathogen from proliferating.

Despite the considerable attention the problem of CAUTI has had, a solution to this problem appears to be no closer. The current guidelines suggest removal of a catheter as soon as is feasible, and to prevent unnecessary catheterisations. Whilst this approach will reduce the overall infection burden on the patient population, it does not offer any solution to the often vulnerable, long term catheterised for whom a urinary catheter is a necessity.

1.7 Bacteriophages

Bacteriophages are obligatory intracellular parasites that hijack the bacterial cellular machinery to propagate themselves. Phage, derived from the Greek 'phagos' means 'a thing that devours', therefore, bacteriophages are 'eaters of bacteria'.

Bacteriophages were first described by Twort in 1915. He noticed a “glassy transformation” in micrococci colonies that were contaminating his attempts at propagating the vaccinia virus on cell-free agar plates. These plaques were dead bacteria and Twort demonstrated that these zones were transmissible via a sterile needle, and specific to the bacteria from which they were isolated. Independently of Twort, D’Herelle isolated what he later called ‘bacteriophages’ whilst working with soldiers suffering an outbreak of dysentery in 1917. It is D’Herelle who is credited with the discovery of bacteriophages and he proposed that they were an “ultravirus” that infected bacteria (D’Herelle, 1917). In fact, D’Herelle not only identified the nature of bacteriophages, he also recognised their therapeutic potential.

To test his theory D’Herelle conducted experiments in rabbits in which phages provided protection against *Shigella*. The old adage of “the enemy of my enemy is my friend”, holds true with phages, however, in Western Europe and the United States their use eventually fell out of favour due to a lack of understanding about their basic biology, that led to a number of unfavourable results. This prompted the American Medical Association’s council on pharmacy and chemistry’s review of the phage literature. Their conclusions did not support the therapeutic use of phages and called for more work to be conducted (Eaton and Bayne-Jones, 1934a). The final compounding factor that caused phage therapy to fall out of favour was the discovery of antibiotics, with a broad, reliable spectrum of activity. Phages were still pursued therapeutically in the Soviet Union, and Eastern Europe, such as Georgia and Poland, and centres were set up that still exist today i.e Eliava Institute in Tbilisi, Georgia.

In the West, the study of a few model phages revealed the central dogma of molecular biology (Salmond and Fineran, 2015). Phages lend themselves to this task because of their relatively simple genomes, in fact the first sequenced organism was phage MS2 (ssRNA) (Fiers *et al.*, 1976). Phages then revealed their ubiquity in nature through work concerning marine environments. It was shown that phages can be present in levels up to 2.5×10^8 PFU/ml of sea water (Bergh *et al.*, 1989) which highlighted their role in the turnover of microorganisms. In fact, phages are estimated to halve the bacterial population every 48 h (Rohwer, Prangishvili and

Lindell, 2009) and hence have a significant impact on carbon cycling in the southern ocean and an important role in the structure and function of oceanic food webs where nitrogen, phosphorous, and carbon, amongst other elements, are made available to other microorganisms in a process termed the “viral shunt” (Wilhelm *et al.*, 1999).

Phages have a significant influence on the evolution and diversity of bacteria both through predation and horizontal gene transfer. Phages and bacteria are locked in an evolutionary arms race best described as antagonistic co-evolution. A concept called “killing the winner” proposed by Thingstad and Lignell (1997) suggests that diversity is maintained within a bacterial community as the species that dominates, due to a selective advantage, will be killed by phages allowing less competitive species to be sustained. Phage infection does indeed seem to be dependent on the density of the bacterial population (Hennes, Suttle and Chan, 1995; Kunin *et al.*, 2008) adding further weight to this theory.

As well as phages accelerating bacterial mutation rates that drive the evolution and adaptability of bacteria (Pal *et al.*, 2007), other mechanisms exist that result in phage mediated changes in bacterial genomes. Horizontal gene transfer can occur through a process termed generalised transduction. Another mechanism that benefits bacteria, termed lysogenic conversion, has been observed where integration of a temperate phage genome provides genes that affect the host cell fitness. An example of this is the conversion of diarrheagenic *Escherichia coli* to a more virulent strain that can potentially cause haemolytic uremic syndrome when infected with a lamboid phage that possesses the Shiga toxin (Schmidt, 2001). The lysogeny of a bacterial cell also offers immunity from further infection by phages that utilise the same receptors, further benefiting the lysogenised host (Labrie, Samson and Moineau, 2010).

Phages are currently the focus of renewed interest due to the rise of antibiotic resistance. It is hoped that, with improved understanding of the fundamental biology of infection and sufficiently controlled trials, phages might become useful tools in the treatment of bacterial infections.

1.7.1 Bacteriophage morphology

A bacteriophage particle consists of genetic material encapsulated by a protein coat. The genetic material can be single or double stranded DNA or RNA, and for some families the protein coat contains lipids which render the particle sensitive to chloroform. The most striking feature of bacteriophage morphology is the sheer diversity that exists amongst them. This is hardly surprising considering 10^{31} are thought to exist in the biosphere (Hendrix *et al.*, 1999). The International Committee on Taxonomy of Viruses (ICTV) recognises 19 families of phages that infect bacteria (Adams *et al.*, 2017). Over 6,300 bacterial viruses have been examined by electron microscopy since 1959 (Ackermann and Prangishvili, 2012). The most abundant group are the dsDNA tailed phages of the Order *Caudovirales*, which account for 96.3 % of those observed (Ackermann and Prangishvili, 2012). The classification system utilised by the ICTV is polythetic meaning that a species is defined by a “set of properties that may or may not be present in any individual” (Van Regenmortel, 1990). Virion morphology is taken into consideration as well as nucleic acid type and structure, nucleotide sequence identity and gene content. With advances in DNA and protein sequence analysis tools, more detailed relationships are being defined (Grose and Casjens, 2014). The fact that similarities exist between tailed bacterial and archaeal viruses suggests that phages existed before the divergence of those two groups and are therefore very ancient (Ackermann, 2009b).

The *Caudovirales* are currently divided into three families, distinguished by their distinct tail morphologies: *Siphoviridae* possess long, flexible non-contractile tails; *Myoviridae* are endowed with contractile tails; and *Podoviridae* have short, stubby tails (Figure 6).

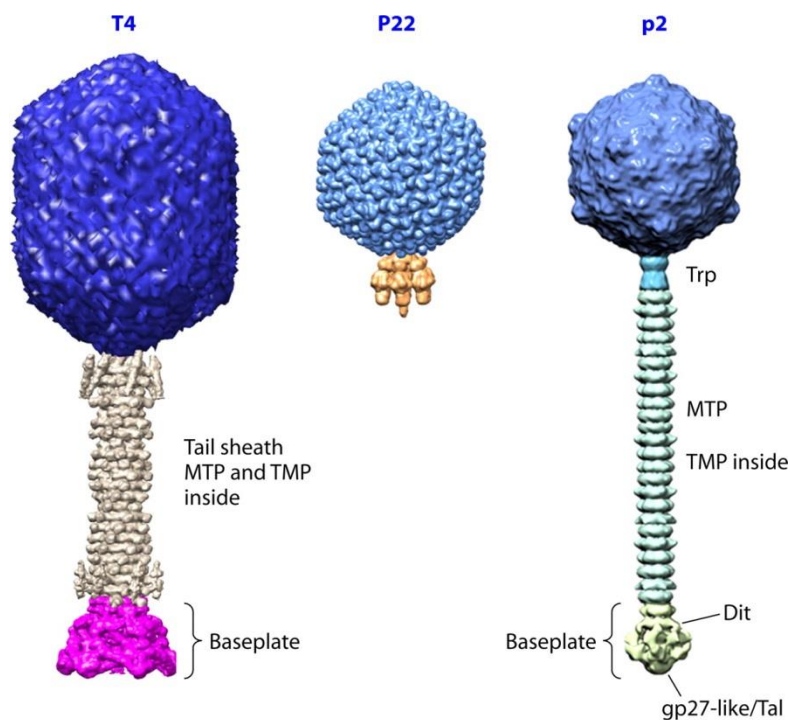


Figure 6. The three families of the Order *Caudovirales* from left to right representatives of *Myoviridae* (T4), *Podoviridae* (P22) and *Siphoviridae* (p2). Image adapted from Veessler and Cambillau (2011) with permission.

The *Siphoviridae* are the most abundant observed, accounting for 61 %, followed by the *Myoviridae* (25 %) and *Podoviridae* (14 %) (Ackermann, 2007). Capsids are isometric consisting of hexa-, icosah-, octa- and dodecahedra or can be elongated by the addition of a ring of capsomers, the units that makes up the capsid, between the two icosahedral end pieces to make a prolate head (Aksyuk and Rossmann, 2011). The formation of a capsid is not unique to bacteriophages and HK97-like protein fold, named after *Escherichia* phage HK97 (Wikoff *et al.*, 2000), is also present in herpesviruses, further providing evidence of an ancient common ancestor. The capsid size is proportional to the quantity of genetic material it contains as a result the DNA is packaged very densely.

The DNA is translocated into the procapsid during the assembly process. Scaffold proteins may still be supporting the procapsid structure at this point in assembly. The terminase molecule that cleaves the DNA interacts with the portal protein and DNA is delivered into the capsid. Scaffold proteins are then released if they have not been already, which provides space for the DNA. The capsid then takes on a

more angular form as it expands to its final shape (Hendrix and Garcea, 1994). In some phages, decoration proteins now bind to the capsid (Casjens and Hendrix, 1988) which are sometimes required for infectivity or stability of the structure in extreme conditions. The terminase then cleaves the DNA and the terminase-DNA complex unbinds and it is thought that this complex then moves on to the next capsid to be assembled. Meanwhile, head completion proteins bind to the portal to prevent premature leakage of the DNA. The tail is now attached to the completed head. For *Podoviridae*, the tail, which is largely recognition and attachment machinery, is sequentially attached to the capsid (Lander *et al.*, 2009) but for *Siphoviridae* and *Myoviridae* the tails are assembled in a separate step and bind to the completed capsids via the neck proteins (Casjens and Hendrix, 1988).

Tail assembly begins with the initiator complex, an intermediary which forms, in phage λ , the conical tip and protruding terminal fibre of the mature tail (Katsura and Köhl, 1975). This structure initiates the polymerisation of the major tail protein (MTP) which forms the tube that acts as the conduit for DNA. In the *Siphoviridae* this forms the tail, whereas in the *Myoviridae* this tube is covered by an outer sheath which contracts upon host binding and DNA injection. The length of the tail is determined by a protein called the tape measure protein (TMP). This protein has been shown to be directly proportional to the length of the tail and acts as a scaffold during polymerisation (Katsura, 1987). It sits within the lumen of the tail and, in addition to its role in length determination, is thought to play a role in infection where it is ejected prior to DNA and assists in DNA entry into the cell (Scandella and Arber, 1976). The tail terminator protein then binds to the tube, halting polymerisation and completing the tail. This protein then interacts with the head completion proteins to join the head and tails together (Pell *et al.*, 2009).

1.7.2 Bacteriophage life cycles

As obligate parasites, bacteriophages lack the cellular machinery required to propagate themselves. As a result they are reliant on their hosts. Phage life cycles begin with adsorption, followed by infection, and finally complete with the release of daughter viruses. There are two main types of life cycle observed in the *Caudovirales*, virulent and temperate (Figure 7). A virulent phage can only replicate by a lytic cycle in which phages infect and rapidly kill their host cells via lysis of the

cell and release of daughter viruses. Temperate phages appear to have a choice when infecting a new cell; they can enter the lytic cycle or the lysogenic, in which the genome assumes a quiescent state termed a prophage, and integrates into the host's genome. Alternatively it can be maintained as a plasmid such as observed in T4 under nutrient limited conditions (Kutter *et al.*, 1994). This state can be maintained indefinitely and, if integrated, the phages genome is copied along with the host chromosome.

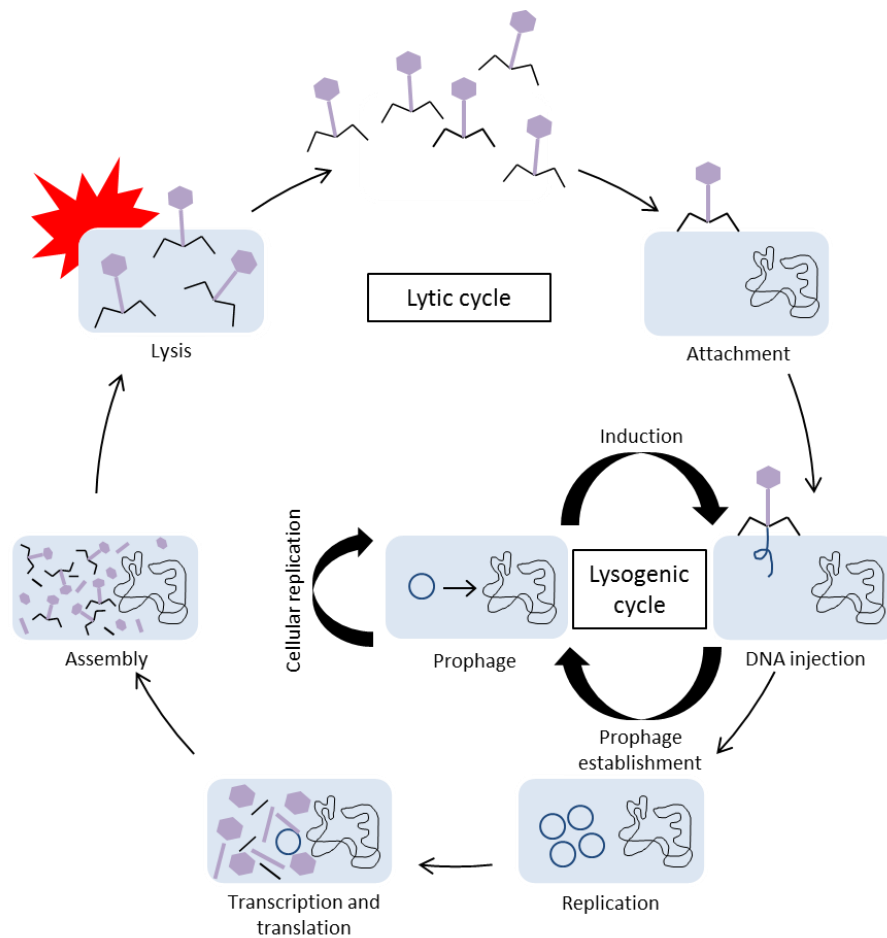


Figure 7. Diagrammatic representation of the life cycle of the tailed bacteriophages. A free phage encounters a susceptible bacterium, attaches to the bacterial cell and injects its DNA. Lysogenic cycle can occur with integration of phage DNA followed by cellular replication. Continuation of lytic cycle, hijack of cellular machinery to produce phages, phages are assembled, lysis occurs releasing daughter phages and killing the bacterial cell.

Infection begins with a phage locating a suitable host. Specific sites on the bacterial cell surface are used for recognition and at this point the phage is only loosely associated with the surface. When a target receptor is recognised the phage irreversibly binds and ejects its DNA into the cell (Hyman and Abedon, 2010). Different phages will utilise different methods for translocating DNA to the cytoplasm and phages have developed certain adaptations to avoid enzymatic degradation once there. Some phage DNA has a modified base, such as that of T4 and SP01, which possess a hydroxymethyldeoxycytidine (hmdC) and a hydroxymethyldeoxyuridine (hmdU), respectively. These bases are resistant to host restriction enzymes (Warren, 1980). Other phages have evolved over time to not possess sites that would be recognised by the restriction enzymes of their common hosts. One tactic is the avoidance of palindromic sequences, as type II restriction endonucleases often recognise symmetrical (palindromic) sequences (Rocha, Danchin and Viari, 2001). Further mechanisms exist to escape degradation including rapid circularization of phage DNA upon entry by means of single stranded genomic termini.

Once the DNA has reached the cytoplasm and avoided bacterial defence mechanisms, it transcribes into messenger RNAs that are then used to direct the cell's ribosomes to produce copies of the viral DNA and produce proteins. These assemble into complete phages then an enzymatic process, mediated by phage proteins, causes the lysis of the bacterial cell and release of progeny virions. The period from infection to when completed virions are detectable inside the bacterial cell is termed the eclipse period and the duration from infection to the release of virions via lysis is referred to as the latent period (Ellis and Delbrück, 1939).

Lysogenic phage infection follows the same initial steps for delivery of DNA to the cytoplasm, then a decision is made to enter into the lytic cycle or to integrate its genome into the bacteria's. Alternatively, the phage can exist as a plasmid within the cell and remain stable and protected through successive bacterial generations (Echols, 1972). The life cycle the phage enters into, at least in the case of phage λ , is based on nutrient availability, high multiplicities of phage absorption and temperature (Ptashne, 2004). In instances of high phage absorption it is relatively safe to assume that other local bacteria are experiencing a similar situation.

Susceptible bacteria are, therefore, declining in the environment. It is not in the phage's interest to completely eradicate its host, and under these conditions, λ enters the lysogenic life cycle. A similar situation exists when a bacterium experiences low nutrient levels; the phage will again enter into the lysogenic life cycle to 'weather the storm' until a point which favours the production of progeny and the likelihood of further hosts being available for those progeny. The genetic switch that controls the decision is mediated by the levels and stability of a protein called cII, a transcriptional activator (Court, Oppenheim and Adhya, 2007). Briefly, high levels of cII result in high levels of production of the λ repressor (cI) and, consequently, P_L and P_R (promoters) are repressed and the recombination genes are transcribed resulting in integration and therefore the lysogenic cycle. Alternatively, lower levels of cII prevent λ repressor production via the action of cro (a repressor) and the phage enters into the lytic phase as P_L and P_R are not repressed resulting in the production of N and Q. N causes the genes for viral DNA replication to be transcribed (by preventing termination). Q then activates the expression of head, tail and lysis genes. cIII also helps establish lysogeny by protecting cII from degradation. Host cell proteases break down cII and are present in greater numbers in high nutrient conditions, this has the effect of low cII and therefore the lytic cycle is selected. When greater numbers of phages enter a cell, higher quantities of cII exist which results in lysogeny. In the laboratory lysis dominates, primarily due to the high nutrient conditions used in the culture of bacteria. This can be problematic as temperate phages may be assumed to be virulent.

Lysogeny is maintained by the presence of cI (Figure 8). It represses transcription from P_L and P_R whilst upregulating its own expression, it's the only phage protein expressed by a lysogenised bacterium and in so doing also provides immunity to superinfection by other lambda phages by repressing transcription of P_L and P_R . A process termed lysogenic conversion has also been shown to provide resistance to superinfection to phage that act on the same receptor by causing conformational changes that prevent phage binding or the loss of the receptor altogether (Chung *et al.*, 2014).

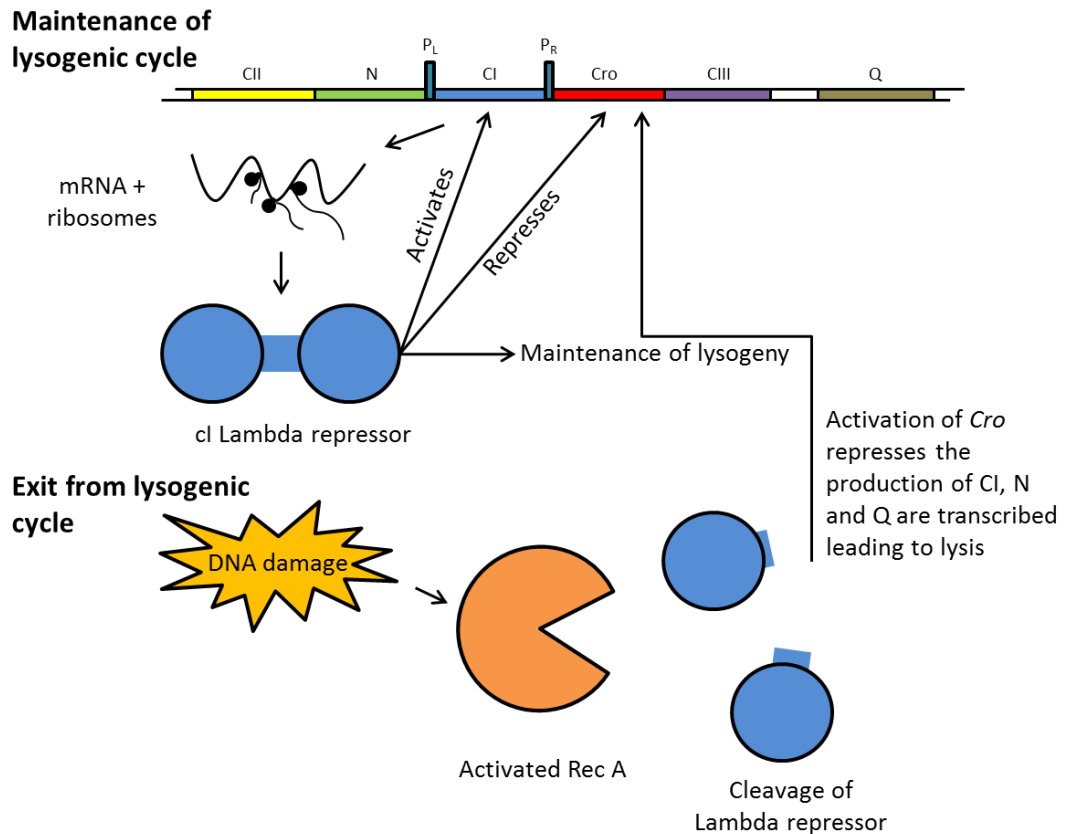


Figure 8. Diagrammatic representation of the maintenance and exit from lysogeny. The lambda repressor (*ci*) represses transcription from P_L and P_R preventing lytic genes from being transcribed, it also up-regulates its own expression. DNA damage causes the exit from lysogeny as the SOS response is activated. Rec A cleaves the *ci* repressor, P_L and P_R are no longer repressed and the lytic genes are sequentially switched on.

The exit from lysogeny is brought about by the bacterial SOS response (Figure 8), commonly induced in the laboratory through DNA damage by mitomycin C or UV irradiation. The SOS response aims to repair DNA damage by arresting the cell cycle and inducing mutagenesis and DNA repair. LexA is a repressor that represses the SOS response genes under normal growth. When DNA damage occurs RecA activates and cleaves LexA preventing it from functioning, decreasing amounts of LexA then sequentially switches on the SOS genes (d'Ari, 1985). In exiting from lysogeny RecA is commandeered and brings about the cleavage of the λ repressor as its structure is similar to LexA. With no λ repressor available to repress transcription, the cell begins the lytic cycle (Ptashne, 2004).

Finally, another facet of bacteriophage life cycles is that of pseudolysogeny. This is where the phage DNA enters into the bacterial cell but does not integrate in a stable way nor initiates the lytic life cycle; instead it remains in this intermediate mode until conditions occur that induce either the temperate or virulent life cycle (Ripp and Miller, 1997). This phage carrier state might confer a number of conditional advantages to the phage, for example it shelters the phage from potentially harsh conditions outside the host. Furthermore it might be an adaptation to overcome a nutrient limited host by preventing an abortive replication or integration event due to the limited nutrients (Łoś and Węgrzyn, 2012). In addition, it might function as a means for a temperate phage to not be entirely reliant on the host's SOS response to escape lysogeny.

1.7.3 Phage therapy

Phage therapy is the “reduction or elimination of pathogenic or undesirable bacteria by the application of bacteria-specific viruses” (Abedon and Thomas-Abedon, 2010). The use of phages to treat human infections has been practiced since just after their discovery. However, the lack of understanding about phage biology and the widespread use of antibiotics in the 1940s resulted in a decline in interest in this potentially useful approach, in the West. Currently, the rise in multi-antibiotic resistant bacteria, and the consequent need for effective alternatives, has led to renewed interest in bacteriophages as therapeutic agents. In 2014 the European parliament proposed a motion for the resolution of antibiotic resistance requesting that member states prioritise phage therapy to complement antibiotic therapy (Parliamentary Assembly, 2014).

1.7.4 Advantages over traditional antimicrobial agents

Bacteriophage therapy has many advantages when compared to conventional antibiotic therapy and should not be overlooked despite difficulties regarding regulatory approval (Section 1.7.6).

As long as virulent phages are used, phages are bactericidal. The same cannot be said for all antibiotics as some are bacteriostatic. If bacteria are not killed they retain the ability to develop resistance or those that have developed resistance are selected for (Stratton, 2003). Additionally, phages increase in number at the site of the infection. This auto dosing is an advantage as numbers increase in the presence

of the bacterial host. The opposite is true for traditional antimicrobial agents where the concentration decreases between doses and potentially reaches sub-inhibitory concentrations depending on how they are employed. This can again lead to the development of resistance.

Another benefit of phages as antimicrobials is specificity. In contrast to conventional antibiotics, phages are species or genus specific. This means that the normal flora of the host is left intact as the pathogen of interest is targeted. This is beneficial to patients as there is less risk of infections from problematic organisms such as *Clostridium difficile* or *Candida albicans*. However, the specificity of the interaction between bacteria and phage can be seen as a disadvantage as well when considering presumptive treatment of infections. This problem can be somewhat overcome with the use of a cocktail of phages with different host ranges or recognition targets. This allows for the coverage of a much wider range of organisms and can contribute to preventing resistance from occurring if there is some overlap in host range.

The FDA (food and drug administration (USA)) considers bacteriophages as generally safe for use in humans (Kutter and Sulakvelidze, 2005). Over the last century there have been no reports of significant adverse reactions from the countries where phage therapy has consistently been practised (Abedon *et al.*, 2011). Considering the abundance of phages in the environment, as well as in and on the human body, they will have been presented to the immune system, for instance, 11 % of healthy controls and 23 % of patients had antibodies against a *Staphylococcus* phage prior to its administration (Kucharewicz-Krukowska and Slopek, 1987). Although humans are exposed to phages on a daily basis concern exists regarding their immunogenicity as high doses of phage proteins has been observed to elicit side effects from immune system stimulation (Dabrowska *et al.*, 2014). Regarding treatment, the concern is that the administered phages will be removed from systemic circulation which would make it difficult to maintain an effective concentration (Goodridge, 2010). However, the emergence of anti-phage antibodies does not exclude a favourable treatment result (Łusiak-Szelachowska *et al.*, 2014), and a couple of studies have reported no adverse effects from administering phage cocktails either topically (Rhoads *et al.*, 2009) or ingesting

them (Bruttin and Brüssow, 2005) so perhaps application needs to be carefully considered.

When compared to traditional antimicrobials, resistance to phages is considered less problematic as many other phages exist that could be utilised that the bacteria are not yet resistant to. Another benefit of phage is that some mutations for resistance negatively impact bacterial fitness or virulence due to the loss or modification of pathogenicity related phage receptors (Skurnik and Strauch, 2006). Antibiotic resistance also does not translate to phage resistance due to the different mechanisms that phages and antibiotics use. As a result phages could be employed to treat antibiotic-resistant bacterial infections (Carlton, 1999; Kaźmierczak, Górski and Dąbrowska, 2014).

In the last 30 years the discovery of new classes of antibiotics has stagnated (Silver, 2011). In contrast, the discovery of novel phages has increased. The advances in high-throughput sequencing technologies has greatly reduced the cost of phage characterisation therefore phages can be obtained for a much reduced cost when compared to the discovery of new antimicrobials (Skurnik, Pajunen and Kiljunen, 2007).

Finally, an advantage of phages is their apparent ability to be able to disrupt and eradicate biofilms. Some phages possess carbohydrate degrading enzymes which have the ability to degrade the EPS of the biofilm, or capsule and O-antigen (Latka *et al.*, 2017). They can be attached to the particles tail spikes, tail fibres or base plates and facilitate access to the bacterial cell for initiating an infection. Presence of this activity is demonstrated by a halo surrounding a plaque that expands upon further incubation. Either phage associated or free depolymerases display this feature (Adams and Park, 1956). The depolymerase enzymes tend to show specificity to a lesser extent than the phages they were derived from (Son *et al.*, 2010). Phage derived depolymerases can be divided into two classes based on their mechanism, lyases and hydrolases. Their ability to disrupt medically relevant biofilms is beneficial as minimal effect should occur on host microbiota as well as human cells. This approach might increase the efficacy of chemical antimicrobial therapy giving the agents access to the bacterial cells, indeed Lu and Collins (2009)

demonstrated enhanced antimicrobial activity utilising engineered temperate phages and Verma, Harjai and Chhibber (2009, 2010) utilised native phages to a similar effect.

1.7.5 Requirements for phage therapy

Phages should ideally be obligately lytic, stable under the chosen storage conditions, subjected to safety and efficacy studies and fully sequenced before being used in phage therapy (Gill and Hyman, 2010). Additionally, they ideally should have good killing potential, be able to evade bacterial defences and survive well within the environment in which they are to be placed. Temperate phages are avoided as they do not kill their hosts and a lysogenic infection can make the bacteria immune to superinfection by another phage which may have been able to kill them otherwise. They may also provide genes that encode toxins or otherwise modify the bacterial genome, enhancing virulence, these are strong arguments for avoiding temperate phages. Skurnik and Strauch (2006) put forward a number of criteria that should ideally be met before phage therapy is attempted;

1. The phage should be well characterised.
2. Phage preparations should comply with all regulatory requirements; specifically such preparations should not contain any bacterial components (e.g. endotoxins) by undertaking adequate purification processes.
3. Phages in the preparation should be viable; stability under storage conditions should be confirmed.
4. The interaction between phage and bacteria should be understood; identification of the receptor and if its loss results in loss of bacterial virulence.
5. The phage should be tested in an animal model as efficacy *in vitro* does not predict efficacy *in vivo*.

Clearly, compliance with these prerequisites requires substantial work and this would not guarantee approval by the regulatory authorities, so further hurdles may exist. This bar to approval of phage therapy is perhaps one reason why it is not yet available in mainstream Western medicine.

1.7.6 Regulatory issues surrounding phage therapy

The problem of regulatory approval of phage therapy, at least in Europe, is the desire for adequately designed and registered clinical trials that include safety assessments and good manufacturing practice (GMP) in regard to phage production. The vast amount of literature that has built up since phage discovery is not considered because these data have not been validated under current regulatory standards. Mullard (2014) estimated the cost of bringing a new drug to market at US\$2.6 billion therefore the ability is limited to organisations which possess the financial resources.

The nature of the phage product can be problematic from a regulatory perspective. Treatment can be derived from a bank of well-defined phages that are tested against the patient's specific pathogen, then a bespoke formulation is produced. This has some similarities to autologous cell-based products (Pelfrene *et al.*, 2016) however the production and characterisation of vast phage libraries are beyond the financial capabilities of most researchers and should ideally be undertaken by government agencies. Alternatively, cocktails against common pathogens can be prepared, however, experience from the Eliava institute, where this has been practiced for a century, has shown that these formulations need to be updated to the current relevant pathogens on a regular basis (Kutter *et al.*, 2010). The regulations that this product would fall under do not allow changes in formulation, especially the introduction of a new phage as it would be considered a new medicinal product and would require separate authorization, a costly and time-consuming endeavour. There is, however, precedence for medical products being allowed an accelerated development pathway circumventing clinical trials for each revision, with the influenza vaccine changing annually, however, the process is still complex (Pelfrene *et al.*, 2016). Additionally, no current guidelines exist for the quality of phages produced for phage therapy (Verbeken *et al.*, 2012). As a result, manufacturers have reverted to existing guidelines for biotechnology products. Clearly, advice is needed to ensure compliance with regulations.

Despite these hurdles, trials are underway with a view to demonstrate efficacy and safety. Clearance for future clinical use, however, may require a new category of

drug licencing to allow for the biological nature of phage products and their requirements for rapid updating.

The issue remains, would pharmaceutical companies be willing to commit to regularly updating their phage preparations, especially as these products would be in direct competition to their other antibiotic products. Furthermore, intellectual property (IP) rights surrounding phages are problematic for companies since this technology has been in the public sphere since the 1920s so is, therefore, unpatentable (Thiel, 2004). Also, natural entities consisting of protein and DNA cannot be patented. This does, however, pave the way for genetically modified phages but significant public scepticism exists surrounding the application of genetically modified organisms (GMOs).

1.7.7 Phage treatment of uropathogens

Relatively few examples of phage use in the treatment of infections of the urogenital tract or of *Proteus mirabilis* exist in the literature. The first mention in English language literature is in the reviews of Eaton and Bayne-Jones (1934b, 1934a, 1934c, 1934d). In these works the authors support the use of phage therapy for the treatment of cystitis despite their critical opinion of phage therapy in general. A later review (Slopek *et al.*, 1987) reported 92.9 % positive outcomes for phage treatment of 42 diseases of the genitourinary tract between 1981 and 1986.

In vitro assessment of a number of phage cocktail products (Pyo, Intesti, Ses and Enko) obtained from the Eliava institute has been reported (Sybesma *et al.*, 2016) and their activity assessed against a library of clinical urinary tract isolates. Good coverage of the clinical isolates was observed (93 %) which, as the authors report, warrants further study.

Phages have been shown to be successful in treating infections in murine models, the seminal work of Smith and Huggins (1982) showed that bacteriophages could be at least as effective as antibiotics at preventing mortality with capsulated *E. coli* K1 infections. Tóthová *et al.* (2011) showed that Injection of phages into the peritoneal cavity of mice resulted in the distribution of phages to all internal organs and titres remained high for 24 h post administration. No adverse reactions

attributed to the administration of phages were noted, providing preliminary data on the safety and efficacy of phage therapy.

Several reports in the literature describe the use of phage therapy in humans. Letkiewicz *et al.* (2009) successfully treated 3 patients suffering *E. faecalis* infections of the prostate. Khawaldeh *et al.* (2011) undertook the treatment of a patient who was suffering a persistent *Pseudomonas aeruginosa* urinary tract infection. Six phage types were selected against the infecting bacterium and instilled into the bladder every 12 h for 10 days. Meropenem and Colistin were administered from day 6 of phage treatment. The patient's urine remained pathogen free for 6 months post treatment, highlighting the benefit of phages as an adjuvant to traditional antimicrobial therapy. However, caution should be exercised, as noted by Torres-Barceló and Hochberg (2016), that double-resistant variants do not develop. Caution is also advised in considering the above results, as so few patients were treated.

Finally, the use of phages to prevent catheter infection has been investigated and is discussed in more detail in Chapter 4. Briefly, Curtin and Donlan (2006) applied phages to hydrogel urinary catheters to prevent *Staphylococcus epidermidis*, often implicated in central venous catheter infections. Fu *et al.* (2010) attempted to prevent infections caused by *P. aeruginosa* in the same model system utilising a cocktail of five phages. The same group subsequently presents work tackling a dual species biofilm consisting of *P. aeruginosa* and *P. mirabilis* (Lehman and Donlan, 2015). Two cocktails, consisting of six and four phages active against *P. aeruginosa* and *P. mirabilis*, respectively, were combined and the activity against dual species biofilms assayed. Melo *et al.* (2016) present data on two phages against *P. mirabilis* isolates in the same model system described by Curtin and Donlan, (2006).

Carson, Gorman and Gilmore (2010) report the use of phages to treat infections caused by *E. coli*, and less successfully, *P. mirabilis*. Nzakizwanayo *et al.* (2015) used a phage bolus to successfully eradicate *P. mirabilis* infections cultured on catheters in an *in vitro* bladder model system. Finally, Milo *et al.* (2017) utilised the previous researchers' phage and incorporated it into a pH sensitive catheter coating, assessed in an *in vitro* bladder model system.

1.7.8 Foreign language literature

A vast amount of Russian, Polish and Georgian language literature exists as phage therapy has been practised in these countries since the 1920s. It has been summarised by Chanishvili and Sharp (2009) however, again, there are relatively few examples of the use of phages in urology. Tsulukidze (1938) describes the application of phage therapy to treat acute and chronic cystitis, pyelocystitis, and purulent paranephritis. Treatment took the form of individual phages or a cocktail called Pio-bacteriophage that contained phages against *E. coli*, *S. aureus*, and *S. epidermidis*. They were administered directly to the bladder or into the pelvis and kidneys. In cases of acute cystitis an effect was observed after 4-5 hours and resulted in relief of pain, a decrease in frequency of urination and a normalisation of the composition of the urine. Full recovery of the 13 patients was observed in 1-3 days, however, in chronic cases of cystitis only moderate improvement was observed. In the treatment of 5 patients with pyelocystitis the authors reported complete cure of 4 patients, however the fifth succumbed to re-infection. For the treatment of four patients with paranephritis, phages were sprayed onto the connective tissues surrounding the kidneys and, after surgery, sprayed onto the wounds; all patients recovered after 2-3 days.

The next reported use of phage was by Tsiskarishvili (1957) who describes 22 cases of paranephritis that were treated with bacteriophage. In 12 cases surgery was not necessary, and in these patients, pus was evacuated by puncture followed by the administration of phages into the site. Additionally 20 ml of phages were administered intramuscularly. Success was measured by duration of hospital stay and this group stayed, on average, 19.5 days. The remaining 10 patients for whom surgery was necessary also received phages in the infective site; their duration was 24.2 days. This compares favourably to the control group, who received the standard treatment of lumbar therapy and tramponization. Their stay was 31.7 days on average.

Pio-bacteriophage preparation was used in the treatment of urinary tract infections against *P. aeruginosa*, *Proteus sp*, *Staphylococcus sp*, and *E. coli* by Perepanova *et al.* (1995). Prior to patient treatment the authors tested the cocktail against 295 isolates from patients. They found that 68.9 % of the isolates tested were lysed.

They managed to enhance this preparation by passage through their bacterial collection and increased efficacy to 84 %. This adapted preparation was then administered orally and locally to patients, and a reported cure was achieved in 92 % of patients.

A review by Voroshilova *et al.* (2000) describes the use of phages to treat cystitis and pyelonephritis. The phages were administered via bladder installations and orally. Infection was eliminated in 88.4 ± 0.9 % for cystitis and 92.2 ± 0.7 % for pyelonephritis. The control group received antibiotics and fared less well, with cure achieved in 39 ± 9.2 % and 58.5 ± 5.5 % for cystitis and pyelonephritis, respectively. Interestingly, the authors monitored immune response and noted that phage treatment caused elevated levels in their markers which was not seen in the antibiotic treated group.

In conclusion, despite a limited number of examples, there is evidence in the literature for safe, efficacious treatment of urinary tract infections by phage therapy. Limitations in experimental design, however, highlight the need for more extensive laboratory investigations and randomised, controlled, clinical trials.

1.8 Study aims

The aim of this study was to assess bacteriophage therapy as a treatment for the infection and eventual blockage of urinary catheters infected with *Proteus mirabilis*. In order to achieve this, the specific aims were:

1. To isolate bacteriophages from environmental samples against clinical *P. mirabilis* isolates.
2. To select the most appropriate phages to take forward for analysis.
3. To characterise the selected phages.
4. To apply the phages as a coating to catheters and assess their impact on infection and blockage in an *in vitro* model system.
5. To investigate if a cocktail of bacteriophages enhances the antimicrobial effect.

Chapter 2 Materials and Methods

2.1 Bacterial strains and growth media

The bacterial isolates used in this study (Table 2) were obtained from the Bristol Urological Institute (BUI) (Bristol, UK), Southmead Hospital (Bristol, UK), and the University of the West of England (Bristol, UK). Isolates obtained from the BUI were of clinical origin from various projects kindly donated by Professor David Stickler of Cardiff University; the isolates were from different geographical locations and chronological time points. Southmead Hospital provided current clinical isolates from infected urines submitted for analysis. Stock bacterial cultures were stored at -80°C in Microbank™ (ProLab Diagnostics, Neston, Cheshire, UK) cryopreservation bead filled tubes. Nutrient media were provided by Oxoid Ltd (Basingstoke, UK) unless stated otherwise. Working cultures were maintained on Cystine-Lactose-Electrolyte-Deficient (CLED) agar and liquid cultures in Tryptone Soya Broth (TSB). Lennox Luria Broth (LB) (Sigma-Aldrich Ltd, Poole, UK) with the addition of 0.6 % w/v Bacteriological Agar for soft media or 1.5 % w/v for solid were used for bacteriophage experiments.

Table 2. Bacterial isolates used in this study. Isolates are numbered according to the original institutions naming scheme.

| No. | Isolate | Source |
|-----|------------------------------|------------------------------|
| 1 | <i>Proteus mirabilis</i> D1 | Bristol Urological Institute |
| 2 | <i>Proteus mirabilis</i> D2 | Bristol Urological Institute |
| 3 | <i>Proteus mirabilis</i> D3 | Bristol Urological Institute |
| 4 | <i>Proteus mirabilis</i> D4 | Bristol Urological Institute |
| 5 | <i>Proteus mirabilis</i> D5 | Bristol Urological Institute |
| 6 | <i>Proteus mirabilis</i> D7 | Bristol Urological Institute |
| 7 | <i>Proteus mirabilis</i> D12 | Bristol Urological Institute |
| 8 | <i>Proteus mirabilis</i> D13 | Bristol Urological Institute |
| 9 | <i>Proteus mirabilis</i> D15 | Bristol Urological Institute |
| 10 | <i>Proteus mirabilis</i> D19 | Bristol Urological Institute |
| 11 | <i>Proteus mirabilis</i> D14 | Bristol Urological Institute |
| 12 | <i>Proteus mirabilis</i> D17 | Bristol Urological Institute |
| 13 | <i>Proteus mirabilis</i> D18 | Bristol Urological Institute |
| 14 | <i>Proteus mirabilis</i> D23 | Bristol Urological Institute |
| 15 | <i>Proteus mirabilis</i> D24 | Bristol Urological Institute |
| 16 | <i>Proteus mirabilis</i> D25 | Bristol Urological Institute |
| 17 | <i>Proteus mirabilis</i> D28 | Bristol Urological Institute |

| No. | Isolate | Source |
|-----|--|-----------------------------------|
| 18 | <i>Proteus mirabilis</i> D32 | Bristol Urological Institute |
| 19 | <i>Proteus mirabilis</i> D33 | Bristol Urological Institute |
| 20 | <i>Proteus mirabilis</i> D35 | Bristol Urological Institute |
| 21 | <i>Proteus mirabilis</i> D36 | Bristol Urological Institute |
| 22 | <i>Proteus mirabilis</i> D37 | Bristol Urological Institute |
| 23 | <i>Proteus mirabilis</i> D41 | Bristol Urological Institute |
| 24 | <i>Proteus mirabilis</i> Releen 18 | Bristol Urological Institute |
| 25 | <i>Proteus mirabilis</i> H24 | Bristol Urological Institute |
| 26 | <i>Proteus mirabilis</i> H25 | Bristol Urological Institute |
| 27 | <i>Proteus mirabilis</i> H26 | Bristol Urological Institute |
| 28 | <i>Proteus mirabilis</i> GS12 | Bristol Urological Institute |
| 29 | <i>Proteus mirabilis</i> GS13 | Bristol Urological Institute |
| 30 | <i>Proteus mirabilis</i> GS14 | Bristol Urological Institute |
| 31 | <i>Proteus mirabilis</i> #3 | Bristol Urological Institute |
| 32 | <i>Proteus mirabilis</i> #10 | Bristol Urological Institute |
| 33 | <i>Proteus mirabilis</i> HI4320 | Bristol Urological Institute |
| 34 | <i>Proteus mirabilis</i> NSM2 | Bristol Urological Institute |
| 35 | <i>Proteus mirabilis</i> NSM 6 | Bristol Urological Institute |
| 36 | <i>Proteus mirabilis</i> NSM 25 | Bristol Urological Institute |
| 37 | <i>Proteus mirabilis</i> NSM 39 | Bristol Urological Institute |
| 38 | <i>Proteus mirabilis</i> NSM 42 | Bristol Urological Institute |
| 39 | <i>Proteus mirabilis</i> NSM 59 | Bristol Urological Institute |
| 40 | <i>Proteus mirabilis</i> NSM 60 | Bristol Urological Institute |
| 41 | <i>Proteus mirabilis</i> 45967 | Southmead Hospital |
| 42 | <i>Proteus mirabilis</i> 46126 | Southmead Hospital |
| 43 | <i>Proteus mirabilis</i> 46453 | Southmead Hospital |
| 44 | <i>Proteus mirabilis</i> 46500 | Southmead Hospital |
| 45 | <i>Proteus mirabilis</i> 46511 | Southmead Hospital |
| 46 | <i>Proteus mirabilis</i> 46546 | Southmead Hospital |
| 47 | <i>Proteus mirabilis</i> 46564 | Southmead Hospital |
| 48 | <i>Proteus mirabilis</i> 46670 | Southmead Hospital |
| 49 | <i>Proteus mirabilis</i> 46708 | Southmead Hospital |
| 50 | <i>Proteus mirabilis</i> 46736 | Southmead Hospital |
| 51 | <i>Proteus mirabilis</i> NCIMB 701880 | University of the West of England |
| | Other Gram-negative bacteria | |
| 1 | <i>Enterococcus faecalis</i> NCIMB 775 | University of the West of England |
| 2 | <i>Klebsiella pneumoniae</i> cc242 | University of the West of England |
| 3 | <i>Serratia marcescens</i> cc12 | University of the West of England |
| 4 | <i>Staphylococcus aureus</i> RN4220 | University of the West of England |
| 5 | <i>Pseudomonas aeruginosa</i> ATCC 15442 | University of the West of England |
| 6 | <i>Salmonella enteritidis</i> PT4 | University of the West of England |
| 7 | <i>Escherichia coli</i> ATCC 15036 | University of the West of England |
| 8 | <i>Acinetobacter baumannii</i> ATCC BAA-1710 | University of the West of England |

2.2 Determination of bacterial numbers

Enumeration of bacteria was achieved by either the drop plate method, the spread plate method or by use of a spiral plating device (WASP, Don Whitley Scientific, Shipley, UK).

2.2.1 Drop plate method

The bacterial suspension was serially diluted in a 1:10 dilution series using ¼ strength Ringers solution (Oxoid Ltd., Basingstoke, UK) as diluent. Ten µL of the well mixed dilutions were plated out in triplicate onto suitable agar plates (see section 2.1) divided into 6 equal sections. Suspensions were pipetted without touching the agar and left to spread and dry before being inverted and incubated overnight at 37°C. Colony forming units (CFU) per ml were calculated by;

$$\text{CFU/ml} = \text{average number of colonies} \times 100 \times \text{reciprocal of counted dilution}$$

2.2.2 Spread plate method

The bacterial suspension was diluted as in 2.2.1. In triplicate, 100 µL of the vortexed suspension was pipetted onto the surface of an agar plate and spread uniformly using an ethanol sterilised glass hockey stick. Plates were allowed to dry before inversion and subsequent incubation over night at 37°C. Colony forming units (CFU) per ml was calculated by;

$$\text{CFU/ml} = \text{average number of colonies from 3 plates} \times 10 \times \text{reciprocal of counted dilution}$$

2.2.3 Spiral plating device

Dilutions of the bacterial suspension were carried out in 10 mL volumes of Ringers solution. Fifty µL was plated by the device (WASP, Don Whitley Scientific, Shipley, UK). Triplicate plating was carried out and plates dried before incubation overnight at 37°C. The bacterial suspension was enumerated following the manufacturer's instructions.

2.3 Pulsed-Field Gel Electrophoresis (PFGE) on bacterial isolates

PFGE is a technique for separating large (> 15 kb) DNA molecules by periodically changing the angle of the electronic field in relation to the agarose gel on which the samples are loaded.

The method was adapted from pulseNet CDC PFGE SOP (Anomyous, 2013). Cultures of the bacterial isolates were grown on NA. The bacteria were collected using a sterile swab, and suspended in 2 mL cell suspension buffer (100 mmol Tris: 100 mmol EDTA, pH8). The optical density of the suspension was modified to 1.0 at 600nm. Suspensions were warmed to 45°C and 200 µL added to an equal volume of molten 2% w/v Agarose (Sigma-Aldrich Ltd, Poole, UK) with 10 µL of Proteinase K (20 mg/mL) (New England Biolabs, Hitchin, UK). The mixtures were aspirated thoroughly and 75 µL transferred to a plug mould (BioRad, Hemel Hempstead, UK). Upon setting, plugs were transferred to 15 mL centrifuge tubes with 5 mL of cell lysis buffer (50 mmol Tris: 50 mmol EDTA, pH 8 + 1 % sarcosyl) with 25 µL of proteinase K (20 mg/ml) (New England Biolabs, Hitchin, UK) and incubated at 55°C for 2 h with vigorous agitation (150 rpm). Sterile ultra-pure water was heated to 55°C and plugs were washed twice for 15 min followed by a further four 15 min washes in TE buffer (10 mmol Tris: 1 mmol EDTA, pH8) that was warmed to 50°C. Slices (approximately 2 mm thick) of the plugs were subjected to restriction digest by 5 U of *Not 1* HF (New England Biolabs, Hitchin, UK) in 200 µL digestion mixture, prepared following the manufacturer's recommendations, for 16 h at 37°C. To cease the reaction the digest mixture was removed and replaced with cold TE buffer. Slices were then loaded onto a 1 % (w/v) agarose gel made with 0.5 X TBE (Sigma-Aldrich Ltd, Poole, UK) and wells sealed with the same agarose. Lambda DNA ladder (New England Biolabs, Hitchin, UK) was included as a size standard and digested genomic DNA from strain HI4320 was loaded onto every gel to check the running efficiency and the accuracy of post-run processing. Macrorestricted DNA was separated (Figure 9) using the CHEF-DR II system (BioRad, Hemel Hempstead, UK) at 6 V/cm with a switch time of 5-50 s for 22 h at 14°C using 0.5 X TBE running buffer. DNA was stained with ethidium bromide (1 µg/ml) for 1 h followed by de-staining with deionised H₂O for 30 min. Bands were visualised under UV light

(FluorChem Q, ProteinSimple, California, USA) and banding patterns analysed with the GelCompar II software package (Applied Maths, Austin, USA) using the Dice similarity coefficient and the UPGMA clustering method.

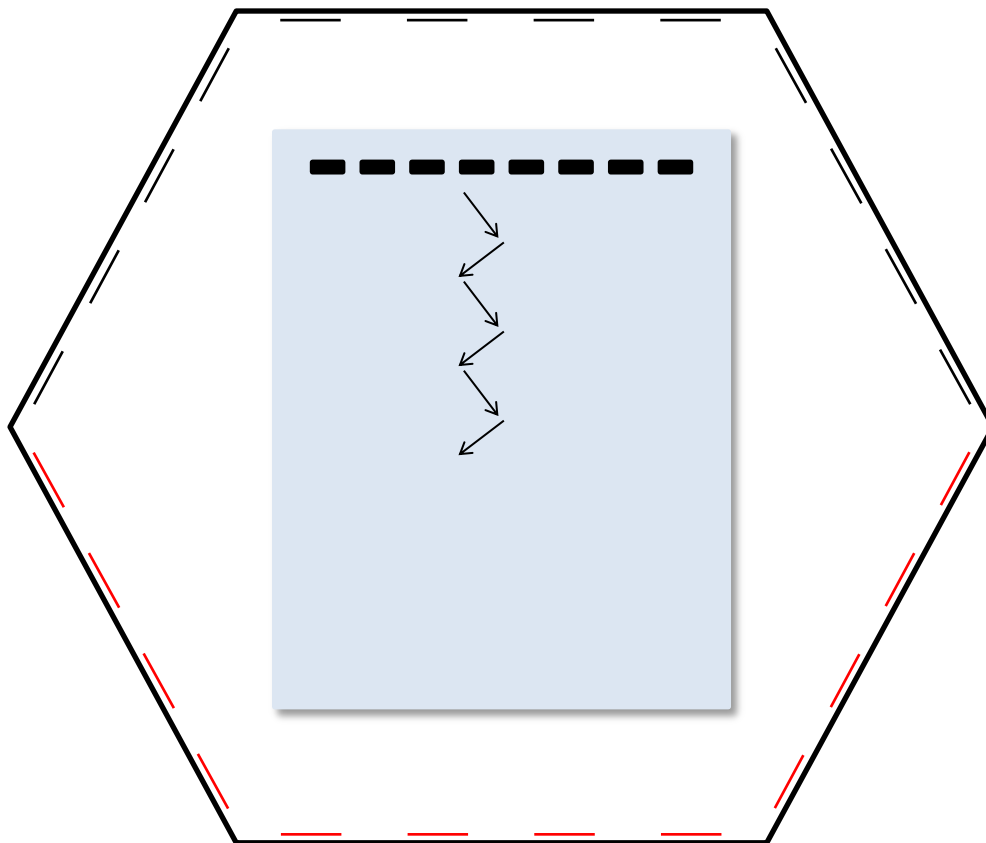


Figure 9. Diagrammatic representation of Pulsed Field Gel Electrophoresis. Large DNA molecules (> 15 kb) are separated by altering the electronic field by 60° from centre (total 120°). The DNA does not move in a straight line through the gel but in a net forward direction depicted by the arrows. The change of direction allows fragments to separate as realignment takes longer for larger fragments. Over the course of the run (22 h) the consistent change of electric field separates the fragments.

2.4 Determination of bacteriophage titres

Enumeration of phage titre was achieved using the double agar overlay plaque assay technique (Kropinski *et al.*, 2009; Adams, 1959). A 100 μ L sample of a log-fold dilution of bacteriophage was added to 100 μ L of early exponential phase host bacteria (OD_{600} 0.1) and allowed to adsorb for 5 min. A 4 ml aliquot of soft LB agar (0.6 % w/v bacteriological agar supplemented with 8 mmol/L $MgSO_4$ and 4 mmol/L $CaCl_2$) was added and subsequently poured on to a 90 mm LB agar plate (supplemented with 8 mmol/L $MgSO_4$ and 4 mmol/L $CaCl_2$) ensuring even coverage was achieved. Prior to inversion and incubation at 37°C for 18-24 h, plates were set for 10 min on the bench. Following incubation, zones of clearing in the bacterial lawn (plaques) were counted on triplicate plates and, where possible, on two consecutive dilutions. The titre of the phage suspension was calculated by;

$$\text{PFU/ml} = \text{average number of plaques from 3 plates} \times 10 \times \text{reciprocal of counted dilution}$$

2.5 Isolation of bacteriophages

Raw influent or activated sludge was acquired from various sewage treatment works within the catchment of Wessex Water. Following the enrichment protocol of Van Twest and Koprinski (2009) sewage samples were centrifuged at 10,000 $\times g$ (Beckman Coulter, Allegra X-30r, High Wycombe, UK) for 10 min followed by filtration (0.2 μ m pore size). A 10 mL aliquot of the filtered sewage was added to an equal volume of double strength NB (Oxoid Ltd., Basingstoke, UK) supplemented with 20 mmol/L $MgSO_4$ and 4 mmol/L $CaCl_2$. A 100 μ L aliquot of a stationary phase culture of each bacterial clinical isolate was added to separate tubes and the enrichments incubated at 37°C for 24 h with gentle mixing (50 rpm). Following incubation, the contents of the enrichments were centrifuged at 10,000 $\times g$ for 10 min, 2.5 % (v/v) of chloroform was added and samples were plated using method 2.4. Any resulting plaques were then excised and suspended in Sodium Magnesium buffer (100 mmol/L Tris-Cl, 8 mmol/L $MgSO_4$, 100 mmol/L NaCl, pH 7.5) at 4°C for 24 h to allow phages to elute. Each excised plaque was plated and excised a further two times to ensure purity.

2.6 Propagation and purification of bacteriophages

Overnight liquid preparations of host bacteria were used to inoculate 1 L of LB (Sigma-Aldrich Ltd, Poole, UK) supplemented with 8 mmol/L MgSO₄ and 4 mmol/L CaCl₂. The optical density (600nm) was monitored until it reached 0.1, at which point titrated plaque suspension was added to achieve an approximate multiplicity of infection (MOI) of 0.1. The propagation was incubated at 37°C with shaking (150 rpm) until post lysis re-growth was observed, which was determined by hourly optical density measurements. Bacterial growth was halted by the addition of chloroform (1 % v/v). The cultures were cooled to room temperature and DNase I and RNase A (1 µg/mL) added and incubated for 30 min. Sodium Chloride (NaCl) was also added to the cultures to a concentration of 1 M and, when dissolved, debris was removed by centrifugation at 11,000 x *g* for 10 min at 4°C. The clarified lysate was transferred to a sterile Duran which contained a magnetic stirrer. PEG 8000 was added (10% w/v) and gently stirred until the powder had dissolved. Lysates were stored at 4°C for 24 h to precipitate bacteriophages prior to their recovery by centrifugation in a fixed angle rotor at 4°C for 10 min at 11,000 x *g*. The pellet was re-suspended in SM buffer (100 mmol/L Tris-Cl, 8 mmol/L MgSO₄, 100 mmol/L NaCl, pH 7.5), 16 mL for every litre of clarified lysate. Re-suspended pellets were mixed by inversion for a minimum of 30 s with an equal volume of chloroform before being centrifuged at 3000 x *g* for 15 min at 4°C. The aqueous phase was retained and the process repeated until no PEG was visible at the interface between the aqueous and organic phases. A two-step Caesium Chloride (CsCl) density-gradient centrifugation was employed (Sambrook and Russell, 2001) to purify phages. Briefly, solid CsCl was added to the phage preparation at a final concentration of 0.5 g/mL and gently agitated. A step gradient was prepared in ultra-clear centrifuge tubes (Beckman Coulter, High Wycombe, UK) by under-laying solutions of higher densities. Solutions were prepared in SM buffer (100 mmol/L Tris-Cl, 8 mmol/L MgSO₄, 100 mmol/L NaCl, pH 7.5) and added as follows; 2 mL of $\rho = 1.3$, 3 mL of $\rho = 1.4$, 3 mL of $\rho = 1.5$, and 2 mL of $\rho = 1.7$. The phage preparation was carefully layered on top of the gradient before centrifugation using an SW40 rotor in an Optima LX-P ultra-centrifuge (Beckman Coulter, High Wycombe, UK) at 87,000 x *g* for 2 h at 4°C. Bacteriophages formed a bluish white band between the ρ

= 1.4 and $\rho = 1.5$ and were collected by puncturing the side of the ultra-clear tube with a 21 G needle attached to a 5 mL syringe (Figure 10). Scotch tape was used to prevent leaks and phages were collected by moving the needle back and forth below the band. A further round of equilibrium centrifugation was carried out. The phage preparation was carefully added to 6 mL of $\rho = 1.5$ g/mL CsCl in SM and centrifuged at $160,000 \times g$ for 24 h at 4°C . Bands were recovered as before, and the sample transferred to a Slide-A-Lyzer (Thermo Scientific, Loughborough, UK) dialysis cassette with a 100 kDa molecular weight cut off to diafiltrate the sample against three 500-fold volume changes of SM buffer at 4°C . Bacteriophages were then titrated and stored at 4°C .

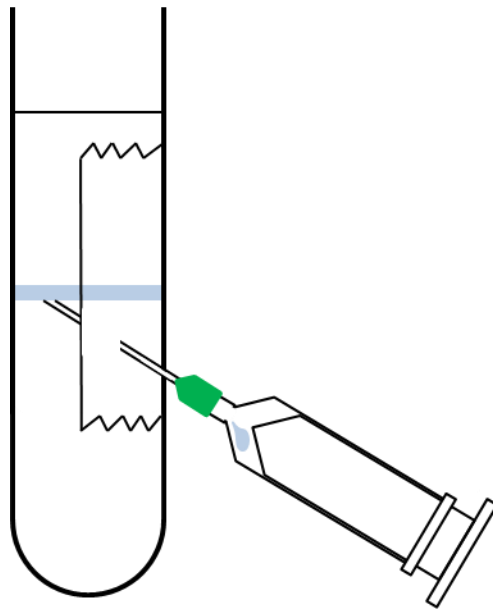


Figure 10. Diagram depicting side puncture method for collecting bacteriophages from CsCl density and equilibrium gradients.

2.7 Transmission electron microscopy

Transmission electron microscopy utilises an accelerated beam of electrons generated by a tungsten filament to acquire an image. Thin samples are negatively stained with heavy metal salts which interact with the electron beam to produce a phase contrast image. The wavelength of the focused electron beam is much shorter than that of light, as a result, higher resolution is achieved when compared to light microscopy.

Morphological examination of bacteriophages was accomplished following the method outlined by Ackermann (2009). Purified bacteriophages were sedimented by centrifugation at 25,000 $\times g$ for 60 min in the Optima LX-P ultra-centrifuge using the 70Ti rotor (Beckman Coulter, High Wycombe, UK). The supernatant was discarded and phage pellets were re-suspended in 0.1 M ammonium acetate (pH 7.0) a total of two times. Formvar carbon-coated 400-mesh TEM grids (TAAB Laboratory Equipment Ltd, Aldermaston, UK) were prepared by the addition of a drop of bacteriophage suspension which was left to absorb for 1 min. Uranyl acetate (1 % v/v, 4.5 pH) was then added for 30 s to stain the particles before being drained off with filter paper. Dry grids were then examined using the CM10 transmission electron microscope (Philips, Eindhoven, NL) at 60 KV. Magnification control was achieved by measuring T4 bacteriophage tails and virion dimensions revealed by measuring at least 20 well preserved intact particles. Phages were attributed to families according to the International Committee on Taxonomy of Viruses (ICTV) recommendations (Anon, 2005).

2.8 Host range

Determination of host range was achieved by following the protocol of Kutter (2009). Square 120 mm plates were prepared with LB (Sigma-Aldrich Ltd, Poole, UK) 1.5 % w/v bacteriological agar (Oxoid Ltd., Basingstoke, UK) supplemented with 8 mmol/L $MgSO_4$ and 4 mmol/L $CaCl_2$. A soft agar overlay was (0.6 % bacteriological agar) mixed with 200 μL of 0.1 OD_{600} culture and poured over the plates to create a lawn of bacteria. Phage stocks were adjusted to yield 5×10^9 PFU/mL and a 10-fold dilution series was carried out. The dilutions were then spotted on to each host in 5 μL aliquots and permitted to absorb (Figure 11). Plates were incubated overnight at

37°C. Phage activity was quantified using a ranking system where; +4 = complete clearing, +3 = clearing throughout but with faintly hazy background, +2 = substantial turbidity throughout the cleared zone, +1 = a few individual plaques, and – = no clearing. A total of 42 *Proteus mirabilis* isolates were tested along with 8 other Gram negative species.

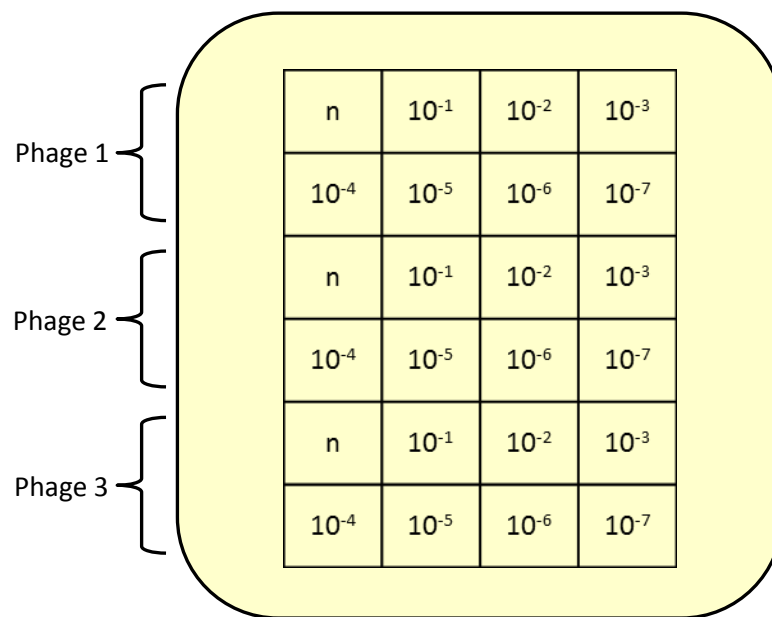


Figure 11. Organisation of bacteriophage dilutions for host range spot plate assay.

2.9 Adsorption rate constant

The adsorption rate constant describes the likelihood of a phage adsorbing to a bacterium over time. Here, it was estimated by measuring free phage loss over time when known quantities of phages and bacteria were mixed.

Measurement of the rate of attachment of bacteriophages to bacterial cells was carried out following the method of Kropinski (2009). Micro-centrifuge tubes were prepared by adding 950 μL of $\frac{1}{4}$ strength Ringers solution (Oxoid Ltd., Basingstoke, UK) to 50 μL of Chloroform and cooled by placing on ice 10 min prior to the commencement of the procedure. Host bacterial strains were grown to an OD_{600} of

0.1 and titrated using method 2.2.1. The approximate cell density was 5×10^7 CFU/mL. A phage suspension was then prepared so that it contained 5×10^5 PFU/mL and pre-warmed to 37°C in a water bath. One mL of phages was then added to 9 mL of bacteria, immediately after, 1 mL of phages was added to 9 mL of broth to provide a means of measuring the number of phages added. At 1 min intervals, 50 µL aliquots from the phage-bacteria suspension were transferred to the micro-centrifuge tubes and retained on ice. The sampling period was 20 min for vB_PmiS_NSM6, and 10 min for vB_PmiP_#3 and vB_PmiM_D3. Immediately on completion of sampling, 100 µL from each time point was plated out via the double agar overlay method (2.4) in triplicate to assess unabsorbed phage numbers. Plates were incubated for 16-24 h at 37°C and absorption rate (K) determined by;

$$K = \frac{-m}{N}$$

where m is the slope of the linear regression of the measured free phage titre over time and N is the initial bacterial density.

2.10 One step growth

One step growth experiments are a means by which the phage growth cycle can be characterised. The method was first described by Ellis and Delbrück (1939) who showed that phage growth is fundamentally different to that of bacteria. Viral infection must be synchronised for efficient measurements in one step growth experiments and measurements of intracellular and extracellular virions are obtained by treating samples with chloroform to lyse bacterial cells. This allows the determination of the eclipse period, which is the time from adsorption until the first daughter virion is assembled, the latent period, which is the time from adsorption until the release of daughter virions, and the burst size, which is the number of daughter virions released per infected cell.

The procedure for one step growth was adapted from the method described by Carlson (2005). Bacteria were grown to 5×10^8 CFU/mL by monitoring optical density (600 nm). A sample was removed and placed on ice, and titrated by plating triplicate spread plates (2.2.2) of the 10^{-5} and 10^{-6} 10-fold dilution series. Bacteriophages were added to the bacteria so that a MOI of 0.1 was achieved. The

mixture was left for 5 min to allow the phage adsorption. A 1 mL sample was then removed and centrifuged at 13,000 x *g* for 1 min, the supernatant was discarded and the pellet re-suspended in an equal volume of LB broth. This was then diluted 10,000 fold by adding 100 µL to 9.9 mL of pre-warmed broth and then transferring 200 µL of the previous dilution to 19.8 mL pre-warmed broth. Immediately, 100 µL was removed and placed in 900 µL SM buffer on ice for infective centre analysis. Every 3 min for 30 min two 100 µL samples were removed simultaneously and added to 900 µL SM buffer, either containing 50 µL chloroform at room temperature, for intra- and extra-cellular quantification, or on ice for extra-cellular quantification. The tubes on ice were plated during the sampling process and the tubes containing chloroform were plated after 30 min incubation post sampling, to allow bacterial cells to lyse. Samples from each time-point were plated in triplicate on double agar overlay plates and plaques counted following overnight incubation at 37°C.

2.11 Extraction of bacteriophage genomic DNA

Bacteriophage genomic DNA was extracted from the product of PEG precipitation Propagation and purification of bacteriophages (2.6). The method was adapted from Phage hunters (Anon, n.d.). Briefly, to 1 mL samples of bacteriophages, 12.5 µL of 1 M MgCl₂ was added and gently mixed. To remove exogenous DNA and RNA, DNase I and RNase A were added to a final concentration of 100 mg/mL. The preparations were incubated at 37°C for 2 h. The digestion was then halted with the addition of 0.5 M EDTA (concentration 20 mmol/L) after which Proteinase K (New England Biolabs, Hitchin, UK; 50 µg/mL in 10 mmol/L Tris pH 8 and 50 mmol/L EDTA) and 10 % SDS (0.5 % final concentration) was added prior to incubation at 56°C for 1 h. Subsequently, 500 µL of the samples were transferred to micro-centrifuge tubes and an equal volume of Phenol:Chloroform:Isoamyl Alcohol (25:24:1) (Sigma-Aldrich Ltd, Poole, UK) was added and thoroughly mixed by inversion. The phases were separated by centrifugation at 13,000 x *g* for 5 min and the top aqueous layer removed avoiding any white material at the interphase. This process was repeated until no white material was seen at the interphase, then the process was repeated once in a 1:1 mixture of equilibrated phenol:chloroform and then in chloroform alone. Bacteriophage DNA was then precipitated by the addition

of two volumes of 100 % ice cold ethanol with Sodium acetate at 0.3 M/L and stored at -20°C overnight. Samples were thawed on ice prior to centrifugation at 15,000 x g at 4°C for 30 min to pellet the DNA. The resulting pellets were washed twice with 70 % (v/v) ethanol by carefully running 500 µL through the pellet followed by centrifugation at 15,000 x g at 4°C for 10 min. Pellets were air dried in a laminar flow cabinet before being re-suspended in TE buffer and stored at -20°C.

2.11.1 Concentration and yield of DNA

Concentration and inferences about purity were achieved by ultraviolet spectroscopy using the Nanodrop 1000 (Thermo Scientific, Loughborough, UK). Upon thorough cleaning of the pedestals of the device with ultra-pure water and lint-free cloth, the machine was blanked with TE buffer prior to a reading. Measurements were carried out in triplicate and the average used to obtain the total yield of DNA;

$$\text{DNA yield } (\mu\text{g}) = \text{Sample concentration (average of 3 measurements)} \times \text{sample volume}$$

Significant absorbance at 270 nm indicated Phenol contamination and repeating chloroform extraction and re-precipitating was employed to remedy this. High concentration DNA samples were heated briefly at 55°C for 10 min to de-aggregate prior to measuring DNA quantity. The accuracy of this method is questionable as it is an indirect means of measuring DNA, it is susceptible to interference from contamination, this however can be controlled by scrutinising the trace that is produced.

2.12 Genome size estimation by pulsed field gel electrophoresis

In order to estimate the size of the bacteriophages' genomes, PFGE was employed following the method of Lingohr *et al.* (2009). Caesium chloride purified phages (2.6) whose titre was modified to approximately 5×10^{10} , were immobilised in 1.2 % (w/v) agarose plugs. The plugs were transferred to 15 mL centrifuge tubes and the immobilised phages lysed by treatment with Proteinase k (New England Biolabs, Hitchin, UK; 20 mg/mL in Phage Lysis Buffer; 50 mmol/L Tris, 50 mmol/L EDTA and 1

% w/v SDS) at 54°C for 2 h. Following lysis, plugs were washed in TE buffer warmed to 54°C, three times for 15 min. Slivers (*approx.* 2 mm) were cut from the plugs and loaded onto a 1 % (w/v) agarose gel made with 0.5 X TBE buffer (Sigma-Aldrich Ltd, Poole, UK). Care was taken to ensure the slivers contacted the front and bottom of the wells. Low range PFGE ladder (New England Biolabs, Hitchin, UK) was used as a size standard and all wells were sealed with the same agarose from which the gel was made. Gels were run in 0.5 X TBE buffer at 6 V/cm for 15 h at 14°C with pulses of 2.2 to 54.2 s using a CHEF-DR II electrophoresis system (BioRad, Hemel Hempstead, UK). DNA was stained with ethidium bromide (1 µg/mL) for 1 h followed by de-staining with deionised H₂O for 30 min. Bands were visualised under UV light (FluorChem Q, ProteinSimple, California USA) and analysed with GelAnalyzer 2010a.

2.13 Restriction digest of genomic DNA

Bacteriophage DNA (2.11) was digested with 10 U of restriction endonuclease; *Bam*HI, *Eco*RV, *Hind*III, *Nde*I, *Not*I HF, *Sma*I and *Xba*I for 1 h at 37°C, with the exception of *Sma*I which was incubated at 25°C, following the manufacture's recommendations (New England Biolabs, Hitchin, UK). Reactions were ceased by heat inactivation, 65°C for 20 min prior to being loaded onto a 0.8 % (w/v) agarose gel, supplemented with 0.5 µg/mL EtBr. Fragments were separated at 5 V/cm in TAE buffer (40 mmol/L Tris-HCL, 20 mmol/L sodium acetate and 50 mmol/L EDTA at pH7.2). To provide size standard a 2-log DNA ladder (New England Biolabs, Hitchin, UK) was run with the samples. Bands were visualized under UV light (FluorChem Q, ProteinSimple, California USA).

2.14 Genomic termini elucidation

2.14.1 Cohesive ends

In order to determine if phage DNA possessed cohesive ends, 1 µg of DNA was digested with *Eco*RV (New England Biolabs, Hitchin, UK). Upon completion of digestion, the samples were heated to 80°C for 15 min in a heating block before being divided equally and cooled by one of two methods either, slowly, by leaving the tube in the heating block to cool to room temperature, or, by placing on wet ice to rapidly cool. The resulting fragments were then separated by gel electrophoresis,

5 V/cm in a 1 % (w/v) agarose gel made with TE buffer (10 mmol/L Tris: 1 mmol/L EDTA, pH 8) and stained with SYBR® safe (Thermo Scientific, Loughborough, UK).

2.14.2 Terminal specificity

To discern whether the genomic termini were fixed or circularly permuted, purified DNA (2.11) was subjected to a time limited digestion with exonuclease BAL-31 (1 U per µg (New England Biolabs, Hitchin, UK)). Reactions were carried out as per manufacturer's recommendations and samples withdrawn at 10, 20, 40 and 60 min. The DNA was immediately precipitated with EtOH and stored on ice. Samples were centrifuged, 13,000 x g for 10 min to recover the DNA which was re-suspended in TE buffer. Following resuspension, the DNA was subject to complete digestion by *EcoRV* before being run on a 1 % agarose gel containing SYBR® safe (Thermo Scientific, Loughborough, UK) made with TAE buffer at 5 V/cm. The 2-log ladder was used as a size standard (New England Biolabs, Hitchin, UK) and gels were visualised under UV light (FluorChem Q, ProteinSimple, California USA).

2.15 Genome sequencing and annotation

Bacteriophages DNA were extracted (2.11) and assessed (2.11.1) to determine yield and purity. Samples were then sent to The Genome Analysis Centre (TGAC, Norwich, UK) for sequencing, utilising p5-c3 chemistry in the PAC Bio RS II sequencer. Severn gaps in the vB_PmiS_NSM6 assembly were closed by targeted Sanger sequencing using the Applied Biosystems 3730 DNA Analyser (Thermo Fisher Scientific, Massachusetts, USA) externally, by the Genomics and Proteomics Facility, University of Birmingham (Birmingham, UK). Primers for Sanger sequencing were designed using New England Biolabs TM calculator (<http://tmcalculator.neb.com/#/>) and supplied by Eurofins MWG Synthesis GmbH (Ebersberg, Germany). UGENE (Unipro, Russia) (Okonechnikov *et al.*, 2012) was then employed to trim, filter and align the Sanger reads. Gaps in Phage vB_PmiP_#3 sequence were closed by creating a hybrid assembly. Purified genomic DNA was re-sequenced externally by the Genomic Services and Development unit at Public Health England by Illumina HiSeq paired-end sequencing. SPAdes (Bankevich *et al.*, 2012) was then used to create the hybrid assembly with the following assembly parameters: k:[27, 31, 33, 42, 53, 63, 73], repeat resolution enabled, mismatch

careful mode turned on, mismatch corrector used and coverage cutoff turned off. Consensus sequences were then opened upstream of the small terminase subunit in accordance with convention. Artemis (Rutherford *et al.*, 2000) was used to visualise the sequence features.

Protein coding regions were identified using Genemark.hmm for viruses, phages and plasmids (Besemer and Borodovsky, 1999) and Prodigal (Prokaryotic Dynamic Programming Gene-finding Algorithm) (Hyatt *et al.*, 2010). Each predicted open reading frame (ORF) was then scrutinised for the presence of an initiation codon with the association of a credible ribosome-binding site (RBS). Size, location and proximity to other ORFs were taken into consideration when assessing predictions. Translated sequences from the predicted ORFs were submitted to BLASTP to look for homology within the extant database and for the presence of conserved domains. These data, combined with results from querying the ORFs with HHpred (Söding, Biegert and Lupas, 2005), enabled the prediction of the function of gene products. Isoelectric point and molecular weight for each putative ORF were predicted with the ExPASy tool: Compute pI/MW (Gasteiger *et al.*, 2005). Regions, 200 bp up-stream from all ORFs were probed using MEME (Bailey and Elkan, 1994) to look for putative promoter sequences and intragenic motifs. ARNold (Lesnik *et al.*, 2001), TranstermHP (Kingsford, Ayanbule and Salzberg, 2007) and WebGESTer (Mitra *et al.*, 2011) were used to look for putative rho-independent terminators. The proximity, presence of poly U tails and the secondary structure as predicted by M-fold (Zuker, 2003) were considered when assessing the predictions. If the stability of the secondary structure was greater than the cut-off, derived by the equation; $\Delta G_{cut-off} = (12/10.5) \times [-0.294 \times (GC\%) + 4.441]$ predictions were considered. Lipo-proteins, signal-peptides and transmembrane helices were predicted with LipoP (Rahman *et al.*, 2008), SignalP (Petersen *et al.*, 2011) and TMHMM 2.0 (Krogh *et al.*, 2001) respectively. Finally, the presence of tRNAs was assessed with tRNAScan-SE (Schattner, Brooks and Lowe, 2005).

2.16 Structural proteins

2.16.1 Bradford assay

Utilising bovine serum albumen (BSA), a series of protein standards were produced (2,000 µg/mL – 125 µg/mL). Absorbance at 595nm was acquired for the standards and phage samples in triplicate employing a microplate reader (Genios Pro, Tecan, Männedorf, Switzerland). The data was plotted to produce a standard curve for which the linear regression line was calculated. Re-arranging the equation of the linear regression enabled concentration to be calculated from absorbance readings from phage samples (Bradford, 1976).

2.16.2 SDS-PAGE

SDS-PAGE is a means of separating proteins electrophoretically through a discontinuous polyacrylamide gel. This method allows the estimation of relative molecular mass. Proteins must be denatured with sodium dodecyl sulphate so that their intrinsic charges are masked and therefore separate based on mass alone.

In order to analyse the proteins within CsCl purified phage preparations, proteins were denatured and reduced by the addition of NuPAGE® LDS sample buffer and reducing agent dithiothreitol (DTT) following the manufacturer's recommendations (Thermo Scientific, Loughborough, UK). Samples were heated for 10 min at 70°C, allowed to cool, and loaded onto the pre cast NuPAGE® bis-tris mini gel immediately. MES SDS running buffer was used, to the upper chamber of the mini cell apparatus, 0.5 mL antioxidant was added to keep the samples reduced. Gels were run for 35 min at 200 V with Novex® sharp unstained protein standard marker (Thermo Scientific, Loughborough, UK). Gels were washed three times for 15 min in deionised water prior to staining with SimplyBlue™ safeStain (Thermo Scientific, Loughborough, UK) for 1 h with gentle agitation. Gels were then washed with deionised water for 1 h before visualisation (FluorChem Q, ProteinSimple, California USA).

2.17 Adherence of bacteriophages to catheter surfaces

Following the method of Curtin and Donlan (Curtin and Donlan, 2006; Carson, Gorman and Gilmore, 2010; Fu *et al.*, 2010; Lehman and Donlan, 2015) phages were

immobilised on to hydrogel coated catheters, 14 ch (lubri-sil™, Bard, Crawley, UK) by incubation with high titre liquid preparations for 2 h at room temperature or for 1 h at 37°C for whole catheter and catheter section experiments, respectively. For whole catheter experiments, catheter syringes were used to supply 6 mL of phage suspension to the inverted catheter whose tip was contained so that it could be immersed, allowing the phages to contact the exterior balloon as well as the interior surfaces.

2.18 Assessment of removal of viable adherent organisms from catheters

Catheter sections 1 cm in length were exposed to 10 mL of approx. 5×10^3 CFU/mL of the three host strains of bacteria for 24 h, shaking 150 rpm at 37°C. Catheter sections were removed from the culture and gently rinsed in phosphate-buffered saline (PBS) to remove planktonic and loosely adhered cells. To remove adhered cells, the method outlined by Curtin and Donlan (2006) was followed with some modifications. Briefly, sections were transferred to universal containers containing 10 mL PBS and subjected to vortex mixing for 30 s, followed by sonication for 10 min. Sections were vortexed for a further 30 s, sonicated for 5 min and finally vortexed for 30 s before a 1 mL aliquot was removed and analysed for viable cells by completing a 10-fold dilution series and plating as per method 2.2.2. The catheter sections were rinsed gently with PBS and transferred to a fresh tube containing 10 mL PBS and subjected to the same sonicating and vortexing procedure as before. A total of 4 rounds of the removal process were completed to test its efficacy.

2.19 Sectioned-catheter suspension tests

Hydrogel coated catheters, 14 ch (lubri-sil™, Bard, Crawley, UK) were exposed to phage suspensions containing 10^3 , 10^6 and 10^9 PFU/mL following method 2.17. The catheter sections in triplicate were added to 10 mL of approx. 5×10^3 CFU/mL of their respective host strain and incubated at 37°C for 24 h with 150 rpm shaking. Following incubation, catheter sections were analysed by removing adherent organisms and enumerated by carrying out 2 rounds of the sonicating and vortexing procedure outlined in 2.18.

2.20 *In vitro* bladder model experiment

A modified version of the model described by Stickler *et al.* (1999) was developed for *in vitro* assessment of bacteriophages ability to prevent the encrustation and blockage of urinary catheters, see

Figure 12. The model consisted of a jacketed glass chamber which was maintained at 37°C by a re-circulating water-bath (ED, JULABO GmbH, Seelbach, Germany). Artificial Urine (AU) was prepared consisting of sodium disulphate (2.3g/litre), magnesium chloride (hexahydrate) (0.65 g/litre), sodium chloride (4.6 g/litre), trisodium citrate (0.65 g/litre), sodium oxalate (0.02 g/litre), potassium dihydrogen orthophosphate (2.8 g/litre), potassium chloride (1.6 g/litre), ammonium chloride (1 g/litre), calcium chloride dihydrate (0.65 g/litre), urea (25 g/litre), gelatine (5 g/litre), the pH was then adjusted to 6.1 using sodium hydroxide. The preparation was then filter sterilised with a 0.2 µm capsule filter (Sartorius Sartobran, Göttingen, Germany). Sterilised TSB (1 g/litre) was added to the urine prior to the commencement of the experiment. AU was supplied to models via a peristaltic pump (323S, Watson-Marlow, Falmouth, UK) with two pumpheads (314MC) at 0.5 mL/min. AU was contained in a sterile glass vessel with an outlet at the bottom. The top was vented with a Millex® (Millipore Ltd, Watford, UK) air filter to maintain the sterility of the vessel and prevent pressure locks. Bladder models were sterilised by autoclaving (121°C, 15 min) and transferred to a laminar flow cabinet. A catheter was inserted into the bottom of the glass chamber through the attached length of silicone tubing, which simulates the urethra and assists in preventing contamination of the model. The catheter's retention balloon was then inflated with the supplied syringe containing 10 mL of sterile water. The taper of the model and the tension applied to the catheter seal the "bladder" chamber preventing leaks. A bed bag (Bard, Crawley, UK) with a 2 L capacity was attached to the catheter to collect run-off and close the sterile drainage system. Six models were set up and run simultaneously. Prior to the commencement of testing, the re-circulating water-bath was operated to ensure experimental temperature was reached. Bacterial inoculum was prepared from overnight cultures in AU and adjusted to 5×10^5 CFU/ml before 10 mL was added directly to the 'bladder' of the model with a sample being plated (2.2.1) to confirm viable numbers. The supply of AU

commenced immediately and samples for zero time point analysis collected from the drainage bag. All successive sampling was achieved by dis-connecting the catheter from the drainage bag and collecting the run-off directly from the catheter's funnel.

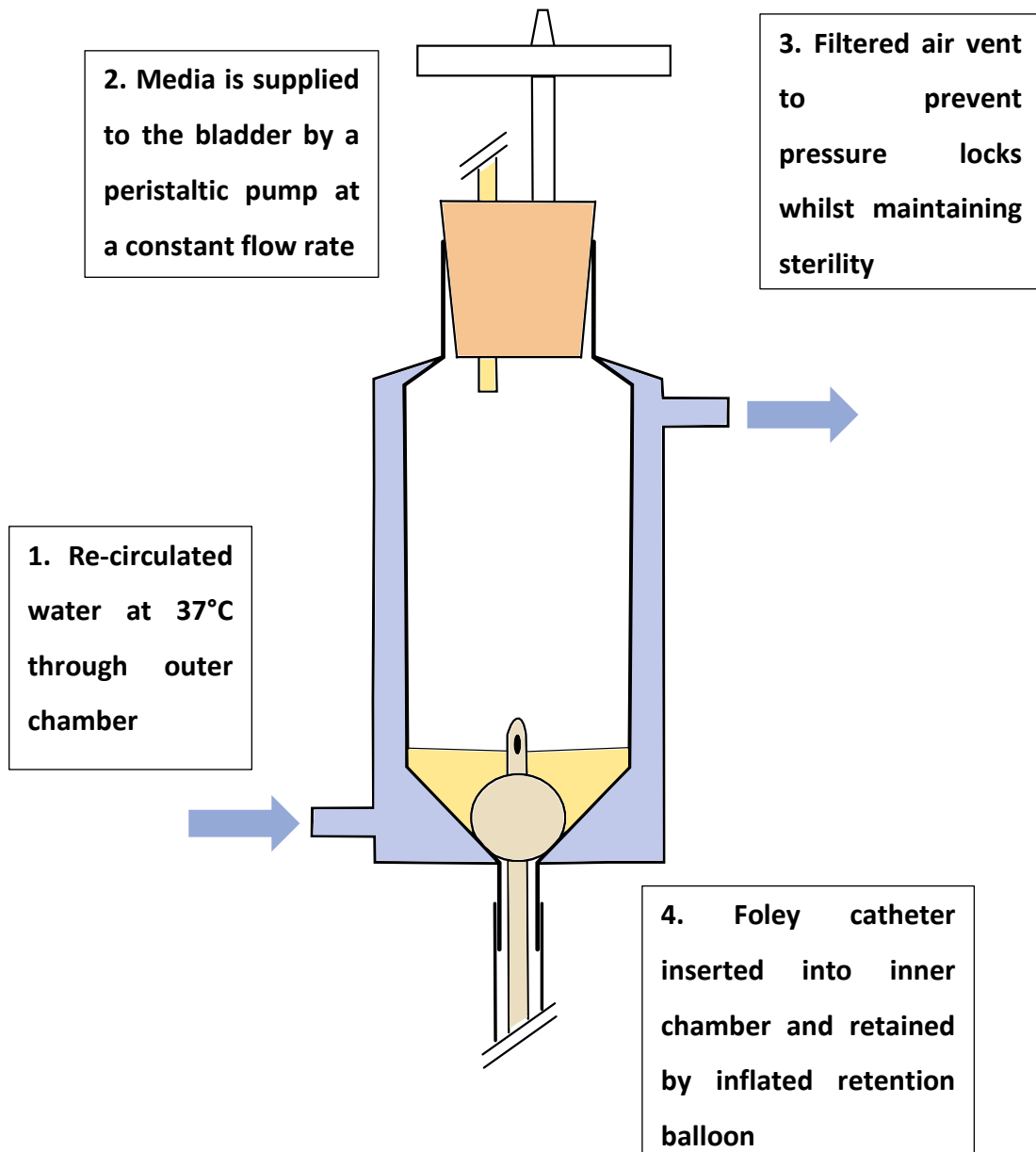


Figure 12. A diagrammatic representation of the *in vitro* bladder model. 1. The jacketed vessel is maintained at 37°C by a re-circulating water bath. 2. Media is supplied to the bladder at a constant flow rate; controlled by a peristaltic pump. 3. The model is vented to allow pressure equalisation, the vent is filtered to prevent contamination. 4. The catheter is inserted into the inner chamber and retained with the inflation of the balloon.

2.21 24 h *in vitro* bladder model experiment

Hydrogel catheters were prepared (2.17) with phage preparations numbering approx. 5×10^{10} PFU. Control catheters were incubated with SM buffer for 2 h at room temperature. Models were set up as 2.20 and run for 24 h. Samples, approx. 5 mL, were collected at 0, 2, 4, 6, and 24 h and assessed for viable bacterial numbers (2.2.1), phages present (2.4) and pH (HI 110, Hanna Instruments Ltd, Leighton Buzzard, UK). Upon completion of the run, catheters were carefully removed from the models and 1 cm sections cut, as shown in Figure 13, before being sliced longitudinally to expose internal surfaces. The sections were assessed for adhered cells as per 2.18 with two repeats of the sonicating and vortexing process. Testing was carried out in triplicate.

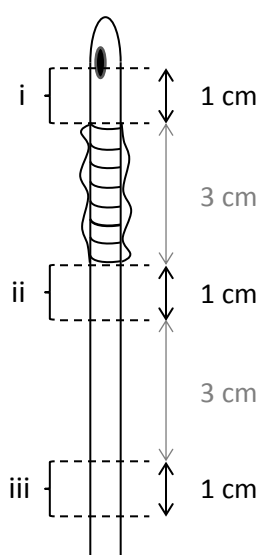


Figure 13. Diagram depicting the sections of Foley catheter excised and examined following the 24 h experiment in the *in vitro* bladder model system.

2.22 Assessment of time to catheter blockage

Hydrogel catheters were prepared (2.17) with phage preparations numbering approx. 5×10^{10} PFU. Control catheters were incubated with SM buffer for 2 h at room temperature. Models were set up as 2.20 and run until the formation of crystalline biofilm occluded the flow of AU. Samples were collected at 24 h intervals and assessed for viable bacterial numbers (2.2.1), phages present (2.4) and pH. Upon blockage the residual volume of AU in the drainage bag was measured and used to calculate the time at which blockage occurred. Models were run in triplicate.

2.23 Scanning electron microscopy of catheter sections

Catheters and models were set up and run (2.21) with assessment of the phage preparation used on the catheters and the bacterial inoculum. Upon completion of the 24 h experiment, catheters were removed from the models and sectioned as in Figure 14, with sections i, iii and iv being sliced longitudinally. Catheter sections were then gently rinsed with PBS, 5 mL for 5 min before fixation in 4 % (v/v) glutaraldehyde (Fisher BioReagents®, Loughborough, UK) in 0.1 M Sorenson's phosphate buffer (0.2 M; 19 mL of 200 mmol/L $\text{NaH}_2\text{PO}_4 \cdot 2\text{H}_2\text{O}$, 81 mL of 200 mmol/L Na_2HPO_4 , pH 7.4) for 24 h at 4°C. Sections were washed three times in 0.1 M Sorenson's phosphate buffer for 1 h at room temperature before dehydration through a series of ethanol solutions (20, 30, 50, 70, 80, 90, 100, 100 and 100 % (w/v) for 5 min). Sections were then air-dried before mounting on aluminium stubs with self-adhesive carbon discs (TAAB Laboratory Equipment Ltd, Reading, UK). Sections were gold sputter coated (SC500A, EMScope Laboratories Ltd, Ashford, UK) and viewed with Philips XL30 microscope at 20 KV using the BSE detector at 0.4 Torr.

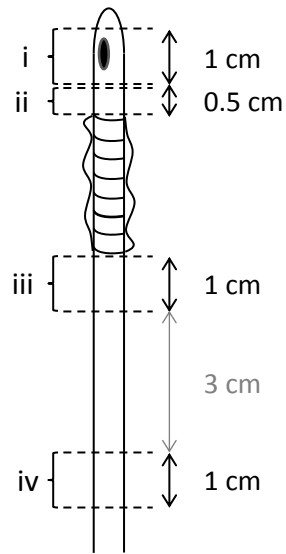


Figure 14. Diagram depicting the sections i to iv of Foley catheter excised and examined by SEM following 24 h exposure to bacteria in the *in vitro* bladder model system.

Chapter 3 Characterisation of the isolated Bacteriophages

3.1 Introduction

In order to investigate the ability of bacteriophages to prevent Catheter Associated Urinary Tract Infections (CAUTI) it was first necessary to isolate distinct bacteriophages against clinically relevant isolates of *P. mirabilis*. Bacteriophages are ubiquitous in nature and their numbers are estimated at 10^{31} (Bergh *et al.*, 1989). Whilst aquatic environments, including their sediments, are where phages are most abundant (Whitman, Coleman and Wiebe, 1998) considerable numbers exist terrestrially in diverse environments. As bacteriophages are obligate parasites, their distribution is likely to be based on that of their hosts. Humans offer unique niches for bacteria where commensalism, as well as mutualism, occurs. The most densely populated area in humans is the gut (Quigley, 2013). Phages infecting gut bacteria will be released from the gut either as free phages, or as prophages, by defaecation. The waste is then processed by the sewage system making sewage a good source for phages that infect enteric bacteria. *Proteus* species are part of the normal flora of the gut, therefore, sewage should potentially be a good source of *Proteus*-infecting phages.

Any phages intended for therapeutic use must be fully characterised to provide information to select the most appropriate phages for the task, and to ensure that they will not introduce any benefit to the bacteria they infect. Bacteriophages have been shown to be agents of horizontal gene transfer (Boyd and Brüssow, 2002). Phage lysogenic conversion can convert a non-virulent bacterium into a virulent one. This selective advantage will result in clonal expansion (Ikebe *et al.*, 2002). This also imparts an advantage upon the lysogen increasing its fitness in a mutually beneficial manner. Broadly speaking, there are two types of transduction that lysogenic bacteriophages participate in, specialised and generalised. Specialised transduction is the packaging of small segments of bacterial DNA along with the phage DNA. These segments can contain genes that are then transferred upon a subsequent infection of another bacterial host. Examples of traits acquired through specialised transduction are the acquisition of bacterial toxins, such as the

Diphtheria, Shiga and Cholera toxins of *Corynebacterium diphtheriae*, *Escherichia coli* and *Vibrio cholera*, respectively (Freeman, 1951; O'Brien *et al.*, 1984; Waldor and Mekalanos, 1996). Generalised transduction occurs when, instead of packaging phage DNA, a headfull of host DNA is packaged. This has been shown to occur in phages P22 and Mu (Canchaya *et al.* 2003). The bacterial DNA is then incorporated into the bacterial chromosome if regions of homology are shared in a similar manner to bacterial recombination. Alternatively, if it was a plasmid in the initial host, it will re-circularise and become a plasmid again or finally, the DNA is not incorporated and is used as spare parts.

Understanding the growth characteristics also enables prediction and control of experimental outcomes; a broad host range and a rapidly lytic phage with high burst size would be an ideal candidate for phage therapy.

This chapter details the results from problematic initial isolations, their characterisation, the re-isolation and the microbiological characterisation, including bioinformatic analysis of the subsequently isolated phages.

3.2 Results

3.2.1 Isolating Bacteriophages

Initially, only isolate NSM 6 was used for phage isolations. The presence of *Proteus* species was crudely confirmed by inoculating an agar plate with a loop full of raw sewage. Swarming behaviour was then used as confirmation of *Proteus* species presence. Following the method of Van Twest and Kropinski (2009), raw influent sewage, activated sewage sludge and sea water were utilised as source material. Multiple plaque types were obtained, often from the same enrichment.

Table 3. Bacteriophages isolated in the first phase of enrichments

| Phage | Date isolated | Source |
|-----------|---------------|---------------------------------------|
| vB_Pmi?_1 | 12/10/10 | Saltford raw influent |
| vB_Pmi?_2 | 12/10/10 | Saltford raw influent |
| vB_PmiS_3 | 13/01/11 | Cam Valley activated sludge |
| vB_PmiS_4 | 13/01/11 | Cam Valley activated sludge |
| vB_PmiS_5 | 13/01/11 | Cam Valley activated sludge |
| vB_PmiS_6 | 22/02/11 | Avon Mouth activated sludge |
| vB_PmiS_7 | 24/03/11 | Sea water –Woolacombe, North Devon |

Phages vB_Pmi?_1 and vB_Pmi?_2 were not taken forward following experimental analysis for lytic or lysogenic behaviour (data not shown) as they appeared to follow temperate life cycles. The remaining isolated phages were propagated and purified prior to electron microscopy and molecular analysis of their extracted DNA.

Figure 15 and Figure 16 detail the restriction profiles obtained utilising *EcoRV*, *XbaI* and *HindIII*. The isolated phages displayed the same profiles for the restriction endonucleases used. This in conjunction with the electron microscopy observations (not shown) suggest the phages are in all likelihood the same.

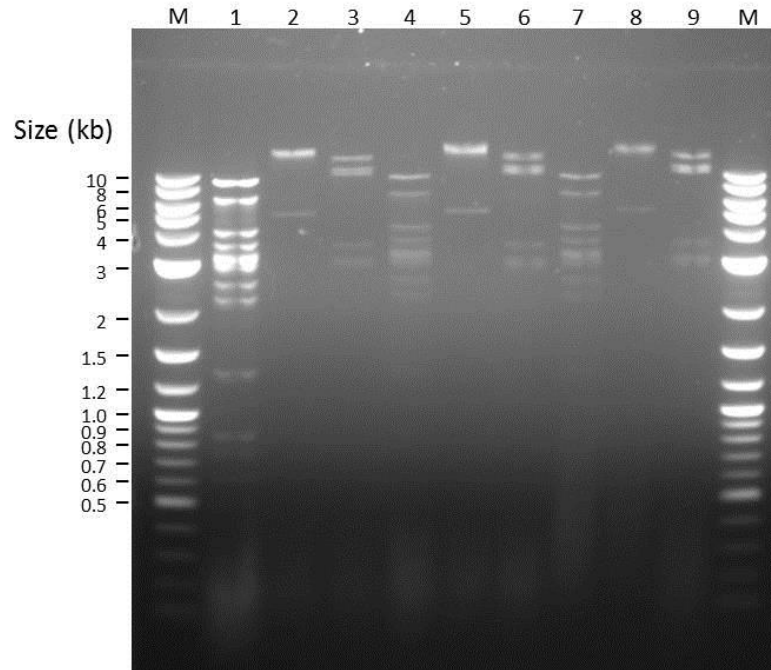


Figure 15. Restriction endonuclease digest of bacteriophages vB_rmiS_3, vB_PmiS_5, vB_PmiS_7. Lane M, 2-Log ladder molecular size marker; Lane 1, vB_PmiS_3 *EcoRV*; Lane 2, vB_PmiS_3 *XbaI*; Lane3, vB_PmiS_3 *HindIII*; Lane 4, vB_PmiS_5 *EcoRV*; Lane 5, vB_PmiS_5 *XbaI*; Lane6, vB_PmiS_5 *HindIII*; Lane 7, vB_PmiS_7 *EcoRV*; Lane 8, vB_PmiS_7 *XbaI*; Lane9, vB_PmiS_7 *HindIII*.

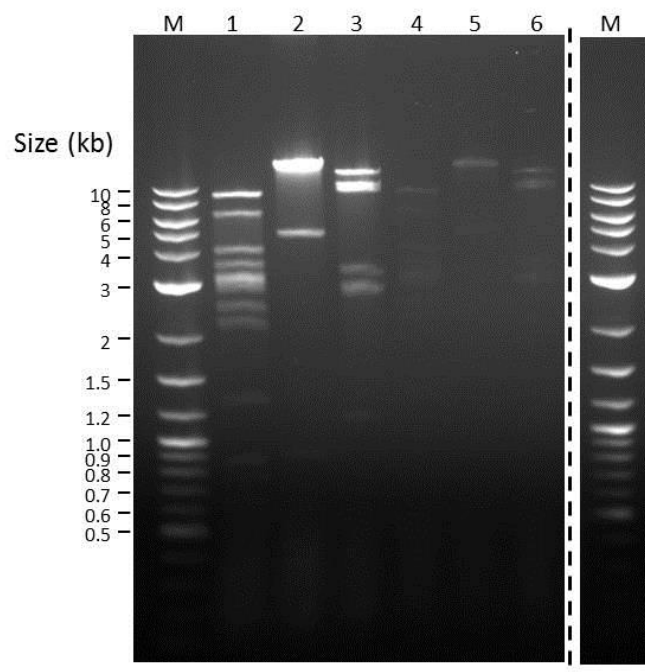


Figure 16. Restriction endonuclease digest of bacteriophages vB_PmiS_4 and vB_PmiS_6. Lane M, 2-Log ladder molecular size marker; Lane 1, vB_PmiS_4 *EcoRV*; Lane 2, vB_PmiS_4 *XbaI*; Lane3, vB_PmiS_4 *HindIII*; Lane 4, vB_PmiS_6 *EcoRV*; Lane 5, vB_PmiS_6 *XbaI*; Lane6, vB_PmiS_6 *HindIII*.

Phage PFGE profiles on the whole genome (Figure 17) shows bands at the same position, approx. 46750 bp in length. This data further supports the assumption that the same phage has been isolated or induced on five separate occasions. It, therefore, became necessary to isolate more phages.

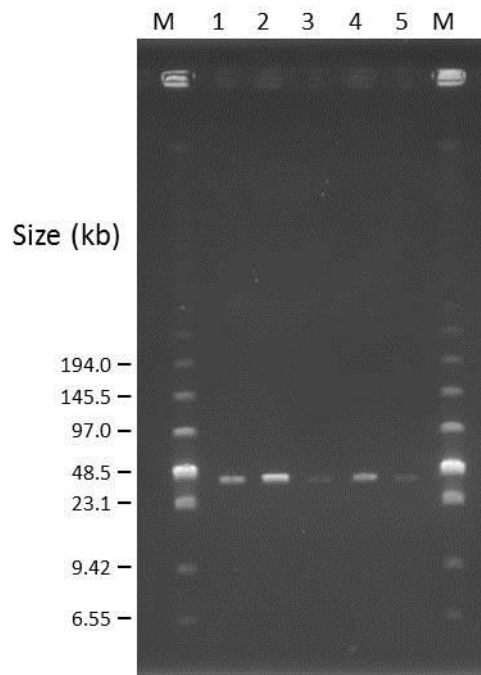


Figure 17. PFGE on whole DNA from the five isolated bacteriophages. Lane M, low range PFG marker; Lane 1, vB_PmiS_3; Lane 2, vB_PmiS_4; Lane 3, vB_PmiS_5; Lane 4, vB_PmiS_6; Lane 5, vB_PmiS_7.

Following a lengthy period of failed isolations, two more bacteriophages were isolated from sewage (Table 4). Instead of using one isolate of *P. mirabilis*, all isolates (42) were used. This approach yielded two phages that were isolated on different isolates, potentially increasing the likelihood of a broader host range. Unfortunately, selection of the most appropriate phages with the broadest host range and most potent lytic activity was not possible with so few phages isolated.

Table 4. Bacteriophages isolated from the second phase of enrichments.

| Phage | Date Isolated | Source |
|------------|---------------|----------------------------------|
| vB_PmiP_#3 | 04/05/13 | Raw sewage pooled from 4 STWs |
| vB_PmiM_D3 | 12/04/13 | Cam Valley activated sludge |

When plated, the isolated phages produced distinct plaques (Figure 18). vB_PmiS_NSM6 produced two morphologies of plaque, a large hazy plaque 6.0 mm (n=15) in diameter when given a longer adsorption than normal, but when adsorbed for 5 min, small turbid plaques were produced that measured 2.15 mm (n=15) (Figure 18, (A)). Phage vB_PmiP_#3 produces bull's eye plaques, often with some resistant micro-colonies in the centre. They were 4.02 mm (n=15) in diameter under the conditions tested (0.6 % top agar, 37°C). Interestingly the plaques had a halo around them (Figure 18, (B)) and this halo continued to expand upon further incubation of the plate at 37°C (Figure 18, (D)). Halos are the consequence of the diffusion and subsequent action of phage produced EPS degrading enzymes, being much smaller than phages, they can diffuse further through the bacterial lawn. The halo was tested for the presence of phages, but none were found, indicating that it is most likely due to an EPS degrading enzyme as opposed to a phage particle, either as an integral part of the virion or released during bacterial cell lysis (Adams and Park, 1956). Phage vB_PmiM_D3 produced relatively large bulls' eye plaques measuring 4.69 mm on average (Figure 18, (C)).

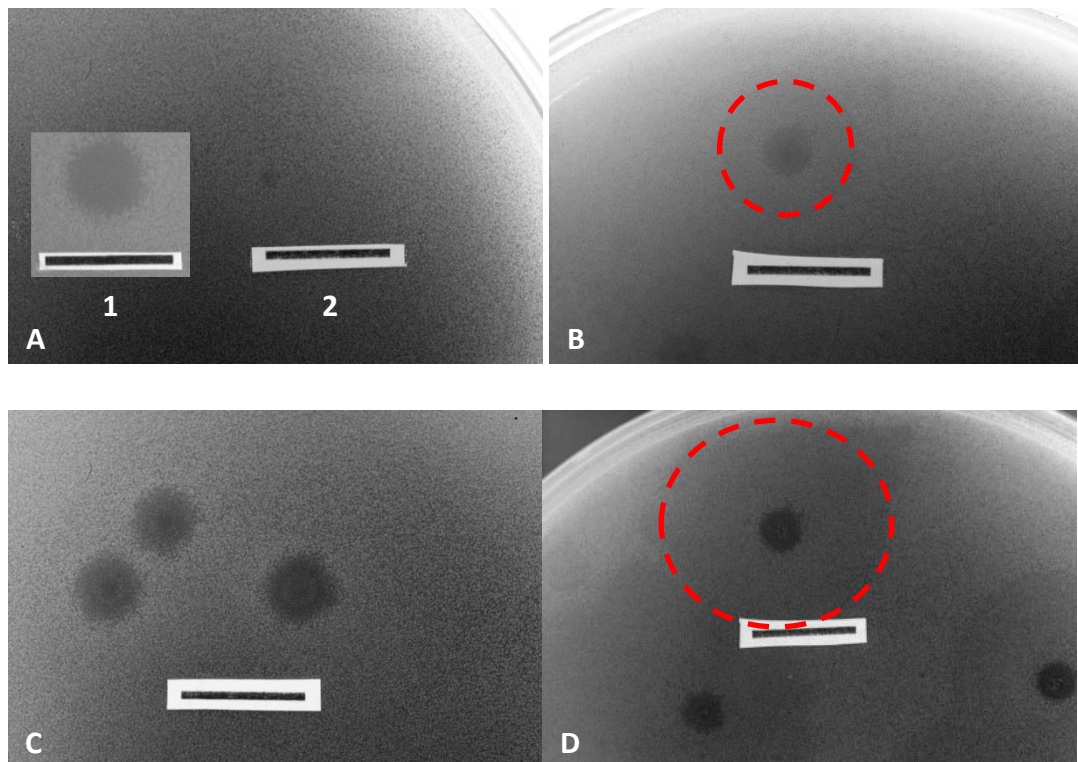


Figure 18. Photograph's of plaques formed by (A), vB_PmiS_NSM6, (B), vB_PmiP_#3, (C) vB_PmiM_D3, (D), vB_PmiP_#3. 0.6 % top agar, incubated at 37°C for 24 h (A),(B) and (C), and 48 h (D). Scale bar represents 10 mm, dashed red circles outline the observed halos.

3.2.2 Restriction analysis and genome size estimation of phages vB_PmiS_NSM6 and vB_PmiP_#3

To ensure the phages were in fact different from one another, restriction analysis and PFGE were carried out on extracted genomic DNA. Unfortunately, it was not possible to purify and extract DNA from phage vB_PmiM_D3. Upon centrifugation, necessary for purification, phage particles would aggregate and not re-dissolve despite many methods and attempts. Procedures were modified to only concentrate and purify with polyethylene glycol to avoid the need for centrifugation. Unfortunately, CsCl density gradients failed as phages did not band at densities near 1.5 g/ml, presumably due to the capsid being impermeable to Cs⁺ ions similar to that of Phage ES18 (Casjens and Gilcrease, 2009). Attempts were made to extract the DNA from vB_PmiM_D3 but it only yielded very low quantities that were insufficient to work with. Again, many attempts and modifications of the

method were trialed unsuccessfully so the decision was made to omit vB_PmiM_D3 from genetic analysis.

The restriction profiles (Figure 19 and Figure 20) are distinct for each phage tested; both phages appear to be resistant to *SmaI*. PFGE (Figure 21) show the genomes have different sizes of approx. 47537 bp and approx. 41900 bp for vB_rmiS_NSM6 and vB_PmiP_#3 respectively, as identified by GelAnalyzer 2010a (Lazar, 2010).

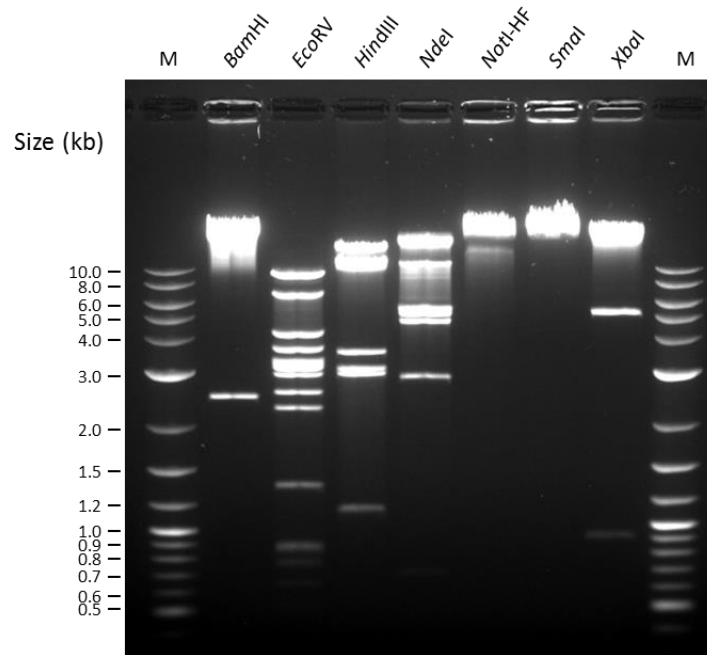


Figure 19. Restriction endonuclease digests of bacteriophage vB_PmiS_NSM6. Lane M, 2-Log ladder molecular size marker.

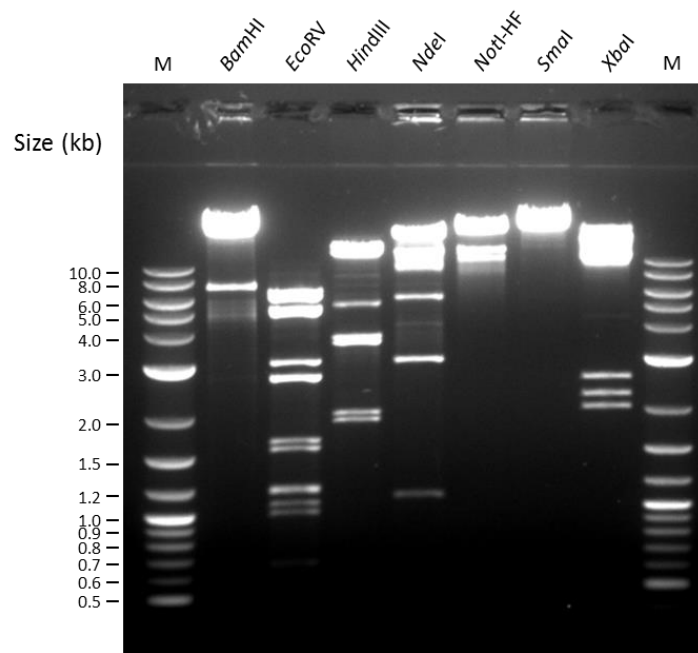


Figure 20. Restriction endonuclease digests of bacteriophage vB_PmiP_#3. Lane M, 2-Log ladder molecular size marker.

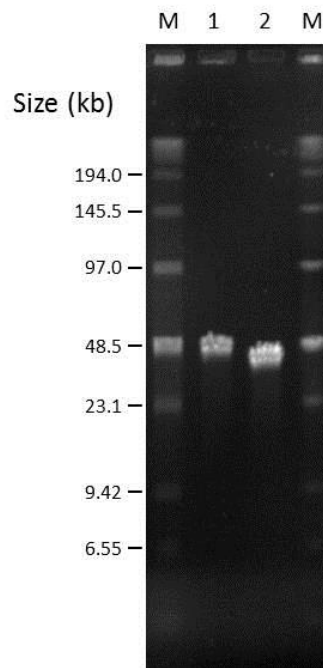


Figure 21. Pulsed field gel electrophoresis of bacteriophages extracted genomic DNA. Lane M, low range molecular size marker; Lane 1, vB_PmiS_NSM6; Lane 2, vB_PmiP_#3.

3.2.3 Transmission electron microscopy of the isolated phages

The virion morphology observed following transmission electron microscopy (Figure 22) revealed that phage vB_PmiS_NSM6 is a member of the *Siphoviridae* family. It has an icosahedral head measuring 64 nm between opposite apices (n=25) and a flexible non-contractile tail that is 165 nm in length and 9.6 nm in width which appears to have horizontal striations and also possesses terminal tail spikes. Phage vB_PmiP_#3 belongs to the *Podoviridae* family of dsDNA bacteriophages. Its head measures 57 nm and it has a short non contractile tail 16 nm in length and 10.6 nm (n=25) wide with terminal tail spikes. Phage vB_PmiM_D3 is a *Myoviridae* family member. It possesses a ridged contractile tail 64 nm in length and 10 nm in width. Its head is 33.5 nm in diameter (n=11).

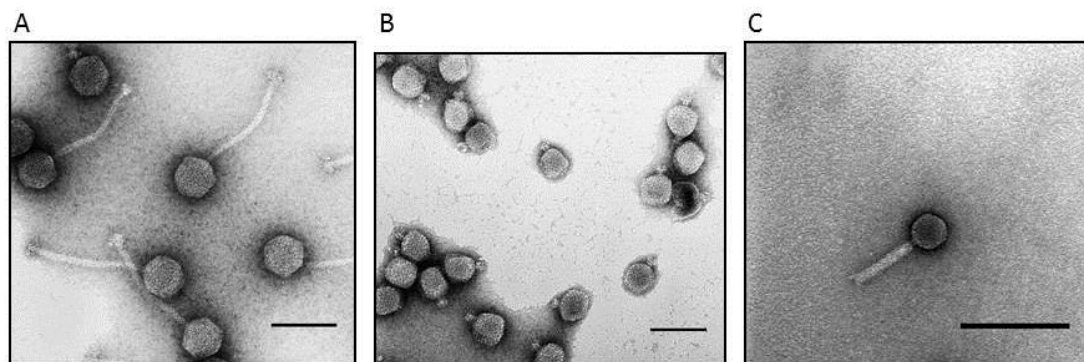


Figure 22. Transmission electron micrographs of A) vB_PmiS_NSM6, B) vB_PmiP_#3, C) vB_PmiM_D3 stained using 2 % uranyl acetate. Scale bars represent 100 nm.

3.2.4 Host range analysis and host library assessment

For host range analyses and bacteriophage isolations, a collection of clinical *P. mirabilis* isolates was required. To ensure no duplicates existed within the collection and to gain an insight into the relatedness and diversity of the group, pulsed field gel electrophoresis typing was employed.

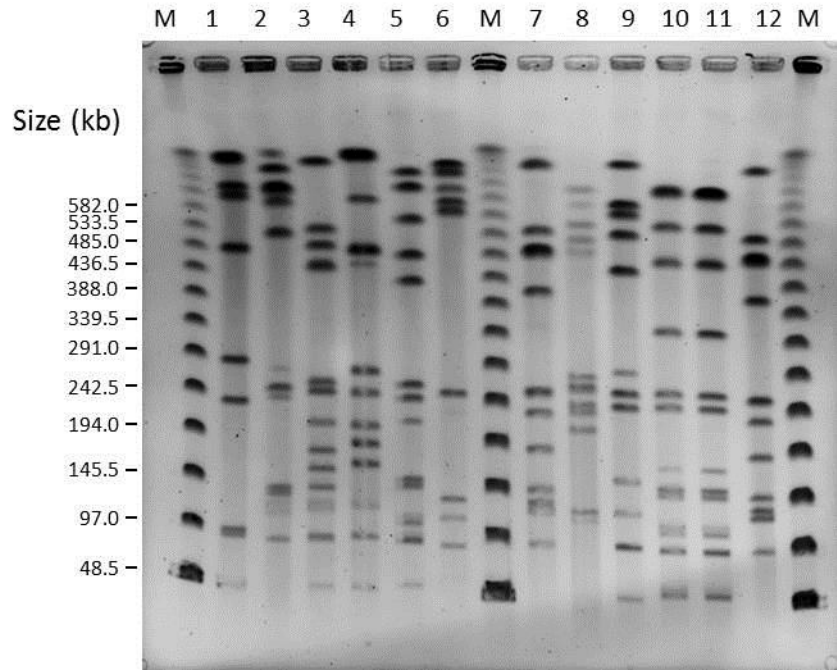


Figure 23. PFGE profiles of *P. mirabilis* isolates digested with *NotI*. Lane M, molecular size markers; lane 1, HI4320; lane 2, D18; lane 3, D23; lane 4, D24; lane 5, D25; lane 6, D28; lane 7, D32; lane 8, D33; lane 9, D35; lane 10, D36; lane 11, D37; lane 12, D41.

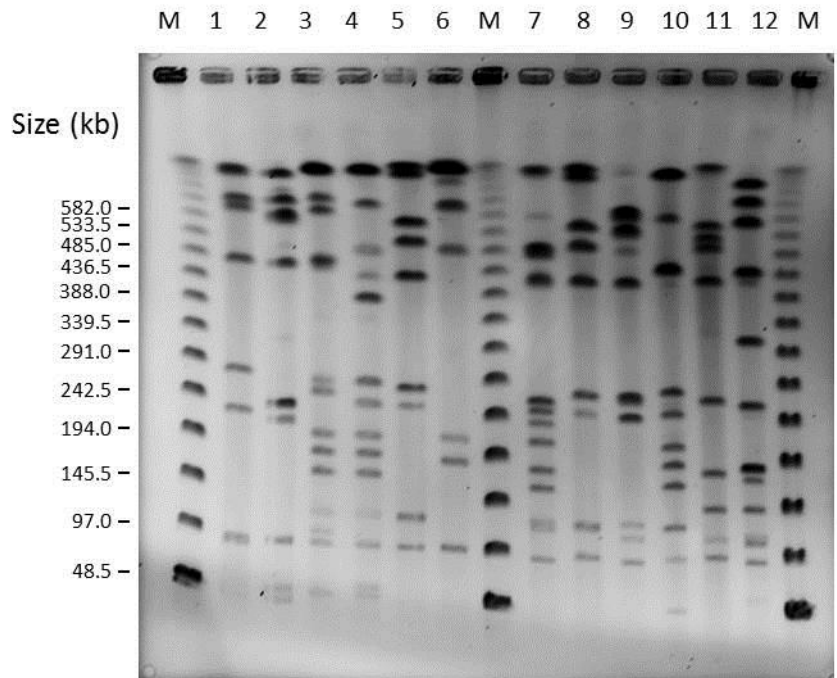


Figure 24. PFGE profiles of *P. mirabilis* isolates digested with *NotI*. Lane M, molecular size markers; lane 1, HI4320; lane 2, D1; lane 3, D2; lane 4, D3; lane 5, D4; lane 6, D5; lane 7, D7; lane 8, D12; lane 9, D14; lane 10, D17; lane 11, Releen 18; lane 12, 701880.

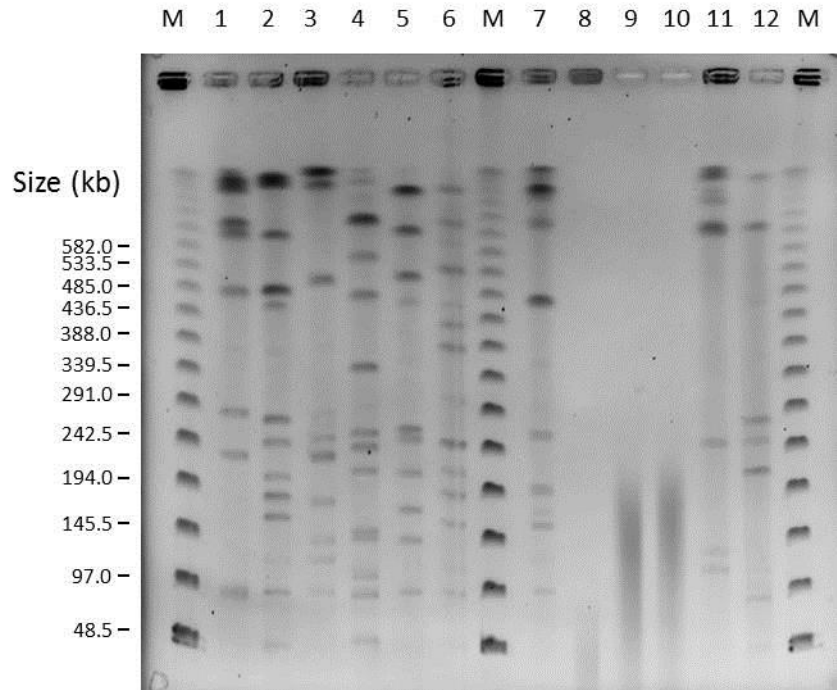


Figure 25. PFGE profiles of *P. mirabilis* isolates digested with *NotI*. Lane M, molecular size markers; lane 1, HI4320; lane 2, D13; lane 3, D15; lane 4, D19; lane 5, H24; lane 6, H25; lane 7, H26; lane 8, GS12; lane 9, GS13; lane 10, GS14; lane 11, #3; lane 12, #10.

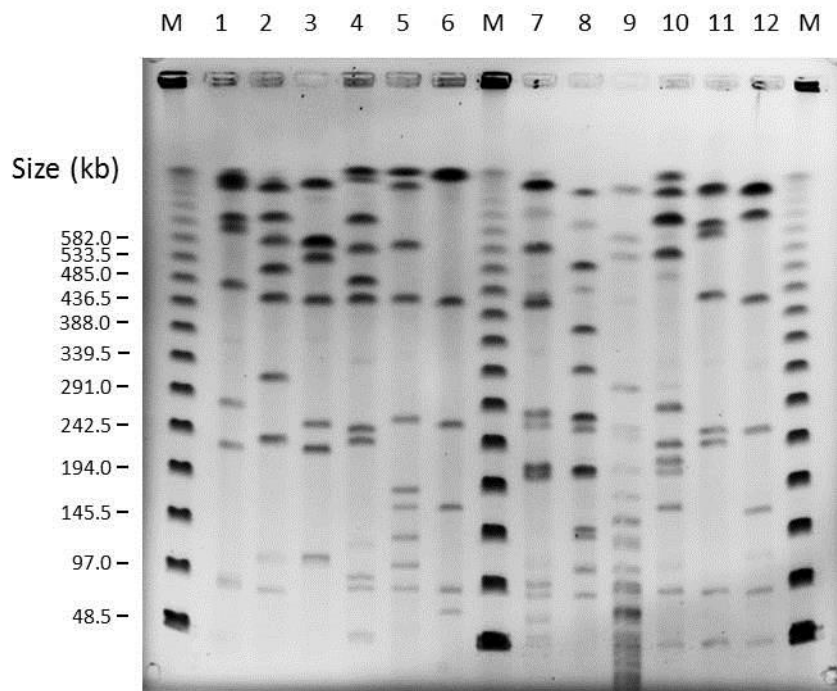


Figure 26. PFGE profiles of *P. mirabilis* isolates digested with *NotI*. Lane M, molecular size markers; lane 1, HI4320; lane 2, 45967; lane 3, 46126; lane 4, 46453; lane 5, 46500; lane 6, 46511; lane 7, 46546; lane 8, 46564; lane 9, 46670; lane 10, 46708; lane 11, 46736; lane 12, NSM 2.

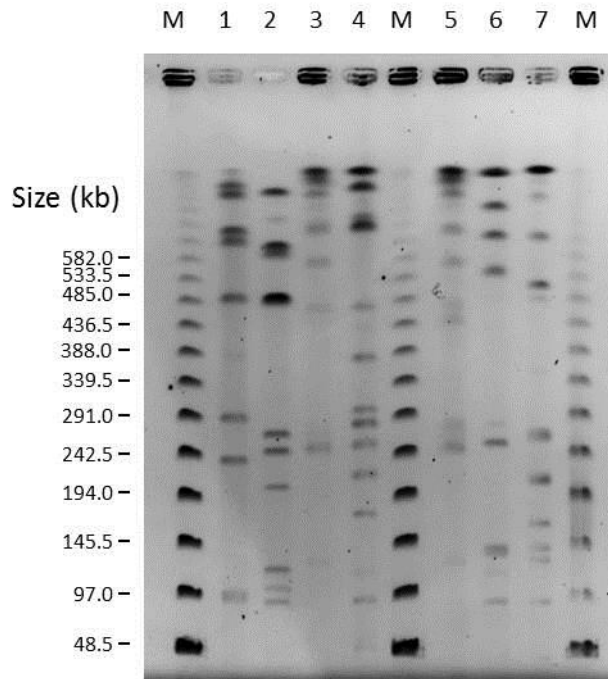


Figure 27. PFGE profiles of *P. mirabilis* isolates digested with *NotI*. Lane M, molecular size markers; lane 1, HI4320; lane 2, NSM 6; lane 3, NSM 25; lane 4, NSM 39; lane 5, NSM 42; lane 6, NSM 59; lane 7, NSM 60.

The restriction fragments generated from digestion with *NotI*-HF restriction endonuclease from each isolate obtained are shown in Figure 23, Figure 24, Figure 25, Figure 26, and Figure 27. Strain HI4320 was added to lane 1 on each gel to act as a control for the clustering parameters applied to the data, molecular size standards were used for band size determination and normalisation across gels. As is common with PFGE, some distortion is apparent at the edges of the gels. Analysis is not affected as it can easily be resolved with computational calibrations. The profiles on Figure 23, lanes 10 and 11, show the same number and size of bands. These isolates, D36 and D37, were from the same study indicating they are epidemiologically related so were designated genetically indistinguishable from one another. The isolates shown on Figure 25, lanes 8, 9 and 10 produced no distinguishable profiles, presumably due to degradation. This produced a smear of DNA that has run off the gel therefore no conclusions can be drawn.

UPGMA analysis (Figure 28) of the profiles using Dice percent coefficient of similarity (at 2 % band tolerance) resulted in 4 clusters being identified. Six pairs of profiles were genetically indistinguishable from each other (indicated with circles)

which resulted in a representative of that type being chosen for further work and the duplicate being removed from the library. The grouping of the 5 profiles of strain HI4320 from separate gels as 100 % similar gives confidence in the reproducibility of the technique across gels.

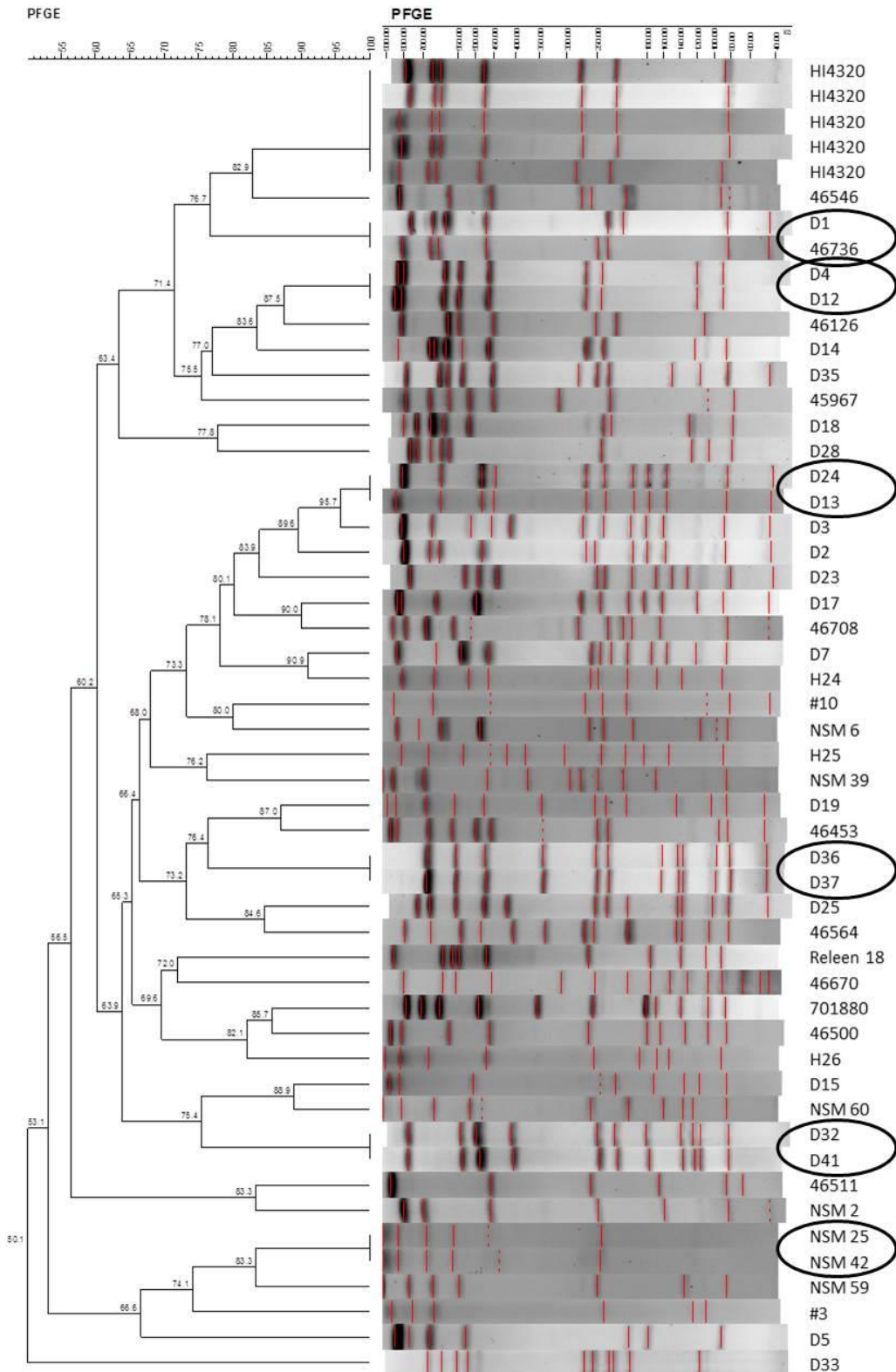


Figure 28. Dendrogram obtained using the Dice similarity coefficient (calculated with a band tolerance of 2 %) and UPGMA analysis (Applied Maths). PFGE profiles of *P. mirabilis* isolates utilising *NotI*. Isolate names are indicated to the right of the profiles.

The 42 isolates of *P. mirabilis* obtained were used for host range analysis. Spots of log fold dilutions of bacteriophage preparations were ranked for their ability to form plaques on lawns of the bacterial isolates. Table 5 details the results obtained. Phage vB_pmiS_NSM6 infected 9.5 % of the *P. mirabilis* isolates. Of the 4 it successfully infected, 3 isolates; NSM 6, D3 and, Releen 18 clustered together on the dendrogram produced from PFGE (Figure 28). NSM 59 was in a different cluster but the difference in profiles is only 3 bands indicating they are closely related (Tenover *et al.*, 1995). Phage vB-PmiP_#3 infected 4 isolates of the library (9.5 %). The most successful infection was in isolates that clustered differently. Phage vB_PmiM_D3 showed the broadest host range, infecting 8 isolates (19 %). Phages vB_PmiS_NSM6 and vB_PmiM_D3 showed good activity against each other's isolating strain enabling a two phage cocktail to be investigated. It is worth noting that isolate D3 and NSM 59 were susceptible to all the isolated phages indicating some common feature and, they would potentially make good isolating strains. No activity was observed in the 8 other Gram-negative bacterial species tested.

Table 5. Host range analysis. Plaque formation was scored visually where; +, complete clearing; +++, clearing throughout but with faintly hazy background; ++, substantial turbidity throughout the cleared zone; +, a few individual plaques; -, no clearing.

| Isolate | vB_rmiS_NSM6 | vB_PmiP_#3 | vB_PmiM_D3 |
|---------------------------------|--------------|------------|------------|
| <i>P. mirabilis</i> , #3 | - | ++++ Host | - |
| <i>P. mirabilis</i> , 701880 | - | - | ++ |
| <i>P. mirabilis</i> , D2 | - | - | +++ |
| <i>P. mirabilis</i> , D3 | +++ | + | ++++ Host |
| <i>P. mirabilis</i> , D13 | - | - | + |
| <i>P. mirabilis</i> , D17 | - | - | + |
| <i>P. mirabilis</i> , D18 | - | - | ++ |
| <i>P. mirabilis</i> , D28 | - | ++++ | - |
| <i>P. mirabilis</i> , NSM 6 | ++++ Host | - | ++++ |
| <i>P. mirabilis</i> , NSM 59 | + | + | ++++ |
| <i>P. mirabilis</i> , Releen 18 | + | - | - |
| <i>P. mirabilis</i> , #10 | - | - | - |
| <i>P. mirabilis</i> , 45967 | - | - | - |
| <i>P. mirabilis</i> , 46126 | - | - | - |
| <i>P. mirabilis</i> , 46453 | - | - | - |

| Isolate | vB_rmiS_NSM6 | vB_PmiP_#3 | vB_PmiM_D3 |
|--|--------------|------------|------------|
| <i>P. mirabilis</i> , 46500 | - | - | - |
| <i>P. mirabilis</i> , 46511 | - | - | - |
| <i>P. mirabilis</i> , 46546 | - | - | - |
| <i>P. mirabilis</i> , 46564 | - | - | - |
| <i>P. mirabilis</i> , 46708 | - | - | - |
| <i>P. mirabilis</i> , 46736 | - | - | - |
| <i>P. mirabilis</i> , D4 | - | - | - |
| <i>P. mirabilis</i> , D5 | - | - | - |
| <i>P. mirabilis</i> , D7 | - | - | - |
| <i>P. mirabilis</i> , D14 | - | - | - |
| <i>P. mirabilis</i> , D15 | - | - | - |
| <i>P. mirabilis</i> , D19 | - | - | - |
| <i>P. mirabilis</i> , D23 | - | - | - |
| <i>P. mirabilis</i> , D25 | - | - | - |
| <i>P. mirabilis</i> , D32 | - | - | - |
| <i>P. mirabilis</i> , D33 | - | - | - |
| <i>P. mirabilis</i> , D35 | - | - | - |
| <i>P. mirabilis</i> , D36 | - | - | - |
| <i>P. mirabilis</i> , GS12 | - | - | - |
| <i>P. mirabilis</i> , GS13 | - | - | - |
| <i>P. mirabilis</i> , GS14 | - | - | - |
| <i>P. mirabilis</i> , H24 | - | - | - |
| <i>P. mirabilis</i> , H25 | - | - | - |
| <i>P. mirabilis</i> , H26 | - | - | - |
| <i>P. mirabilis</i> , HI4320 | - | - | - |
| <i>P. mirabilis</i> , N88 | - | - | - |
| <i>P. mirabilis</i> , NSM 25 | - | - | - |
| <i>P. mirabilis</i> , NSM 39 | - | - | - |
| <i>P. mirabilis</i> , NSM 60 | - | - | - |
| <i>P. mirabilis</i> , NSM 2 | - | - | - |
| <i>E. faecalis</i> , NCIMB 775 | - | - | - |
| <i>K. pneumoniae</i> , cc242 | - | - | - |
| <i>S. marcescens</i> , cc12 | - | - | - |
| <i>S. aureus</i> , RN4220 | - | - | - |
| <i>P. aeruginosa</i> , ATCC 15442 | - | - | - |
| <i>S. enteritidis</i> , PT4 | - | - | - |
| <i>E. coli</i> , ATCC 15036 | - | - | - |
| <i>A. baumannii</i> , ATCC BAA-1710 | - | - | - |

3.2.5 Adsorption rate determination and one step growth

To determine the adsorption rate of the isolated bacteriophages free phage loss was measured as a function of time. Individual experiments were repeated three times under identical conditions. Phage vB_PmiS_NSM6 has an adsorption rate at 37°C of $6.21 \times 10^{-9} \text{ ml/min}^{-1}$ ($R^2 = 0.989$). Phage vB_PmiP_#3 and vB_PmiM_D3 have similar rates of $8.90 \times 10^{-9} \text{ ml/min}^{-1}$ ($R^2 = 0.977$) and $6.80 \times 10^{-9} \text{ ml/min}^{-1}$ ($R^2 = 0.986$), respectively (Figure 29).

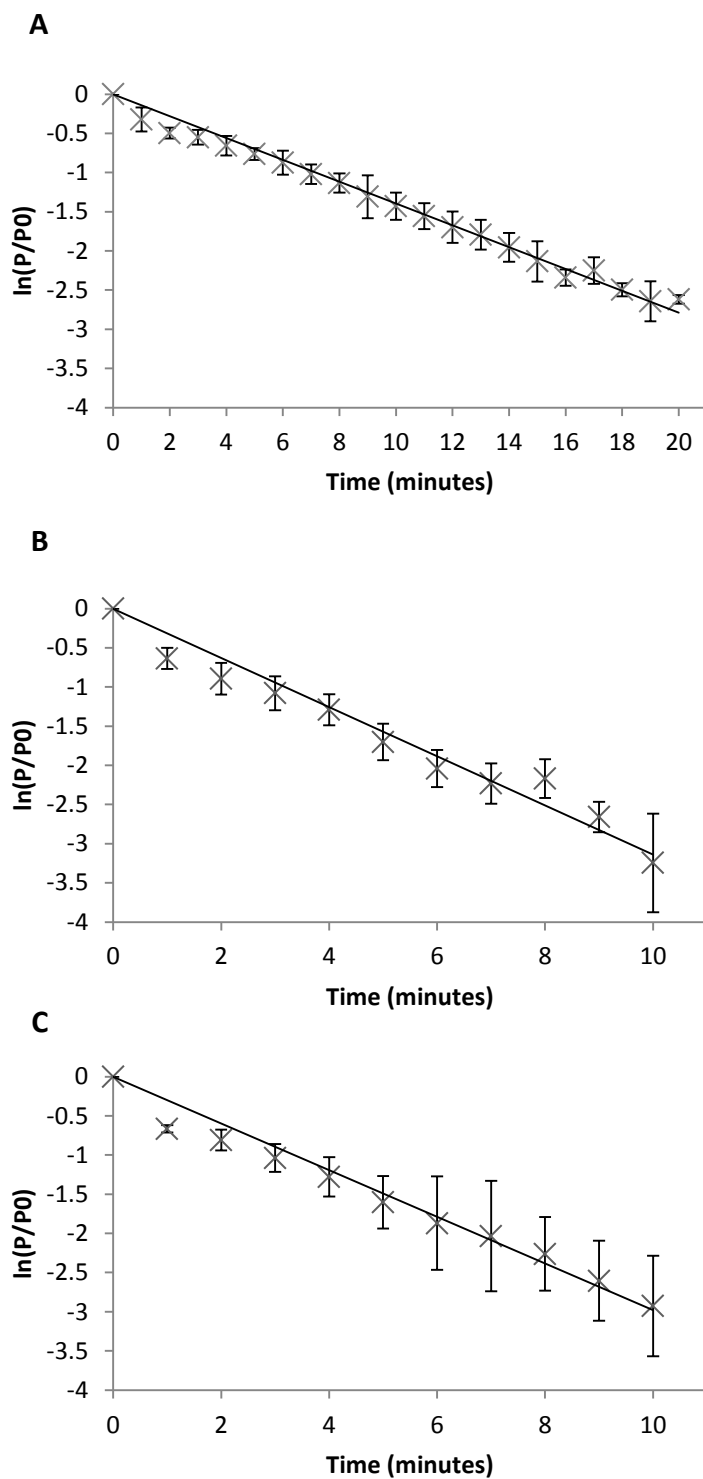


Figure 29. Adsorption rate constant for; A, vB_PmiS_NSM6; B, vB_PmiP_#3; C, vB_rmiM_D3. The results represent the natural log of the mean and standard deviation of three independent experiments.

One step growth analysis (Figure 30) showed that phage vB_PmiS_NSM6 has an eclipse period of 12.5 min and a latent period of 15 min. The rise period commenced after 12 min and host cell lysis completed after 35 min. The burst size was 250 progeny virions per infected cell. Phage vB_PmiP_#3 had an eclipse of 7.5 min and a latent period of 20 min. Its rise period began after 20 min and host cell lysis was complete after 32.5 min releasing 322 progeny virions per infected cell. Phage vB_PmiM_D3 had an eclipse period of 24.5 min with a latent period of 26 min. The rise period began after 27 min and lysis was complete after 55 min releasing 126 progeny virions per infected cell.

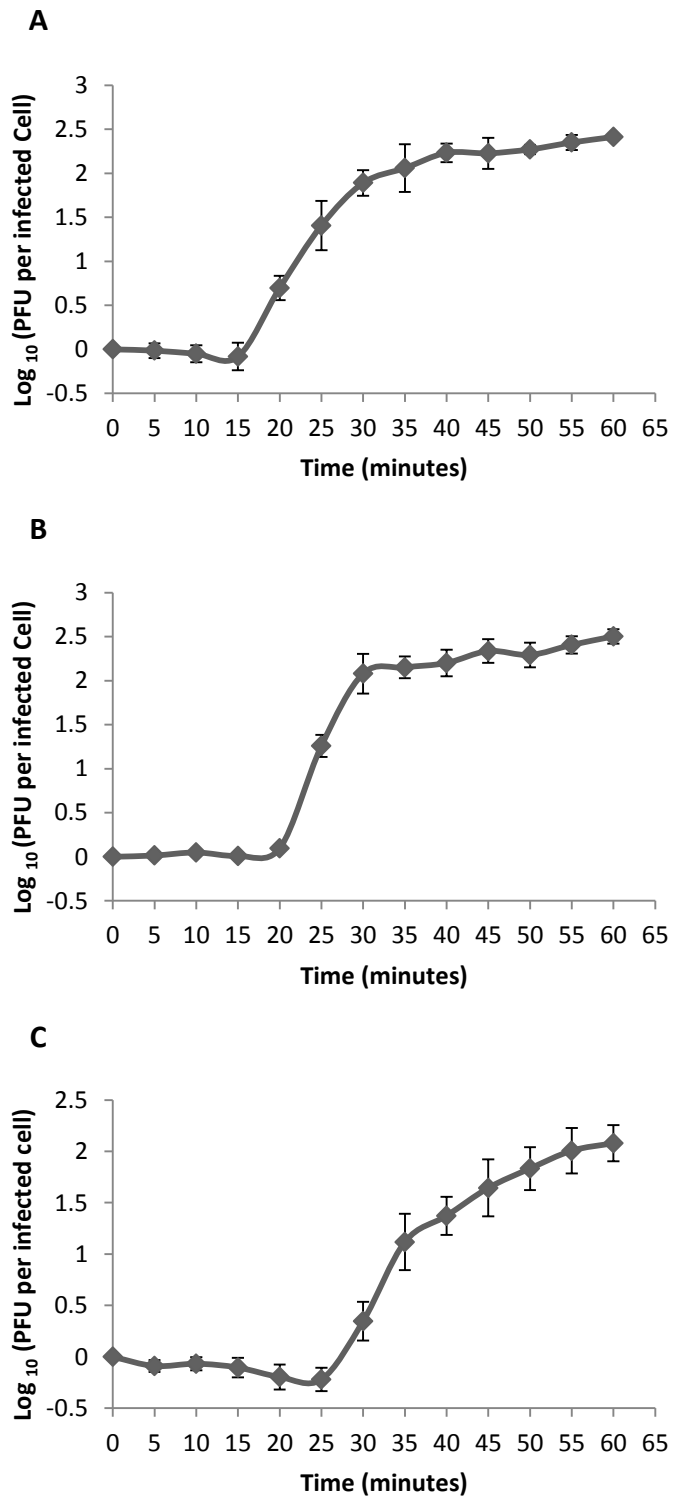


Figure 30. One step growth curve for; A, vB_PmiS_NSM6; B, vB_PmiP_#3; C, vB_PmiM_D3. The results represent the log₁₀ of the mean and standard deviation of three independent experiments.

3.2.6 Genomic sequencing and analysis phage vB_PmiS_NSM6

Genomic DNA from phage vB_PmiS_NSM6 was sequenced by PacBio RS using p5-c3 chemistry. *De novo* assembly was performed using HGAP, followed by polishing using Quiver and resulted in a single contig of 215 x coverage. The contig was apparently circular, consisting of the whole phage NSM6 genome and a large duplication. Comparisons performed between the duplicated regions led to the identification of 7 gaps that were closed with targeted Sanger sequencing. Phage NSM6 has a double stranded DNA genome of 47745 bp in length. Circular phage genome assemblies indicate that the genome is either circularly permuted or has a non-permuted terminal redundancy (e.g. direct terminal repeats).

The length of the sequenced genome agrees with the genome size estimation of 47.5 kb realised by PFGE (Figure 21). The G+C content is 39.72 % which is similar to that of its host *P. mirabilis* at 38.88 % (Pearson *et al.*, 2008). A total of 79 open reading frames (ORFs) were predicted, with an average length of 555 bp and a coding density of 1.675 genes per kb. The coding potential was calculated to be 93 %. High coding potential has been repeatedly observed in bacteriophage genomes; structural constraints of the capsid limit the size of the genetic material that they can contain so genomes must be efficient (Chirico, Vianelli and Belshaw, 2010; Fiddes, 1977). A total of 50 ORFs (63.3%) exhibited some homology to proteins in the extant sequence databases which allowed assignment of putative protein function (Appendix, Table 1). The remaining 36 % are unique, exhibiting no sequence similarity to known proteins. The majority of the ORFs have an ATG start codon (69 ORFs, 86.25 %), whereas 9 (11.4 %) start with GTG and 2 (2.5 %) with TTG. No tRNAs were detected.

Phage vB_PmiS_NSM6 exhibits a modular genomic architecture (Figure 31), a characteristic common among members of the *Siphoviridae*. The high degree of conservation of gene order among members of the *Siphoviridae*, particularly within the module encoding virion structural and assembly genes, allows for the identification of gene products by syntenic organisation (Veesler and Cambillau, 2011). The NSM6 genome is comprised of four main modules that consist of genes involved in DNA replication/regulation, virion structural and morphogenesis, genome packaging and lysis. Phage NSM6 also possesses an integration cassette

that is located to the right of the packaging, structure and assembly genes, a common position for such elements (Hatfull, 2008). The putative *attP* site was identified as a 111 bp sequence located downstream of the putative integrase in this region. This sequence was also located at the boundaries of putative prophages in the genomes of *P. mirabilis* strains BB2000, AOUC-100, CYPM1 and HI4320. The presence of an integrase indicates that vB_PmiS_NSM6 could be a temperate bacteriophage.

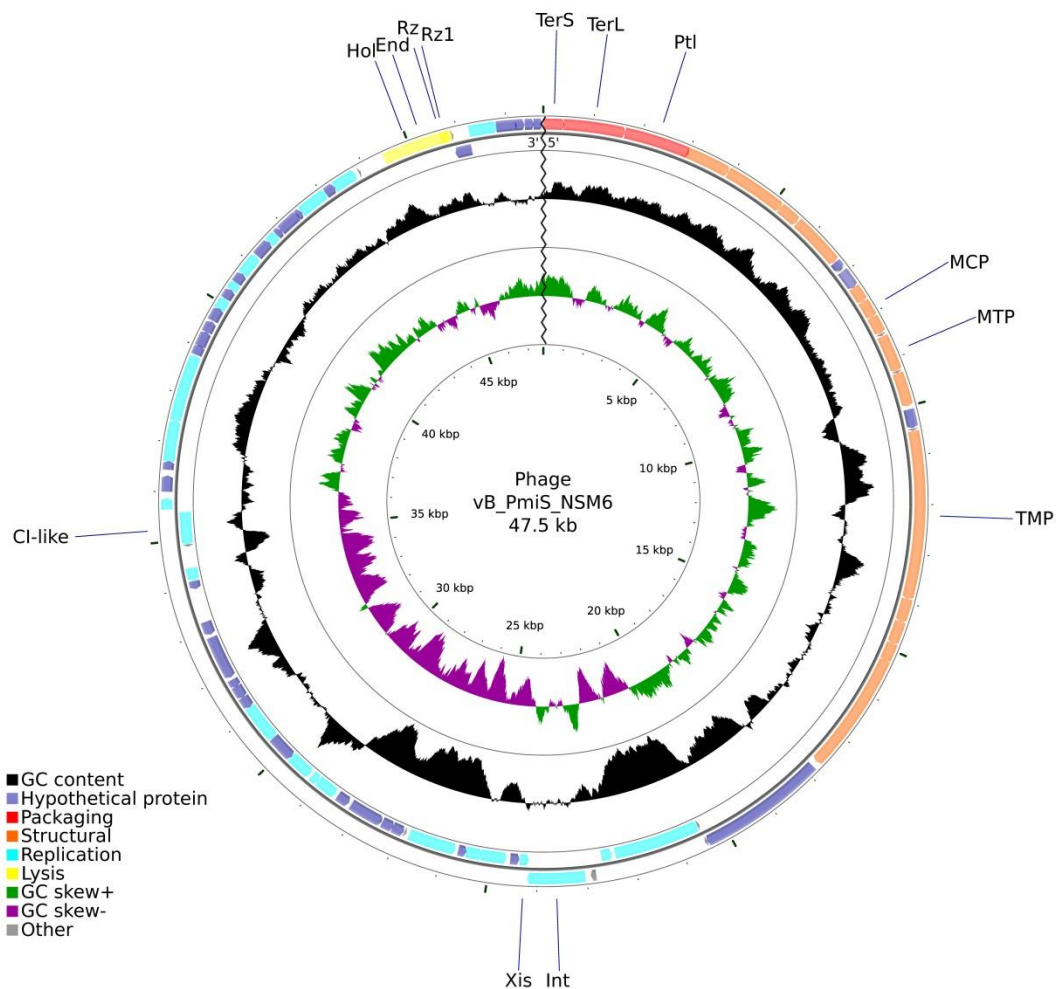


Figure 31. Genome map of vB_PmiS_NSM6. The outer ring illustrates the CDS, coloured according to their putative protein function as shown in the key. Some genes are labelled, *TerS* = small terminase subunit, *TerL* = large terminase subunit, *Ptl* = portal, *MCP* = major capsid protein, *MTP* = major tail protein, *TMP* = tape measure protein, *Int* = integrase, *Xis* = excisionase, *ci*-like = similar to the lambda repressor, *Hol* = holin, *End* = endolysin, *Rz* and *Rz1* are not shortened. GC content is depicted in black, whilst positive skew is depicted in green and negative skew in purple.

Purified viral structural proteins were separated by 1D SDS-PAGE (Figure 32). A total of eight bands were observed, consisting of three major bands at 204 115 and 52 kDa and five minor bands of 98, 87, 72, 35 and 17 kDa. The sizes of proteins resolved by 1D SDS-PAGE were compared to the *in silico* predicted molecular mass for structural proteins and the predicted function inferred from protein homologs identified using BLASTP and HHpred.

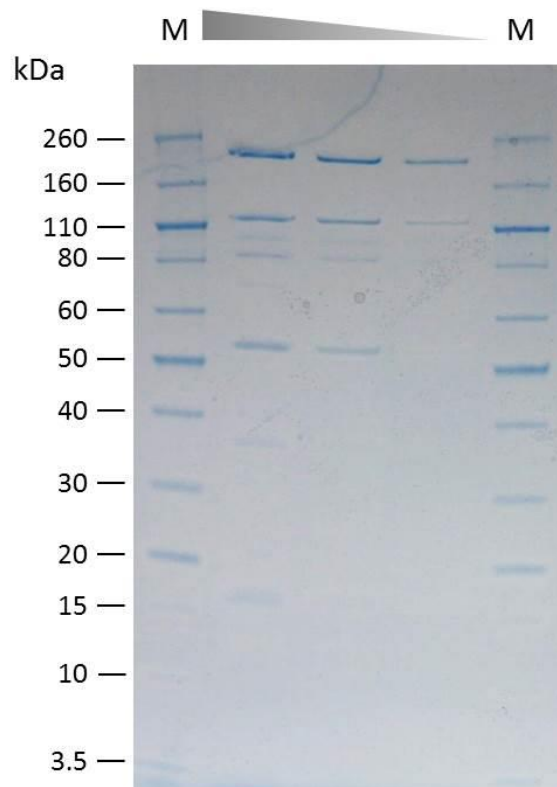


Figure 32. vB_PmiS_NSM6 structural proteins resolved by 1D SDS PAGE.

3.2.7 Genes involved in genome packaging, virion structure and morphogenesis

The NSM6 phage genome was opened at the predicted small terminase subunit, a convention first seen in P22 and Lambda. Gp01 contains a conserved domain, GP3_package (Pfam: PF16677) and exhibits 91 % amino acid sequence identity to the putative small terminase subunit of *Acinetobacter* phage YMC-13-01-C62 using

BLASTP. Gp02 was identified as the large terminase subunit with a good match in the database to Enterobacteria phage ES18 (100%). This ORF contains a Terminase_3 (Pfam: PF04466) superfamily domain. These gene products are concerned with packaging the DNA into the prohead. The small terminase forms a nucleoprotein that aligns the large terminase at the packaging initiation site (Black, 1988). Gp03 was assigned as the portal vertex protein and it usually follows the terminase enzymes as it acts as a recognition site for them. It also acts as a duct for DNA passage and as the site of tail attachment. Database searches showed similarity to the portal vertex protein of *Salmonella* phage vB_SosS_Oslo and 1D SDS-PAGE identified a protein of 52 kDa which is close to the predicted 50 kDa molecular weight of the product.

Continuing downstream, genes concerned with structure and morphology are encountered. Gp04 was putatively identified as a head morphogenesis protein, and contains a conserved domain, Phage_Mu_F. These minor head proteins are thought to be essential for infectivity (Aksyuk and Rossmann, 2011) as is the case for gpD in phage lambda, capsid expansion creates openings in the lattice structure of the capsid. GpD is required to strengthen the structure allowing for the packaging of the complete chromosome. Mutants deficient in gpD have capsid failure due to the pressure exerted by the packaged DNA (Fuller *et al.*, 2007). A minor band identified on the SDS PAGE gel of 35 kDa could represent this product. No function could be assigned for either gp05 or gp06. Gp06 did, however, exhibit similarity to gene products 06, 0006, and gp08 of *Salmonella* phages vB_SosS_Oslo, SPN3UB and ES18, respectively. Gp07 was assigned as the major capsid protein based on sequence similarity to the capsid protein of *Cronobacter* phage ES2 (100% query cover) and structural similarity to the major capsid protein of HK97 (Pfam: PF05065). No band could be identified on SDS PAGE gels that matched the predicted molecular weight of 39 kDa but a much larger band exists that is unidentified, and it is possible the individual proteins have formed a trimer or another complex and appear larger on the gel. Gp08 and gp09 could not be assigned a putative function, gp10-12 are concerned with head to tail joining. Gp13 was designated as the major tail protein due to the presence of three conserved domains; Big_2, Phage_tail_2 and YjdB. Big_2 represents bacterial immunoglobulin-

like domain that has been suggested to facilitate weak bonds between carbohydrates on the cell surface that keeps the phage associated with the cell before final attachment occurs (Fraser, Maxwell and Davidson, 2007). The Phage_tail_2 is a family of proteins whose characterised members are major tail tube proteins. YjdB has Immunoglobulin like domains which probably function in a similar manor to Big_2. Gp14 is likely to be a tail assembly chaperone based on its position between the tail tube and tape measure proteins, a common location for such elements (Pell *et al.*, 2013), however, no structural or sequence similarity was observed. The presence of a conserved SmpA OmlA domain and LipoP results suggest that Gp15 is a lipoprotein. It possesses a single transmembrane helix (confirmed by TMHMM and HMMTOP). Gp15 is predicted to be a ribosomal binding site and is followed by a terminator (Ter₀₄). It has similar characteristics to moron elements, such as that seen in phage HK97 (Cumby *et al.*, 2012). These elements are only seen in temperate phages and it is suggested they either infer some benefit to the host bacterium (i.e. moron = more on). For example, the temperate *Salmonella* phage GFSY-2 possess an moron that encodes a superoxide dismutase which provides lysogenised *Salmonella* cells with increased resistance against reactive oxygen species produced by the mammalian host (Figueroa-Bossi and Bossi, 1999). A further example includes genes involved in lysogenic conversion, whereby the host cell receptor is modified by genes encoded by a resident prophage conferring resistance to further phage infection. Examples of lipoproteins are superinfection exclusion (sie) elements whose action is proposed to prevent injection of DNA into a lysogenised cell, thus preventing prophage destruction (Donnelly-Wu, Jacobs and Hatfull, 1993). It is possible that gp15 might represent a sie element but further experimental work would be required to confirm this hypothesis.

The tape-measure protein (TMP) is encoded by Gp16; 95 % query coverage at 40 % identity with that of phage ES18 was observed. It contains conserved domain; phage_HK97_TLTM (Pfam: PF06120) which is the tape-measure protein first identified in phage HK97. Studies performed with Enterobacteria phage Lambda demonstrated that the length of this gene correlated precisely to the actual length of the tail (Katsura and Hendrix, 1984). In phage NSM6, the TMP is the longest gene

in the genome. For some phages, it has been suggested that the TMP might also be involved with genome translocation by forming a conduit that spans the bacterial cell envelope. Interaction with host proteins is essential for this role as TMPs are not predicted to form transmembrane proteins on their own (Cumby *et al.*, 2015). Gp17 was ascribed as the minor tail protein due to structural similarities between that of GpM from phage lambda (Interpro: IPR010265), however little sequence similarity was observed. Gp18 contains the conserved domain DUF1833 (Pfam: PF08875), NlpC peptidase and ubiquitin domain containing genes exist in close association to this domain and their function has been predicted to be involved with tail assembly. Gp19 was putatively identified as a virion-associated peptidoglycan hydrolase (InterPro: IPR008044). The proposed mechanism of action is to facilitate degradation of the peptidoglycan cell wall, allowing the injection of DNA (Rodríguez-Rubio *et al.*, 2013; Lehnerr, Hansen and Ilyina, 1998). Conserved domain NlpC_P60 is present. Gp20 encodes a tail tip or baseplate structural protein. A conserved domain COG4733 is present which is identified as a tail component of bacteriophages, it exists at the N-terminal of the protein and homology was observed across varying phages which suggests it is phage binding. Similarity was seen with the tail tip protein gpJ of lambda (InterPro: IPR032876) when searched against the Pfam database using HHsearch. In Lambda gpJ initiates distal tail tip assembly through interactions with gpI, gpL and gpK. When interacting with the host, gpJ binds irreversibly to a host receptor which induces structural changes in the tail that leads to DNA ejection (Roessner and Ihler, 1984). Gp21 contains a conserved domain; DUF3359 no known functional information is available for this domain. Structural similarity was observed with phage phi297 tail spike protein and many glycoside hydrolase enzymes. It would seem probable, therefore, that gp21 is a tail spike that possesses some enzymatic activity concerned with degrading carbohydrates.

3.2.8 Genes involved in Lysogeny

Gp22 is encoded on the complimentary strand and represents the beginning of a new module of genes concerned with recombination and integration. Gp22 itself codes for an acetyl transferase and contains a conserved OafA domain, which is involved with Peptidoglycan/LPS O-acetylase OafA/YrhL activity, and a SGNH-

hydrolase domain which is involved with Cell wall/membrane/envelope biogenesis. Good similarity was seen with that of *Enterobacter* phage Tyrion but limited functional information is available on this seemingly bacterial enzyme. If Gp22 is involved in the modification of a component of the bacterial cell surface, there is a possibility that it might be happening for phage immunity from superinfection, although further work would be required to test this hypothesis. Gp23 encodes a homologue for the theta subunit of DNA polymerase III. This replicative protein has good similarity (HHpred) to HOT from phage P1. It has been suggested that the HOT homologue to theta binds more tightly in the DNA polymerase III complex and is more thermally stable as a result (Derose *et al.*, 2004). A 111 bp sequence (5'-CTCGTTATATCCATTTAACTAAGGGAACATTTTGCAGAGGGTGCTTAACTGTTTCTCAGTGCCGTATAGTACCGTTTTTGTGGTGAATGAATCAAGTTGTTAGTTCATT-3'), representing the predicted *attP* site, was identified just upstream from gp24. Searches of complete *P. mirabilis* genomes using BLASTN identified this sequence to be duplicated at the right and left boundaries of putative prophages. The *attP* site is the location where site specific recombination occurs. The *int* and *xis* encoding regions usually occur immediately downstream of their site of action and this is the case for phage NSM6. Gp24, transcribed in the opposite direction, is the integrase. In Lambda, the product of *int* catalyses the integration of the phage genome into the bacterial chromosome if conditions in the cell allow *clI* to achieve a high enough concentration to activate its promoters. As there is only one specific *attB* site, only one copy can be contained within the bacterial genome (Bushman *et al.*, 1985).

Exit from lysogeny is carried out by an excisionase. Gp25 has been identified as the excisionase with good structural similarity to phage Lambda and sequence similarity to *coliphage* vB_EcoP_24B. It contains a conserved domain, AlpA, that is a DNA-binding transcriptional regulator. Again, in Lambda Xis initiates excision by organising the assembly of a higher-order complex called the excisive intrasome (Abbani *et al.*, 2007). This structure excises the phage genome allowing lytic development to follow. Xis also inhibits reintegration by altering the *attP* site into a catalytically inactive structure (Moitoso de Vargas and Landy, 1991). The control of these processes, in phage Lambda, is carried out in part by the *cl* repressor. Gp47 was identified as a *cl*-like repressor. The *cl* repressor prevents lytic growth by

repressing two promoters necessary for lysis to occur. Interestingly, *cl* can autoregulate its synthesis, up-regulating when in low concentration and down-regulating when high. It forms loops in the DNA, binding dimers attached to distant operators, termed long-range cooperativity. These loops are thought to enhance autoactivation and autorepression (Lewis *et al.*, 2011) allowing for more efficient prophage induction. Mirroring the control region of Lambda, gp48 encodes a Cro-like protein on the rightward strand. Cro blocks the promoter of *cl* allowing lysis to occur. The expression of *cl* and *Cro* is controlled by the concentration of bacterial proteases present in the cell. Proteases degrade a transcriptional activator *cII*; *cII* activates transcription of *cl* and *int*. GP49 encodes a *cII*-like transcriptional activator. When high concentrations of proteases are present under favourable growing conditions (e.g. high nutrients), *cII* is degraded, *cl* is not produced and the phage undergoes a lytic life cycle. Low concentrations of proteases result in lysogeny as *cl* is active. So the decision to enter the lysogenic lifecycle or lytic is due, ultimately, to environmental factors. Continuing rightward, no significant matches could be detected for gp50. Gp51 has good sequence similarity to O-like replication proteins. In Lambda, the O and P proteins initiate replication of the phage chromosome as part of the lytic life cycle. O binds at the *Ori* site and P binds the DnaB subunit of the host replication machinery; this allows the phage to use the host DNA polymerase and rolling circle replication initiates (Ptashne, 2004).

3.2.9 Nin-like gene cassette

Gene products 53-58 exhibited no similarity in the databases but fall within a 4.9 kb Nin-like region. Nin seems to control N-dependant transcriptional terminations and temporal expression of the late genes (Leason and Friedman, 1988). Gp 57 contains DUF551 (Pfam: PF04448), found in dsDNA viruses with no tRNAs like Lambda and P22, no function has been determined. Gp58 had no homologues in BlastP or HHsuite searches but gp59 was identified as Lar-like protein and contains conserved domain Lar_restr_allev (Pfam: PF14354). This protein modulates the activity of the hosts restriction and modification system (Toothman, 1981). Gp60 had no similarity in the databases but GP61 had similarity to NinB protein from *Escherichia* phage HK639 and contains conserved domain NinB (Pfam: PF05772). In Lambda, NinB is involved when the RecF and RecBCD recombination pathways operate (Tarkowski

et al., 2002). No function could be determined for gp62. Gp63 contains a domain of unknown function, DUF3310 (Pfam: PF11753) which is bacteriophage specific and conserved. Gp64 has low similarity in the databases so no function could be inferred. Gp65 has no sequence similarity in the databases but structural similarity to DNA binding proteins that have a transcriptional regulatory role. The product of gp66 has sequence similarity to NinF-like proteins from *Salmonella* phage ES18, *Salmonella* phage SEN22 and vB_SemP_Emek. No known function has been reported for this protein. A NinG-like protein has been identified as the product of gp67. Conserved domain NinG (Pfam: PF05766) is present. In Lambda it participates in the RecBCD homologous recombination pathway, NinG is a DNA structure specific endonuclease that cleaves Holliday junction branch points (Casjens and Hendrix, 2015). No similarity was observed for gp68. Gp69 had significant similarity to antiterminator Q and contains a conserved domain of unknown function, DUF1133 (Pfam: PF06576) which consists of a range of unknown proteins from *E. coli* 0157:H7 and *S. enterica* serovar typhi. In Lambda, antiterminator Q positively regulates expression of the phage early and late gene operons. It modifies host RNA polymerases so they transcribe through termination sites that would otherwise prevent expression (Yarnell and Roberts, 1992).

3.2.10 Lysis Cassette

Genes 70-74 represent phage NSM6s lysis cassette, ORFs gp70-74, follows an organisation typical of dsDNA phages. It possesses a holin inhibitor (anti-holin; gp70), holin (gp71), endolysin (gp72) which is followed by RZ (gp73) and RZ1 (gp74) homologues. RZ and RZ1 are unique genes in that the RZ1 cistron is embedded within the RZ coding sequence, albeit in the +1 reading frame (Berry *et al.*, 2008) which is the case in phage NSM6. The anti-holin is thought to act as a specific negative regulator of holin function. In T4 this is achieved by the binding of the anti-holin to the holin upon superinfection. The anti-holin blocks holins from triggering and prolongs the infection cycle. This allows phages to build up intracellularly and demonstrates how environmental conditions can influence the infection cycle (Moussa *et al.*, 2012). Holins are characterised by the presence of transmembrane domains and function to form a pore in the inner cytoplasmic membrane, allowing endolysin access to the peptidoglycan substrate. Holins have been demonstrated to

play a role in scheduling the lysis event, ensuring a programmed release of virions at the optimal time (Young, 2014). Phage NSM6 encodes a class I holin due to the presence of three transmembrane domains predicted by TMHMM, alongside a low probability of the N-terminal being on the cytoplasmic side (Young, 2002). A function for RZ and RZ1 has been proposed by Berry *et al.* (2008) who postulate that the gene products form a complex with each other and fuse the inner and outer membranes, allowing phages to be released without barrier. The proposed RZ and RZ1 coding genes have similarity to criteria set out by Berry *et al.* (2008) that the RZ has an N-terminal transmembrane domain and a C-terminal periplasmic domain that is rich in acidic and basic residues (39 of 155 total) although not quite as rich as observed, 25 % vs 37 %. The RZ1 protein is slightly longer (58 vs 41) with less Pro (6 vs 10) residues but is devoid of secondary structure.

3.2.11 Regulatory Sequences: Promoters and Terminators

Regions 150 bp upstream of the ORFs were tested for the presence of statistically over-represented motifs using MEME (Bailey *et al.*, 2006). None were observed with the parameters used so identification of promoter sequences was not possible.

The presence of rho-independent terminators was assessed by use of three programs, ARNold (Naville *et al.*, 2011), Transterm HP (Kingsford, Ayanbule and Salzberg, 2007) and GeSTer (Mitra *et al.*, 2011). Agreement between the predicted locations, presence of appropriate characteristics and the stability of the folded structure were considered when assessing predictions. A ΔG cut off of -8.27 kcal/mol of the stability of the stem loop structure as calculated by MFold (Markham and Zuker, 2008) was used for terminator predictions. A total of eleven rho-independent terminators were identified in the NSM6 genome that satisfied these criteria (Table 6). Four terminators are located in the structural and morphogenesis gene module. Between gp20 and gp21 on the boundary between recombination and the structure and morphogenesis modules is a convergent, or x-type terminator, structure where complementary terminators exist on opposite strands to each other. Three terminators are then present in the recombination region and one at the end of the Nin region within the replication genes before the

lysis cassette. The final terminator was predicted to reside at the end of the lysis cassette after the sequence encoding the putative RZ protein.

Table 6. The position and sequence of the putative rho independent terminators

| Name | Coordinates | Strand | Sequence | Stability (ΔG) (kcal/mol) |
|--------------------|--------------|--------|--|--|
| T _{ORF8} | 6903..6923 | + | <u>AGCCGCGAAAGCGGTTTTTTT</u> | -9.05 |
| T _{ORF12} | 8456..8478 | + | <u>AGGTCGCTTATGCGCCTTTTTT</u> | -11.91 |
| T _{ORF13} | 9266..9297 | + | <u>AAGGGTGCITTCGAGTGCCCTTGATAATATTC</u> | -10.73 |
| T _{ORF15} | 10470..10500 | + | <u>AACCCTGCCAACTGGCGGGGTTTTTCATTTT</u> | -15.14 |
| T _{ORF22} | 20458..20488 | - | <u>AAGGCATCTATATGATGCCITTAATAAATAA</u> | -10.80 |
| T _{ORF21} | 20468..20496 | + | <u>AAGGCATCATATAGATGCCITTTATTTTTT</u> | -10.70 |
| T _{ORF31} | 26854..26895 | - | <u>GGATATGTATTACTGCTTGTAAATACAGGGTTCTGCTGTACCT</u> | -9.58 |
| T _{ORF33} | 27438..27460 | - | <u>ACCCTGCACTAGCAGGGTTTTTTT</u> | -10.63 |
| T _{ORF47} | 34857..34885 | - | <u>AGCCCTCTACATGAGGGTTATCTCATACA</u> | -9.88 |
| T _{ORF69} | 43860..43886 | + | <u>GACCTCGCTACGCGGGGTTTTTTGTT</u> | -13.04 |
| T _{ORF73} | 45876..45900 | + | <u>GCCTCGCTCAATAGCGGGGTTTTTT</u> | -12.63 |

The underlined nucleotides form the stem of the structure.

3.2.12 Determination of physical genome ends/termini

Several forms of termini have been observed in dsDNA bacteriophage genomes. These include cohesive ends, circularly permuted direct terminal repeats, short or long direct terminal repeats, covalently bound terminal proteins or terminal host DNA sequence. The genome ends of vB_PmiS_NSM6 do not appear to be cohesive, since the restriction profiles generated by EcoRV were not altered after exposure to heat followed by either fast or slow cooling (Figure 33). If COS ends were present, the slow cooled sample would have one larger band in place of two smaller ones expected in the fast cooled gel as when cooled slowly the cohesive ends have time to anneal together (Casjens and Gilcrease, 2009). The genome appears to be circularly permuted as time-limited digestion with exonuclease BAL-31 (Figure 34) followed by restriction enzyme digestion showed an even, simultaneous degradation across all fragments. This agrees with the circular genome assemblies produced during sequencing. If the NSM6 chromosome were flanked by exact repeats (defined ends), the restriction fragments containing these repeats would be expected to decrease in size concomitantly with the time exposed to BAL-31

exonuclease activity. Casjens *et al.* (2005) and Casjens and Gilcrease (2009) demonstrated that comparative sequence analysis of the large terminase subunit can be used as a basis to predict packaging strategy and, therefore, the genome ends as similar functionalities cluster together. This approach has been confirmed with phages whose genomic termini have been experimentally validated. Multiple sequence alignment of the large Terminase subunit of NSM6 and other phages, demonstrates that the NSM6 large terminase subunit forms a clade with the Sf6-like headful packing (Figure 35). These data strongly suggest that the NSM6 genome is circularly permuted and terminally redundant. A headful packing strategy perhaps explains the diffuse band observed in PFGE (Figure 21) as packaging is imprecise so different lengths of DNA are packaged (Tavares *et al.*, 1996).

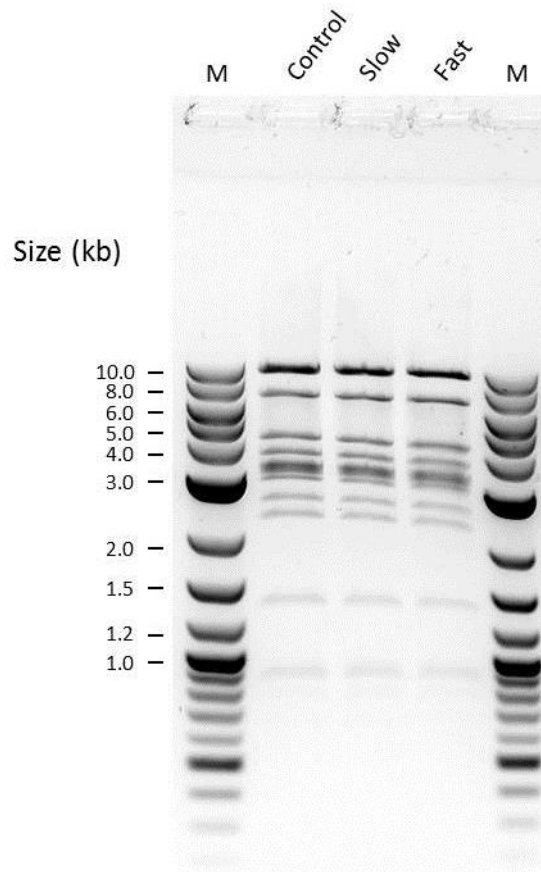


Figure 33. Assay for the determination of cohesive genome termini. Phage genomic DNA was cut with the restriction enzyme EcoRV, denatured and subsequently cooled rapidly or slowly. Samples are denoted above each lane. M represents the size standard in kb.

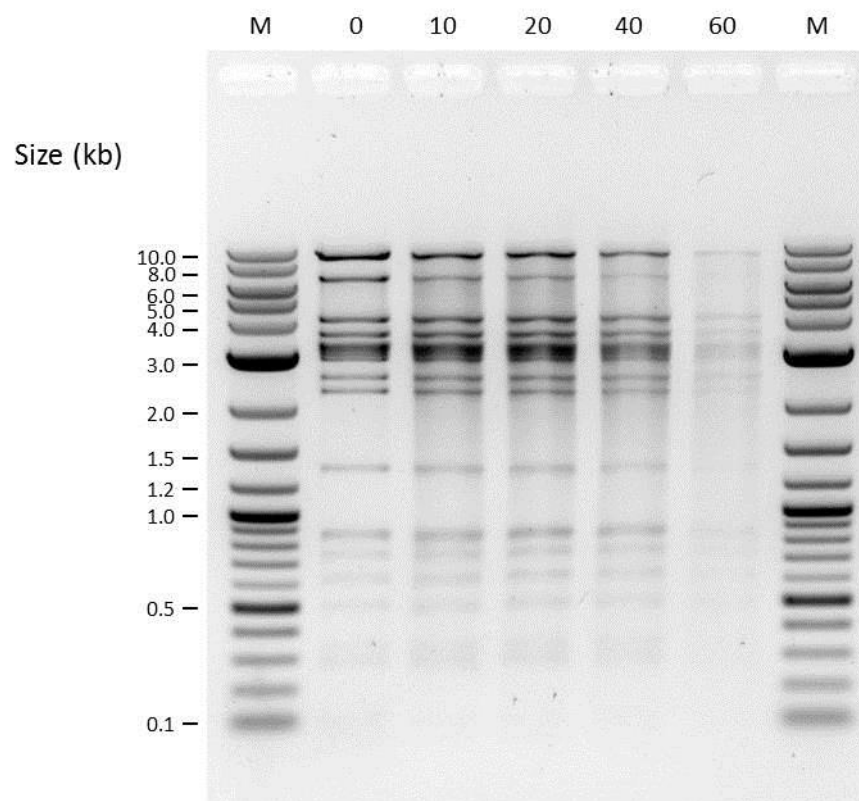


Figure 34. Time dependent digestion of genomic DNA with exonuclease BAL-31. M is the size standard and the numerical values refer to the length of exposure to BAL-31 in minutes.

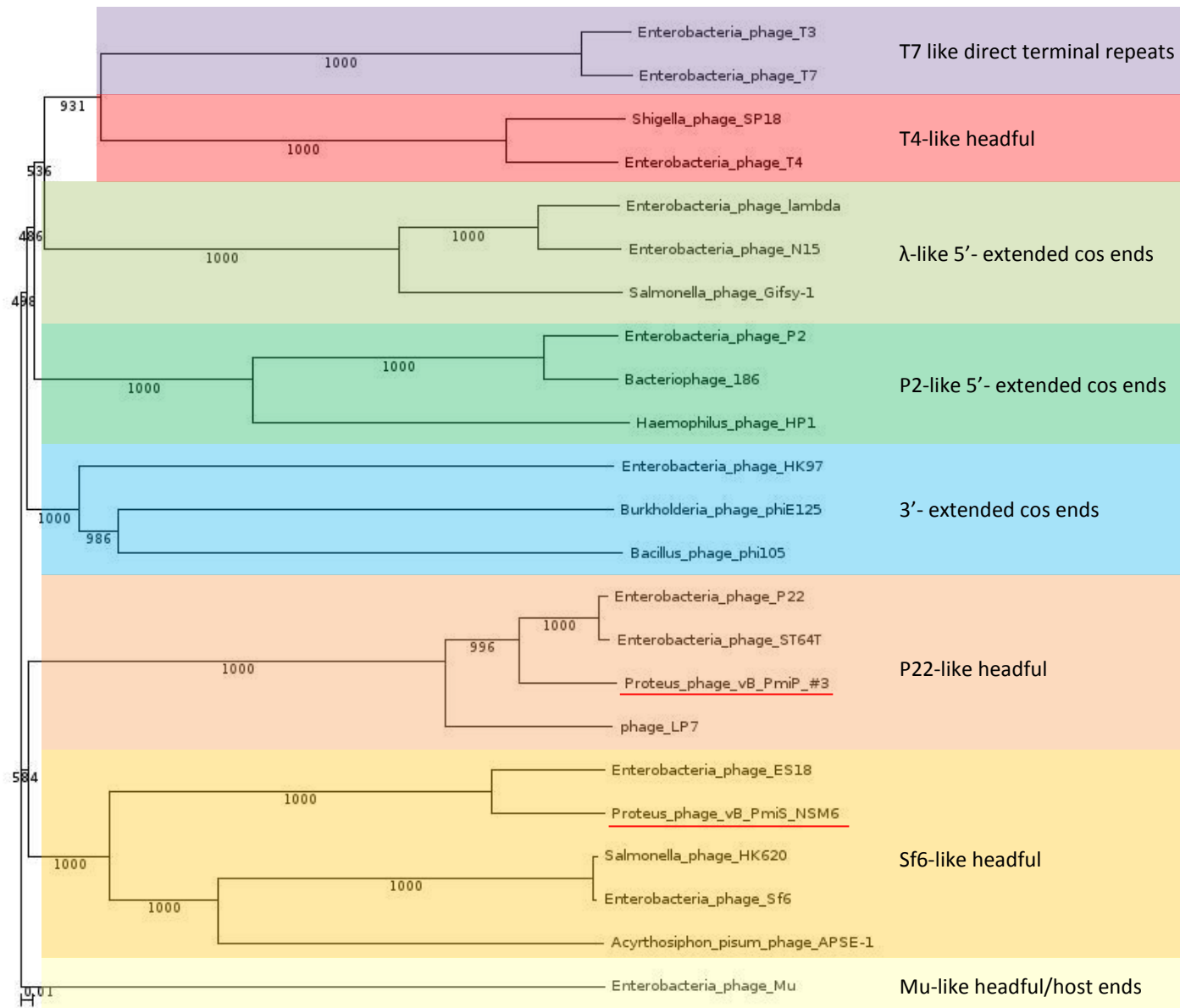


Figure 35. Neighbour-joining tree of large terminase sub unit amino acid sequences. The numbers near bifurcations are bootstrap values for 1000 trials. Major related groups of packaging strategy are highlighted with coloured boxes and the prototype is written to the right.

3.2.13 Genomic sequencing and analysis phage vB_PmiP_#3

The complete consensus sequence for phage vB_PmiP_#3 was obtained by a hybrid assembly approach utilising both Pac-Bio RS sequencing and Illumina HiSeq. The hybrid assembly was performed using SPAdes (Bankevich *et al.*, 2012) and resulted in a single contig of 627 x coverage. Phage vB_PmiP_#3 has a double stranded DNA genome of 41184 bp in length that is circularly permuted. This is only slightly less than the result seen in PFGE of ~41,900 bp (Figure 21). The G+C content is 40.28 % which is slightly higher than its host which is 38.88 % (Pearson *et al.*, 2008). A single tRNA was detected therefore slightly reducing the reliance on host translational machinery, possibly allowing for the greater G+C content. The tRNA was identified as an initiator. These tRNAs carry a methionine at the N terminal of the protein and differ from elongation tRNAs. They bind directly to the P site on the ribosome causing conformational changes that allow translation to occur. The genome encodes 75 ORFs with an average length of 508 bp and a density of 1.821 genes per kb. A total of 92.6 % of the genome has coding potential with 52 % of the predicted ORFs exhibiting some likeness to proteins in the extant sequence databases. Phage genomes are constrained by the size of the capsid they must package their DNA into therefore coding tends to be dense. Similarity to sequences deposited in the extant sequence databases allowed prediction of putative protein function (appendix table 2). The remaining 41.33 % were assigned as hypothetical proteins of unknown function. The predominant start codon is ATG with 68 genes (90.67 %) whereas 6 genes start with GTG (8 %) and one with TTG (1.33 %).

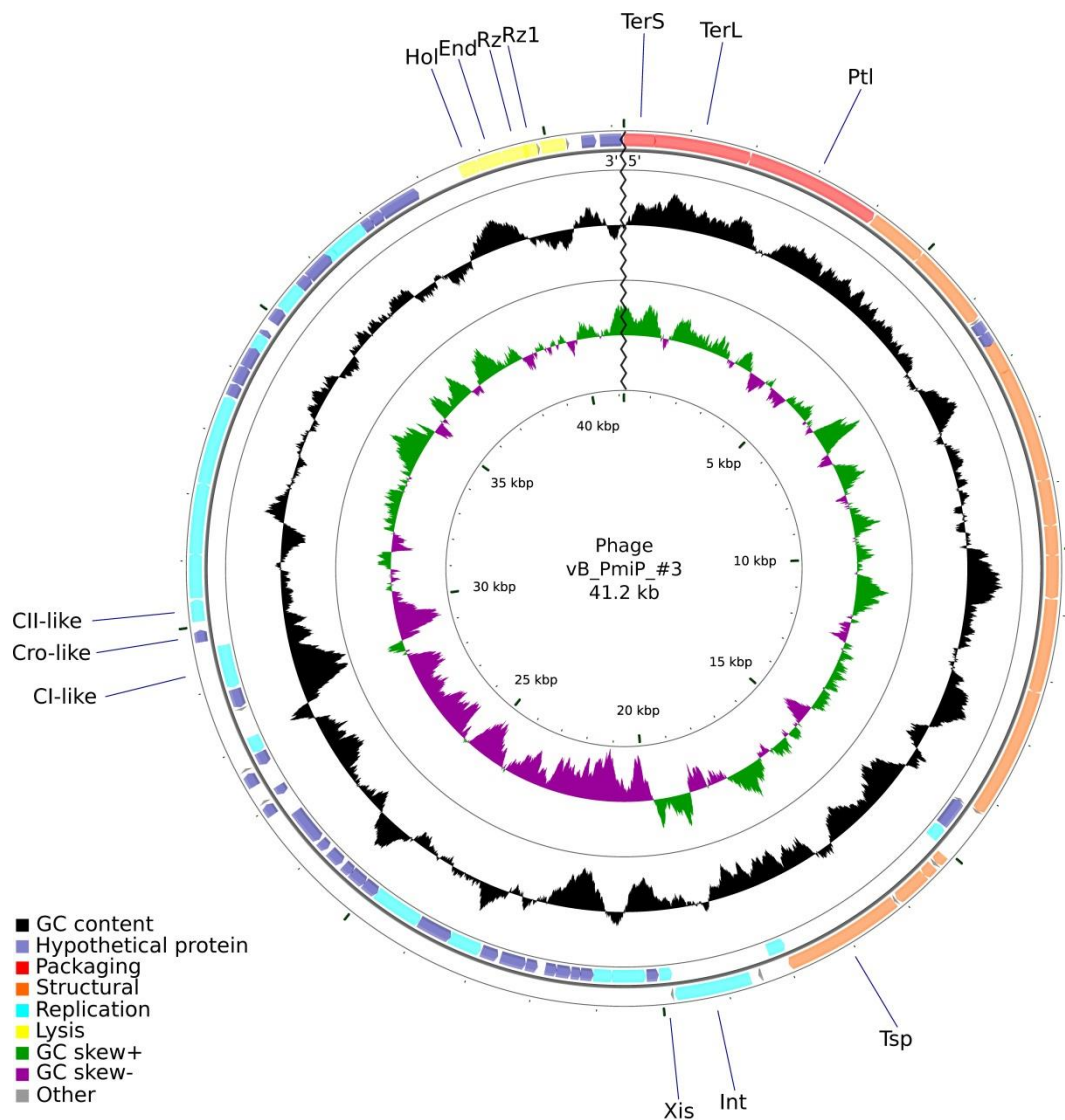


Figure 36. Genome map of vB_PmiP_#3. The outer ring illustrates the CDS, coloured according to their putative protein function as shown in the key. Some genes are labelled, *TerS* = small terminase subunit, *TerL* = large terminase subunit, *Ptl* = portal, *Tsp* = tail spike, *Int* = integrase, *Xis* = excisionase, *cl*-like = similar to the lambda repressor, *Cro*-like = similar to lambda's *Cro* transcriptional repressor, *cII*-like = similar to lambda's *cII* transcriptional activator, *Hol* = holin, *End* = endolysin, *Rz* and *Rz1* are not shortened. GC content is depicted in black, whilst positive skew is depicted in green and negative skew in purple.

The vB_PmiP_#3 genome (Figure 36) exhibits the same modular architecture as vB_PmiS_NSM6. It comprises four discrete regions that can be assigned as replication and regulation, structure and morphogenesis, packaging, and lysis according to the functional annotation of gene products. vB_PmiP_#3 also possesses an integration cassette located to the right of the packaging, structure and assembly genes, again, a similar position to vB_PmiS_NSM6 and a common

location for dsDNA viruses. The presence of such genes would indicate that vB_PmiP_#3 may also be a temperate bacteriophage.

Purified viral structural proteins were separated by SDS-PAGE (Figure 37). Three bands were observed, with one band, at 47 kDa being more dense than the others. The other two bands were 84 and 65 kDa. Predicted molecular mass was then used in corroboration with protein homologues from BLASTP and HHpred to annotate the predicted ORFs based on similarity of amino acid sequence, and secondary protein structure, respectively.

BlastP searches of gp01 returned similarity to the small terminase subunit of *Salmonella* phage vB_SemP_Emek and HHpred returned structural similarity to the small terminase subunit of P22 (pdb: 3p9a). A GP3_package conserved domain (Pfam: PF16677), a bacteriophage DNA packaging protein, was also predicted, lending further weight to this assignment. Gp02 was assigned as the large terminase subunit. Structural and sequence likeness was observed with *Shigella* phage SF6 and *Salmonella* phage AT64T, respectively. The COG5565 conserved domain, a member of Terminase_6 superfamily, was present in this ORF. The small and large terminases are often adjacent to one another in phage genomes (Casjens, 2011). Gp03 putatively encodes the portal protein, identified by the presence of the P22_portal conserved domain (Pfam: PF16510) as well as by sequence and structural similarity (pdb: 3lj5) to phage P22. The portal is a dodecameric structure situated at the vertex between the capsid and tail and acts as a channel for the phage DNA to enter upon assembly by attaching to the terminase complex, and allows the linear dsDNA to leave upon ejection. The portal forms a tube-like structure that extends into the capsid (Casjens *et al.*, 1992). This structure assists with efficient packaging of the DNA, prevents circularisation and stabilises the pressure driven exit of DNA ensuring accurate delivery (Olia *et al.*, 2011). The molecular weight of the portal vertex is 79 kDa and is likely to be the uppermost band whose weight was determined to be 84 kDa on the SDS PAGE gel (Figure 37).

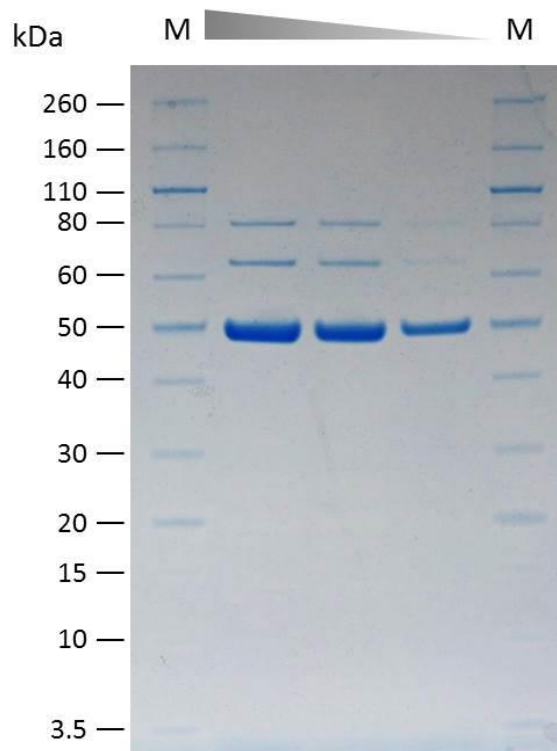


Figure 37. vB_PmiP_#3 structural proteins resolved by 1D SDS PAGE.

3.2.14 Structure and Morphogenesis Module

Genes comprising virion structural proteins and those involved in virion morphogenesis are encoded immediately downstream from the packaging genes. There are 15 genes in this module of which 13 were putatively assigned a function. Gp04 putatively encodes a scaffold protein. The top search results for HHpred and BlastP are with P22 and a conserved domain, phage-scaffold (Pfam: PF09306) is present that is found in many bacteriophages. Scaffold proteins catalyse the assembly of the capsid and bind to the capsid proteins forming an intermediate structure called the procapsid. Scaffold proteins are released around the time DNA is packaged into the capsid, leaving a structure that could not have formed alone (Sun *et al.*, 2000). Scaffold proteins are recycled and catalyse capsid formation up to five times (Casjens and King, 1974). The major capsid protein is encoded by gp05. Again, sequence and structural homology are similar to phage P22, and, in addition, this protein contains a conserved domain, P22_coatprotein (cl22542). In P22, the major capsid protein consists of two protease stable domains connected by a flexible loop region. The loop region is susceptible to proteolytic enzymes when in a

procapsid but not in mature capsids. This suggests hinge bending can occur which accounts for the morphological changes that happen during construction and maturation of the capsid (Lanman, Tuma and Prevelige, 1999; Teschke and Parent, 2010). No putative function could be determined for either gp06 or gp07. Gp08 encodes a tail accessory protein and has conserved domain P22_tail-4 (Pfam: PF11650). In P22 this protein is essential and is the first protein to bind to the tail structure after DNA is packaged. Its function, along with two others (gp10 and gp26), is to stabilise the portal vertex protein and prevent chromosomal leakage (Strauss and King, 1984). A conserved phage stabilisation domain (Pfam:PF11134) is present in gp09 and sequence similarity was present (66 % amino acid identity) with gp10 from P22, which further emphasises the structural similarity between vB_PmiP_#3 and phage P22. HHpred returns a match for gp10 with P22 gp26 at high probability. So the function, in part, is to retain DNA in the capsid by completing the portal vertex. The structure of gp26 has been shown to be a trimeric coiled-coil and due to the similarity to viral membrane fusion proteins is suggested to be a thin needle-like fibre emanating from the centre of the tail that may play a role in piercing the outer membrane (Andrews *et al.*, 2005).

Gp11 is predicted to encode a Gcn5-related N-acetyltransferase (Pfam: PF13420) and gp12 a DNA injection protein which has similarity to gene 11 from phage Sf6 (63 % identity). Gp13 has conserved domain inj_translocase (Pfam: PF16928) which is involved in the injectosome mechanism/assembly. This protein has similarity to gp20 in P22 which is one of the four E proteins that are ejected into the cell upon infection. It is hypothesised that gp20 forms a complex within the bacteria that is essential for effective infection. It is not required for DNA ejection or E protein ejection and may help the DNA cross the plasma membrane or protect it from degrading enzymes (Israel, 1977). Gp14 also appears to be an E protein and is similar to gp16 in P22. In P22 gp16 seems to be necessary for ejection of some of the other E proteins and in the active transport of DNA across the cytoplasmic membrane (Perez *et al.*, 2009).

No putative function could be identified for gp15 which occurs on the opposite strand along with gp16. Gp16, 17 and 18 show homologies to *mnt*, *arc* and *ant*, respectively. These proteins are concerned with the maintenance of lysogeny and

superinfection immunity in P22 and termed the *imml* region (Sauer *et al.*, 1983). The control of lysogeny is conducted by a similar set of genes as seen in vB_PmiS_NSM6 and phage Lambda (*immC*), the *cl* repressor binds to operators to prevent the transcription of early genes. However, the *cl* repressor (termed *cli* in P22) is inactivated by *ant* which would lead to prophage induction. To maintain lysogeny, the product of *mnt* is continuously required to repress the *ant* gene. *Arc* similarly acts to repress *ant*, binding to the promoter and repressing its synthesis (Susskind and Botstein, 1978).

The product of *gp19* is predicted to encode an HNH homing endonuclease and contains the conserved domain HNH_3 (Pfam: PF13392). These genes are efficient parasitic elements and utilise host break-repair mechanisms for their propagation (Chevalier and Stoddard, 2001). Homing is the lateral transfer of an intervening sequence to a homologous allele that lacks the sequence, and this allows propagation and maintenance within the population as they appear to confer no selective advantage. They can splice within introns or inteins and therefore do not affect host phenotype. They have also been shown to be free standing and can tolerate changes in the specific homing sequence (Bonocora and Shub, 2009).

The putative tail spike protein is encoded by *gp20* and is a candidate for the middle band estimated to be 68.8 kDa on the SDS-PAGE gel (Figure 37). It possesses a conserved domain associated with P22 called *head_binding* (Pfam: PF09008). In P22 the tailspike is comprised of a trimer of the product of *gp09* and recognises the repeating units of the O antigen of the hosts lipopolysaccharide (Israel, Anderson and Levine, 1967). The P22 tailspike possesses enzymatic activity (Baxa *et al.*, 1996). The kinetics of the binding have been shown to be fast and reversible which suggests the phage can scan over the surface of the cell searching for its receptor (Baxa *et al.*, 1996; Steinbacher *et al.*, 1997).

Gp21 is encoded immediately downstream of the putative tailspike on the opposite strand. This gene encodes a product exhibiting similarity to a DNA polymerase III theta subunit present in *Escherichia* phage HK639. Chikova and Schaaper (2007) postulated that the phage encoded theta subunit enhances the activity of the

polymerase complex for optimal phage replication. However, no loss in virulence was observed in mutants where this gene was knocked out.

A candidate *attP* site was identified at position 18447 on the #3 genome, spanning 53 bases on the forward strand, located just upstream of gp22, a predicted tyrosine family integrase. It possesses conserved domain INT_P4_C (cd00801) which is a P4-like integrase (Nunes-Düby *et al.*, 1998). Integrases function to integrate the phage genome into the bacterial chromosome at the *attB* site, a region of homology shared with the *attP* site. Integrases are classified into two major families depending on the amino acid sequence similarity and catalytic residues, either tyrosine or serine (Groth and Carlos, 2004). A putative excisionase (gp23) is encoded immediately downstream of the integrase.

Gp24 had no likeness in the databases. Gp25 putatively encodes a DNA (N-6-adenine)-methyltransferase, with similarity to that of phage Lahn2. Orphan methyltransferases are utilised by phages to methylate their DNA so that it is not susceptible to restriction enzymes thereby avoiding this form of host defence (Murphy *et al.*, 2013). Gp26 encodes a Nin X-like protein with greatest similarity to *Serratia* phage Sta. No function is currently known for this product (Denyes *et al.*, 2014). No putative function could be identified for gene products 27-33. Gp34 encodes a protein with similarity to a single stranded DNA binding protein. Concerned with recombination, replication and repair, single stranded DNA binding proteins (ssb) prevent annealing from occurring prematurely, protect against nuclease digestion and prevent the formation of secondary structures from forming thus enabling the effective function of other enzymes (Marceau, 2012). Ssb conserved domain is present within this CDS (cog0629). The product of gp35 could not be determined through similarity in the databases but gp36 showed good likeness to exodeoxyribonuclease VIII, a 5'-3' linear exonuclease. No functions could be assigned to gp37-44.

3.2.15 Genes Involved in Lysogeny

No significant matches were observed for gp45-6 but gp47 was putatively identified as an N-like regulatory protein and is the first gene encountered in the immediate early replication segment of the genome. In phage Lambda, *N* along with *cro* are

expressed early in infection (Calendar, 2006). Gp50 has insufficient similarity to identify a function, however, it is likely to be similar to a cro-like repressor due to structural likeness. No putative function could be determined for gp48. Gp49 was putatively identified as a ci-like repressor, due to high sequence similarity observed by searches using BLASTp. Continuing downstream gp51 putatively encodes a cII-like transcriptional activator. Gp52 is predicted to be involved with the decision between lysogeny and lysis. It contains two conserved domains, phage_pRha (Pfam: PF09669) and KilAC (COG3645). Phage_pRha containing genes are dependent on integration host factor (IHF) for their regulation and in hosts deficient in IHF, phage growth does not occur (Iyer, Koonin and Aravind, 2002). KilAC is an auxiliary repressor of ci, controlled by the ci promoter and is not essential for replication and lytic development (Hansen, 1989).

The genomic module encoding genes involved in DNA replication begins at gp53, a putative O-like replication protein. In lambda, the O protein along with the P protein hijack the host DNA polymerase initiating replication that will ultimately end in lysis (Zylicz *et al.*, 1984). Gp54 is a P-like regulatory protein containing a conserved DnaB domain (InterPro: IPR007692).

3.2.16 Nin-like Region

Proteins encoded by gp55-60 could not be identified by database searches. Gp61 putatively encodes a NinB like protein and represents the beginning of the Nin region of the genome. NinB binds to single stranded DNA and has roles in the hijacking of the recombination pathways of the bacterial host (Tarkowski *et al.*, 2002). Structural similarity (HHpred) was seen with that of phage Lambda's NinB and conserved domain NinB (Pfam: PF05772) is present. Gp64 was putatively identified as NinF-like although the nucleotide and amino acid sequence similarity is weak. A NinG-like product has been predicted from the sequence for gp65 due to the presence of a conserved NinG domain (Pfam: PF05766) and similarity within the extant sequence databases. In Lambda, NinG plays a role in the Red recombination pathway (Tarkowski *et al.*, 2002). Gene products 66-8 could not be identified.

3.2.17 Lysis Cassette

Gene products 69-72 were identified as the lysis cluster and represent the holin, endolysin, Rz and Rz1, respectively. The holin proteins oligomerise to form a pore in the inner cell membrane, allowing the endolysin access to the periplasm and exposing the cell wall to endolysin-mediated degradation. RZ and RZ1 then complete the lysis process allowing the release of progeny virions.

Downstream from the lysis cassette is gp63 which putatively encodes a gp63-like protein seen in phiKO2, which has no known function. No homologues were identified for gp74 and gp75 in the extant sequence database.

3.2.18 Regulatory Sequences: Promoters and Terminators

As for vB_PmiS_NSM6, regions 150 bp upstream of the ORFs were analysed for the presence of over represented motifs. No over-represented motifs with high significance were detected with the parameters used so identification of promoter sequences was, again, not possible.

The presence and location of rho independent terminators was predicted by the use of three programs, ARNold, Transterm HP and GeSTer. Agreement between the programs predictions, location, presence of appropriate characteristics and the stability of the folded structure were considered when assessing predictions. A ΔG cutoff of 8.46 kcal/mol of the stability of the stem loop structure as calculated by QuickFold (Markham and Zuker, 2008) was employed for terminator predictions. However, on two occasions (T_{ORF48} and T_{ORF71}) the ΔG fell below the cut-off but, due to convincing predicted secondary structures, these putative terminators were retained in the annotation. A total of eleven terminators were identified that satisfied the criteria (Table 7). Five are present in the structure morphogenesis region of the genome. Between gp14 and gp15 within the structure and morphogenesis region is a convergent, or x-type, terminator structure where complementary terminators exist on opposite strands to each other. One terminator was predicted immediately downstream of the integrase, three in the replication region with one after the lysis cassette and finally one after gp73.

Table 7. The position and sequence of the putative rho independent terminators

| Name | Coordinates | Strand | Sequence | Stability (ΔG) (kcal/mol) |
|--------------------|--------------|--------|---|--|
| T _{ORF5} | 6285..6306 | + | <u>GGGAGCTTCGGCTCCCTTTTTT</u> | -12.27 |
| T _{ORF15} | 14231..14257 | - | <u>GAAGGGCTATTGCCCTTCCTTTATTT</u> | -10.94 |
| T _{ORF14} | 14240..14265 | + | <u>GAAGGGCAATAGCCCTCTTTAATAT</u> | -11.20 |
| T _{ORF19} | 15258..15300 | + | <u>GAAGCCCCAACTACTTGCATAGTCAGGGCTTCTAGTTTAGTT</u> | -11.80 |
| T _{ORF19} | 16089..16114 | + | <u>AAGGTCACTTAATGTGACCTTTTTT</u> | -11.96 |
| T _{ORF22} | 19835..19875 | + | <u>AGGGCAACGAGCATTATTAATTCGTTGCTCTATCCATTCAT</u> | -12.98 |
| T _{ORF43} | 27101..27138 | + | <u>AGAGCGAGCAAGTTCTTCGCTTGCTCTTATCTGGAT</u> | -14.72 |
| T _{ORF45} | 27665..27704 | + | <u>GCGGAACTAATTCATAATGGTTGTTCCGCAATTTAGAGT</u> | -9.81 |
| T _{ORF48} | 28565..28589 | - | <u>ATCCCTCTTTAATGAGGGATTTTTT</u> | -5.58 |
| T _{ORF71} | 39856..39884 | + | <u>AGCCTCTAAGTAATTAGGGGCTTTTTTTT</u> | -7.40 |
| T _{ORF72} | 40312..40334 | + | <u>GCCTCGCAATAGCGGGGCTTTTTT</u> | -12.00 |

The underlined nucleotides form the stem of the structure.

3.2.19 Packaging strategy

To ascertain if the genomic termini possess cohesive ends or not, vB_PmiP_#3's DNA was digested with EcoRI then denatured by heating at 80°C followed by rapid or slow cooling (Figure 38). If the genome has cohesive ends, the two restriction fragments possessing those ends will anneal in the slow cooled sample and form a single larger fragment (Casjens and Gilcrease, 2009). No difference to the restriction profile was observed between the rapid and slow cooled samples ruling out cohesive ends. To determine if the genomic termini are fixed or variable, time limited digestion with the exonuclease BAL-31 followed by digestion with restriction endonuclease was carried out. This resulted in an even, simultaneous degradation of all restriction fragments (Figure 39). This result discounts the presence of fixed termini, where a progressive shortening of two restriction fragments that contain the fixed termini would have occurred (Loessner *et al.*, 2000). Circularly permuted genomes are indicative of a head-full packaging strategy. The packaged DNA length can be between 102 and 110% of the total genome length, resulting in terminal redundancy (Casjens and Gilcrease, 2009). To confirm the experimental observations the amino acid sequence of the large terminase subunit was compared to phages with experimentally confirmed packaging strategies. Casjens *et al.* (2005) revealed that packaging strategies cluster together and therefore can be used to predict the genomic termini. Figure 35 shows the neighbour-joining tree of

the amino acid sequences produced by ClustalW2. vB_PmiP_#3 clusters with the terminases of the P22-like headful packing group, corroborating what was observed experimentally, that the genome of vB_PmiP_#3 is circularly permuted and terminally redundant.

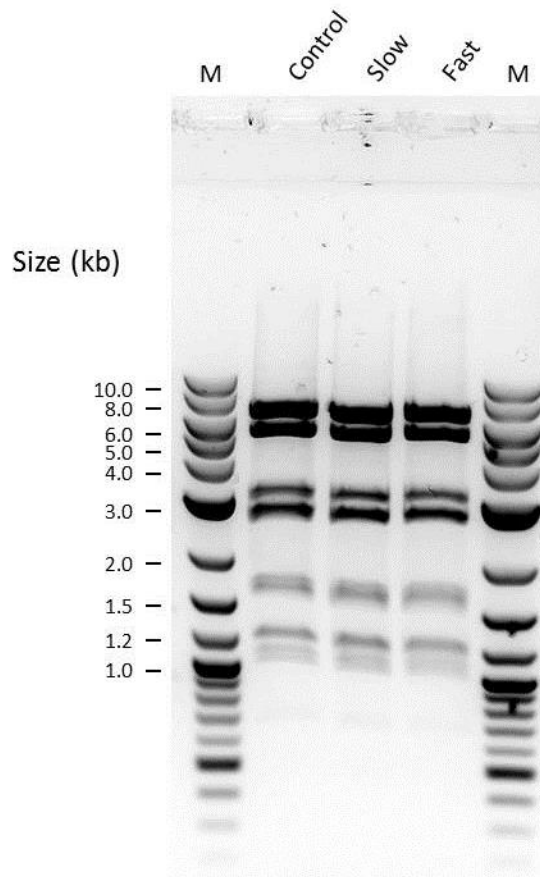


Figure 38. Assay for the determination of cohesive genome termini. Phage vB_PmiP_#3 genomic DNA was cut with the restriction enzyme EcoRV, denatured and subsequently cooled rapidly or slowly. Samples are denoted above each lane. M represents the size standard.

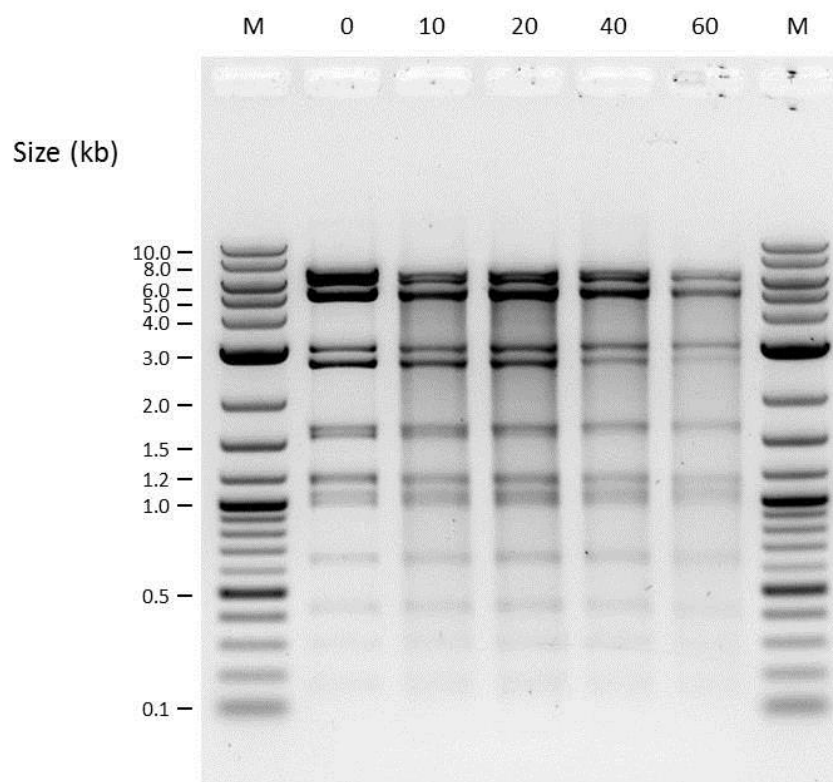


Figure 39. Time dependant digestion of genomic DNA with exonuclease BAL-31. M is the size standard and the numerical values refer to the length of exposure to BAL-31 in minutes.

3.3 Discussion

The aims of the work described in this chapter were to isolate distinct phages lytic against clinical isolates of *P. mirabilis* and to characterise them, both microbiologically and genetically.

Three distinct viruses were isolated and characterised. A representative of each family from the *Caudovirales* (i.e. *Siphoviridae*, *Myoviridae* and *Podoviridae*) were obtained (

Figure 22). There was significant difficulty experienced when isolating bacteriophages against *P. mirabilis* for this study. The number of phages reported in the literature for *Proteus* species is comparatively small, possibly due to their scarcity in nature. Initially only a single bacterial isolate was used to obtain phages. Although this approach is acceptable, it would limit the number of phages acquired due to host range constraints, especially considering the narrow host ranges of the

phages presented in this study. Experimental methods were scrutinised to determine if error was occurring, however, when *E. coli* was used with the techniques and environmental samples, many phages were isolated. If funds had allowed, tangential flow filtration would have been employed to concentrate any viruses present in the environmental samples allowing the processing of greater quantities of raw influent sewage. The isolation technique used biases the results to rapidly propagating lytic phages that produce visible plaques with the concentration of top agar used. Whilst biasing rapidly propagating phages selects for the most lytic, an attribute beneficial for phage therapy, other phages that do not produce so many plaques are being missed. The visibility of the plaques is associated with the phage capsid size; larger phages only produce tiny plaques due to their inability to migrate through the agarose matrix. This bias is shown in the prevalence of phages with genomes between 30-50 kb in the sequence database (50 %) as the largest genomes are 100-200 kb and only marginally represented (6 %) (Hatfull, 2008; Serwer *et al.*, 2007).

The finding that the 5 initial phages were indistinguishable from one another was unfortunate. Differences in plaques observed and culture kinetics lead to a false assumption of uniqueness. On the second round of isolations, performing DNA extraction from crude lysates and restriction digests on the extracted DNA was a priority before any further analyses were carried out. This was done to ensure they were different before commencing with purification and the other time consuming characterisation techniques.

The second round of isolations was labour intensive due to using every isolate (42) in the host library. Despite this considerable increase in potential hosts, very few phages were isolated indicating low numbers with the ability to infect members of the library being present in the environmental samples or perhaps a low diversity of the host library. This supports the presumption that *P. mirabilis* phages are relatively scarce in the environmental samples processed.

The collection of *P. mirabilis* isolates was acquired from diverse sources, separated geographically and chronologically. Detailed epidemiological analysis was not the aim of this piece of work. Pulsed Field Gel Electrophoresis adequately characterised

the library, removing duplicates, necessary for the isolation of bacteriophages as well as host range determination of the isolated bacteriophages. The library was originally populated with 51 isolates; 10 were obtained from Southmead Hospital at the time of experimentation from infected urine samples. After analysis, 42 strains remained with varying degrees of relatedness. Interestingly, the duplicates which existed were often from the same studies, however, one pair that was genetically indistinguishable was 46736 and D1, a current clinical isolate and a isolate from a previous study, respectively. The discriminatory power of PFGE is reported as being high when compared to other commonly used typing methods (Olive and Bean, 1999) so it was assumed the isolates were very closely related despite their geographical and chronological separation.

PFGE using restriction endonuclease *NotI* produced between 4 – 15 bands for the isolates in the library. *NotI* was used because an infrequent cutter is required for PFGE and Sabbuba *et al.* (2003) found it to produce profiles that were readily interpretable. At the time of experimentation PFGE was considered the “gold standard” for strain typing. Its discriminatory power surpasses phenotypic methods and, although technically demanding, labour-intensive and time-consuming (Sabat *et al.*, 2013) it is relatively cheap to perform. Modern whole genome sequencing (WGS) technology has surpassed PFGE in terms of accuracy but bioinformatic analysis of the sequences produced requires specialist knowledge. The cost and lack of standardised protocols has prevented the widespread application of this technique, however, over the course of this project the cost has already dramatically reduced and automation of bioinformatics will result in this method becoming the new “gold standard” (Salipante *et al.*, 2015).

The failure of attempts to purify phage vB_PmiM_D3 and for its DNA to be extracted was a hindrance that would have prevented the phage from being taken forward if it were not so difficult to isolate phages against *P. mirabilis* isolates. Many attempts were made to purify and extract the DNA but finally a decision was made to pursue this no further. The phage was not able to be re-suspended following centrifugation; instead it aggregated into a distinct pellet that could only be broken up. This prevented purification by CsCl gradients as individual phages are required to go through the gradient and band at the appropriate location. Purifying with

polyethylene glycol was still possible and re-suspending in smaller volumes of SM buffer enabled concentration of the samples to a point sufficient for the completed works. High titre preparations were put through CsCl density gradients but they produced no band at the expected density, just debris at the top and bottom of the gradient. Similarly, extracting the DNA was not possible using the methods detailed in chapter 2. The DNA containing phase of the extractions was almost completely devoid of DNA and what was there was fragmented, as when the result of many isolations were combined and run on a gel (not shown), smeared profiles with no discrete bands resulted. Casjens *et al.* (2005) describe a similar situation with phage ES18; it would not form a discrete band in CsCl equilibrium gradients at or near the expected density of 1.5 g/ml. They proposed that the capsid was impermeable to Cs⁺ ions and overcame the issue by partial purification by differential centrifugation utilising sucrose gradients, therefore separating based on size. If time had permitted this alternative approach may have provided a means of purifying phage D3, although experimentation would be necessary to confirm if this approach is viable in this instance.

Despite the ability of the isolated bacteriophages to lyse liquid cultures and titrate as expected on solid media, genetic sequencing of vB_PmiS_NSM6 and vB_PmiP_#3 have shown them to contain elements only associated with temperate phages. This would omit these phages from being used therapeutically as temperate phages could act as a means of transduction between bacteria, potentially allowing the spread of antibiotic resistance genes or virulence factors leading to enhanced pathogenicity (Abedon *et al.*, 2011). Additionally, lysogenised bacteria do not die as a result of a temperate infection and the infection may make the bacterial host resistant to superinfection which might have otherwise led to lysis by a virulent phage utilising the same cellular receptor. This result highlights the importance of genetic characterisation for any potential therapeutic bacteriophages. This result was not obtained until after all laboratory testing was complete and no indication was present that hinted that this might be the case. It has been shown by Reyes *et al.* (2010) through metagenomic analysis that the majority of phages present in the human gut are temperate, therefore it is reasonable to assume temperate phages are more prevalent in sewage as well. It is not currently clear if the phages isolated

in this study were isolated from the sewage samples or induced from the bacteria as a by-product of the enrichment process. Testing resistant colonies from the centre of plaques for resistance to reinfection gave conflicting results (data not shown) partly due to the uncertainty in picking the tiny resistant colonies. A preferable method of determining the source would be to probe the bacterial hosts' DNA for the presence of the phages' DNA contained within as a prophage or plasmid. This could be achieved with PCR using primers designed from important genes in the known phage sequence. Many attempts at phage isolations were carried out, particularly with isolate NSM 6. If the technique was inducing a prophage, it is estimated that it would have appeared more than it did. Prophage induction usually comes about through DNA damage eliciting the SOS response and it is possible some component of the raw sewage brought this about.

No sequences were observed in the databases with greater than or equal to 95 % similarity indicating that the phages sequenced in this work are novel. The genome sequencing of the phages vB_PmiS_NSM6 and vB_PmiP_#3 was conducted externally. Gaps in the sequence occurred due to the nature of PacBio RSII sequencing and, to close the gaps, other sequencing approaches were used. For the vB_PmiS_NSM6 assembly, targeted Sanger sequencing was undertaken and for vB_PmiP_#3, Illumina HiSeq was utilised. Both methods effectively closed the gaps in the sequence, however, Illumina provided much more detailed information confirming the PacBio data, additionally, it was a simpler process to undertake. Hybrid assembly allows the shortcomings of second and third generation sequencing technologies to be controlled. For example, resolving repeated regions in assemblies becomes possible as PacBio often provides long reads that span the suspect regions. Accuracy is provided by second generation approaches that often produce short reads thereby the two approaches complement each other.

The presence of homologues to genes from Lambda's Red recombination pathway (NinB and NinR) in vB_PmiS_NSM6 is interesting as they could be utilised as tools to recombine genes in *P. mirabilis* or other similar bacteria. The Lambda recombineering pathway is a powerful tool for making targeted genetic changes in the form of insertions, deletions and point mutations (Mosberg, Lajoie and Church, 2010). No virulence factors or antibiotic resistance genes were identified in either

phage, which is a key factor in selecting phages for phage therapy. It is worth noting, however, that not all the genes had a putative function identified and, until all genes are identified in a therapeutic phage, caution should be exercised in its use. The identification of these gene products might lead to the discovery of novel proteins with medical relevance or further the understanding of phage-host interactions (Lima-Mendez, Toussaint and Leplae, 2011).

Chapter 4 Phage therapy in an *in vitro* model system

4.1 Introduction

The assessment of bacteriophages' utility in preventing the encrustation and eventual blockage of urinary catheters presents a number of experimental challenges that require validation prior to testing the approach in an *in vitro* bladder model system. For example, the removal of adhered bacteria from catheter surfaces, required to measure the reduction of viable counts following exposure to bacteriophages, is one such method that requires validation. Methods for the removal of biofilm and enumeration were modified from Fu *et al.* (2010) where a series of vortexing and sonication steps were employed to remove adherent cells from sections of catheters.

Another challenge was to develop a method of delivery for the bacteriophages. Curtin and Donlan (2006) presented a method of adhering bacteriophages to catheters manufactured with a hydrogel coating, by incubating the catheters with high titre phage preparations. It was suggested that the phages embed in the gel matrix on the catheters' surface. This method was trialled as a convenient, if slightly crude, method of delivery for the phages as it mimics a coating which would otherwise be difficult to produce, yet represents ideal placement for the phages.

In order to test the phage-coated catheters, a model system is required that challenges the approach in a way that mimics the situation *in vivo* as closely as possible. The *in vitro* bladder model first described by Stickler *et al.* (1999) provides a model of the catheterised urinary tract used extensively within the literature. The benefits of this system are that it tests whole urinary catheters connected to the closed drainage system that is used in the real world, providing a closer approximation of the pressures and fluid flow observed *in vivo*. Furthermore, this system allows a sump of urine to build up in the "bladder" that is akin to what is

observed in patients due to the design of the catheters placing the eye holes above the retention balloon.

This chapter details the proof of principle of these techniques and their utilisation in assessing the isolated phages' ability to prevent infection and the eventual blockage of the catheters in the *in vitro* bladder model system.

4.2 Results

4.2.1 Assessment of biofilm removal

To assess the method of viable biofilm recovery, four rounds of the washing procedure described in section 2.18 were carried out in triplicate. Figure 40 shows the percentage of bacteria recovered from each of the four rounds of the removal process on hydrogel coated catheters.

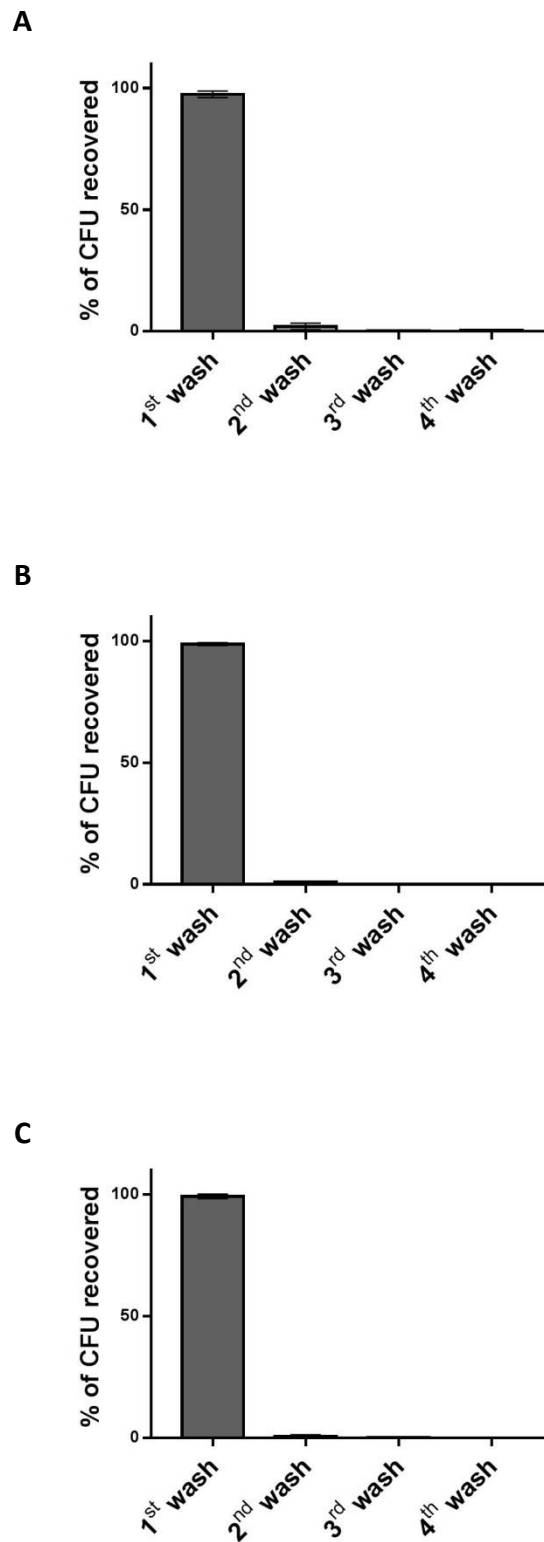


Figure 40. Viable recovered bacteria as a percentage of the total recovered following four rounds of the removal process from 1 cm catheter sections. (A) = bacterial isolate NSM 6, (B) = bacterial isolate #3, and, (C) = bacterial isolate D3. Error bars represent the standard deviation of the mean of three independent experiments.

These data demonstrate that the majority of the biofilm is recovered from the first round of the removal process corresponding to 97.49 %, 98.84 % and 99.32 % for total viable counts of *P. mirabilis* isolates NSM 6, #3 and D3, respectively. Upon completion of the second round of the removal process >99% of the total recovered viable organisms were obtained. Further rounds of removal did not result in a significant gain in recovery, and two rounds of the process were employed within future experiments.

4.2.2 Catheter section suspension tests

To assess the ability of bacteriophages to prevent bacterial attachment and biofilm formation, catheter section suspension testing was performed by pre-treating catheters with bacteriophages at three different concentrations. Figure 41 (A) shows the recovered bacteria for host NSM 6 treated with phage vB_PmiS_NSM6. Despite the 10^9 phage pre-treatment resulting in a 2 log reduction in adhered recovered bacteria, none of these data are statistically significant ($P= 0.2132$). Bacterial isolate #3 and vB_PmiP_#3 showed no discernible difference in recovered bacteria with phage pre-treatment, compared to control. D3 with phage vB_PmiM_D3 however, showed a statistically significant difference between the control treatment and 10^9 phage treatment ($P=0.0160$), but with more bacteria being recovered from the phage treated catheter, all other treatments showed no statistically significant difference.

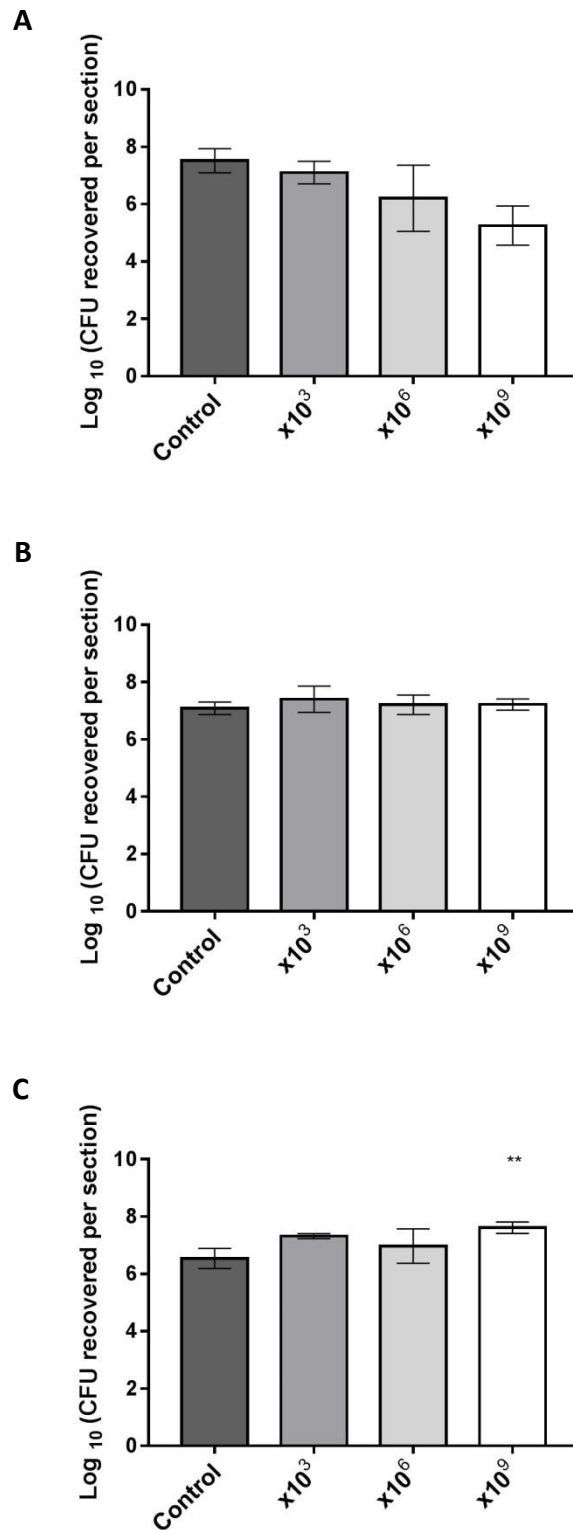


Figure 41. Catheter section suspension tests. One cm sections of hydrogel coated catheters were exposed to different phage concentrations before submersion in $\sim 5 \times 10^3$ CFU/ml of host bacteria for 24 h at 37 °C. (A) isolate NSM 6, catheters treated with vB_PmiS_NSM6. (B) isolate #3, catheters treated with vB_PmiP_#3. (C) isolate D3, catheters treated with vB_PmiM_D3. The results represent the mean and standard deviation of 3 independent experiments that have been log transformed. (**, P<0.01).

4.2.3 Quantification of phages adhered to catheters

Since the number of phages adhering to the catheters could not be directly measured an indirect quantification method was employed to estimate the fraction of phages that had adsorbed to the catheter surface. The adsorbed fraction was calculated as the difference between the titres measured before and after incubation in the presence of catheters. Adhered numbers ranged between 10^8 and 10^{10} PFU, and they were distributed along the whole internal length of the catheter and externally on the tip and inflation balloon (Figure 42).

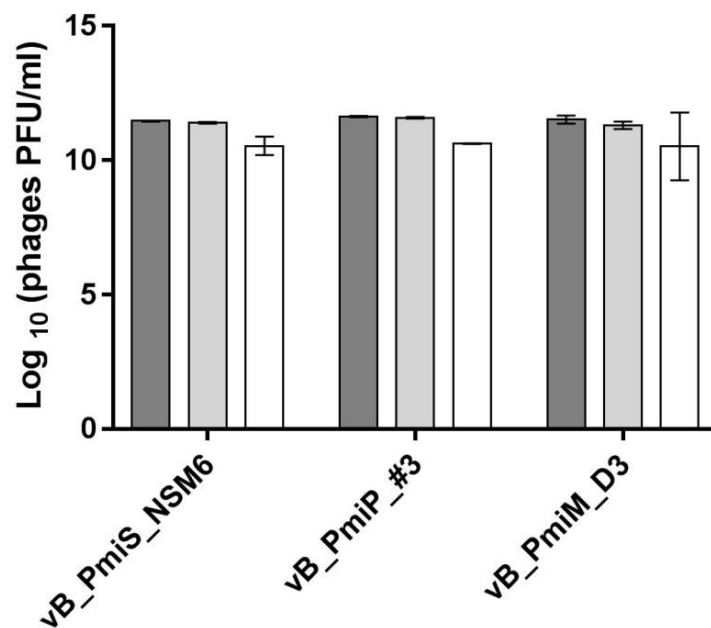


Figure 42. Adhered phages. Phage preparations were titrated and instilled into hydrogel catheters (Bard Hydrosil, ch 14) at approx. 5×10^{10} PFU/ml. After incubation, the solution was removed and titrated, the difference between applied and recovered being what was embedded in the hydrogel. The data represent two independent replicates, error bars are standard deviation. ■ = Applied, □ = Recovered, □ = Remains.

4.2.4 *In vitro* bladder models, 24 h experiment, *P. mirabilis* NSM 6

Phage vB_PmiS_NSM6 was embedded in the hydrogel of the catheters as described previously. Models were set up (Figure 43) with bacterial loads of approximately 5×10^5 CFU per ml, corresponding to the concentration of bacteria designated as the threshold of a clinically diagnosed UTI (Wilson and Gaido, 2004). It was revealed that there were, on average 3.99×10^{10} phages on the catheter distributed throughout its internal lumen, on the inflation balloon and tip. The multiplicity of infection is, therefore, not exact but approximately 8,000:1 phage to bacteria.



Figure 43. Photograph of the bladder model set up. (A) The re-circulating water bath that aimed to retain the models at 37°C, (B) the peristaltic pump that supplied the models (C) with artificial urine stored in the vented bottles (D).

After 24 h the supply of urine to the model was arrested, and following removal of the catheters, three sections were excised; from the top just above the retention balloon, immediately below the retention balloon and 3 cm beneath the retention balloon (2.21). Each section was assessed for adherent viable bacteria. All sections showed a reduction in the average numbers of recovered viable adherent bacteria on the phage treated catheters compared to the untreated control (Figure 44 (A)). Section i experienced a reduction of $3.65 \log_{10}$, section ii a $3.9 \log_{10}$ reduction, and section iii a reduction of $3.44 \log_{10}$. All these data are significant with $p < 0.0001$,

$p < 0.0001$ and $p = 0.0001$ for sections i, ii, and iii, respectively. Viable counts of both bacterial cells and phages in the effluent over the course of the experiment were determined (Figure 44 (B)). Counts of both bacteria and phages decreased after commencement of the experiment. Phage-treated catheters consistently showed reduced numbers of colony forming units in the effluent. The concentration of viable phages in the effluent increased after 4 hours, providing an indication that productive infection was occurring. At 24 h, the difference between planktonic bacterial numbers in the effluent of phage-treated and control catheters was significantly different ($p = 0.0092$). Despite the application of phages, bacterial numbers did increase after the initial drop. A possible explanation for this observation is that the continual perfusion of the model with artificial urine washed out some of the planktonic bacteria and time was then required for the bacteria to adhere to the catheter surfaces and proliferate.

The pH of the effluent was monitored at time points throughout the experiment (Figure 44 (C)). An initial drop in pH was observed after 2 h, presumably due to the dilution of the culture that remained in the residual volume in the bladder. The pH then remained relatively stable for the first 6 h despite bacterial numbers increasing after the first 4 h. The pH of the control models rose to pH 8 by 24 h whereas the pH of the phage-treated catheters remained stable at around pH 6.1 indicating that no crystal formation could have occurred. This assumption was confirmed by the images obtained by scanning electron microscopy (Figure 45). The phage-treated catheters have significantly less visible encrustation compared to control catheters. There is a clear difference around the eye hole, an area that typically becomes encrusted due to the flow of urine through it and its uneven topology, which is due, in part, to how the holes are stamped out from the material (Stickler *et al.*, 2003). The greatest differences in encrustation, after the tip of the catheters, are seen from the images of the internal lumens in sections iii and iv (Figure 45). A large quantity of mineral deposits formed in the control catheters whereas the phage-treated catheters appeared almost entirely free from encrustation.

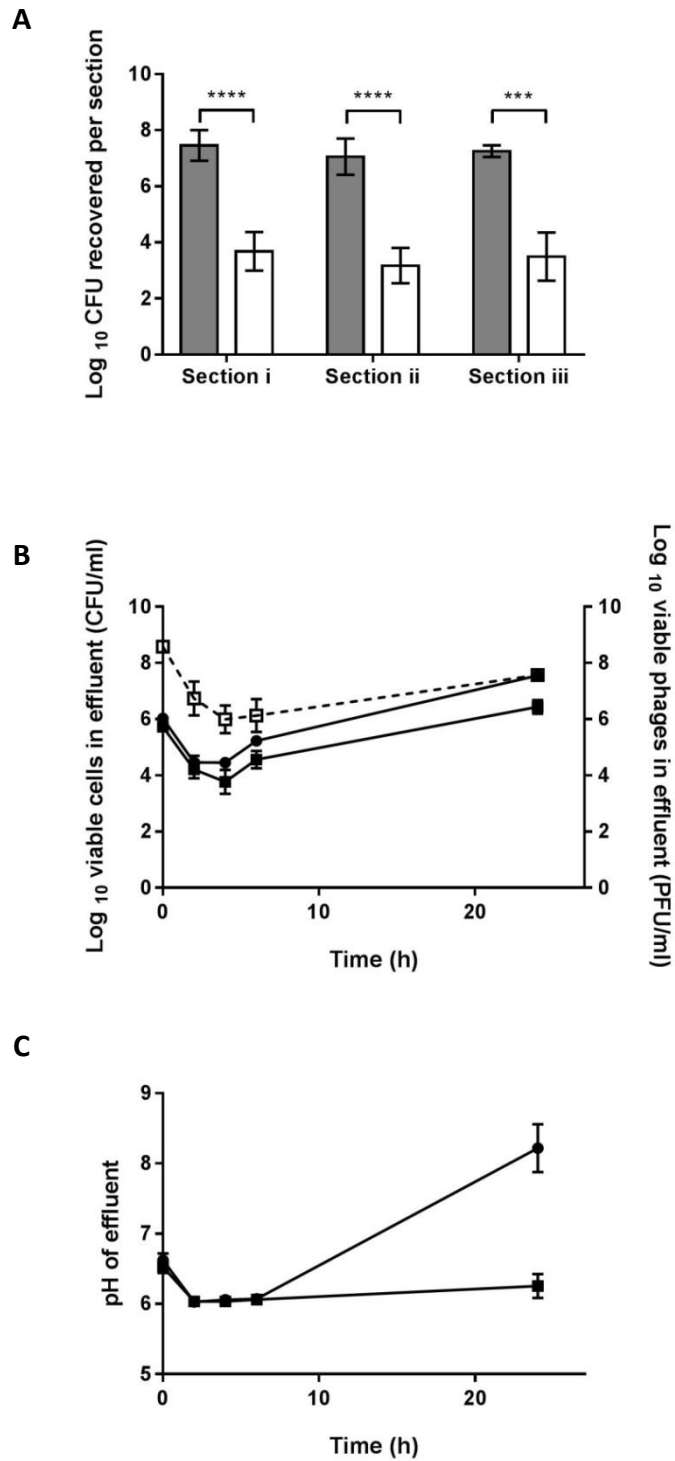


Figure 44. Impact of phage pre-treatment on bacterial biofilm formation by *P. mirabilis* NSM6. (A) Bacteria recovered from each section i, ii, and, iii. ■ = control and □ = phage treated. (B) Viable bacteria and phages in the effluent of the models, ● = bacteria from control models, ■ = bacteria from phage treated models, and, ◻ = phages from phage treated models. (C) pH of the effluent of the models. ● = control models, ■ = phage treated models. Data points represent the average of three experiments, error bars are standard deviation. Statistical analysis was performed by one way ANOVA with the Bonferroni *post hoc* test, (***) = $P \leq 0.001$, and (****) = $P \leq 0.0001$).

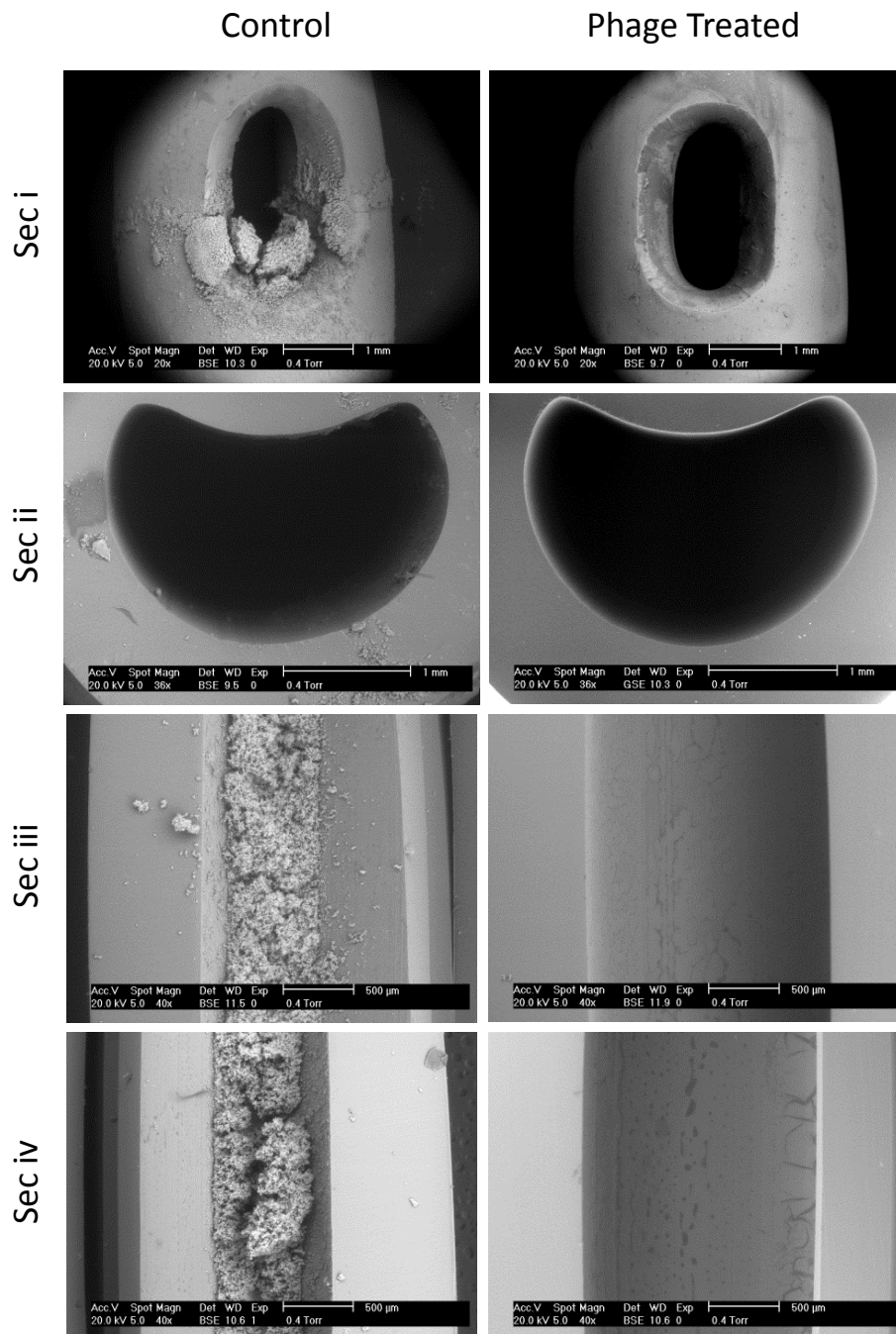


Figure 45. Scanning electron micrographs of un-treated and phage treated catheters removed from the *in vitro* bladder model system after 24 h. The models were challenged with *P. mirabilis* NSM6 at 5×10^6 CFU. The control models show the encrustation that formed as a result of urease activity elevating the urinary pH, leading to the formation of mineral deposits. Section i shows the eye hole of the catheter. Section ii is a cross section, distal to section i. Section iii is from 3 cm below section i and section iv is from 3 cm below section iii. Arbitrary regions were chosen for visualisation.

4.2.5 *In vitro* bladder models, 24 h experiment, *P. mirabilis* #3

Phage vB_PmiP_#3 was embedded in the hydrogel coating of the catheters and models were set up with the same concentration of bacteria as previously described at an approximate concentration of Ca. 5×10^5 CFU/ml determined by optical density and viable counts. Approximately 4.11×10^{10} phages were attached to the catheter surface, giving a MOI of 8,220:1 phages to bacteria, slightly greater than numbers achieved for vB_PmiS_NSM6.

Figure 46 details the results obtained from removal and analysis of the adhered bacteria on sections i – iii of the catheters. Analysis of the viable counts of adherent bacteria revealed a $0.92 \log_{10}$ reduction in viable adhered bacteria for section i when compared to control. Section ii, from below the retention balloon therefore only the internal lumen was exposed to both phages and bacteria, experienced a $1.97 \log_{10}$ reduction vs the control catheters. Section iii reduced by $1.53 \log_{10}$ compared to controls. When these data were analysed with Bonferroni's *post hoc* analysis none of the reductions were statistically significant between the control and their respective test sections.

The effluent was monitored at 0, 2, 4, 6 and 24 h for both bacteria and phages. There was an initial drop in numbers for both bacteria and phages as seen in the previous tests. Interestingly, there was an increase of phages at 4 h that presumably was due to a release of progeny virions overcoming the dilution effect of the continually perfused model. Phage numbers exhibited a reduction at 6 h but then increased by 24 h, finishing at 1.66×10^7 which is a $1.18 \log_{10}$ reduction compared to time 0. The numbers of bacteria in the effluent were significantly reduced in the phage treated models. After 24 h, viable counts were 9.33×10^6 CFU/ml in phage treated catheters compared to 1.24×10^8 CFU/ml in untreated control catheters, representing a statistically significant ($p=0.0204$) $1.12 \log_{10}$ reduction. The pH of the models remained very similar between the treated verses control until the end of the experiment when pH raised marginally in the treated, from pH 6.08 to pH 6.55 at 24 h. In contrast the pH in the untreated models rose to pH 7.98 after 24 h. Again, this is consistent with what was observed with electron microscopy and what is expected as crystal formation has been shown to occur in patients at pHs above 7.58 (Choong *et al.*, 2001). Scanning electron micrographs (Figure 47) for

vB_PmiP_#3 exposed catheters show minimal crystal formation in the control catheter that was further reduced in the phage treated catheter. The eye hole which typically collects some crystalline biofilm, appears comparable to the control and the only observable difference was seen in section iv where deposits had started to form in the lumen of the control catheter.

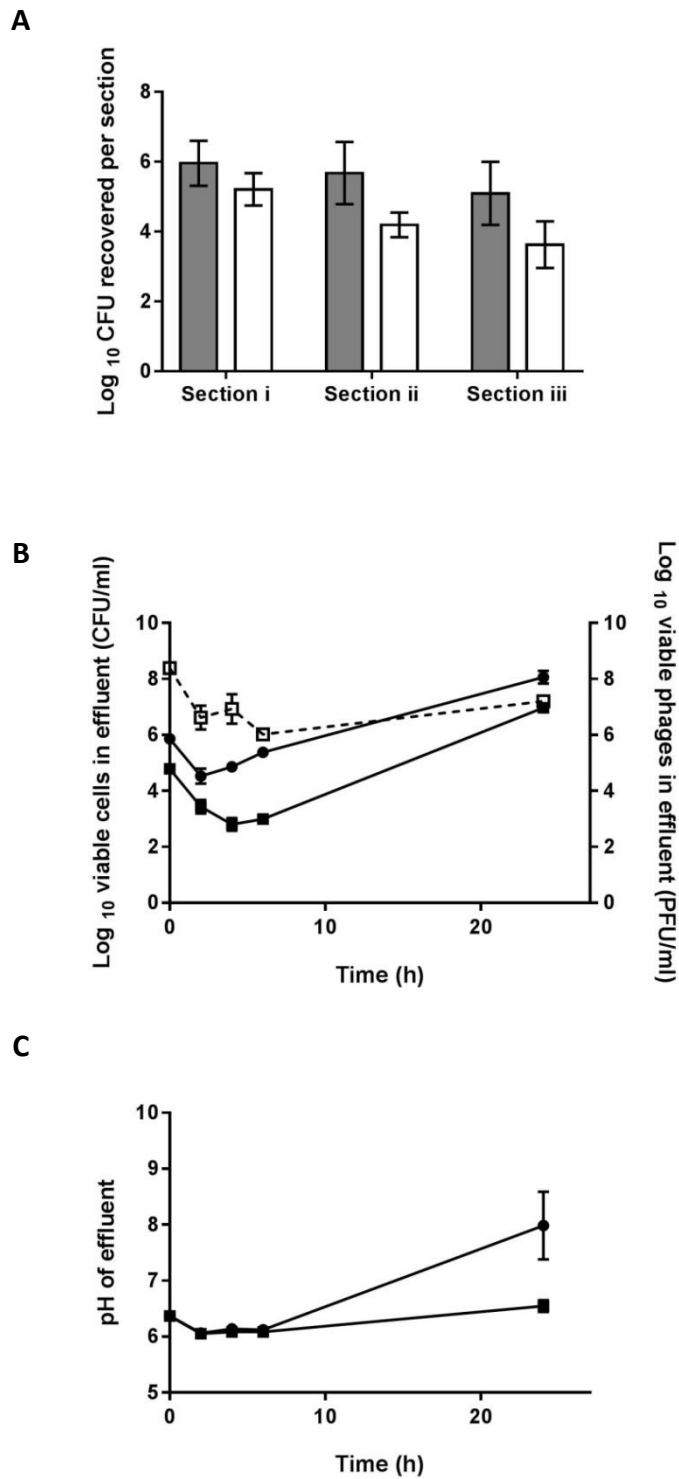


Figure 46. Impact of phage pre-treatment on bacterial biofilm formation by *P. mirabilis* #3. (A) Bacteria recovered from each section i, ii, and, iii. ■ = control and □ = phage treated. (B) Viable bacteria and phages in the effluent of the models, ● = bacteria from control models, ■ = bacteria from phage treated models, and, ◻ = phages from phage treated models. (C) pH of the effluent of the models. ● = control models, ■ = phage treated models. Data points represent the average of three experiments, error bars are standard deviation. Statistical analysis was performed by one way ANOVA with the Bonferroni *post hoc* test.

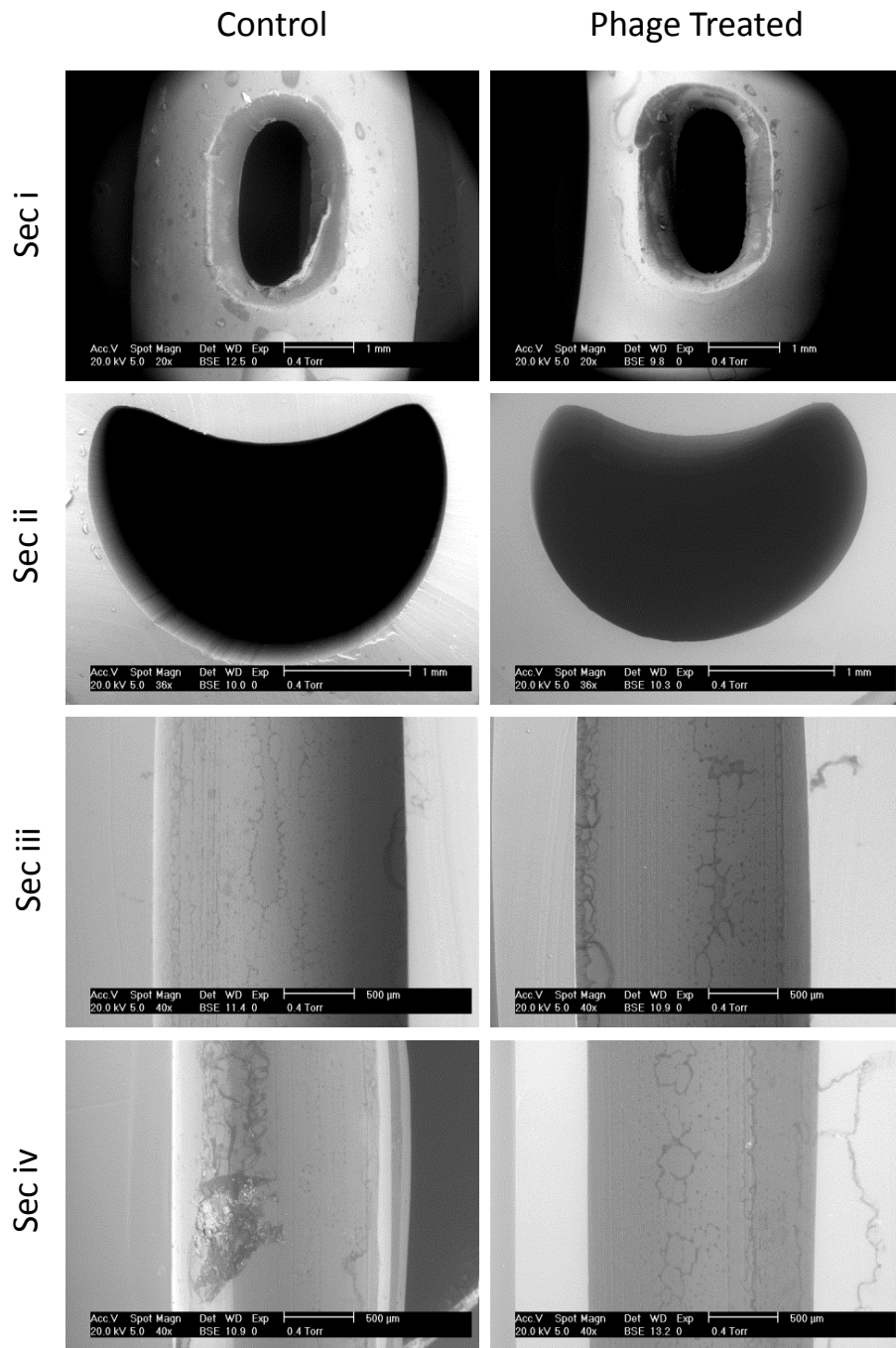


Figure 47. Scanning electron micrographs of un-treated and phage treated catheters removed from the *in vitro* bladder model system after 24 h. Models challenged with *P. mirabilis* #3 at 5×10^6 CFU. The control models show the encrustation that formed as a result of urease activity elevating the urinary pH leading to the formation of mineral deposits. Section i shows the eye hole of the catheter. Section ii is a cross section, distal to section i. Section iii is from 3 cm below section i and section iv is from 3 cm below section iii. Arbitrary regions were chosen for visualisation.

4.2.6 *In vitro* bladder models, 24 h experiment, *P. mirabilis* D3

Phage vB_PmiM_D3 was embedded in the hydrogel coating of the catheters prior to challenge with 5×10^6 CFU. Approximately 1.30×10^{11} PFU were associated with the catheter surfaces giving a MOI of 26,000:1 phages to bacteria, greater than titres obtained for vB_PmiS_NSM6 and vB_PmiP_#3 which were approximately 8,000:1.

After 24 h there was a $1.32 \log_{10}$ reduction in bacterial numbers as seen on section i from the tip of the catheter, compared to the control. Section ii experienced a $1.71 \log_{10}$ reduction, and section iii a $1.92 \log_{10}$ reduction in adhered bacteria (Figure 48). Bonferroni's *post hoc* analysis revealed that between sections from the same regions the differences observed were not statistically significant.

As observed for the models using the different phages, numbers of bacteria dropped initially and then increased from 4 h in the control models, but was delayed until 6 h in the phage treated models. Initial numbers of bacteria differed in the phage treated models with fewer bacteria being present in the effluent at the time of plating, despite the same homogenised culture being used for all models. Presumably lysis had begun before numbers could be analysed. From 6 h numbers of bacteria increased until 24h where the numbers of bacteria for both phage treated and control were similar with 2.97×10^7 CFU/ml and 2.99×10^7 CFU/ml respectively. The concentration of phages in the effluent of phage treated catheters reduced from the start of the experiment, suggesting that a proportion might be eluting from the hydrogel. After 2 h, the numbers in the effluent plateaued and from 6 h onwards numbers increased indicating productive infections releasing progeny virions. The numbers of phages at 24 h roughly equalled the numbers in the effluent at commencement with 1.89×10^8 PFU at the start and 2.69×10^8 PFU at the end of the experiments. The pH of the effluent was very similar for both phage treated and the control catheters, with only a marginal difference in the final pH of 8.53 and 8.31 for the control and phage treated, respectively.

The scanning electron micrographs obtained (Figure 49) show a clear difference between phage treated and control. Section i had very little encrustation forming round the eyehole of the catheter whereas the control has large amounts of mineralised deposits. Unfortunately some of the deposits at the base of the eye

hole broke off during the processing of the sample, but it is possible to see the depth of the deposit in the cross-section. In the transverse section of the catheter (section ii) encrustation is clearly visible on the control catheter but absent on the phage treated catheter. The difference between sections iii and iv is similarly pronounced, with the control catheter having substantial amounts of mineralised deposits that are lacking for the phage-treated sections.

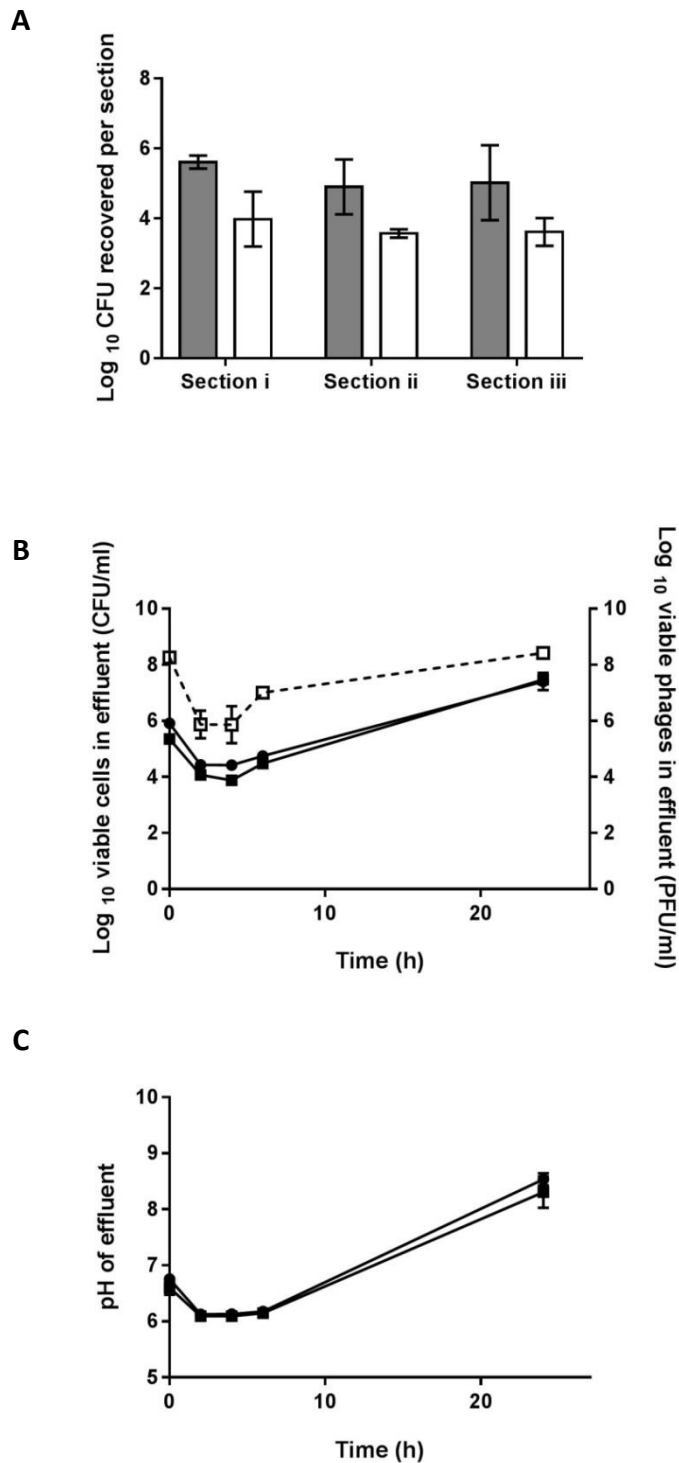


Figure 48. Impact of phage pre-treatment on bacterial biofilm formation by *P. mirabilis* D3. (A) Bacteria recovered from each section i, ii, and, iii. ■ = control and □ = phage treated. (B) Viable bacteria and phages in the effluent of the models, ● = bacteria from control models, ■ = bacteria from phage treated models, and, □ = phages from phage treated models. (C) pH of the effluent of the models, ● = Control models, ■ = phage treated models. Data points represent the average of three experiments, error bars are standard deviation. Statistical analysis was performed by one way ANOVA with the Bonferroni *post hoc* test.

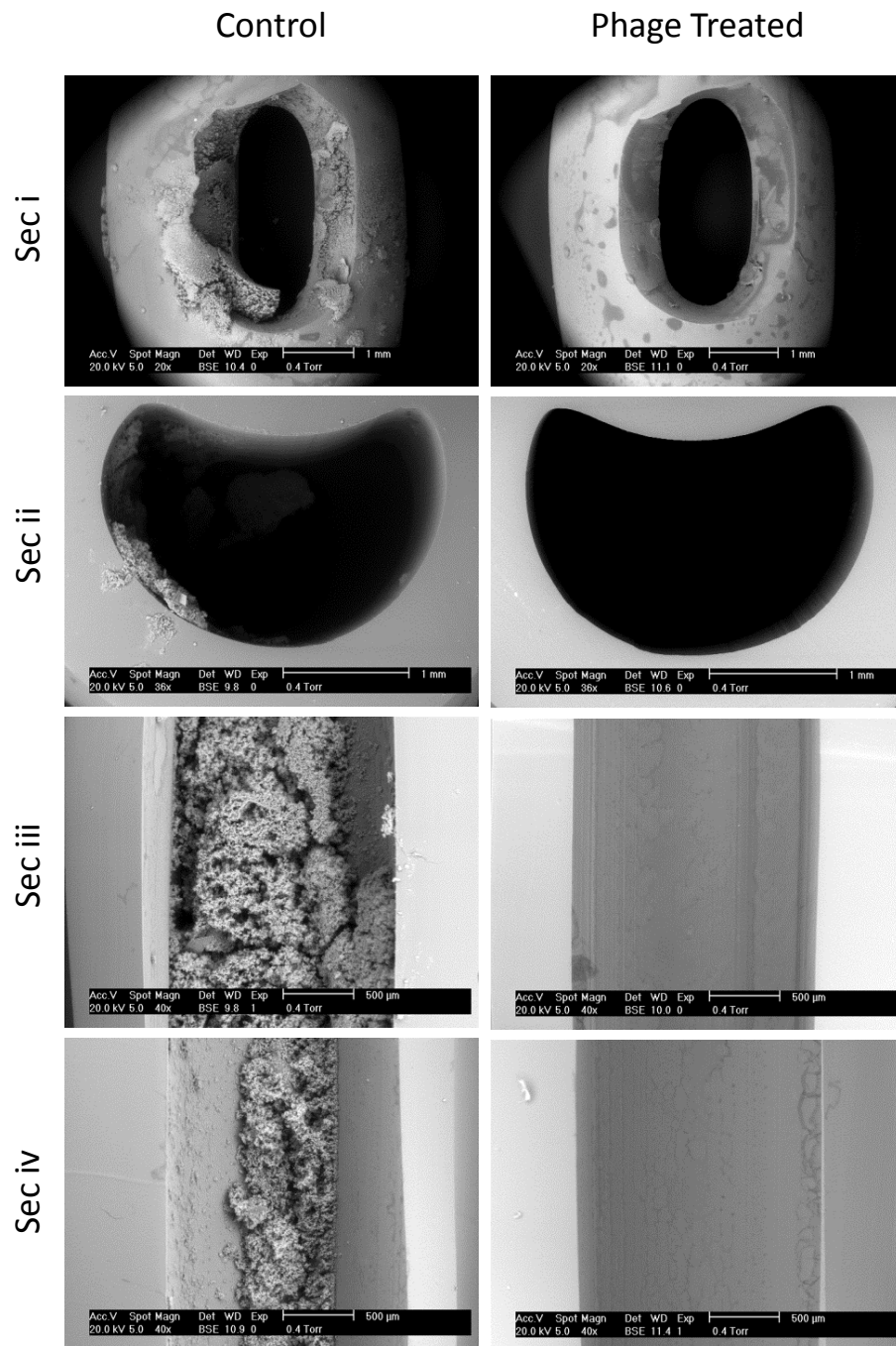


Figure 49. Scanning electron micrographs of un-treated and phage treated catheters removed from the *in vitro* bladder model system after 24 h. Models challenged with *P. mirabilis* D3 at 5×10^6 CFU. The control models show the encrustation that formed as a result of urease activity elevating the urinary pH leading to the formation of mineral deposits. Section i shows the eye hole of the catheter. Section ii is a cross section, distal to section i. Section iii is from 3 cm below section i and section iv is from 3 cm below section iii. Arbitrary regions were chosen for visualisation.

4.2.7 *In vitro* bladder models: Time to blockage experiments

In order to determine time to blockage, the model system (2.21) was inoculated and perfused until urine flow to the drainage bag ceased due to the formation of crystalline biofilm causing occlusion of the catheter lumen (Figure 50).

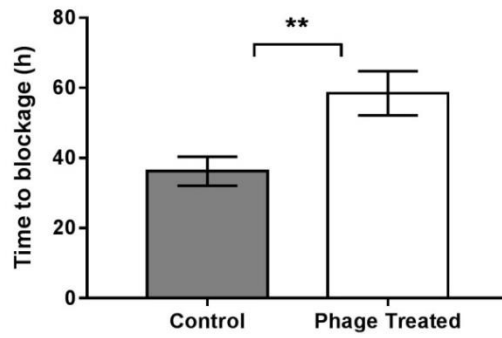


Figure 50. Photograph of a blocked catheter removed from the *in vitro* bladder model system. Crystalline deposits have completely occluded the eye hole and are visible on the tip and balloon. Cuffing, the creases and ridges that form as the retention balloon fails to return to its original size, is also evident.

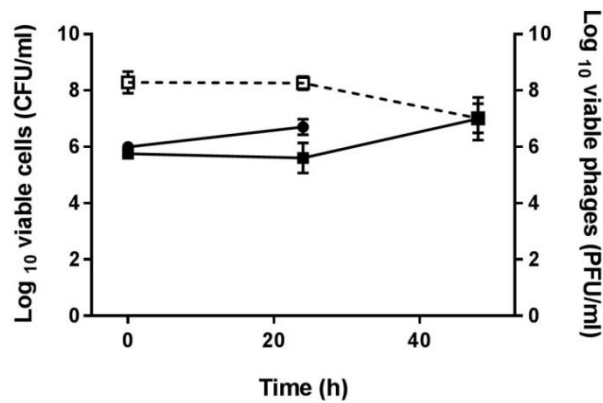
The volume of urine in the drainage bag was used to determine the time the blockage event occurred as the peristaltic pump provided a constant flow rate. Bacteria were added to the models at a density of 1.43×10^6 CFU and phage numbers embedded in the catheter were approximately 4×10^{10} PFU giving a MOI of 28,000:1. The phages were embedded throughout the catheter, however, the bacteria were only added to the residual volume of the model's bladder therefore not all phages initially could come into contact with the bacteria. Bacteria, phages and pH were quantified at 24 hourly intervals. The time to blockage was significantly extended ($p=0.0069$) in the vB_PmiS_NSM6 phage treated models by 61.49 % from 36.2 h for the control to 58.47 h for phage-treated (Figure 51 (A)). The number of bacteria in the effluent appeared to slightly reduce for the phage-treated catheters over the first 24 h, whilst rising in the control to 0.75 \log_{10} higher than at $t=0$. Bacterial numbers in the phage treated models increased after 48 h. Phage numbers in the effluent were similar to the start after 24 h, then, by 48 h their numbers decreased in line with the blockage event occurring. The rise in pH of the effluent corresponds to the blockage event, and elevated pH occurred sooner in the

control models than in the phage treated models (Figure 51(C)) which maintained a relatively stable pH for the first 24 h. The pH of the phage-treated models became elevated prior to blockage events.

A



B



C

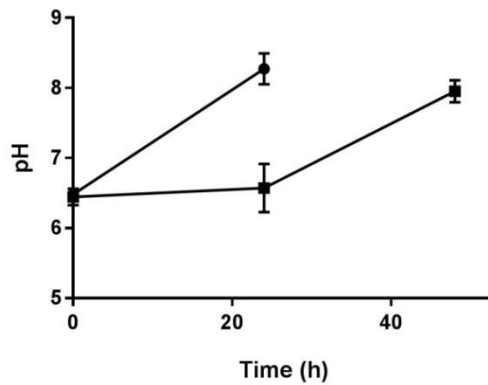
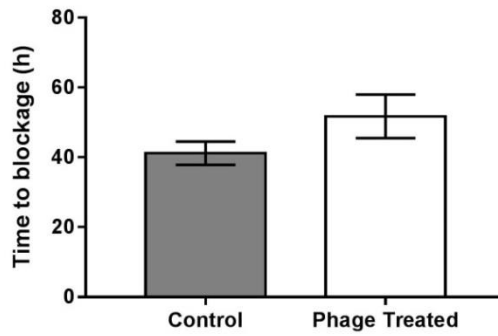


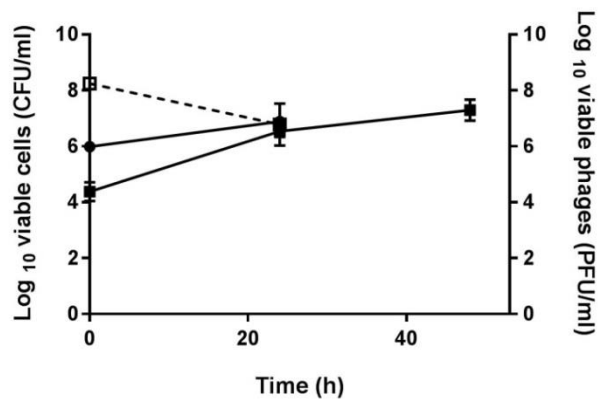
Figure 51. Impact of phage vB_PmiS_NSM6 pre-treatment on time to blockage by *P. mirabilis* NSM6. (A) Time taken for control (■) and phage treated (□) models to block. (B) Viable bacteria and phages in the effluent of the models, ● = bacteria from control models, ■ = bacteria from phage treated models, and, ◻ = phages from phage treated models. (C) pH of the effluent of the models, ● = control models, ■ = phage treated models. Data points represent the average of three experiments, error bars are standard deviation. Statistical analysis was performed by two way student's *t* test, (** = $P \leq 0.01$).

For Phage vB_PmiP_#3, the time to blockage for treated catheters was 51.73 h compared to 41.17 h in the control catheters, representing an increase of 25.67 % (Figure 52) but was not statistically significant when analysed with a two way student's *t* test. Compared to vB_PmiS_NSM6, the bacterial counts in the effluent for phage treated catheters increased during the first 24 h and were only marginally ($0.33 \log_{10}$) less than the control. After 48 h, bacterial counts in the effluent had risen slightly to 2.37×10^7 CFU/ml, however one replicate model had blocked at 44.57 h. As previously observed, the numbers of phages decreased by 24 h from initiation, then dramatically increased and by 48 h were 3.89×10^9 PFU/ml, $1.34 \log_{10}$ above starting titres. Despite bacterial numbers increasing throughout the experiment for phage-treated catheters, the pH remained relatively stable for the first 24 h but reached pH 9 by the end of the experiment.

A



B



C

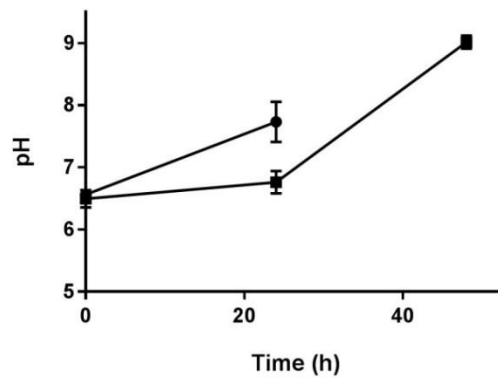


Figure 52. Impact of phage vB_PmiP_#3 pre-treatment on time to blockage by *P. mirabilis* #3. (A) Time taken for control (■) and phage treated (□) models to block. (B) Viable bacteria and phages in the effluent of the models, ● = bacteria from control models, ■ = bacteria from phage treated models, and, -□ = phages from phage treated models. (C) pH of the effluent of the models, ● = control models, ■ = phage treated models. Data points represent the average of three experiments, error bars are standard deviation. Statistical analysis was performed by two way student's *t* test.

Treatment of catheters with phage vB_PmiP_D3 increased the time to blockage by 52.31 %, from 40.97 h for the control models to 62.40 h for the phage-treated models (Figure 53). This increase is statistically significant ($p=0.0029$). The bacterial numbers in the effluent remained relatively stable throughout the course of the experiment with a 0.26 log increase in the control models after 24 h. Effluent from the phage-treated catheters contained fewer bacteria than controls ($0.22 \log_{10}$) at 24 h, but numbers then increased slightly by 48 h to $0.11 \log_{10}$ greater than at $t=0$. The numbers of phages in the effluent of phage-treated models increased $0.77 \log_{10}$ at 24 h, but had reduced by 48 h, albeit still $0.44 \log_{10}$ greater than at time 0. The pH of the control and phage-treated models rose steadily in line with the blockage event, the pH in the phage treated models was lower at 6.9 at 24 h in comparison to 8.16 for the controls. It then rose to pH 8.13 on average after 48 h.

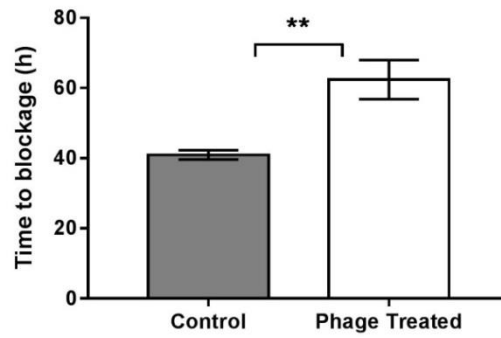
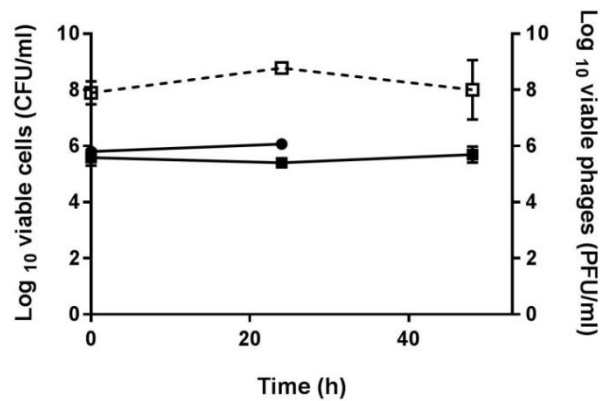
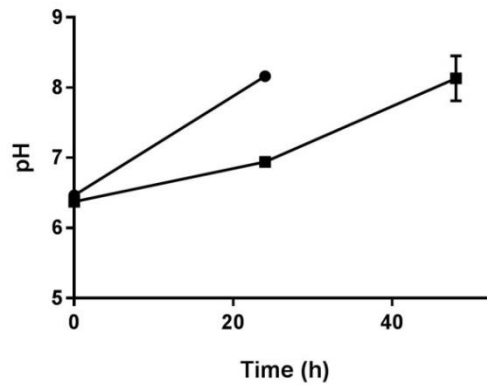
A**B****C**

Figure 53. Impact of phage vB_PmiP_D3 pre-treatment on time to blockage by *P. mirabilis* D3. (A) Time taken for control (■) and phage treated (□) models to block. (B) Viable bacteria and phages in the effluent of the models, ● = bacteria from control models, ■ = bacteria from phage treated models, and, □ = phages from phage treated models. (C) pH of the effluent of the models, ● = control models, ■ = phage treated models. Data points represent the average of three experiments, error bars are standard deviation. Statistical analysis was performed by two way student's *t* test, (** = $P \leq 0.01$).

4.2.8 24 hour *In vitro* bladder models utilising a two phage cocktail

From the host range analysis, it was noted that phages vB_PmiS_NSM6 and vB_PmiM_D3 exhibit lytic activity on each of the propagating strains. This characteristic allowed for the assessment of a two-phage cocktail on the prevention of crystalline biofilm formation in the whole urinary catheter model. The cocktail consisted of a 1:1 ratio of phage and the same total titre was achieved as in the 24 h tests with single phages, in order to allow for direct comparison. As described previously, models were run for 24 h at which point the catheters were removed, and sections excised to quantify adhered bacteria.

For models inoculated with *P. mirabilis* isolate NSM6, a reduction in adhered organisms compared to control sections from untreated models was observed. Section i experienced a 1.43 log₁₀ reduction, section ii a 3.89 log₁₀ reduction and section iii a 2.41 log₁₀ reduction (Figure 54). High error was observed rendering the section ii result the only result that was statically significant. For two replicates of section ii and one of section iii no bacteria were recovered. This, combined with the detection limit of the counting method accounts for the large variability in the observed counts. The pH of the effluent was monitored and followed a similar trend to that seen in single phage 24 h testing. After 6 h the pH of the control models rose with a concomitant rise in viable counts in the effluent. Phages in the effluent of the control models also rose towards the end of the experiment, roughly equivalent to the concentrations observed in the effluent at the beginning of the experiment, indicating that active infection had occurred. Phage treated models had consistently fewer bacteria in the effluent compared to an untreated control, suggesting a phage mediated antimicrobial effect.

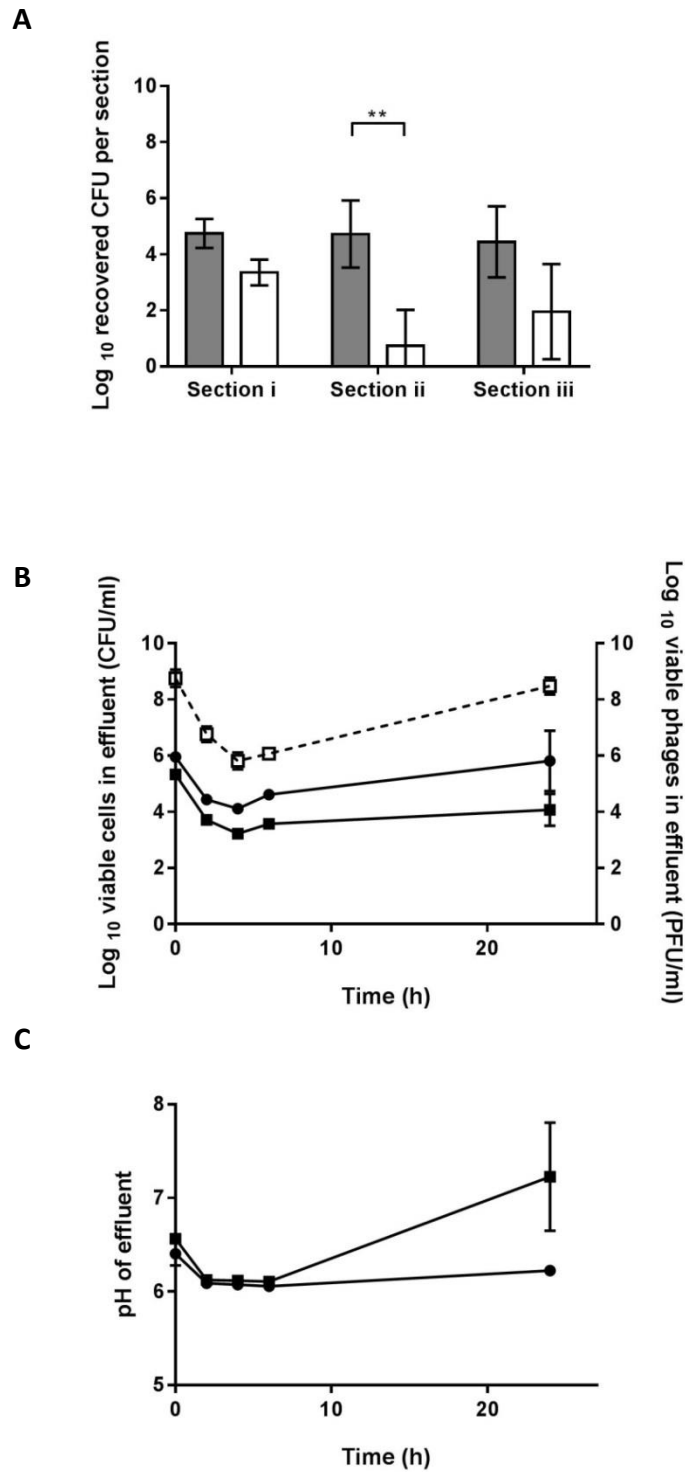


Figure 54. Impact of phage cocktail pre-treatment on bacterial biofilm formation by *P. mirabilis* NSM6. (A) Bacteria recovered from each section i, ii, and iii. □ = control and ■ = phage treated. (B) Viable bacteria and phages in the effluent of the models. ● = bacteria from control models, ■ = bacteria from phage treated models, and, ◻ = phages from phage treated models. (C) pH of the effluent of the models, ● = control models, ■ = phage treated models. Data points represent the average of three experiments, error bars are standard deviation. Statistical analysis was performed by one way ANOVA with the Bonferroni *post hoc* test, (** = $P \leq 0.01$).

For models challenged with *P. mirabilis* D3, the phage treated catheters consistently returned fewer adhered bacteria for the three sections cut from the catheters at the conclusion of the experiments (Figure 55). Section i had a reduction of 2.06 \log_{10} , section ii a reduction of 2.12 \log_{10} and section iii a 2.03 \log_{10} reduction. These data are significant with $p = 0.0050$, 0.0199 and 0.0329 for sections i, ii and iii, respectively. The pH of the effluent was lower at the end of the test compared to the control but exhibit a rise to pH 6.91 from the initial reading of pH 6.36, correlating with a rise in bacterial numbers in the effluent of the control from 1.84×10^4 CFU/ml at 6 h to 3.00×10^5 CFU/ml at 24 h. These data indicate that the phage treatment was not as effective at reducing bacterial numbers especially when compared with the untreated control which only had a marginally higher count of 1.12×10^6 CFU/ml at the conclusion of the experiment. The numbers of phages increased during the experiment indicating a successful continuing infection.

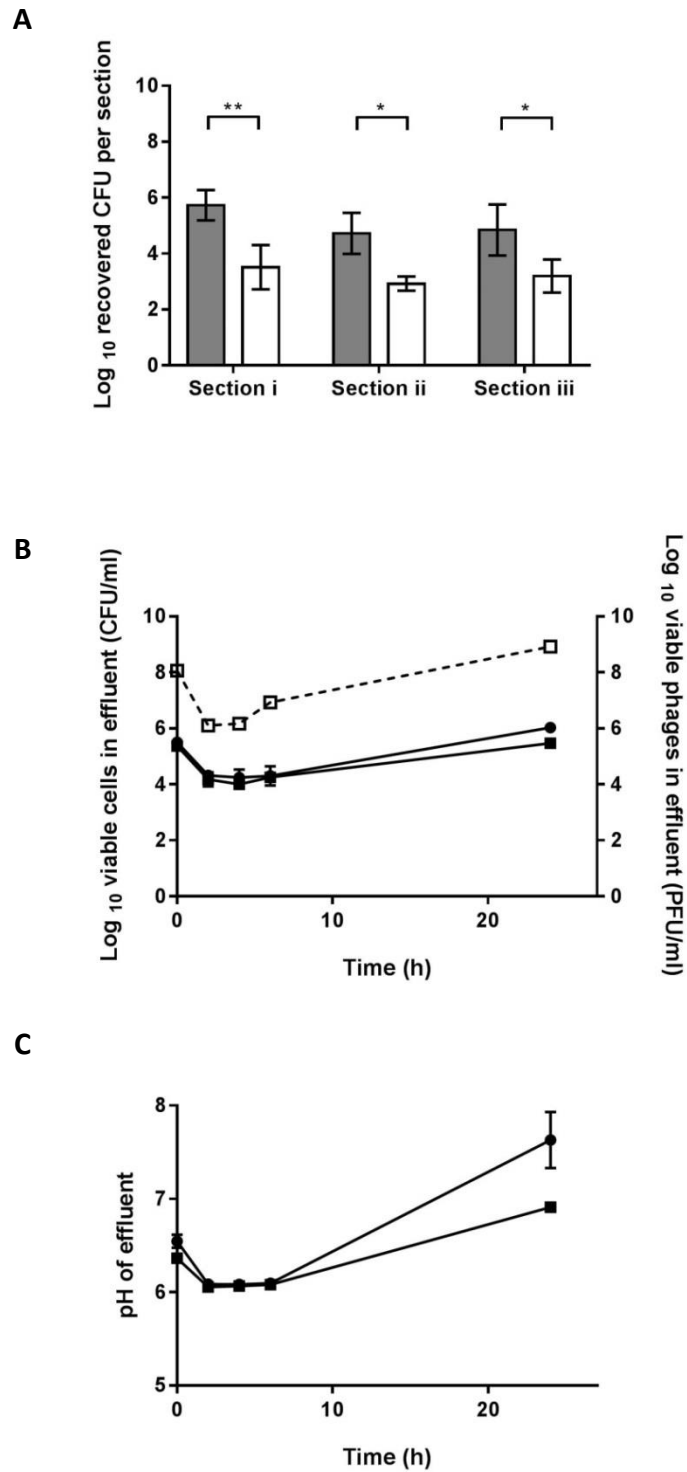


Figure 55. Impact of phage cocktail pre-treatment on bacterial biofilm formation by *P. mirabilis* D3. (A) Bacteria recovered from each section i, ii, and, iii. ■ = control and □ = phage treated. (B) Viable bacteria and phages in the effluent of the models, ● = bacteria from control models, ■ = bacteria from phage treated models, and, □ = phages from phage treated models. (C) pH of the effluent of the models, ● = control models, ■ = phage treated models. Data points represent the average of three experiments, error bars are standard deviation. Statistical analysis was performed by one way ANOVA with the Bonferroni *post hoc* test, (* = $P \leq 0.05$, and, ** = $P \leq 0.01$).

It was important to determine the relative activity of each phage in the cocktail individually in order to assess the activity seen in concert. Phage vB_PmiS_NSM6 was therefore challenged with isolate D3. The sections obtained from the 24 h experiment indicate a very low activity or ability to prevent biofilm formation as sections of phage treated catheters returned greater numbers of adhered bacteria compared to the control (Figure 56(A)). None of these data display a statistically significant difference between phage treated and control. The result for the effluent monitoring tells the same story, with pH (Figure 56(C)) being almost exactly the same over the course of the experiment and bacterial numbers (Figure 56(B)) being almost equal as well.

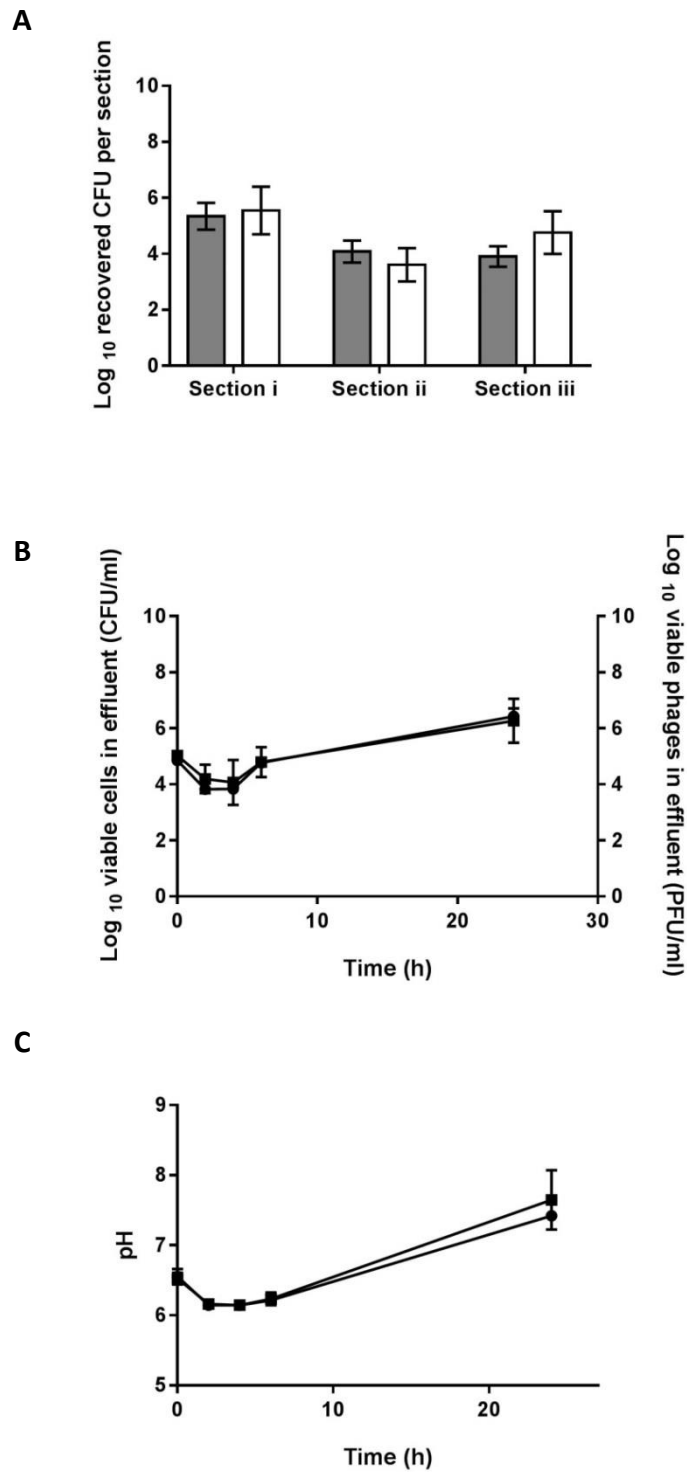


Figure 56. Impact of vB_PmiS_NSM6 pre-treatment on bacterial biofilm formation by *P. mirabilis* D3. (A) Bacteria recovered from each section i, ii, and, iii. ■ = control and □ = phage treated. (B) Viable bacteria in the effluent of the models, no data for phages are available, ● = bacteria from control models, ■ = bacteria from phage treated models. (C) pH of the effluent of the models, ● = control models, and, ■ = phage treated models. Data points represent the average of three experiments, error bars are standard deviation. Statistical analysis was performed by one way ANOVA with the Bonferroni *post hoc* test.

For models where phage vB_PmiM_D3 was challenged with isolate NSM 6 (Figure 57) fewer adherent bacteria were recovered from excised catheter sections after 24 h. Section i yielded 1.96 log₁₀ fewer bacterial cells than control (p = 0.0039), for section ii viable counts were 2.81 log₁₀ less than the control (p = 0.0002) and a 1.83 log₁₀ reduction was observed for section iii (p = 0.0075). The pH of the effluent remained stable in the phage treated models in contrast to control catheters where it increased to > pH 8. The bacteria in the effluent of the phage treated models were reduced overall by 0.13 log₁₀ after 24 h. However, viable counts at 24 h were greater than those quantified at 6 h reading, indicating the bacteria could be overcoming the phage's activity. Indeed, phages in the effluent decreased initially by 2 h, increased to near original levels then slowly reduced by 24 h to marginally less than at the commencement of the experiment.

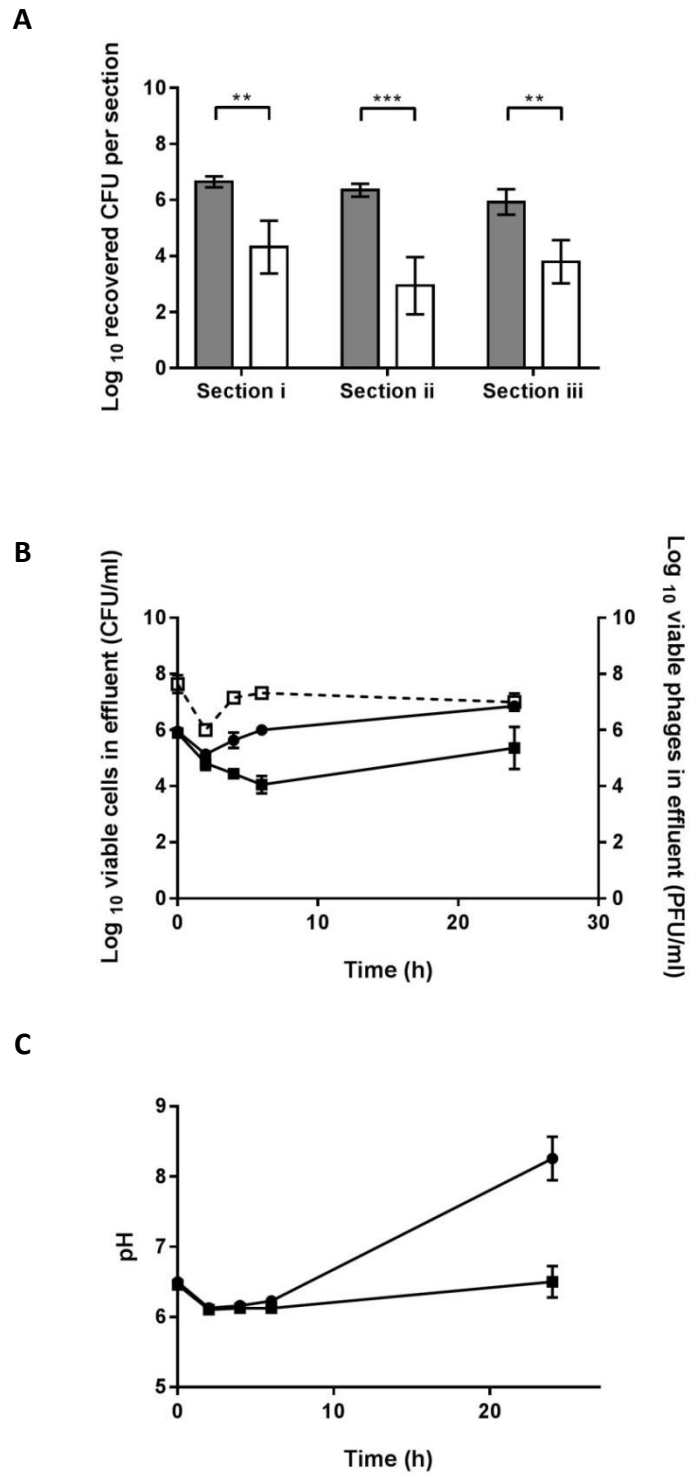
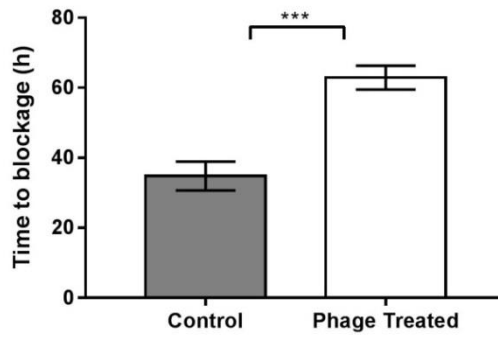


Figure 57. Impact of vB_PmiM_D3 pre-treatment on bacterial biofilm formation by *P. mirabilis* NSM6. (A) Bacteria recovered from each section i, ii, and iii. ■ = control and □ = phage treated. (B) Viable bacteria and phages in the effluent of the models, ● = bacteria from control models, ■ = bacteria from phage treated models, and, □ = phages from phage treated models. (C) pH of the effluent of the models. ● = control, ■ = phage treated. Data points represent the average of three experiments, error bars are standard deviation. Statistical analysis was performed by one way ANOVA with the Bonferroni *post hoc* test, (** = $P \leq 0.01$, and, *** = $P \leq 0.001$).

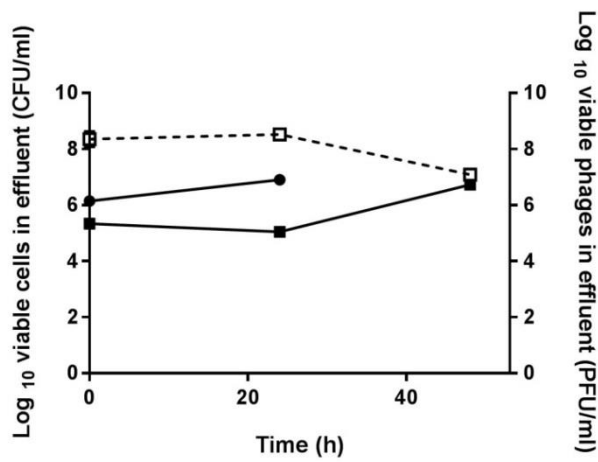
4.2.9 Time to blockage experiments for *In vitro* bladder models treated with a two phage cocktail

Time to blockage experiments were set up as previously described. The model was challenged with approximately 5×10^6 CFU of isolate NSM6 added directly to the bladder. The un-treated control models blocked after 34.8 h in contrast to the phage treated catheters which blocked after 62.92 h (Figure 58). This equates to an increase in time to blockage of 80.81 % and is statistically significant ($p= 0.0008$). The viable bacteria in the effluent marginally decreased in the phage treated models by $0.28 \log_{10}$ after 24 h, but were increased to $1.41 \log_{10}$ greater than at time 0 after 48 h. The number of bacteria in the control models effluent increased $0.76 \log_{10}$ at 24 h. The concentration of phages was slightly increased in the phage treated models after 24 h but decreased by $1.32 \log_{10}$ at 48 h. The pH of the effluent for the control model steadily increased over the duration of the experiment and by 24 h post inoculation reached pH 8.32, up 1.81 units from the beginning of the experiment. The pH of the phage treated models remained relatively stable for the first 24 h of the experiment, exhibiting a slight decrease from pH 6.5 to pH 6.37. After 48 h the pH had risen to pH 8.57, but despite this, blockage did not occur for a further 14.92 h.

A



B



C

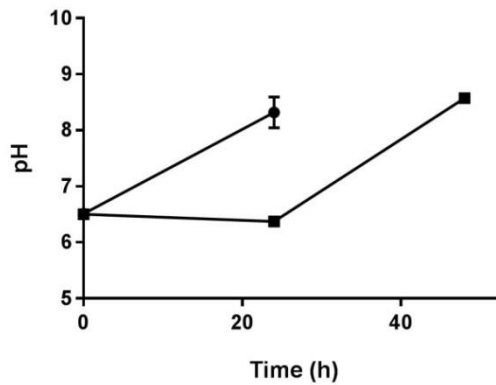
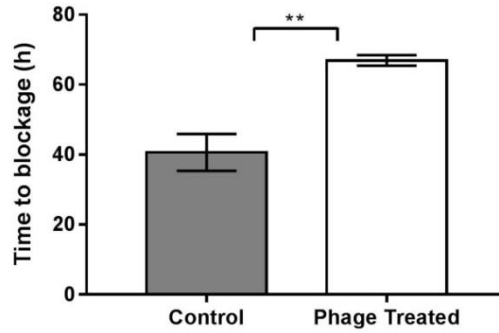


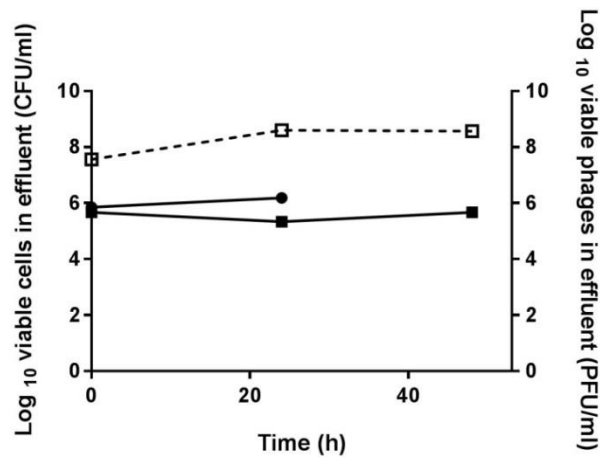
Figure 58. Impact of phage cocktail pre-treatment on time to blockage by *P. mirabilis* NSM6. (A) Time taken for control (■) and phage treated (□) models to block. (B) Viable bacteria and phages in the effluent of the models. ● = bacteria from control models, ■ = bacteria from phage treated models, and, □ = phages from phage treated models. (C) pH of the effluent of the models, ● = control models, ■ = phage treated models. Data points represent the average of three experiments, error bars are standard deviation. Statistical analysis was performed by two way student's *t* test, (***) = $P \leq 0.001$).

The same cocktail was then trialled against isolate D3 (Figure 59) using the same titre of phages and bacteria as before. The time to blockage showed a statistically significant increase ($p= 0.0011$) of 64.61 % from 40.65 h for the control models to 66.92 h for the phage treated catheters. The concentration of viable bacteria in the effluent exhibited a similar trend to that observed previously for the different combinations of phage and host. Viable counts rose for the control model after 24 h by 0.31 \log_{10} , the viable bacteria in the effluent of the phage treated models showed an initial decrease of 0.32 \log_{10} compared to $t=0$, but showed a slight increase of 0.01 \log_{10} after 48 h. The concentration of phages in the effluent of the phage treated models increased after 24 h by 1.04 \log_{10} and then remained relatively stable and reduced only slightly by 0.02 \log_{10} at 48 h compared to at 24 h. The pH of the effluent increased from pH 6.45 to 7.78 at 24 h for the control models whereas for the phage treated models it increased from pH 6.33 to 6.95 after 24h and rose to pH 7.75 by 48 h.

A



B



C

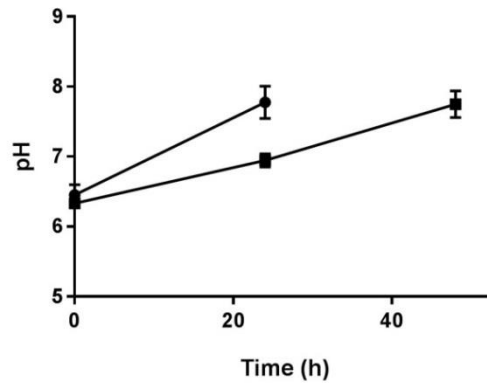


Figure 59. Impact of phage cocktail pre-treatment on time to blockage by *P. mirabilis* D3. (A) Time taken for control (■) and phage treated (□) models to block. (B) Viable bacteria and phages in the effluent of the models, ● = bacteria from control models, ■ = bacteria from phage treated models, and, □ = phages from phage treated models. (C) pH of the effluent of the models, ● = control models, ■ = phage treated models. Data points represent the average of three experiments, error bars are standard deviation. Statistical analysis was performed by two way student's *t* test, (** = $P \leq 0.01$).

4.3 Discussion

The aims of this work were to validate methods for removing and quantifying adherent bacteria from catheter sections and to assess the use of an *in vitro* bladder model for investigating the use of bacteriophages to prevent the encrustation and eventual blockage of urinary catheters.

In order to remove adhered organisms a method was adapted from Curtin and Donlan, (2006) and Fu *et al.* (2010). The method effectively removed the majority of adhered organisms within two rounds of the process. When removing adhered organisms, a fine balance must be struck between recovery and maintaining viability. It was interesting to note that, in contrast to results presented by other researchers, it was not possible to remove all the bacteria present using this technique (Curtin and Donlan, 2006; Fu *et al.*, 2010). This observation might be explained by the adhesion characteristics of *Proteus mirabilis* (highlighting why this is such a problematic bacterium). Differences in equipment and organisms could explain the differences observed between the reported results of this removal procedure. Whilst it was not possible to remove all the adhered organisms, a consistent approach that removed greater than 99% of the adhered bacteria was sufficient to act as a measure of adhered organisms. [Some researchers (Holling *et al.*, 2014; Melo *et al.*, 2016) have utilised a staining procedure in order to quantify the adherent bacteria by measurements of absorbance. This approach was not considered here due to unacceptable error and reproducibility experienced with this technique at our institution.]

As a delivery method for bacteriophages in a commercial product, immobilisation within a coating is a rational solution. It would require no extra intervention from healthcare professionals and would place the phages where they need to be to prevent the migration of bacteria over the catheter surface. The advent of the closed drainage system has ensured that bacteria initially gain access to the bladder extra-luminally, unless the bladder is already contaminated from a previous CAUTI. Placing the antimicrobial at the site of initial infection should, in theory, improve the chances of tackling the infection before it reaches the bladder and proliferates. Following the procedure of Curtin and Donlan (2006) phages were immobilised in

the hydrogel coating of the lubri-sli catheter (C R BARD™). BARD designed the catheter to be more lubricious to ease insertion and removal, an issue associated with all designs of silicone catheters. Whilst allowing phages to embed in the matrix, it also improves the ability of bacteria to adhere to the catheter surface reducing time to blockage (Morris, Stickler and Winters, 1997). This method was utilised to adhere phages to the catheter surfaces as it is convenient and has proven to be effective. It was necessary to know the quantity of phages that were immobilised within the catheter hydrogel coating so phage PFU/ml was determined for the solutions that were applied and after application, the difference between the two measures being what was left on the catheters' surfaces. Whilst some phages are lost to the stripettes, syringe and the container that held the inverted catheter, this loss was assumed to be minimal and unavoidable. The approach was considered the only option available as any attempt to remove the phages from the surfaces using sonication or vortex mixing would result in shearing of the tails of phage rendering them non-infective (Schatten and Eisenstark, 2007). It would also be quite difficult to ensure all virions were removed by the processes described here, as no direct means of visualisation is easily possible. It is interesting to note that the numbers of adhered phages differed for each phage type and those possessing shorter tails obtained higher levels of immobilisation. The reasons for this remain undetermined and would require a lot more variation in virion sizes to enable testing. A potential drawback of the passive immobilisation approach employed here is that the orientation of the phages is not known nor controlled in any way. This would not be an issue when phages elute from the surface but when bacteria come into contact with the surface, a "tails up" orientation might make their presence more effective. Hosseinidoust *et al.* (2011) showed that efficacy of infection is reduced for asymmetric (tailed) phages immobilised onto surfaces and postulated it was due to the orientation of the phages preventing the recognition machinery coming into contact with the host cell receptor. Enhanced efficacy of immobilisation has been demonstrated by Pearson *et al.* (2013) through the use of microwave plasma reactions in the presence of maleic anhydride to bind phages to polyethylene (PE) and polytetrafluoroethylene (PTFE) surfaces. The orientation of the phages was favourable and phage activity was maintained. Whilst this approach is attractive, in the catheter environment the release of free phages is beneficial, as

infection could be tackled more rapidly than waiting for bacteria to reach the catheter, therefore, a combined approach would represent an ideal delivery method.

Prior to the use of the *in vitro* bladder model system testing was undertaken utilising a method adapted from Carson, Gorman and Gilmore (2010) on sections of catheters suspended in broth that were incubated for 24 h at 37°C. The results obtained indicated that phage pre-treatment of catheter sections was not effective in reducing biofilm formation. In fact, in many instances the use of phages was associated with increased numbers of adhered viable organisms verses a control, as was seen for the statically significant result using bacterial isolate D3, with its respective phage at 10^9 PFU/ml. Whilst the data for isolate NSM6 seemed to show reduced adhered bacterial numbers, none of these data are statistically significant. The problem with this approach was that the numbers of phages were too low to be able to prevent bacterial growth in the 10 ml of culture in which the sections were suspended. A small proportion of the phages would have eluted from the surface but they would have not been sufficiently numerous to exert an effect over the planktonic bacteria. It is possible that resistance occurred to the phages but more likely they were overwhelmed by the volume of the media and the quantity of bacteria that grew within it. The fact that the results for #3 and D3 show greater numbers of adhered bacteria could be due to a conditioning film of lysed bacterial cells masking any phage effect and providing a stickier surface to adhere to. In fact, lysed cells formed a sticky mass in the bottoms of the tubes and the constant rotation of the vessels kept this mass in contact with the catheter sections. Despite the result observed from this analysis, due to the perceived issues with the test, it was still deemed worthwhile to continue with testing the phage-treated catheters in the *in vitro* bladder model system as it provides a more realistic challenge.

The bacteriophage vB_PmiS_NSM6 displayed an ability in the 24 h *in vitro* bladder model tests to reduce bacterial numbers adhered to the catheter sections. The three sections, i, ii, and iii, had reduced counts by 3.65 \log_{10} , 3.9 \log_{10} , and, 3.44 \log_{10} , respectively. This result compares favourably to what other researchers have reported for *P. mirabilis*. Carson *et al.* (2010) and Melo *et al.* (2016) observed a 1 \log_{10} reduction with their respective methods and organisms used. A slightly better

reduction was obtained by Lehman and Donlan (2015) of 2.5 log₁₀, however, this result was from a four phage cocktail after 48 h, as no difference was observed after 24 h. For other bacterial species, better-phage mediated reductions on catheter surfaces are reported in the literature. Fu *et al.* (2010) observed a 4.03 log₁₀ reduction by pre-treating a catheter with phage M4 and challenging it with *P. aeruginosa*. Similarly, Curtin and Donlan (2006) saw a reduction in *S. epidermidis* biofilms of 4.47 log₁₀ when supplementing the media with divalent cations, and 2.34 log₁₀ without. Divalent cations appear to be essential for adsorption by a number of phages. It is worthwhile noting that the catheter experiments in the above examples did not use whole catheters and therefore cannot be directly compared. Instead, the tip and funnel were removed from the catheters leaving just the tube and fluids were passed directly through the tube allowing biofilms to form on the internal surfaces. This approach is relevant and can provide useful information but does not take into consideration some of the challenges faced in the real world setting. Specifically, there is no sump of urine in the bladder to act as a reservoir for the bacteria and potentially phages. Similarly, there is no eye hole which usually sits in the sump of urine, which has been shown to be the site of blockage events and significant bacterial attachment due to its irregular topology (Stickler *et al.*, 2003). The fluid flow is likely to be different in the cut catheter models as a solid column of fluid slowly advances whereas in the *in vitro* bladder model the flow is in fits and starts due, in part, to the surface tension of the urine around the eye hole, and the closed drainage system causing a pressure lock. The other main difference with some of the reported experiments is the medium used to perfuse the models. *Proteus* biofilms have been shown to form differently with different media (Jones *et al.*, 2007). Biofilms grown in artificial urine are structurally less well organised, contain crystalline deposits and more swarmer cells are present, when compared to biofilms grown with LB. It was obvious that urea would be required to produce the crystalline deposits indicative of a *Proteus* infection *in vivo*. The exact composition of the artificial urines used differs; some researchers have utilised a composition described by Brooks and Keevil (1997) that contains lactate and citrate as the carbon source and it is thought that this is the reason the biofilms are flatter than with LB. For the work detailed here, an artificial urine recipe was used following that of Griffith, Musher and Itin (1976) formulated to mimic the concentrated urine

of an elderly patient (Stickler and Morgan, 2006). It differs quite significantly from the Brooks and Keevil artificial urine and causes encrustation to occur at a faster rate as there is almost double the concentration of urea. The pH of the Griffith formulation was lower at pH 6.1 versus pH 6.8 for the Brooks and Keevil formulation, which may have an effect on the rate of mineral formation.

Monitoring the effluent for the duration of the 24 h experiments has given an insight into the dynamics of bacterial and bacteriophage interactions. For the NSM6 24 h models, numbers of bacteria and phages reduce for the first 4 h of the experiment. This observation can be attributed to the washing out of the catheters with artificial urine that flowed at 0.5 ml/min through the models. Whilst large numbers of phages appeared in the effluent, it does not seem reasonable that they just were washed out but, rather, represent a combination of elution and productive infection. A similar situation was observed for the bacteria. The bacterial inoculum was directly placed in the bladder of the models and a similar concentration was eluted at $t=0$ to that which was initially added to the models. Numbers of viable bacteria in the effluent then decreased due to the constant perfusion of the model diluting the residual volume in the bladder. The bacteria would require some time to form biofilms on the surfaces and numbers increased from 4 h. A similar increase was seen in phages after the 4 h sample, indicating productive infection and that they were controlling bacterial populations, albeit not completely eradicating them. It is interesting to compare the pH of the effluent with the above data. The pH of the control models increased after 6 h and finished the experiment at pH 8.22 on average. The phage treated models maintained the pH at levels not too dissimilar to the media supplied. This ability to maintain a lower pH, presumably due to the reduced numbers of bacteria, prevented the formation of crystals and, therefore, the mineralisation of the biofilm that had formed on the catheters' surfaces. This finding is corroborated with the scanning electron micrographs obtained (Figure 45) as no mineralised deposits are present on the phage treated catheters. This is directly a result of the pH as crystals only form once the nucleation pH of the urine is achieved. Bacteria had still adhered to the catheters' surfaces but had not begun the process that would eventually lead to blockage.

Models that were challenged with isolate #3 and its phage vB_PmiP_#3, showed no statistically significant reduction in bacterial adherence to the sections after 24 h, although there were consistently fewer adhered bacteria on the catheter sections pre-treated with phages. One reason for this is that this isolate's ability to produce mineralised biofilm is not as effective as NSM6 and D3. This can be seen in the scanning electron micrographs (Figure 47). Only a small amount of crystal formation had occurred in section iv of the control model but only to a minimal degree. Different *Proteus* strains do have different potencies of urease activity and, therefore, varying abilities to cause blockage of a urinary catheter. Whilst some isolates can be deficient, #3 is able to utilise urea and eventually block the catheter. The results obtained for sections i-iii (Figure 46) show $> 1 \log_{10}$ reductions versus control. This is not too dissimilar to the experience of other researchers' attempts to reduce *P. mirabilis* on catheters (Carson, Gorman and Gilmore, 2010; Melo *et al.*, 2016). When monitoring the effluent the effect of phage was clear. The control models' numbers of bacteria increased after 2 h and continued to do so until the end of the experiment. The bacteria in the effluent of the phage-treated models only increases after 4 h and at 6 h was only marginally higher. An increase in phages in the effluent at 4 h was observed (Figure 46 (C)) in line with the reduction of bacteria. Again, no increase in effluent pH was seen in the phage-treated model therefore preventing the precipitation of calcium and magnesium phosphates. The control models' pH increased but not to the extent seen with models challenged with NSM6 or D3, perhaps highlighting the isolates lack of ability to form mineralisation as rapidly as some of the other isolates.

For 24 h experiments with bacterial isolate D3 and phage vB_PmiM_D3, a statistically significant difference was seen with the numbers of adhered bacteria on section i versus a control. The other sections did not return a statistically significant difference despite $> 1 \log_{10}$ reductions for section ii and iii across the three repeats. Presumably this is due to the variation observed with these results as a high standard deviation of measurements was observed. Perhaps further repeats of the experiment would reduce the standard deviation. The results of the effluent monitoring detail a different story as seen with the other *P. mirabilis* strains. Phage treated models did not produce significantly fewer bacteria in the effluent when

compared to the control and pH was not vastly different compared to the control either. This is interesting as > 1 log reductions in bacterial numbers were occurring after 24 h and the scanning electron micrographs show a clear difference between the phage treated and control models (Figure 48). Phages in the effluent did increase after the initial drop in numbers so productive infections were occurring just not at a rate fast enough to reduce bacterial numbers in the effluent. It is possible that the phages were exerting an effect on the surfaces of the catheter but the residual volume in the bladder was supplying the effluent with the bacterial numbers observed. The pH increase is more difficult to explain; the scanning electron micrographs show that no encrustation had formed in the phage treated models but the pH was not dissimilar to the control models. It is possible that a phage resistant mutant arose that was less able to form biofilm and this could be the reason for the observed results, but without confirming this hypothesis no real conclusions can be drawn. Another possibility is the action of EPS degrading enzymes disrupting the biofilms, thus leading to less surface growth and attachment. Whilst this phage did not show the halos around plaques on semi-solid media, EPS degrading enzymes could still be present on the tail/attachment machinery of the phage, or released during lysis, and it is possible that these may be responsible for the reduced mineralised biofilm formation.

The application of bacteriophages significantly increased the time to catheter blockage by 61.49 %, 25.67 %, and, 52.31 % for catheters treated with vB_PmiS_NSM6, vB_PmiP_#3, and, vB_PmiM_D3, respectively. This represents a significant increase in the time a catheter could be in place, especially considering only one phage type was utilised against the isolates. It is worth noting that the model system used here represents a worst case scenario, with highly concentrated urine being supplied at a slow rate and a reasonably high initial bacterial challenge delivered directly to the bladder. In the clinical setting, patient catheters typically block in weeks, not days. Nzakizwanayo *et al.* (2015) investigated the effect of bacteriophage treatment, with time to blockage as a therapeutic end point in a very similar bladder model system. They observed a 3 fold increase in time to blockage when modelling a late-stage infection and complete eradication of bacteria in an early-stage infection. Some key differences might explain the enhanced activity.

Firstly, they were using a three phage cocktail in their model system. This should give enhanced efficacy as resistance can be overcome if it arises if members of the cocktail utilise different bacterial receptors. It was not reported if their three phages targeted different receptors but this cannot be ruled out. Secondly, the delivery method and quantity of phages were different. They simply supplied bacteriophages to the bladder, which would ensure a high initial MOI. The way the models were infected also differed as, after adding the bacteria to the residual volume of the bladder, they allowed 45 min for the bacteria to establish. Following the establishment period, they added phages and then waited 15 min before beginning the flow of urine. This would allow the phages time to infect the bacteria and prevent any washout, further enhancing the effects of the phages. Two scenarios, early and established infection, were investigated. It is not clear how they decided upon the numbers of bacteria to add to simulate these infections, but they chose 10^{10} , and, 10^3 CFU for established and early phase, respectively. They added 10^{10} PFU of the three phage cocktail thus achieving a 1:1 MOI for established infection and $1:10^{-7}$ MOI for early. At such a high MOI it is clear why the early model was so effective with very high numbers of phages present and a period of phage-bacterial absorption, lysis from without would almost certainly be occurring, adding another mechanism to the approach's success. It is unfortunate the effluent was not monitored as it would be interesting to know if viable bacteria existed after the initial incubation period. Whilst these approaches differed from the ones detailed in this study, the data is still valid and shows the potential of this treatment in tackling CAUTI.

A significant issue with the work detailed in this study is the finding that the phages employed here are predicted to encode genes involved in lysogeny. This would have an effect on the infection dynamics as lysogeny does not kill the bacteria. Despite the lytic behaviour of the phages they should not be utilised in an *in vivo* setting due to the possibility of reduced efficacy and of horizontal gene transfer imparting some benefit onto the bacteria. With the exception of Melo *et al.* (2016) none of the other researchers discussed above sequenced the genomes of the phages they used, best practise in the West suggests that this is a requirement to prevent unintended consequences occurring from phage therapy. The result obtained in this

work was surprising, especially for phage vB_PmiP_#3 as it showed no sign of being temperate. This really highlights the need to determine as much as possible about any phage used therapeutically, including a detailed study of life cycle characteristics.

The activity of vB_PmiS_NSM6 and vB_PmiM_D3 on each other's isolating strain warranted investigation of the phages activity as a two phage cocktail to determine if a longer lasting antimicrobial effect could be enacted. Clear reductions in adherent bacteria on the treated catheters were observed after 24 h. The reductions were not as great as the reductions observed for vB_PmiS_NSM6 alone. One problem encountered is that the control sections did not return as high counts as for single phage treatment, so the reductions do not seem as great. In some instances, no bacteria were recovered for phage treated sections and, in these instances, the limit of detection causes the data have a large standard deviation which affects the statistics. In retrospect, samples with low counts should have been plated by a more accurate means. Whilst there is always a detection limit, pour plates could have been conducted using greater volumes of sample. This would have provided greater accuracy for samples that fell below the detection limit used in this study.

The cocktail was also used to challenge *P. mirabilis* D3. Phage cocktail pre-treatment lead to a statistically significant reduction in adhered bacteria after 24 h across all catheter sections. The results compare favourably to results using a single phage.

It was necessary to test the phages against the bacterial isolates that they were not isolated against to gain an understanding of the effect they have in the cocktail. When phage vB_PmiM_D3 was used with isolate NSM6 (Figure 57) statistically significant reductions, not too dissimilar from when the phage was used with its isolating strain were obtained across all catheter sections. The pH stayed relatively stable and effluent counts confirmed that productive infections were occurring. The same cannot be said for phage vB_PmiS_NSM6 and isolate D3 (Figure 56). No statistically significant difference was observed in the catheter sections and, in fact, phage treated catheters had increased numbers in some instances. This is unexpected as the cocktail seemed to have a better effect than the single phage

alone but it is clear the other phage cannot have been contributing to this effect from the results obtained. As this could only be carried out on one occasion, it is not possible to draw firm conclusions from the outcome of the experiment.

Time to blockage experiments utilising the two phage cocktail show an increase in the time it takes for the blockage event to occur. For strain NSM6 the increase is from 61.49 % for individual phage treatment to 80.81 % for the cocktail. For isolate D3 the time to blockage again increased slightly from 52.3 % with a single phage to 64.61 % for the two phage cocktail. It is clear that the cocktail is not preventing the blockage event from occurring. Phage treatment did prevent crystal formation for a time but eventually the bacteria overcome this and blockage occurred. Whilst this is not due to resistance occurring as high counts of phages are apparent in the effluent, the bacteria are overcoming the phages' effect. The numbers and, therefore MOI are an important issue when tackling an infection with phages. Work by other researchers has shown phages' efficacy when used in excess. In a real-world setting phages could be useful in preventing or significantly slowing an infection, although clinical trials would be required to confirm this hypothesis.

Chapter 5 Discussion

The objective of this project was to assess the ability of novel bacteriophages, applied as a catheter coating, to prevent the mineralisation and eventual blockage of urinary catheters in an *in vitro* bladder model system. To fulfil this aim it was necessary to characterise the isolated phages fully. Three novel phages were isolated and their antimicrobial ability was assessed.

An essential step in this work was to have a well-defined bacterial collection to facilitate the isolation of phages, and, to allow host range analysis. All the *P. mirabilis* strains used in this study were of clinical origin; a proportion (20.83 %) were collected from Southmead Hospital, to provide current isolates, and the remainder were from previous studies from different places at different points in time. The aim was to obtain a diverse, representative group of strains to act as a panel which, in theory, should increase the diversity of the bacteriophages isolated, to cover a greater range of strains that are of clinical interest. To gain an understanding of the strains compiled for this work it was decided to carry out PFGE RFLP analysis as, at the time of experimentation, it was considered the gold standard. The information that was gained allowed the removal of duplicates from the library and the formation of clusters that could inform which strains to use for isolations. The best method of choosing different representative bacterial “phage types” is to submit the bacterial library to a set of typing phages. This would contain phages that act on different receptors, therefore ensuring a bacterial representative of each “type” is present in the isolations to facilitate obtaining phages with a diverse receptor targets. Unfortunately, no set of typing phages was available so the only means of defining the library was via the properties of the bacteria. With hindsight, the method was probably too involved and time consuming. It provided more information than is required to remove duplicates from the library, as a simple Dienes reaction should have given similar results, albeit with less discriminatory power (Sabbuba, Mahenthalingam and Stickler, 2003). Other researchers investigating phage prevention of catheter infections (Curtin and Donlan, 2006; Carson, Gorman and Gilmore, 2010; Fu *et al.*, 2010; Nzakizwanayo *et al.*, 2015) made no attempt to define the host range of their phages therefore

limiting the scope of the treatment. Melo *et al.* (2016) did attempt host range analysis; 11 strains were obtained from culture collections (CECT) and 7 obtained from infected urine samples. No analysis was made of the collection. It is reasonably safe to assume strains purchased from culture collections were distinct but the strains isolated from urines could be similar or identical. This invalidates the host range analysis and could lead to a false assumption of broad coverage. A similar situation was observed in the work of Lehman and Donlan (2015). Ten isolates of *P. mirabilis* were obtained from the CDC and used in mixed strain enrichments. Strains were selected for bacteriophage isolations based on their ability to form biofilms in microtiter plates. The host range of the isolated phages, that was likely to contain duplications, was assessed and used to remove duplicate phages from the library. Whilst this approach is legitimate, basing the decision on the ability to form consistent biofilms rather than phage type could limit the breadth of the isolated phages. Proof of principle laboratory testing does not require the same approach as isolating phages for a phage therapy; nonetheless, best practises should be followed to increase diversity.

Isolations were often unsuccessful and ultimately only 3 phages were obtained, preventing selections to be made of the most appropriate phage. For an effective phage, factors that can enhance efficacy are a broad host range and sufficient virulence so that they replicate at a rate faster than they are removed from their site of action. It is also helpful if they are amenable in the laboratory. The lack of a broad host range can be overcome by the application of a phage cocktail, and through various techniques such as Appelmans passage (Appelmans, 1921), but no method exists for improving virulence. The method used in this study to isolate phages from environmental samples is known to introduce a bias in the types of phages that are isolated (Gill and Hyman, 2010). The enrichment technique tends to result in phages that are virulent, as rapidly propagating phages become dominant in the preparations. Moreover, phages tend to have a narrow host range. These characteristics are beneficial when considering phage therapy but prevent the isolation of broader host range or polyvalent phages. One of the purported benefits of phage therapy is the specificity of the interaction, leaving normal flora intact therefore limiting the risks of secondary infections caused by *Candida* or *Clostridium*

difficile for example. A broader host range would still maintain this benefit as, compared to chemical antimicrobials, phages are still very specific. The above observations were experienced with the phages isolated for this study. The host ranges were very narrow. The approach of this study was to isolate phages against a library of strains, whilst the approach in institutions that have practised phage therapy for decades seems to be the maintenance of a well described bank of phages from which bespoke preparations can be constructed (i.e. the Hirsfeld institute) (Kutter *et al.*, 2010). The latter approach would be much quicker, once the library is in place, but the commencement and maintenance of a phage bank was beyond the scope of this project.

For the work detailed here, sewage was used as the environmental source for phages. A great many phages have been isolated from sewage and any source that contains the pathogen of interest should contain phages that infect it (Chibani-Chennoufi *et al.*, 2004). Difficulty was experienced when isolating phages. Initially only strain NSM6 was used for isolations but this approach failed to yield sufficient viruses. Using a panel of isolating strains should have provided more diversity amongst the isolated phages. Every isolate was utilised from the bacterial library in an attempt to increase the likelihood of isolating phages, but this approach still proved to be problematic. One approach that yielded a phage was to pool the samples of sewage from different STWs. Pooling the sample should increase the diversity of the material and increase the numbers of phages present. This resulted in the isolation of vB_PmiP_#3. Using every strain from the library was very labour intensive and required considerable amounts of raw sample. An approach by Lehman and Donlan (2015) and Melo *et al.* (2016) was to combine bacterial strains, 10 and 13 respectively, into single enrichments. This had the effect of widening the diversity of potential hosts within the enrichment although the isolating strain is not known immediately. Another modification that may have yielded more phages could have been to use a greater volume of sewage in the reactions. Nzakizwanayo *et al.* (2015) used 100 ml of sewage in 490 ml total reaction volume and incubated statically, resulting in the isolation of three phages. Lehman and Donlan (2015) and Melo *et al.* (2016) used 50 ml in their enrichment reactions. Unfortunately, the amount of sample available was limited as it had to be supplied by a trained worker

who supplied 500 ml bottles on a bi-weekly basis. Activated sewage sludge was used as a source for enrichments with some success with the isolation of vB_PmiM_D3, however, a great many attempts were made as this material is further along in the processing of sewage and phages may have been removed or rendered avirulent. Curtin and Donlan (2006) and Fu *et al.* (2010) chose to obtain their phages from outside sources (Colindale, HPA) and Carson, Gorman and Gilmore (2010) used LGC standards and isolated phages from a commercially available preparation, Bacteriophage coli-proteic (microgen pharma, Russia). This is a much more convenient approach as no isolation is required and some information is available about the phages to enable selecting the most suitable, however, pre-existing phages would be considered “prior art” and therefore not be patentable. There appear to be few *Proteus* phages described in the literature and only a relatively small number of sequences deposited in the databases; whether this is due to a genuine scarcity in nature, inherent difficulties in their isolation, or a lack of interest experimentally remains to be seen.

The isolated phages that were subject to genetic analysis possessed genes associated with lysogeny, a characteristic that would usually omit phages from further consideration for bio-control or phage therapy. This information was not obtained until after the work utilising the phages as catheter coatings had been completed. This highlights the importance of conducting detailed characterisation prior to any further work. Monitoring the propagation the phages did not hint at lysogenic behaviour, as it is notoriously difficult to identify under standard laboratory conditions. vB_PmiS_NSM6 did produce turbid plaques but not initially and they seemed to be a feature of adsorption time rather than being due to temperate infection. Figure 18 (chapter 3) displays the two plaque types observed after a short (<5 min) and long (10 min) adsorption. Temperate phages are omitted from therapeutic formulations due to the risk of lysogenic conversion, which could confer enhanced virulence upon the bacteria, generalised transduction, where large amounts of DNA are copied across and could potentially transfer genes detrimental to treatment, and, also because they do not lyse their hosts and render them immune to superinfection by similarly acting phages. No bias towards lysogeny was observed with the phages in this study at high MOIs and growth seems to continue

in a lytic manner. This is expected when phages are parasitizing bacteria that are grown in high nutrient conditions as host cell proteases are present in high amount and degrade repressors that control the lytic or lysogenic decision (Ptashne, 2004). Alternatively, it could be possible that the phages are defective mutants that renders them obligatorily virulent, or perhaps they are temperate on a different strain. Further investigation would be required to elucidate their true nature.

The sequence analysis of the phages did not highlight any known antibiotic resistance genes or virulence factors, which is important for considering phages for therapeutic use. Whilst virulent phages are the preferred choice for phage therapy, some success has been observed in laboratory trials with temperate phages. A cocktail that contains different phage types and possesses a tendency towards lytic growth could prevent the prospect of lysogeny not killing the bacteria as another phage that the bacteria are not resistant to is included in the mixture. Matsuzaki *et al.* (2003) and Capparelli *et al.* (2007) both utilised temperate phages successfully in treating *S. aureus* infections in a murine model. The phages were acquired by induction with mitomycin C. It was postulated that it would be possible to render temperate phages virulent by the artificial modification of elements necessary for the integration of phage DNA into the host cell, providing a means of obtaining virulent phages from bacteria for which it is difficult to isolate phages.

Phage vB_PmiM_D3 proved recalcitrant in attempts at purification and DNA extraction. It would not have been taken forward for further study if more phages had been isolated but it was deemed worthwhile as it had a broader host range than the other isolated phages and facilitated the production of a two phage cocktail. As no information is available as to the lifecycle of the phage it would be precluded from therapeutic use until such information was available. It showed no signs of lysogeny when grown in the lab, but this is to be expected in the high nutrient conditions in which it was propagated. A different approach would be required to purify and extract DNA from this phage but potentially useful phages should not be discounted due to difficulty with standard laboratory techniques.

The genetic analysis of the two amenable phages yielded information about their composition and allowed comparisons to be made with similarly described phages.

The method of finding similarity in the sequence/protein databases and inferring function is a standard approach in this field although to date there are few (8) comparable *P. mirabilis* phage genomes deposited in the sequence database. It would be beneficial to confirm the predictions experimentally although this can be labour intensive. Knock out mutations can be created by various approaches, and the effects on infection monitored to assess the possible function. Whilst many genes' functions were determined, many had no match in the sequence databases and remained "hypothetical". The function of these genes might lead to useful discoveries that could have wide ranging applications and provide further information on phage lifecycles.

Catheter-associated urinary tract infection (CAUTI) is the most common healthcare-associated infection globally and accounts for approximately 150–250 million cases per year (Zowawi *et al.*, 2015). The most severe CAUTI complications occur as a result of an infection by *P. mirabilis*. A range of approaches have been evaluated to prevent bacterial colonisation of the catheter, however, all preventative measures have been unsuccessful in clinical use (Morris, Stickler and Winters, 1997; Morgan, Rigby and Stickler, 2009). CAUTIs respond poorly to traditional antimicrobial therapy (Zowawi *et al.*, 2015) and the increase in antimicrobial resistance is exacerbating the problem (Wang *et al.*, 2014). A solution must be sought that can effectively control catheter infection and encrustation. Bacteriophages were selected as a potential antimicrobial agent due to the benefits they are purported to possess. For example, they replicate at the site of infection, are specific and possess low toxicity (Loc-Carrillo and Abedon, 2011).

In this study, whole natural phages were isolated and, after characterisation, used as a catheter coating following the procedure of Curtin and Donlan (2006). Testing the isolated bacteriophages' ability to prevent infection in the *in vitro* bladder model system provided a convenient measure of efficacy in a system that closely mimics the conditions experienced *in vivo*. The phages used in this study showed varying abilities in preventing bacterial colonisation of the catheter surfaces and their use resulted in a reduction in crystal formation after 24 h. Complete eradication of *P. mirabilis* was not observed, mirroring the results of other published work (Carson, Gorman and Gilmore, 2010; Lehman and Donlan, 2015;

Melo *et al.*, 2016; Milo *et al.*, 2017). Only one study to date has achieved complete eradication in a catheter model utilising bacteriophages. Nzakizwanayo *et al.* (2015) achieved this by adding a very high MOI of phages and incubated with no flow for 15 min, allowing for phage adsorption/action. This eradicated the bacteria present and shows that phages might be better at controlling infections initially before numbers of bacteria increase, taking advantage of high MOIs. Utilising lysis from without as a control method negates the issue of resistance occurring which, with single phage treatment, is beneficial. Using phages vB_PmiS_NSM6 and vB_PmiP_#3, the pH of the AU remained around 6.1 for the duration of the 24 h experiments despite numbers of bacteria increasing steadily after 6 hours. The relative suppression of bacterial numbers presumably resulted in less urease production and, consequently, a slower increase in pH. This is corroborated by the SEM images that show little to no crystal formation in the phage treated models. The use of Phage vB_PmiM_D3, however, resulted in only marginally fewer bacteria in the effluent and, therefore, pH increased nearly in line with control models. Despite this rise in pH, the SEM images showed only scant crystal aggregation on the catheter surfaces when compared to control models. This is not easy to explain as crystal formation should have been comparable at the pHs reached. It is possible phage infection led to the emergence of a bacterial strain that had decreased biofilm forming ability and, therefore, fewer crystals formed on the catheter surfaces. It is also possible a component of phage or a product released during lysis had some effect on biofilm. Between 1.32 and 1.92 \log_{10} reductions were observed in phage treated models but these reductions were not statistically significant.

In time to blockage experiments, increase in catheter lifespan was observed with all phages used in this study. The ability to delay the blockage of catheters is beneficial and worthy of further study. Whilst these phages had an effect, bacterial dominance did ultimately occur and, for this reason, other phages active on different receptors would be required to prolong the effect. A two phage cocktail was tested to determine whether resistance could be avoided, but this did not prevent the eventual blockage of the catheter. It is possible that the two phages utilise the same receptor, however further investigation would be required to confirm this assumption. Again, a broader cocktail containing more phages may

overcome this limitation. One factor to consider is that *P. mirabilis* has two distinct physiologies (Jones and Park, 1967) and it is possible that the phages are only active on one type and the conformational changes that occur make the other type resistant to infection. Phage isolations were carried out in liquid culture so it is possible that the swarmer form of the cells are resistant to the phages. Resistance has been reported previously in similar experiments (Fu *et al.*, 2010) and could result from alterations or loss of the cell surface receptor, restriction modification, or other mechanisms of abortive infection such as the presence of clustered regularly interspaced short palindromic repeats (CRISPRs) within the bacterial genome (Labrie, Samson and Moineau, 2010). Resistant bacteria are usually less virulent than the wild type (León and Bastías, 2015) and this is beneficial to treatment outcomes. The other factor to consider is the phages used in this study possessed lysogenic genes therefore it is possible they were entering into the lysogenic lifecycle due to environmental conditions and this could be the reason for the eventual blockage of the catheters.

The investigation of phages has shed light on some important components that might be utilised as antimicrobial agents. Phage vB_PmiP_#3 displayed an expanding halo around plaques formed on agar plates (Figure 18, chapter 3). It has been suggested that these halos can be due to a depolymerase enzyme that can potentially degrade the EPS matrix of the biofilm to facilitate infections (Adams and Park, 1956). Indeed, the lack of crystal formation in bladder models, despite relatively high numbers of bacteria present, hints at some other factor preventing the formation of mineralised biofilm despite *P. mirabilis* #3's comparatively reduced urease activity. The presence of halos was first noted in 1956 by Adams and Park but it was not until work carried out by Hughes, Sutherland and Jones (1998) that the effect was tested on biofilms grown in the laboratory. Depolymerase enzymes facilitate bacteriophage infection by either degrading structural or capsular polysaccharides on the bacterial surface or the EPS in bacterial biofilms. So far 160 putative depolymerases have been identified from 143 phages in the extant databases (Pires *et al.*, 2016). It has been suggested that these enzymes could be used as an adjuvant to traditional antimicrobial therapy, facilitating contact with cells previously encased within the biofilm. Endolysins, holins and spanins have also

been suggested as bactericidal agents (Roach and Donovan, 2015). This approach is perhaps more suited to gram positive bacteria due to the ability to directly access the peptidoglycan layer that the endolysin acts on, but the use of spanins or peptides with outer-membrane disrupting abilities may allow this approach in the gram negative bacteria. There have been some endolysins reported in the literature that are able to permeate the outer membrane, due to the possession of highly cationic or amphipathic regions that interact with lipid polysaccharides in the outer membrane (Carvalho *et al.*, 2017). The aforementioned elements can be used to disrupt the cell wall causing osmotic lysis and cell death. Nelson, Loomis and Fischetti (2001) demonstrated that it was possible, in a mouse model, to reduce carriage of group A streptococci using the endolysin PlyC from phage C₁. Due to the specificity of the enzyme, the commensal community was left intact. Wide ranging applications exist for this technology and the relative ease of production make this an attractive alternative to traditional antimicrobials.

Not all phages possess EPS degrading abilities and it has been postulated that possession of these enzymes may enhance their antimicrobial activity. Lu and Collins (2007) engineered phage T7 to express dispersin B. The engineered phage performed better than the wild type at reducing bacterial biofilms. Indeed, advances in molecular techniques have made it possible to modify phages to perform wide ranging tasks. Technologies seem to focus on using the phage as a delivery vehicle or to tackle a perceived negative aspect of phage infections. For example, Matsuda *et al.* (2005) utilised an engineered phage, LyD, a mutant of T4 that produces a defective holin. An infection still results in cell death but lysis does not occur, limiting endotoxin release. When tested in mice, survival was enhanced. Another approach has been to redirect the host range of bacteriophages. Pouillot, Blois and Iris (2010) introduced point mutations in the receptor binding domain genes of T4. This led to a shift in hosts from *Escherichia coli* to *Pseudomonas aeruginosa* and *Yersinia ruckeri*. Phages have been modified to act as carriers of antimicrobial agents, usually bound to the phage capsid. For example, Yacoby, Bar and Benhar (2007) attached chloramphenicol to filamentous phage fUSE5-ZZ. This approach allowed targeted use of an antimicrobial that is generally not used systemically. The authors reported an improvement factor of 20,000 in growth

inhibition when compared to the free drug *in vitro*. In a similar vein, phages have been trialled as carriers of antigens in the field of vaccinology, a technique termed phage display. The capsid is modified so components that elicit an immune response are displayed. The phages are then administered in the same way as standard vaccines. Sathaliyawala *et al.* (2006) modified T4 phage to display multiple HIV antigens on its capsid. In mice, a strong immune response, both humoral and cellular, was observed. The benefit of this approach is that no HIV genomic sequences are present in the immunogen.

Recombinant phages have also been used in an attempt to increase bacterial susceptibility to antimicrobial agents. Lu and Collins (2009) engineered filamentous phage M13 to overexpress a repressor (*lexA3*) that represses the SOS response in bacteria. Challenge of *E. coli* EMG2 with fluoroquinolones, thought to exert their bactericidal effect via damage of DNA (Kohanski *et al.*, 2007) was more effective in the presence of engineered phages. An interesting finding of this study was that, when testing the approach against a bacterium that already had resistance to quinolones, the application of phages as an adjuvant improved response by 3.5 orders of magnitude and, the authors proposed, could restore obsolete antibiotics back into clinical use (Lu and Collins, 2009). Some concern, however, exists with the use/release of genetically modified phages, in particular that the modified genes will be released and affect the natural population of both phages and bacteria. This problem could be abated by modifying phages to be non-replicative (Paul *et al.*, 2011). However, Gladstone, Molineux and Bull (2012) noted that engineered phages with a gain of function lost the ability to compete with natural phages on the same host as the engineered advantage benefited other genomes and therefore was selected against. This suggests that engineered genomes might not persist in the wild.

A clear benefit of engineered phages is that they can be the subject of patents. Utilising natural phages as antimicrobials is not considered patentable due to being an approach that has been widely used for about a hundred year (Thiel, 2004). Individual phages that have been completely characterised can be patented but the prospect of another similar phage being isolated with better characteristics is likely with so many phages in the biosphere. This, along with other issues, has acted as a

barrier to phage therapy being adopted widely. The regulatory issues around the use of bacteriophages also inhibit the development and implementation of this technology in the therapeutic field. The regulatory framework in the West is largely built around the development of chemical drugs, such as antibiotics. Bacteriophages as self-replicating and self-limiting natural entities are not comparable to single chemical molecules and thus do not fit into the scope of the existing framework. The European Medical Association has been consulted in regard to making a new category for phages, however they expressed only a desire to apply existing regulations (Verbeken *et al.*, 2012). Contradictions exist relative to phages within the existing regulations that further complicate the matter, for example exemptions exist for DNA products but not proteins and polypeptides. Phages contain both. A few trials have been granted permission, usually under the auspices of medical ethical committees, so it seems that there is some hope. Furthermore, the FDA in the USA has designated phages as GRAS (Generally Regarded as Safe) (Kutter *et al.*, 2010). Despite the study of therapeutic applications of phages since shortly after their discovery, there is a lack of high quality scientific studies into their efficacy. This is partly due to the majority of the work being conducted in Georgia and Poland, where emphasis was not placed on double blind clinical trials with the standards considered necessary in the West. There is also concern that the general public might misconstrue the term virus and think that it could cause harm to humans. This may be an issue if this approach is taken up and used more widely, however, it is of benefit that the viruses of bacteria are known as bacteriophages (Loc-Carrillo and Abedon, 2011).

Despite the challenges faced, in a world of increasing antimicrobial resistance, alternatives to traditional antibiotics must be utilised. The work detailed within this thesis offers an insight into the prevention of CAUTI, however, much more work would be required to improve, refine and validate the method. Bacteriophages potentially represent a good option for treating urinary tract infections due to fewer immunological interactions in the bladder than elsewhere in the body (e.g. circulatory system) and the relative ease of delivery. However, the problems inherent with catheter design may not be overcome with the use of any antimicrobial. Phages may be able to reduce the frequency of blockage events,

especially utilising phages as an adjuvant to traditional antimicrobial therapy. If we are to face a post antibiotic future it might be worth remembering the proverb “the enemy of my enemy, is my friend”.

5.2 Further work

Some unanswered questions exist regarding the origin of the phages obtained in this work. As the two sequenced phages are temperate, it is possible that they were induced rather than isolated from the environment. This is especially true for phage vB_PmiS_NSM6, as the same phage was isolated on different occasions during the initial round of enrichment experiments. Therefore, it should be determined whether they are lysogens of the isolating strains by identifying the presence of their genetic material in the bacterial cell. The genomic analysis of the phages yielded the full genetic sequence for two of them, therefore this information could be used to generate PCR primers for conserved regions within the phage genome. If PCR products correspond to the size of the predicted product, then the phages were most likely induced. There are reports in the literature of the isolation of virulent phages against *P. mirabilis* (Melo *et al.* 2016; Nzakizwanayo *et al.* 2015) so further attempts at isolation are warranted. Perhaps the use of virulent phages that are selected for their ability to lyse cultures and infect a wide range of clinical isolates would produce a better result. This hypothesis should be tested to develop this approach further.

The recalcitrant nature of phage vB_PmiP_D3 to purification and DNA extraction is something that could be addressed with further work. The implementation of a sucrose gradient and cushion could be trialled as a means of obtaining a pure sample (Casjens *et al.* 2005). An alternative method of DNA extraction should be sought that does not utilise phenol or chloroform in case these chemicals are preventing DNA extraction. There exists commercially available kits that extract with a spin column format that might be successful. Running samples on gels from each stage of the process could determine if degradation is occurring and if DNA is indeed present.

Further comparative analysis of the phage genomes should be conducted to acquire more information about where they should be placed in the family tree of viruses and potentially find out more information about their life styles. The sequences should be submitted to the database.

The method of attaching phages to catheters used in this work requires further development and refinement. Utilising the hydrogel layer already deposited on catheters was convenient but a coating applied that embeds the phages in a desirable orientation and in a manner that releases phages at a consistent rate, at a sufficiently high titre, would be preferable. It was noticed during electron microscopy that phages aligned in the same orientation when the grids were pre-charged, perhaps offering insight into how orientation could be controlled. Bacteriophages have been bonded to polymeric surfaces in a tails up orientation that retains biological viability (Pearson *et al.*, 2013). This is another option that should be assessed in a catheter model system; although no phages are released, an active infection would produce daughter virions that would be released into the system. Recently Milo *et al.* (2017) described a coating that degrades when alkaline pH occurs. This is an interesting concept, however, arguably, releasing phages when bacteria have reached a high enough titre to alter pH is too late in the infection process and perhaps a coating that just degrades from insertion represents a better approach to tackling infection before it establishes.

Further work regarding the application of this technology should be undertaken to assess its ability to prevent the colonisation of catheters. There exists scope to investigate the ready to use, cocktail strategy verses made to measure approach with the latter representing a favourable method despite the regulatory difficulties, and the need for large phage banks that require characterising and updating on a constant basis. When considering the ready to use cocktail approach detailed in this study, once a cocktail has been assembled that infects a majority of clinically relevant isolates, work should be undertaken to assess the optimum concentration for the cocktail. Using the *in vitro* bladder model, a method of infecting the model could be developed that more closely mimics how an infection occurs in patients rather than the high titre bolus added directly to the bladder as described in this work. The drainage bag of the assembled model system could be infected, allowing

the bacteria the opportunity to migrate to the bladder. Alternatively as extraluminal contamination tends to be the more common source of infection in patients, a method to simulate this should be developed.

Using the phage cocktail as an antimicrobial lock should be investigated to assess if this approach extends catheter longevity. This would be straight forward to test in the model system and analysis could be carried out on the catheters to visualise biofilm removal. Clearly this approach would benefit from phages that possess degradative enzymes that may facilitate removal of the biofilm.

Once a cocktail of phages and a delivery method have been determined for optimal activity, the work could progress to *in vivo* pre-clinical trials using an animal model, such as a murine model, to assess phage activity *in vivo*. Rigorous assessment of immune response and phage resistance, as well as overall efficacy and safety would be required before proceeding to human clinical trials. Clearly, if phages can be used to prevent or inhibit *P. mirabilis* colonisation of urinary catheters, a similar approach would be warranted with respect to the other significant urological pathogens as infections are often multispecies. A catheter that inhibits the most common bacterial urinary pathogens would be beneficial to both patients and healthcare providers.

Finally, the presence of EPS-degrading ability, evidenced by phage vB_PmiP_#3's expanding halos (Pires *et al.*, 2016), warrants further study. The presumptive depolymerase enzyme must first be isolated and purified. Alternatively, if the gene could be identified and then expressed in a suitable host, the resultant enzyme could be assessed in the model of the catheterised bladder, either as a preventative coating or as an antimicrobial lock approach where the enzyme would be instilled into the catheter to clear biofilm. The host range of the enzyme should be assessed on *Proteus* strains and other closely related bacteria. Depolymerase enzymes have been shown to increase the effectiveness of antibiotic (Bansal, Harjai and Chhibber, 2014) therapies, therefore, enzyme-antibiotic combinations could be investigated using the *in vitro* bladder model to determine the potential of depolymerases as adjuncts to conventional treatment of catheter-associated infection.

References

- Abbani, M.A., Papagiannis, C. V, Sam, M.D., Cascio, D., Johnson, R.C. and Clubb, R.T. (2007) Structure of the cooperative Xis–DNA complex reveals a micronucleoprotein filament that regulates phage lambda intasome assembly. *PNAS*. 104pp. 2109–2114.
- Abedon, S. and Thomas-Abedon, C. (2010) Phage Therapy Pharmacology. *Current Pharmaceutical Biotechnology*. 11 (1), pp. 28–47.
- Abedon, S.T., Kuhl, S.J., Blasdel, B.G. and Kutter, E.M. (2011) Phage treatment of human infections. *Bacteriophage*. 1 (2), pp. 66–85.
- Abrams, P., Cardozo, L., Fall, M., Gri, D., Rosier, P., Ulmsten, U., Kerrebroeck, P. Van, Victor, A. and Wein, A. (2002) *The Standardisation of Terminology of Lower Urinary Tract Function : Report from the Standardisation Sub-committee of the International Continence Society*. 61 (1), pp 37-49
- Ackermann, H.-W. (2007) 5500 Phages examined in the electron microscope. *Archives of Virology*. 152 (2), pp. 227–243.
- Ackermann, H.-W. (2009a) Basic Phage Electron Microscopy. *Methods in molecular biology (Clifton, N.J.)*. 501pp. 113–126.
- Ackermann, H.-W. (2009b) Phage Classification and Characterization. In: *Methods in molecular biology (Clifton, N.J.)*. pp. pp. 127–140.
- Ackermann, H.-W. and Prangishvili, D. (2012) Prokaryote viruses studied by electron microscopy. *Archives of Virology*. 157 (10), pp. 1843–1849.
- Adams, M.H. (1959) *Bacteriophages*. New York (and London): Inter-science Publishers.
- Adams, M.H. and Park, B.H. (1956) An enzyme produced by a phage-host cell system. II. The properties of the polysaccharide depolymerase. *Virology*. 2 (6), pp. 719–736.
- Adams, M.J., Lefkowitz, E.J., King, A.M.Q., Harrach, B., Harrison, R.L., Knowles, N.J., Kropinski, A.M., Krupovic, M., Kuhn, J.H., Mushegian, A.R., Nibert, M., Sabanadzovic, S., Sanfaçon, H., Siddell, S.G., et al. (2017) Changes to taxonomy and the International Code of Virus Classification and Nomenclature ratified by the International Committee on Taxonomy of Viruses. *Archives of Virology*. 162 (8), pp. 2505–2538.
- Ahluwalia, R.S., Johal, N., Kouriefs, C., Kooiman, G., Montgomery, B.S.I. and Plail, R.O. (2006) The surgical risk of suprapubic catheter insertion and long-term sequelae. *Annals of the Royal College of Surgeons of England*. 88 (2), pp. 210–213.
- Aksyuk, A.A. and Rossmann, M.G. (2011) Bacteriophage assembly. *Viruses*. 3 (3), pp. 172–203.

- Allison, C., Lai, H.C. and Hughes, C. (1992) Co-ordinate expression of virulence genes during swarm-cell differentiation and population migration of *Proteus mirabilis*. *Molecular microbiology*. 6 (12), pp. 1583–1591.
- Alteri, Christopher J. Himpsl, Stephanie D. Pickens, Shannon R. Lindner, Jonathon R. Zora, J.S., Miller, J.E., Arno, P.D. and Straight, Samuel W. Mobley, H.L.T. (2013) Multicellular Bacteria Deploy the Type VI Secretion System to Preemptively Strike Neighboring Cells. *PLoS pathogens*. 9 (9), e0013608.
- Amtul, Z., Follmer, C., Mahboob, S., Atta-Ur-Rahman, Mazhar, M., Khan, K.M., Siddiqui, R.A., Muhammad, S., Kazmi, S.A. and Choudhary, M.I. (2007) Gamma-lactones as novel inhibitors of bacterial urease activity. *Biochemical and Biophysical Research Communications*. 356 (2), pp. 457–463.
- Andrews, D., Butler, J.S., Al-Bassam, J., Joss, L., Winn-Stapley, D.A., Casjens, S. and Cingolani, G. (2005) Bacteriophage P22 tail accessory factor GP26 is a long triple-stranded coiled-coil. *The Journal of biological chemistry*. 280 (7), pp. 5929–5933.
- Anomyous (2013) *PlusNet PFGE Manual*. Available from: <http://www.cdc.gov/pulsenet/PDF/ecoli-shigella-salmonella-pfge-protocol-508c.pdf>
- Anon (n.d.) *PCI/SDS DNA Extraction*. Available from: <http://phagesdb.org/workflow/Extraction/>
- Appelmans, R. (1921) De dosage du bactériophage. *C R Soc Biol*. 85, pp. 1098.
- Armbruster, C.E., Hodges, S.A. and Mobley, H.L.T. (2013) Initiation of swarming motility by *Proteus mirabilis* occurs in response to specific cues present in urine and requires excess L-glutamine. *Journal of bacteriology*. 195 (6), pp. 1305–1319.
- Armbruster, C.E. and Mobley, H.L.T. (2012) Merging mythology and morphology: the multifaceted lifestyle of *Proteus mirabilis*. *Nature reviews. Microbiology*. 10 (11), pp. 743–754.
- Bailey, T.L. and Elkan, C. (1994) Fitting a mixture model by expectation maximization to discover motifs in biopolymers. *Proceedings / ... International Conference on Intelligent Systems for Molecular Biology ; ISMB. International Conference on Intelligent Systems for Molecular Biology*. 2pp. 28–36.
- Bailey, T.L., Williams, N., Mischak, C. and Li, W.W. (2006) MEME: discovering and analyzing DNA and protein sequence motifs. *Nucleic acids research*. 34 (Web Server issue), pp. W369-73.
- Bankevich, A., Nurk, S., Antipov, D., Gurevich, A.A., Dvorkin, M., Kulikov, A.S., Lesin, V.M., Nikolenko, S.I., Pham, S., Pribelski, A.D., Pyshkin, A. V, Sirotkin, A. V, Vyahhi, N., Tesler, G., et al. (2012) SPAdes: a new genome assembly algorithm and its applications to single-cell sequencing. *Journal of computational biology : a journal of computational molecular cell biology*. 19 (5), pp. 455–477.

- Bansal, S., Harjai, K. and Chhibber, S. (2014) Depolymerase improves gentamicin efficacy during *Klebsiella pneumoniae* induced murine infection. *BMC Infectious Diseases*. 14 (1), pp. 456.
- Baxa, U., Steinbacher, S., Miller, S., Weintraub, A., Huber, R. and Seckler, R. (1996) Interactions of phage P22 tails with their cellular receptor, Salmonella O-antigen polysaccharide. *Biophysical journal*. 71 (4), pp. 2040–2048.
- Belas, R., Manos, J. and Suvanasuthi, R. (2004) *Proteus mirabilis* ZapA metalloprotease degrades a broad spectrum of substrates, including antimicrobial peptides. *Infection and immunity*. 72 (9), pp. 5159–5167.
- Bergh, O., Borsheim, K.Y., Bratbak, G. and Heldal, M. (1989) High abundance of viruses found in aquatic environments. *Nature*. 340 (6233), pp. 467–468.
- Berry, J., Summer, E.J., Struck, D.K. and Young, R. (2008) The final step in the phage infection cycle: the Rz and Rz1 lysis proteins link the inner and outer membranes. *Molecular Microbiology*. 70 (2), pp. 341–351.
- Besemer, J. and Borodovsky, M. (1999) Heuristic approach to deriving models for gene finding. *Nucleic Acids Research*. 27 (19), pp. 3911–3920.
- Bibby, J.M. and Hukins, D.W. (1993) Acidification of urine is not a feasible method for preventing encrustation of indwelling urinary catheters. *Scandinavian journal of urology and nephrology*. 27 (1), pp. 63–65.
- Bjarnsholt, T. (2013) The role of bacterial biofilms in chronic infections. *APMIS*. 121 (s136), pp. 1–58.
- Black, L. (1988) DNA packaging in dsDNA bacteriophages. *Annual review of microbiology*. 43pp. 267–292.
- Bonocora, R.P. and Shub, D.A. (2009) A likely pathway for formation of mobile group I introns. *Current biology : CB*. 19 (3), pp. 223–228.
- Boyd, E.F. and Brüssow, H. (2002) Common themes among bacteriophage-encoded virulence factors and diversity among the bacteriophages involved. *Trends in Microbiology*. 10 (11), pp. 521–529.
- Bradford, M.M. (1976) A rapid and sensitive method for the quantitation of microgram quantities of protein utilizing the principle of protein-dye binding. *Analytical Biochemistry*. 72 (1–2), pp. 248–254.
- Bridier, A., Piard, J.-C., Pandin, C., Labarthe, S., Dubois-Brissonnet, F. and Briandet, R. (2017) Spatial Organization Plasticity as an Adaptive Driver of Surface Microbial Communities. *Frontiers in microbiology*. 8pp. 1364.
- Brooks, T. and Keevil, C.W. (1997) A simple artificial urine for the growth of urinary pathogens. *Letters in applied microbiology*. 24 (3), pp. 203–206.
- Bruce, A.W., Sira, S.S., Clark, A.F. and Awad, S.A. (1974) The problem of catheter encrustation. *Canadian Medical Association journal*. 111 (3), pp. 238–9.

- Bruttin, A. and Brüssow, H. (2005) Human volunteers receiving Escherichia coli phage T4 orally: a safety test of phage therapy. *Antimicrobial agents and chemotherapy*. 49 (7), pp. 2874–2878.
- Budding, A.E., Ingham, C.J., Bitter, W., Vandenbroucke-Grauls, C.M. and Schneeberger, P.M. (2009) The Dienes phenomenon: competition and territoriality in Swarming Proteus mirabilis. *Journal of bacteriology*. 191 (12), pp. 3892–3900.
- Busby-Whitehead, J. M., and Johnson, T.M. (1999) Urinary incontinence. *Clin Geriatr Med*. 14pp. 285–296.
- Bushman, W., Thompson, J.F., Vargas, L. and Landy, A. (1985) Control of directionality in lambda site specific recombination. *Science (New York, N.Y.)*. 230 (4728), pp. 906–911.
- Busscher, H.J. and van der Mei, H.C. (2012) How do bacteria know they are on a surface and regulate their response to an adhering state? *PLoS pathogens*. 8 (1), pp. e1002440.
- Calendar, R. (2006) *The bacteriophages*. Oxford University Press.
- Canchaya, C., Fournous, G., Chibani-Chennoufi, S., Dillmann, M.-L. and Brüssow, H. (2003) Phage as agents of lateral gene transfer. *Current Opinion in Microbiology*. 6 (4), pp. 417–424.
- Capparelli, R., Parlato, M., Borriello, G., Salvatore, P. and Iannelli, D. (2007) Experimental Phage Therapy against Staphylococcus aureus in Mice. *Antimicrobial Agents and Chemotherapy*. 51 (8), pp. 2765–2773.
- Carey, D.E. and McNamara, P.J. (2014) The impact of triclosan on the spread of antibiotic resistance in the environment. *Frontiers in microbiology*. 5pp. 780.
- Carey, D.E., Zitomer, D.H., Kappell, A.D., Choi, M.J., Hristova, K.R. and McNamara, P.J. (2016) Chronic exposure to triclosan sustains microbial community shifts and alters antibiotic resistance gene levels in anaerobic digesters. *Environmental science. Processes and impacts*. 18 (8), pp. 1060–1067.
- Carlson, K. (2005) *Appendix: Working with bacteriophages*. In *Bacteriophages: Biology and Applications*. Elizabeth Kutter and Alexander Sulakvelidze (eds.). CRC Press.
- Carlton, R.M. (1999) Phage therapy: past history and future prospects. *Archivum immunologiae et therapiae experimentalis*. 47 (5), pp. 267–274.
- Carson, L., Gorman, S.P. and Gilmore, B.F. (2010) The use of lytic bacteriophages in the prevention and eradication of biofilms of Proteus mirabilis and Escherichia coli. *FEMS immunology and medical microbiology*. 59 (3), pp. 447–455.
- Carvalho, C., Costa, A., Silva, F. and Oliveira, A. (2017) Bacteriophages and their derivatives for the treatment and control of food-producing animal infections. *Crit Rev Microbiol*. 10pp. 1–19.

- Casjens, S. and Hendrix, R. (1988) Control Mechanisms in dsDNA Bacteriophage Assembly. In: *The Bacteriophages*. Boston, MA: Springer US. pp. 15–91.
- Casjens, S. and King, J. (1974) P22 morphogenesis I: Catalytic scaffolding protein in capsid assembly. *Journal of Supramolecular Structure*. 2 (2–4), pp. 202–224.
- Casjens, S., Wyckoff, E., Hayden, M., Sampson, L., Eppler, K., Randall, S., Moreno, E.T. and Serwer, P. (1992) Bacteriophage P22 portal protein is part of the gauge that regulates packing density of intravirion DNA. *Journal of molecular biology*. 224 (4), pp. 1055–1074.
- Casjens, S.R. (2011) The DNA-packaging nanomotor of tailed bacteriophages. *Nature Reviews Microbiology*. 9 (9), pp. 647–657.
- Casjens, S.R. and Gilcrease, E.B. (2009) Determining DNA packaging strategy by analysis of the termini of the chromosomes in tailed-bacteriophage virions. *Methods in molecular biology (Clifton, N.J.)*. 502pp. 91–111.
- Casjens, S.R., Gilcrease, E.B., Winn-Stapley, D.A., Schicklmaier, P., Schmieger, H., Pedulla, M.L., Ford, M.E., Houtz, J.M., Hatfull, G.F. and Hendrix, R.W. (2005) The generalized transducing Salmonella bacteriophage ES18: complete genome sequence and DNA packaging strategy. *Journal of bacteriology*. 187 (3), pp. 1091–1104.
- Casjens, S.R. and Hendrix, R.W. (2015) Bacteriophage lambda: Early pioneer and still relevant. *Virology*. 479–480pp. 310–330.
- Chakravarti, A., Gangodawila, S., Long, M.J., Morris, N.S., Blacklock, A.R.E. and Stickler, D.J. (2005) An Electrified Catheter to Resist Encrustation by Proteus Mirabilis Biofilm. *The Journal of Urology*. 174 (3), pp. 1129–1132.
- Chanishvili, N. and Sharp, R.A. (2009) *Literature Review of the Practical Application of Bacteriophage Research*.
- Chevalier, B.S. and Stoddard, B.L. (2001) Homing endonucleases: structural and functional insight into the catalysts of intron/intein mobility. *Nucleic acids research*. 29 (18), pp. 3757–3774.
- Chibani-Chennoufi, S., Bruttin, A., Dillmann, M.-L. and Brüssow, H. (2004) Phage-host interaction: an ecological perspective. *Journal of bacteriology*. 186 (12), pp. 3677–3686.
- Chikova, A.K. and Schaaper, R.M. (2007) The bacteriophage P1 hot gene, encoding a homolog of the E. coli DNA polymerase III theta subunit, is expressed during both lysogenic and lytic growth stages. *Mutation research*. 624 (1–2), pp. 1–8.
- Chirico, N., Vianelli, A. and Belshaw, R. (2010) Why genes overlap in viruses. *Proceedings of the Royal Society B: Biological Sciences*. 277 (1701), pp. 3809–3817.

- Choong, S., Wood, S., Fry, C., Whitfield, H., Mulhall, A.B., Chapman, R.G., Crow, R.A., Slade, N., Gillespie, W.A., Kohler-Ockmore, J., Feneley, R.C.L., Getliffe, K., Kunin, C.M., Sassoon, E., et al. (2001) Catheter associated urinary tract infection and encrustation. *International Journal of Antimicrobial Agents*. 17 (4), pp. 305–310.
- Chrisp, J.M. and Nacey, J.N. (1990) Foley catheter balloon puncture and the risk of free fragment formation. *British journal of urology*. 66 (5), pp. 500–502.
- Chung, I.-Y., Jang, H.-J., Bae, H.-W. and Cho, Y.-H. (2014) A phage protein that inhibits the bacterial ATPase required for type IV pilus assembly. *Proceedings of the National Academy of Sciences*. 111 (31), pp. 11503–11508.
- Conlon, B.P., Rowe, S.E. and Lewis, K. (2015) *Persister Cells in Biofilm Associated Infections*. In: Springer, Cham. pp. 1–9.
- Costerton, W., Veeh, R., Shirtliff, M., Pasmore, M., Post, C. and Ehrlich, G. (2003) The application of biofilm science to the study and control of chronic bacterial infections. *The Journal of clinical investigation*. 112 (10), pp. 1466–1477.
- Court, D.L., Oppenheim, A.B. and Adhya, S.L. (2007) A new look at bacteriophage lambda genetic networks. *Journal of bacteriology*. 189 (2), pp. 298–304.
- Cox, A.J. (1990) Comparison of catheter surface morphologies. *British journal of urology*. 65 (1), pp. 55–60.
- Cumby, N., Edwards, A.M., Davidson, A.R. and Maxwell, K.L. (2012) The bacteriophage HK97 gp15 moron element encodes a novel superinfection exclusion protein. *Journal of bacteriology*. 194 (18), pp. 5012–5019.
- Cumby, N., Reimer, K., Mengin-Lecreulx, D., Davidson, A.R. and Maxwell, K.L. (2015) The phage tail tape measure protein, an inner membrane protein and a periplasmic chaperone play connected roles in the genome injection process of *E. coli* phage HK97. *Molecular Microbiology*. 96 (3), pp. 437–447.
- Curtin, J.J. and Donlan, R.M. (2006) Using bacteriophages to reduce formation of catheter-associated biofilms by *Staphylococcus epidermidis*. *Antimicrobial agents and chemotherapy*. 50 (4), pp. 1268–1275.
- d’Ari, R. (1985) The SOS system. *Biochimie*. 67 (3–4), pp. 343–347.
- D’Herelle, F. (1917) Sur un microbe invisible antagoniste des bacillus dysentérique. *Acad Sci Paris*. 165pp. 373–375.
- Dabrowska, K., Miernikiewicz, P., Piotrowicz, A., Hodyra, K., Owczarek, B., Lecion, D., Ka mierzak, Z., Letarov, A. and Gorski, A. (2014) Immunogenicity Studies of Proteins Forming the T4 Phage Head Surface. *Journal of Virology*. 88 (21), pp. 12551–12557.
- Dance, D.A., Pearson, A.D., Seal, D. V and Lowes, J.A. (1987) A hospital outbreak caused by a chlorhexidine and antibiotic-resistant *Proteus mirabilis*. *The Journal of hospital infection*. 10 (1), pp. 10–16.

- Darouiche, R.O., Smith, J.A., Hanna, H., Dhabuwala, C.B., Steiner, M.S., Babaian, R.J., Boone, T.B., Scardino, P.T., Thornby, J.I. and Raad, I.I. (1999) Efficacy of antimicrobial-impregnated bladder catheters in reducing catheter-associated bacteriuria: a prospective, randomized, multicenter clinical trial. *Urology*. 54 (6), pp. 976–981.
- Darouiche, R.O., Thornby, J.I., Stewart, C.C., Donovan, W.H. and Hull, R.A. (2005) Bacterial Interference for Prevention of Urinary Tract Infection: A Prospective, Randomized, Placebo-Controlled, Double-Blind Pilot Trial. *Clinical Infectious Diseases*. 41 (10), pp. 1531–1534.
- Delcaru, C., Alexandru, I., Podgoreanu, P., Grosu, M., Stavropoulos, E., Chifiriuc, M.C. and Lazar, V. (2016) Microbial Biofilms in Urinary Tract Infections and Prostatitis: Etiology, Pathogenicity, and Combating strategies. *Pathogens (Basel, Switzerland)*. 30;5 (4), pii: E65.
- Denyes, J.M., Krell, P.J., Manderville, R.A., Ackermann, H.-W., She, Y.-M. and Kropinski, A.M. (2014) The genome and proteome of Serratia bacteriophage η which forms unstable lysogens. *Virology journal*. 11 (1), pp. 6.
- Derose, E.F., Kirby, T.W., Mueller, G.A., Chikova, A.K., Schaaper, R.M. and London, R.E. (2004) Phage like it HOT: solution structure of the bacteriophage P1-encoded HOT protein, a homolog of the theta subunit of E. coli DNA polymerase III. *Structure (London, England : 1993)*. 12 (12), pp. 2221–2231.
- Dienes, L. (1946) Reproductive processes in Proteus cultures. *Proceedings of the Society for Experimental Biology and Medicine. Society for Experimental Biology and Medicine (New York, N.Y.)*. 63 (2), pp. 265–270.
- Donlan, R.M. (2002) Biofilms: microbial life on surfaces. *Emerging infectious diseases*. 8 (9), pp. 881–890.
- Donlan, R.M. (2001) Biofilms and device-associated infections. *Emerging infectious diseases*. 7 (2), pp. 277–281.
- Donnelly-Wu, M.K., Jacobs, W.R. and Hatfull, G.F. (1993) Superinfection immunity of mycobacteriophage L5: applications for genetic transformation of mycobacteria. *Molecular microbiology*. 7 (3), pp. 407–417.
- Dumanski, A.J., Hedelin, H., Edin-Liljegren, A., Beauchemin, D. and McLean, R.J. (1994) Unique ability of the Proteus mirabilis capsule to enhance mineral growth in infectious urinary calculi. *Infection and immunity*. 62 (7), pp. 2998–3003.
- Durack, D.T. (1975) Experimental bacterial endocarditis. IV. Structure and evolution of very early lesions. *The Journal of Pathology*. 115 (2), pp. 81–89.
- Eaton, M.D. and Bayne-Jones, S. (1934a) Bacteriophage Therapy. *Journal of the American Medical Association*. 103 (23), pp. 1769.
- Eaton, M.D. and Bayne-Jones, S. (1934b) Bacteriophage Therapy. *Journal of the American Medical Association*. 103 (23), pp. 1780.

- Eaton, M.D. and Bayne-Jones, S. (1934c) Bacteriophage Therapy. *Journal of the American Medical Association*. 103 (24), pp. 1847.
- Eaton, M.D. and Bayne-Jones, S. (1934d) Bacteriophage Therapy. *Journal of the American Medical Association*. 103 (25), pp. 1934.
- Echols, H. (1972) Developmental Pathways for the Temperate Phage: Lysis VS Lysogeny. *Annual Review of Genetics*. 6 (1), pp. 157–190.
- Ellis, E.L. and Delbrück, M. (1939) The Growth Of Bacteriophage. *The Journal of general physiology*. 22 (3), pp. 365–384.
- Evans, L. V. (2000) *Biofilms : recent advances in their study and control*. Harwood Academic.
- CM Fauquet, MA Mayo, J Maniloff, U Desselberger, and LA Ball (eds.) (2005) *Virus Taxonomy, VIIIth Report of the ICTV*. London: Elsevier/Academic Press.
- Feneley, R.C.L., Hopley, I.B. and Wells, P.N.T. (2015) Urinary catheters: history, current status, adverse events and research agenda. *Journal of medical engineering and technology*. 39 (8), pp. 459–470.
- Feneley, R.C.L., Kunin, C.M. and Stickler, D.J. (2012) An indwelling urinary catheter for the 21st century. *BJU International*. 109 (12), pp. 1746–1749.
- Feng, Q.L., Wu, J., Chen, G.Q., Cui, F.Z., Kim, T.N. and Kim, J.O. (2000) A mechanistic study of the antibacterial effect of silver ions on *Escherichia coli* and *Staphylococcus aureus*. *Journal of biomedical materials research*. 52 (4), pp. 662–668.
- Fiddes, J.C. (1977) The nucleotide sequence of a viral DNA. *Sci Am*. 237pp. 54–67.
- Fiers, W., Contreras, R., Duerinck, F., Haegeman, G., Iserentant, D., Merregaert, J., Min Jou, W., Molemans, F., Raeymaekers, A., Van den Berghe, A., Volckaert, G. and Ysebaert, M. (1976) Complete nucleotide sequence of bacteriophage MS2 RNA: primary and secondary structure of the replicase gene. *Nature*. 260 (5551), pp. 500–507.
- Figueroa-Bossi, N. and Bossi, L. (1999) Inducible prophages contribute to *Salmonella* virulence in mice. *Molecular microbiology*. 33 (1), pp. 167–176.
- Fisher, L.E., Hook, A.L., Ashraf, W., Yousef, A., Barrett, D.A., Scurr, D.J., Chen, X., Smith, E.F., Fay, M., Parmenter, C.D.J., Parkinson, R. and Bayston, R. (2015) Biomaterial modification of urinary catheters with antimicrobials to give long-term broadspectrum antibiofilm activity. *Journal of Controlled Release*. 202pp. 57–64.
- Fiss, E.M., Rule, K.L. and Vikesland, P.J. (2007) *Formation of Chloroform and Other Chlorinated Byproducts by Chlorination of Triclosan-Containing Antibacterial Products*.
- Flemming, H.-C. (2016) EPS—Then and Now. *Microorganisms*. 4 (4), pp. 41.

- Foo, L.Y., Lu, Y., Howell, A.B. and Vorsa, N. (2000) The structure of cranberry proanthocyanidins which inhibit adherence of uropathogenic P-fimbriated *Escherichia coli* in vitro. *Phytochemistry*. 54 (2), pp. 173–181.
- Fraser, J.S., Maxwell, K.L. and Davidson, A.R. (2007) Immunoglobulin-like domains on bacteriophage: weapons of modest damage? *Current opinion in microbiology*. 10 (4), pp. 382–387.
- Freeman, V.J. (1951) Studies on the virulence of bacteriophage-infected strains of *Corynebacterium diphtheriae*. *Journal of bacteriology*. 61 (6), pp. 675–688.
- Fu, W., Forster, T., Mayer, O., Curtin, J.J., Lehman, S.M. and Donlan, R.M. (2010) Bacteriophage cocktail for the prevention of biofilm formation by *Pseudomonas aeruginosa* on catheters in an in vitro model system. *Antimicrobial agents and chemotherapy*. 54 (1), pp. 397–404.
- Fuller, D.N., Raymer, D.M., Rickgauer, J.P., Robertson, R.M., Catalano, C.E., Anderson, D.L., Grimes, S. and Smith, D.E. (2007) Measurements of Single DNA Molecule Packaging Dynamics in Bacteriophage λ Reveal High Forces, High Motor Processivity, and Capsid Transformations. *Journal of Molecular Biology*. 373 (5), pp. 1113–1122.
- Garibaldi, R.A., Burke, J.P., Dickman, M.L. and Smith, C.B. (1974) Factors predisposing to bacteriuria during indwelling urethral catheterization. *The New England journal of medicine*. 291 (5), pp. 215–219.
- Gasteiger, E., Hoogland, C., Gattiker, A., Duvaud, S., Wilkins, M., Appel, R. and Bairoch, A. (2005) Protein Identification and Analysis Tools on the ExpASY Server. *The Proteomics Protocols Handbook*. pp. 571–607.
- Getliffe, K.A. (1994) The characteristics and management of patients with recurrent blockage of long-term urinary catheters. *Journal of Advanced Nursing*. 20 (1), pp. 140–149.
- Gibbs, K.A., Urbanowski, M.L. and Greenberg, E.P. (2008) Genetic determinants of self identity and social recognition in bacteria. *Science (New York, N.Y.)*. 321 (5886), pp. 256–259.
- Gill, J.J. and Hyman, P. (2010) Phage choice, isolation, and preparation for phage therapy. *Current pharmaceutical biotechnology*. 11 (1), pp. 2–14.
- Gladstone, E.G., Molineux, I.J. and Bull, J.J. (2012) Evolutionary principles and synthetic biology: avoiding a molecular tragedy of the commons with an engineered phage. *Journal of biological engineering*. 6 (1), pp. 13.
- Goodridge, L.D. (2010) Designing phage therapeutics. *Current pharmaceutical biotechnology*. 11 (1), pp. 15–27.
- Griffith, D.P., Musher, D.M. and Itin, C. (1976) Urease. The primary cause of infection-induced urinary stones. *Investigative urology*. 13 (5), pp. 346–350.

- Grose, J.H. and Casjens, S.R. (2014) Understanding the enormous diversity of bacteriophages: The tailed phages that infect the bacterial family Enterobacteriaceae. *Virology*. 468pp. 421–443.
- Groth, A.C. and Carlos, M.P. (2004) Phage Integrases: Biology and Applications. *Journal of Molecular Biology*. 335 (3), pp. 667–678.
- Hachem, R., Reitzel, R., Borne, A., Jiang, Y., Tinkey, P., Uthamanthil, R., Chandra, J., Ghannoum, M. and Raad, I. (2009) Novel antiseptic urinary catheters for prevention of urinary tract infections: correlation of in vivo and in vitro test results. *Antimicrobial agents and chemotherapy*. 53 (12), pp. 5145–5149.
- Hall-Stoodley, L., Costerton, J.W. and Stoodley, P. (2004) Bacterial biofilms: from the Natural environment to infectious diseases. *Nature Reviews Microbiology*. 2 (2), pp. 95–108.
- Hansen, E.B. (1989) Structure and regulation of the lytic replicon of phage P1. *J Mol Biol*. 5pp. 135–149.
- Hashmi, S., Kelly, E., Rogers, S.O. and Gates, J. (2003) Urinary tract infection in surgical patients. *American journal of surgery*. 186 (1), pp. 53–56.
- Hatfull, G.F. (2008) Bacteriophage genomics. *Current Opinion in Microbiology*. 11 (5), pp. 447–453.
- Haylen, B.T., de Ridder, D., Freeman, R.M., Swift, S.E., Berghmans, B., Lee, J., Monga, A., Petri, E., Rizk, D.E., Sand, P.K., Schaer, G.N., International Urogynecological Association and International Continence Society (2009) An international urogynecological association (IUGA)/international continence society (ICS) joint report on the terminology for female pelvic floor dysfunction. *Neurourology and Urodynamics*. 29 (1), pp. n/a-n/a.
- Hedelin, H., Eddeland, A., Larsson, L., Petersson, S. and Öhman, S. (1984) The Composition of Catheter Encrustations, including the Effects of Allopurinol Treatment. *British Journal of Urology*. 56 (3), pp. 250–254.
- Hendrix, R.W. and Garcea, R.L. (1994) Capsid assembly of dsDNA viruses. *Seminars in Virology*. 5 (1), pp. 15–26.
- Hendrix, R.W., Smith, M.C., Burns, R.N., Ford, M.E. and Hatfull, G.F. (1999) Evolutionary relationships among diverse bacteriophages and prophages: all the world's a phage. *Proceedings of the National Academy of Sciences of the United States of America*. 96 (5), pp. 2192–2197.
- Hennes, K.P., Suttle, C.A. and Chan, A.M. (1995) Fluorescently Labeled Virus Probes Show that Natural Virus Populations Can Control the Structure of Marine Microbial Communities. *Applied and environmental microbiology*. 61 (10), pp. 3623–3627.

- Hentzer, M., Wu, H., Andersen, J.B., Riedel, K., Rasmussen, T.B., Bagge, N., Kumar, N., Schembri, M.A., Song, Z., Kristoffersen, P., Manefield, M., Costerton, J.W., Molin, S., Eberl, L., et al. (2003) Attenuation of *Pseudomonas aeruginosa* virulence by quorum sensing inhibitors. *The EMBO Journal*. 22 (15), pp. 3803.
- Hoener, J.F.M. (1965) Development of Flagella by *Proteus mirabilis*. *Journal of General Microbiology*. 40 (1), pp. 29–42.
- Høiby, N., Bjarnsholt, T., Givskov, M., Molin, S. and Ciofu, O. (2010) Antibiotic resistance of bacterial biofilms. *International Journal of Antimicrobial Agents*. 35 (4), pp. 322–332.
- Holling, N., Lednor, D., Tsang, S., Bissell, A., Campbell, L., Nzakizwanayo, J., Dedi, C., Hawthorne, J.A., Hanlon, G., Ogilvie, L.A., Salvage, J.P., Patel, B.A., Barnes, L.M. and Jones, B. V (2014) Elucidating the genetic basis of crystalline biofilm formation in *Proteus mirabilis*. *Infection and immunity*. 82 (4), pp. 1616–1626.
- Hooton, T.M., Bradley, S.F., Cardenas, D.D., Colgan, R., Geerlings, S.E., Rice, J.C., Saint, S., Schaeffer, A.J., Tambayh, P.A., Tenke, P., Nicolle, L.E. and Infectious Diseases Society of America (2010) Diagnosis, prevention, and treatment of catheter-associated urinary tract infection in adults: 2009 International Clinical Practice Guidelines from the Infectious Diseases Society of America. *Clinical infectious diseases : an official publication of the Infectious Diseases Society of America*. 50 (5), pp. 625–663.
- Hosseinidoust, Z., Van de Ven, T.G.M. and Tufenkji, N. (2011) Bacterial Capture Efficiency and Antimicrobial Activity of Phage-Functionalized Model Surfaces. *Langmuir*. 27 (9), pp. 5472–5480.
- Howell, A.B. (2007) Bioactive compounds in cranberries and their role in prevention of urinary tract infections. *Molecular Nutrition and Food Research*. 51 (6), pp. 732–737.
- Hughes, K.A., Sutherland, I.W. and Jones, M. V (1998) Biofilm susceptibility to bacteriophage attack: the role of phage-borne polysaccharide depolymerase. *Microbiology (Reading, England)*. 144 (Pt 1) pp. 3039–3047.
- Hyatt, D., Chen, G.-L., LoCascio, P.F., Land, M.L., Larimer, F.W., Hauser, L.J., Delcher, A., Bratke, K., Powers, E., Salzberg, S., Lukashin, A., Borodovsky, M., Benson, D., Karsch-Mizrachi, I., et al. (2010) Prodigal: prokaryotic gene recognition and translation initiation site identification. *BMC Bioinformatics*. 11 (1), pp. 119.
- Hyman, P. and Abedon, S.T. (2010) Bacteriophage host range and bacterial resistance. *Advances in applied microbiology*. 70 pp. 217–248.
- Ikebe, T., Wada, A., Inagaki, Y., Sugama, K., Suzuki, R., Tanaka, D., Tamaru, A., Fujinaga, Y., Abe, Y., Shimizu, Y., Watanabe, H. and Working Group for Group A Streptococcus in Japan (2002) Dissemination of the phage-associated novel superantigen gene *speL* in recent invasive and noninvasive *Streptococcus pyogenes* M3/T3 isolates in Japan. *Infection and immunity*. 70 (6), pp. 3227–3233.

- Irwin, D.E., Milsom, I., Hunskar, S., Reilly, K., Kopp, Z., Herschorn, S., Coyne, K., Kelleher, C., Hampel, C., Artibani, W. and Abrams, P. (2006) Population-Based Survey of Urinary Incontinence, Overactive Bladder, and Other Lower Urinary Tract Symptoms in Five Countries: Results of the EPIC Study. *European Urology*. 50 (6), pp. 1306–1315.
- Israel, J. V, Anderson, T.F. and Levine, M. (1967) *in vitro* Morphogenesis of Phage P22 from Heads and Base-Plate Parts. *Proceedings of the National Academy of Sciences of the United States of America*. 57 (2), pp. 284–291.
- Israel, V. (1977) E proteins of bacteriophage P22. Identification and ejection from wild-type and defective particles. *J Virol*. 23pp. 91–97.
- Israni, A.K. and Kasiske, B.L. (2011) Laboratory assessment of kidney disease: glomerular filtration rate, urinalysis, and proteinuria. In: M Taal, G Chertow, P Marsden, K Skorecki, A Yu, and B Brenner (eds.). *Brenner and Rector's the Kidney*. 9th edition. Saunders. pp. pp. 868–896.
- Iyer, L.M., Koonin, E. V and Aravind, L. (2002) Extensive domain shuffling in transcription regulators of DNA viruses and implications for the origin of fungal APSES transcription factors. *Genome biology*. 3 (3), pp. RESEARCH0012.
- Jacobsen, S.M., Stickler, D.J., Mobley, H.L.T. and Shirtliff, M.E. (2008) Complicated catheter-associated urinary tract infections due to *Escherichia coli* and *Proteus mirabilis*. *Clinical microbiology reviews*. 21 (1), pp. 26–59.
- Jahn, P., Beutner, K. and Langer, G. (2012) Types of indwelling urinary catheters for long-term bladder drainage in adults. In: Patrick Jahn (ed.). *Cochrane Database of Systematic Reviews*. Chichester, UK: John Wiley and Sons, Ltd. p. Available from:
<http://doi.wiley.com/10.1002/14651858.CD004997.pub3>
[doi:10.1002/14651858.CD004997.pub3](http://doi.org/10.1002/14651858.CD004997.pub3)
- Jansen, B., Rinck, M., Wolbring, P., Strohmeier, A. and Jahns, T. (1994) In vitro Evaluation of the Antimicrobial Efficacy and Biocompatibility of a Silver-Coated Central Venous Catheter. *Journal of Biomaterials Applications*. 9 (1), pp. 55–70.
- Jepson, R.G., Williams, G. and Craig, J.C. (2012) Cranberries for preventing urinary tract infections. In: Ruth G Jepson (ed.). *Cochrane Database of Systematic Reviews*. Chichester, UK: John Wiley and Sons, Ltd. p. pp. CD001321. Available from:
<http://www.ncbi.nlm.nih.gov/pubmed/23076891>
[doi:10.1002/14651858.CD001321.pub5](http://doi.org/10.1002/14651858.CD001321.pub5)
- Johnson, J.R., Johnston, B. and Kuskowski, M.A. (2012) In vitro comparison of nitrofurazone- and silver alloy-coated foley catheters for contact-dependent and diffusible inhibition of urinary tract infection-associated microorganisms. *Antimicrobial agents and chemotherapy*. 56 (9), pp. 4969–4972.

- Jones, B. V, Young, R., Mahenthiralingam, E., Stickler, D.J. and Mmun, I.N.I. (2004) Ultrastructure of *Proteus mirabilis* Swarmer Cell Rafts and Role of Swarming in Catheter-Associated Urinary Tract Infection. *Infection and immunity*. 72 (7), pp. 3941–3950.
- Jones, B.D. and Mobley, H.L. (1987) Genetic and biochemical diversity of ureases of *Proteus*, *Providencia*, and *Morganella* species isolated from urinary tract infection. *Infection and immunity*. 55 (9), pp. 2198–2203.
- Jones, G.L., Muller, C.T., O'Reilly, M. and Stickler, D.J. (2006) Effect of triclosan on the development of bacterial biofilms by urinary tract pathogens on urinary catheters. *Journal of Antimicrobial Chemotherapy*. 57 (2), pp. 266–272.
- Jones, H.E. and Park, R.W.A. (1967) The Short Forms and Long Forms of *Proteus*. *J. gen. Microbiol.* 47pp. 359–367.
- Jones, S.M., Dang, T.T. and Martinuzzi, R. (2009) Use of quorum sensing antagonists to deter the formation of crystalline *Proteus mirabilis* biofilms. *International Journal of Antimicrobial Agents*. 34 (4), pp. 360–364.
- Jones, S.M., Yerly, J., Hu, Y., Ceri, H. and Martinuzzi, R. (2007) Structure of *Proteus mirabilis* biofilms grown in artificial urine and standard laboratory media. *FEMS Microbiology Letters*. 268 (1), pp. 16–21.
- Katsura, I. (1987) Determination of bacteriophage λ tail length by a protein ruler. *Nature*. 327 (6117), pp. 73–75.
- Katsura, I. and Hendrix, R. (1984) Length determination in bacteriophage lambda tails. *Cell*. 39pp. 691–698.
- Katsura, I. and Kühn, P.W. (1975) Morphogenesis of the tail of bacteriophage lambda. *Journal of Molecular Biology*. 91 (3), pp. 257–273.
- Kaźmierczak, Z., Górski, A. and Dąbrowska, K. (2014) Facing antibiotic resistance: *Staphylococcus aureus* phages as a medical tool. *Viruses*. 6 (7), pp. 2551–2570.
- Kazmierska, K.A., Thompson, R., Morris, N., Long, A. and Ciach, T. (2010) In Vitro Multicompartmental Bladder Model for Assessing Blockage of Urinary Catheters: Effect of Hydrogel Coating on Dynamics of *Proteus mirabilis* Growth. *Urology*. 76 (2), pp. 515.e15-515.e20.
- Kearns, D.B. (2010) A field guide to bacterial swarming motility. *Nature reviews. Microbiology*. 8 (9), pp. 634–644.
- Khawaldeh, A., Morales, S., Dillon, B., Alavidze, Z., Ginn, A.N., Thomas, L., Chapman, S.J., Dublanchet, A., Smithyman, A. and Iredell, J.R. (2011) Bacteriophage therapy for refractory *Pseudomonas aeruginosa* urinary tract infection. *Journal of Medical Microbiology*. 60 (11), pp. 1697–1700.
- Kingsford, C.L., Ayanbule, K. and Salzberg, S.L. (2007) Rapid, accurate, computational discovery of Rho-independent transcription terminators illuminates their relationship to DNA uptake. *Genome biology*. 8 (2), pp. R22.

- Kohanski, M.A., Dwyer, D.J., Hayete, B., Lawrence, C.A. and Collins, J.J. (2007) A Common Mechanism of Cellular Death Induced by Bactericidal Antibiotics. *Cell*. 130 (5), pp. 797–810.
- Krogh, A., Larsson, B., von Heijne, G. and Sonnhammer, E.L.. (2001) Predicting transmembrane protein topology with a hidden markov model: application to complete genomes. *Journal of Molecular Biology*. 305 (3), pp. 567–580.
- Kropinski, A.M. (2009) Measurement of the rate of attachment of bacteriophage to cells. *Methods in molecular biology (Clifton, N.J.)*. 501pp. 151–155.
- Kropinski, A.M., Mazzocco, A., Waddell, T.E., Lingohr, E. and Johnson, R.P. (2009) Enumeration of Bacteriophages by Double Agar Overlay Plaque Assay. *Methods in molecular biology (Clifton, N.J.)*. pp. 69–76.
- Kucharewicz-Krukowska, A. and Slopek, S. (1987) Immunogenic effect of bacteriophage in patients subjected to phage therapy. *Archivum immunologiae et therapiae experimentalis*. 35 (5), pp. 553–561.
- Kunin, C.M. (1989) Blockage of urinary catheters: role of microorganisms and constituents of the urine on formation of encrustations. *Journal of clinical epidemiology*. 42 (9), pp. 835–842.
- Kunin, C.M. (1997) *Urinary tract infections: detection, prevention, and management*. Williams and Wilkins.
- Kunin, C.M., Chin, Q.F. and Chambers, S. (1987) Indwelling urinary catheters in the elderly. Relation of catheter life to formation of encrustations in patients with and without blocked catheters. *The American journal of medicine*. 82 (3), pp. 405–411.
- Kunin, C.M. and McCormack, R.C. (1966) Prevention of Catheter-Induced Urinary-Tract Infections by Sterile Closed Drainage. *New England Journal of Medicine*. 274 (21), pp. 1155–1161.
- Kunin, V., He, S., Warnecke, F., Peterson, S.B., Garcia Martin, H., Haynes, M., Ivanova, N., Blackall, L.L., Breitbart, M., Rohwer, F., McMahon, K.D. and Hugenholtz, P. (2008) A bacterial metapopulation adapts locally to phage predation despite global dispersal. *Genome Research*. 18 (2), pp. 293–297.
- Kutter, E. (2009) Phage host range and efficiency of plating. *Methods in molecular biology (Clifton, N.J.)*. pp. 141–150.
- Kutter, E., Kellenberger, E., Carlson, K., Eddy, S., Neitzel, J., Messinger, L., North, J. and Guttman, B. (1994) Effects of bacterial growth condition and physiology on T4 infection. In: JD Karam (ed.). *Molecular Biology of Bacteriophage T4*. Washington DC: . pp. 406–418.
- Kutter, E. and Sulakvelidze, A. (2005) *Bacteriophages : biology and applications*. CRC Press.

- Kutter, E., De Vos, D., Gvasalia, G., Alavidze, Z., Gogokhia, L., Kuhl, S. and Abedon, S.T. (2010) Phage therapy in clinical practice: treatment of human infections. *Current pharmaceutical biotechnology*. 11 (1), pp. 69–86.
- Labrie, S.J., Samson, J.E. and Moineau, S. (2010) Bacteriophage resistance mechanisms. *Nature Reviews Microbiology*. 8 (5), pp. 317–327.
- Lander, G.C., Khayat, R., Li, R., Prevelige, P.E., Potter, C.S., Carragher, B. and Johnson, J.E. (2009) The P22 Tail Machine at Subnanometer Resolution Reveals the Architecture of an Infection Conduit. *Structure*. 17 (6), pp. 789–799.
- Lange, D., Elwood, C.N., Choi, K., Hendlin, K., Monga, M. and Chew, B.H. (2009) Uropathogen Interaction With the Surface of Urological Stents Using Different Surface Properties. *The Journal of Urology*. 182 (3), pp. 1194–1200.
- Lanman, J., Tuma, R. and Prevelige, P.E. (1999) Identification and characterization of the domain structure of bacteriophage P22 coat protein. *Biochemistry*. 38 (44), pp. 14614–14623.
- Latka, A., Maciejewska, B., Majkowska-Skrobek, G., Briers, Y. and Drulis-Kawa, Z. (2017) Bacteriophage-encoded virion-associated enzymes to overcome the carbohydrate barriers during the infection process. *Applied Microbiology and Biotechnology*. 101 (8), pp. 3103–3119.
- Lazar, I. (2010) *Gel Analyzer 2010 a*. Available from: <http://www.gelanalyzer.com>
- Leason, K.R. and Friedman, D.I. (1988) Analysis of transcription termination signals in the nin region of bacteriophage lambda: the roc deletion. *Journal of bacteriology*. 170 (11), pp. 5051–5058.
- Lehman, S.M. and Donlan, R.M. (2015) Bacteriophage-mediated control of a two-species biofilm formed by microorganisms causing catheter-associated urinary tract infections in an in vitro urinary catheter model. *Antimicrobial agents and chemotherapy*. 59 (2), pp. 1127–1137.
- Lehnherr, H., Hansen, A.-M. and Ilyina, T. (1998) Penetration of the bacterial cell wall: a family of lytic transglycosylases in bacteriophages and conjugative plasmids. *Molecular Microbiology*. 30 (2), pp. 454–457.
- León, M. and Bastías, R. (2015) Virulence reduction in bacteriophage resistant bacteria. *Frontiers in microbiology*. 6pp. 343.
- Lesnik, E.A., Sampath, R., Levene, H.B., Henderson, T.J., McNeil, J.A. and Ecker, D.J. (2001) Prediction of rho-independent transcriptional terminators in *Escherichia coli*. *Nucleic Acids Research*. 29 (17), pp. 3583–3594.
- Letkiewicz, S., Międzybrodzki, R., Fortuna, W., Weber-Dąbrowska, B. and Górski, A. (2009) Eradication of *Enterococcus faecalis* by phage therapy in chronic bacterial prostatitis — case report. *Folia Microbiologica*. 54 (5), pp. 457–461.

- Lewis, D., Le, P., Zurla, C., Finzi, L. and Adhya, S. (2011) Multilevel autoregulation of λ repressor protein CI by DNA looping in vitro. *Proceedings of the National Academy of Sciences of the United States of America*. 108 (36), pp. 14807–14812.
- Liao, K.S., Lehman, S.M., Tweardy, D.J., Donlan, R.M. and Trautner, B.W. (2012) Bacteriophages are synergistic with bacterial interference for the prevention of *Pseudomonas aeruginosa* biofilm formation on urinary catheters. *Journal of applied microbiology*.
- Liaw, S.J., Lai, H.C. and Wang, W.B. (2004) Modulation of Swarming and Virulence by Fatty Acids through the RsbA Protein in *Proteus mirabilis*. *Infection and Immunity*. 72 (12), pp. 6836–6845.
- Liedl, B. (2001) Catheter-associated urinary tract infections. *Current opinion in urology*. 11 (1), pp. 75–79.
- Lima-Mendez, G., Toussaint, A. and Lepiae, R. (2011) A modular view of the bacteriophage genomic space: identification of host and lifestyle marker modules. *Research in Microbiology*. 162 (8), pp. 737–746.
- Lingohr, E., Frost, S. and Johnson, R.P. (2009) Determination of Bacteriophage Genome Size by Pulsed-Field Gel Electrophoresis. *Methods in molecular biology (Clifton, N.J.)*. 2pp. 19–25.
- Liu, Y., Black, M.A., Caron, L. and Camesano, T.A. (2006) Role of cranberry juice on molecular-scale surface characteristics and adhesion behavior of *Escherichia coli*. *Biotechnology and Bioengineering*. 93 (2), pp. 297–305.
- Lo, J., Lange, D. and Chew, B.H. (2014) Ureteral Stents and Foley Catheters-Associated Urinary Tract Infections: The Role of Coatings and Materials in Infection Prevention. *Antibiotics (Basel, Switzerland)*. 3 (1), pp. 87–97.
- Loc-Carrillo, C. and Abedon, S.T. (2011) Pros and cons of phage therapy. *Bacteriophage*. 1 (2), pp. 111–114.
- Loessner, M.J., Inman, R.B., Lauer, P. and Calendar, R. (2000) Complete nucleotide sequence, molecular analysis and genome structure of bacteriophage A118 of *Listeria monocytogenes*: implications for phage evolution. *Molecular Microbiology*. 35 (2), pp. 324–340.
- Łoś, M. and Węgrzyn, G. (2012) Pseudolysogeny. In: *Advances in virus research*. pp. 339–349.
- Lu, T.K. and Collins, J.J. (2007) Dispersing biofilms with engineered enzymatic bacteriophage. *Proceedings of the National Academy of Sciences of the United States of America*. 104 (27), pp. 11197–11202.
- Lu, T.K. and Collins, J.J. (2009) Engineered bacteriophage targeting gene networks as adjuvants for antibiotic therapy. *Proceedings of the National Academy of Sciences of the United States of America*. 106 (12), pp. 4629–4634.

- Łusiak-Szelachowska, M., Żaczek, M., Weber-Dąbrowska, B., Międzybrodzki, R., Kłak, M., Fortuna, W., Letkiewicz, S., Rogóż, P., Szufnarowski, K., Jończyk-Matysiak, E., Owczarek, B. and Górski, A. (2014) Phage Neutralization by Sera of Patients Receiving Phage Therapy. *Viral Immunology*. 27 (6), pp. 295–304.
- Macleod, S.M. and Stickler, D.J. (2007) Species interactions in mixed-community crystalline biofilms on urinary catheters. *Journal of Medical Microbiology*. 56 (11), pp. 1549–1557.
- Maki, D.G. and Tambyah, P. a (2001) Engineering out the risk for infection with urinary catheters. *Emerging infectious diseases*. 7 (2), pp. 342–347.
- Malic, S., Jordan, R.P.C., Waters, M.G.J., Stickler, D.J. and Williams, D.W. (2014) Biocide activity against urinary catheter pathogens. *Antimicrobial agents and chemotherapy*. 58 (2), pp. 1192–1194.
- Marceau, A.H. (2012) Functions of Single-Strand DNA-Binding Proteins in DNA Replication, Recombination, and Repair. In: *Single-Stranded DNA Binding Proteins*. Totowa, NJ: Humana Press. pp. pp. 1–21.
- Markham, N.R. and Zuker, M. (2008) *UNAFold*. In: pp. 3–31. Available from: http://link.springer.com/10.1007/978-1-60327-429-6_1doi:10.1007/978-1-60327-429-6_1
- Mathoera, R.B., Kok, D.J., Verduin, C.M. and Nijman, R.J.M. (2002) Pathological and therapeutic significance of cellular invasion by *Proteus mirabilis* in an enterocystoplasty infection stone model. *Infection and immunity*. 70 (12), pp. 7022–7032.
- Matsuda, T., Freeman, T.A., Hilbert, D.W., Duff, M., Fuortes, M., Stapleton, P.P. and Daly, J.M. (2005) Lysis-deficient bacteriophage therapy decreases endotoxin and inflammatory mediator release and improves survival in a murine peritonitis model. *Surgery*. 137 (6), pp. 639–646.
- Matsuzaki, S., Yasuda, M., Nishikawa, H., Kuroda, M., Ujihara, T., Shuin, T., Shen, Y., Jin, Z., Fujimoto, S., Nasimuzzaman, M.D., Wakiguchi, H., Sugihara, S., Sugiura, T., Koda, S., et al. (2003) Experimental Protection of Mice against Lethal *Staphylococcus aureus* Infection by Novel Bacteriophage ϕ MR11. *The Journal of Infectious Diseases*. 187 (4), pp. 613–624.
- McGill, S. (1982) Catheter management: it's the size that's important. *Nursing mirror*. 154 (14), pp. 48–49.
- McNamara, P.J. and Levy, S.B. (2016) Triclosan: an Instructive Tale. *Antimicrobial agents and chemotherapy*. 60 (12), pp. 7015–7016.
- McOsker, C.C. and Fitzpatrick, P.M. (1994) Nitrofurantoin: mechanism of action and implications for resistance development in common uropathogens. *The Journal of antimicrobial chemotherapy*. 33 Suppl App. 23–30.

- Melo, L.D.R., Veiga, P., Cerca, N., Kropinski, A.M., Almeida, C., Azeredo, J. and Sillankorva, S. (2016) Development of a Phage Cocktail to Control *Proteus mirabilis* Catheter-associated Urinary Tract Infections. *Frontiers in Microbiology*. 7, pp. 1024.
- Milles, G. (1965) Catheter-Induced Hemorrhagic Pseudopolyps of the Urinary Bladder. *JAMA*. 193pp. 968–969.
- Milo, S., Hathaway, H., Nzakizwanayo, J., Alves, D.R., Esteban, P.P., Jones, B. V. and Jenkins, A.T.A. (2017) Prevention of encrustation and blockage of urinary catheters by *Proteus mirabilis* via pH-triggered release of bacteriophage. *J. Mater. Chem. B*. 5 (27), pp. 5403–5411.
- Mitra, A., Kesarwani, A.K., Pal, D. and Nagaraja, V. (2011) WebGeSTer DB--a transcription terminator database. *Nucleic acids research*. 39, pp. D129-35.
- Mobley, H.L., Belas, R., Lockatell, V., Chippendale, G., Trifillis, A.L., Johnson, D.E. and Warren, J.W. (1996) Construction of a flagellum-negative mutant of *Proteus mirabilis*: effect on internalization by human renal epithelial cells and virulence in a mouse model of ascending urinary tract infection. *Infection and immunity*. 64 (12), pp. 5332–5340.
- Mobley, H.L., Chippendale, G.R., Swihart, K.G. and Welch, R.A. (1991) Cytotoxicity of the HpmA hemolysin and urease of *Proteus mirabilis* and *Proteus vulgaris* against cultured human renal proximal tubular epithelial cells. *Infection and immunity*. 59 (6), pp. 2036–2042.
- Mobley, H.L., Chippendale, G.R., Tenney, J.H., Mayrer, A.R., Crisp, L.J., Penner, J.L. and Warren, J.W. (1988) MR/K hemagglutination of *Providencia stuartii* correlates with adherence to catheters and with persistence in catheter-associated bacteriuria. *The Journal of infectious diseases*. 157 (2), pp. 264–271.
- Mobley, H.L. and Warren, J.W. (1987) Urease-positive bacteriuria and obstruction of long-term urinary catheters. *Journal of clinical microbiology*. 25 (11), pp. 2216–2217.
- Moitoso de Vargas, L. and Landy, A. (1991) A switch in the formation of alternative DNA loops modulates lambda site-specific recombination. *Proceedings of the National Academy of Sciences of the United States of America*. 88 (2), pp. 588–592.
- Morgan, S.D., Rigby, D. and Stickler, D.J. (2009) A study of the structure of the crystalline bacterial biofilms that can encrust and block silver Foley catheters. *Urological Research*. 37 (2), pp. 89–93.
- Morris, N.S. and Stickler, D.J. (1998) The effect of urease inhibitors on the encrustation of urethral catheters. *Urological research*. 26 (4), pp. 275–279.
- Morris, N.S., Stickler, D.J. and Winters, C. (1997) Which indwelling urethral catheters resist encrustation by *Proteus mirabilis* biofilms? *BJU International*. 80 (1), pp. 58–63.

- Mosberg, J.A., Lajoie, M.J. and Church, G.M. (2010) Lambda Red Recombineering in *Escherichia coli* Occurs Through a Fully Single-Stranded Intermediate. *Genetics*. 186 (3), pp. 793-799.
- Moussa, S.H., Kuznetsov, V., Tran, T.A.T., Sacchettini, J.C. and Young, R. (2012) Protein determinants of phage T4 lysis inhibition. *Protein science: a publication of the Protein Society*. 21 (4), pp. 571–582.
- Mullard, A. (2014) New drugs cost US\$2.6 billion to develop. *Nat. Rev. Drug Discov*. 13, pp. 887.
- Murphy, J., Mahony, J., Ainsworth, S., Nauta, A. and van Sinderen, D. (2013) Bacteriophage orphan DNA methyltransferases: insights from their bacterial origin, function, and occurrence. *Applied and environmental microbiology*. 79 (24), pp. 7547–7555.
- Naville, M., Ghuillot-Gaudeffroy, A., Marchais, A. and Gautheret, D. (2011) ARNold: a web tool for the prediction of Rho-independent transcription terminators. *RNA Biol*. 8pp. 11–13.
- Nelson, D., Loomis, L. and Fischetti, V.A. (2001) Prevention and elimination of upper respiratory colonization of mice by group A streptococci by using a bacteriophage lytic enzyme. *Proceedings of the National Academy of Sciences of the United States of America*. 98 (7), pp. 4107–4112.
- Nichols, W.W., Dorrington, S.M., Slack, M.P. and Walmsley, H.L. (1988) Inhibition of tobramycin diffusion by binding to alginate. *Antimicrobial agents and chemotherapy*. 32 (4), pp. 518–523.
- Niël-Weise, B.S., van den Broek, P.J., da Silva, E.M.K. and Silva, L.A. (2012) Urinary catheter policies for long-term bladder drainage. *Cochrane database of systematic reviews (Online)*. 8pp. CD004201.
- Nishikawa, H., Yasuda, M., Uchiyama, J., Rashel, M., Maeda, Y., Takemura, I., Sugihara, S., Ujihara, T., Shimizu, Y., Shuin, T. and Matsuzaki, S. (2008) T-even-related bacteriophages as candidates for treatment of *Escherichia coli* urinary tract infections. *Archives of Virology*. 153 (3), pp. 507–515.
- Nunes-Düby, S.E., Kwon, H.J., Tirumalai, R.S., Ellenberger, T. and Landy, A. (1998) Similarities and differences among 105 members of the Int family of site-specific recombinases. *Nucleic acids research*. 26 (2), pp. 391–406.
- Nzakizwanayo, J., Hanin, A., Alves, D.R., McCutcheon, B., Dedi, C., Salvage, J., Knox, K., Stewart, B., Metcalfe, A., Clark, J., Gilmore, B.F., Gahan, C.G.M., Jenkins, A.T.A. and Jones, B. V (2015) Bacteriophage Can Prevent Encrustation and Blockage of Urinary Catheters by *Proteus mirabilis*. *Antimicrobial agents and chemotherapy*. 60 (3), pp. 1530–1536.
- O'Brien, A., Newland, J., Miller, S., Holmes, R., Smith, H. and Formal, S. (1984) Shiga-like toxin-converting phages from *Escherichia coli* strains that cause hemorrhagic colitis or infantile diarrhea. *Science*. 226 (4675), pp. 694-6.

- Okonechnikov, K., Golosova, O., Fursov, M. and UGENE team, the U. (2012) Unipro UGENE: a unified bioinformatics toolkit. *Bioinformatics (Oxford, England)*. 28 (8), pp. 1166–1167.
- Olaniyan, L.W.B., Mkwetshana, N. and Okoh, A.I. (2016) Triclosan in water, implications for human and environmental health. *SpringerPlus*. 5 (1), pp. 1639.
- Olia, A.S., Prevelige, P.E., Johnson, J.E., Cingolani, G. and Cingolani, G. (2011) Three-dimensional structure of a viral genome-delivery portal vertex. *Nature structural and molecular biology*. 18 (5), pp. 597–603.
- Olive, D.M. and Bean, P. (1999) Principles and applications of methods for DNA-based typing of microbial organisms. *Journal of clinical microbiology*. 37 (6), pp. 1661–1669.
- Pal, C., Maciá, M.D., Oliver, A., Schachar, I. and Buckling, A. (2007) Coevolution with viruses drives the evolution of bacterial mutation rates. *Nature*. 450 (7172), pp. 1079–1081.
- Panáček, A., Kvítek, L., Smékalová, M., Večeřová, R., Kolář, M., Röderová, M., Dyčka, F., Šebela, M., Pruček, R., Tomanec, O. and Zbořil, R. (2018) Bacterial resistance to silver nanoparticles and how to overcome it. *Nature Nanotechnology*. 13 (1), pp. 65–71.
- Parida, S. and Mishra, S.K. (2013) Urinary tract infections in the critical care unit: A brief review. *Indian journal of critical care medicine : peer-reviewed, official publication of Indian Society of Critical Care Medicine*. 17 (6), pp. 370–374.
- Parkin, J., Scanlan, J., Woolley, M., Grover, D., Evans, A. and Feneley, R.C.L. (2002) Urinary catheter 'deflation cuff' formation: clinical audit and quantitative in vitro analysis. *BJU international*. 90 (7), pp. 666–671.
- Parliamentary Assembly (2014) Phage therapy, a public health issue. *Doc. 13480*. Available from: <http://www.assembly.coe.int/nw/xml/XRef/Xref-XML2HTML-en.asp?fileid=20704&lang=en>
- Paul, V.D., Sundarrajan, S., Rajagopalan, S.S., Hariharan, S., Kempashanaiah, N., Padmanabhan, S., Sriram, B. and Ramachandran, J. (2011) Lysis-deficient phages as novel therapeutic agents for controlling bacterial infection. *BMC microbiology*. 11, pp. 195.
- Pearson, H.A., Sahukhal, G.S., Elasri, M.O. and Urban, M.W. (2013) Phage-bacterium war on polymeric surfaces: can surface-anchored bacteriophages eliminate microbial infections? *Biomacromolecules*. 14 (5), pp. 1257–1261.
- Pearson, M.M., Rasko, D.A., Smith, S.N. and Mobley, H.L.T. (2010) Transcriptome of Swarming *Proteus mirabilis*. *Infection and Immunity*. 78 (6), pp. 2834–2845.

- Pearson, M.M., Sebahia, M., Churcher, C., Quail, M.A., Seshasayee, A.S., Luscombe, N.M., Abdellah, Z., Arrosmith, C., Atkin, B., Chillingworth, T., Hauser, H., Jagels, K., Moule, S., Mungall, K., et al. (2008) Complete genome sequence of uropathogenic *Proteus mirabilis*, a master of both adherence and motility. *Journal of bacteriology*. 190 (11), pp. 4027–4037.
- Peerbooms, P.G., Verweij, A.M. and MacLaren, D.M. (1984) Vero cell invasiveness of *Proteus mirabilis*. *Infection and immunity*. 43 (3), pp. 1068–1071.
- Pelfrene, E., Willebrand, E., Cavaleiro Sanches, A., Sebris, Z. and Cavaleri, M. (2016) Bacteriophage therapy: a regulatory perspective. *Journal of Antimicrobial Chemotherapy*. 71 (8), pp. 2071–2074.
- Pell, L.G., Cumby, N., Clark, T.E., Tuite, A., Battaile, K.P., Edwards, A.M., Chirgadze, N.Y., Davidson, A.R. and Maxwell, K.L. (2013) A conserved spiral structure for highly diverged phage tail assembly chaperones. *Journal of molecular biology*. 425 (14), pp. 2436–2449.
- Pell, L.G., Liu, A., Edmonds, L., Donaldson, L.W., Howell, P.L. and Davidson, A.R. (2009) The X-Ray Crystal Structure of the Phage λ Tail Terminator Protein Reveals the Biologically Relevant Hexameric Ring Structure and Demonstrates a Conserved Mechanism of Tail Termination among Diverse Long-Tailed Phages. *Journal of Molecular Biology*. 389 (5), pp. 938–951.
- Perepanova, T.S., Darbeeva, O.S., Kotliarova, G.A., Kondrat'eva, E.M., Maïskaia, L.M., Malysheva, V.F., Baïguzina, F.A. and Grishkova, N. V (1995) [The efficacy of bacteriophage preparations in treating inflammatory urologic diseases]. *Urologiia i nefrologiia*. (5), pp. 14–17.
- Perez, G.L., Huynh, B., Slater, M. and Maloy, S. (2009) Transport of Phage P22 DNA across the Cytoplasmic Membrane. *Journal of Bacteriology*. 191 (1), pp. 135–140.
- Persat, A. (2017) Bacterial mechanotransduction. *Current Opinion in Microbiology*. 36, pp. 1–6.
- Petersen, T.N., Brunak, S., von Heijne, G. and Nielsen, H. (2011) SignalP 4.0: discriminating signal peptides from transmembrane regions. *Nature Methods*. 8 (10), pp. 785–786.
- Pires, D.P., Oliveira, H., Melo, L.D.R., Sillankorva, S. and Azeredo, J. (2016) Bacteriophage-encoded depolymerases: their diversity and biotechnological applications. *Applied microbiology and biotechnology*. 100 (5), pp. 2141–2151.
- Pouillot, F., Blois, H. and Iris, F. (2010) Genetically engineered virulent phage banks in the detection and control of emergent pathogenic bacteria. *Biosecurity and bioterrorism : biodefense strategy, practice, and science*. 8 (2), pp. 155–169.
- Powers, J. (2016) Impact of an aseptic procedure for breaking the integrity of the urinary drainage system on the development of catheter-associated urinary tract infections in the intensive care unit. *Intensive and Critical Care Nursing*. 37pp. 82–85.

- Prasad, A., Cevallos, M.E., Riosa, S., Darouiche, R.O. and Trautner, B.W. (2009) A bacterial interference strategy for prevention of UTI in persons practicing intermittent catheterization. *Spinal cord*. 47 (7), pp. 565–569.
- Ptashne, M. (2004) *A genetic switch : phage lambda revisited*. Cold Spring Harbor Laboratory Press.
- Quigley, E.M.M. (2013) Gut bacteria in health and disease. *Gastroenterology and hepatology*. 9 (9), pp. 560–569.
- Rahman, O., Cummings, S.P., Harrington, D.J. and Sutcliffe, I.C. (2008) Methods for the bioinformatic identification of bacterial lipoproteins encoded in the genomes of Gram-positive bacteria. *World Journal of Microbiology and Biotechnology*. 24 (11), pp. 2377–2382.
- Reddy, S.T., Chung, K.K., McDaniel, C.J., Darouiche, R.O., Landman, J. and Brennan, A.B. (2011) Micropatterned surfaces for reducing the risk of catheter-associated urinary tract infection: an in vitro study on the effect of sharklet micropatterned surfaces to inhibit bacterial colonization and migration of uropathogenic *Escherichia coli*. *Journal of endourology / Endourological Society*. 25 (9), pp. 1547–1552.
- Van Regenmortel, M.H. (1990) Virus species, a much overlooked but essential concept in virus classification. *Intervirology*. 31 (5), pp. 241–254.
- Reitz, A., Haferkamp, A., Wagener, N., Gerner, H. and Hohenfellner, M. (2006) Neurogenic bladder dysfunction in patients with neoplastic spinal cord compression: Adaptation of the bladder management strategy to the underlying disease. *Neurorehabilitation*. 21 (1), pp. 65–69.
- Reyes, A., Haynes, M., Hanson, N., Angly, F.E., Heath, A.C., Rohwer, F. and Gordon, J.I. (2010) Viruses in the faecal microbiota of monozygotic twins and their mothers. *Nature*. 466 (7304), pp. 334–338.
- Rhoads, D.D., Wolcott, R.D., Kuskowski, M.A., Wolcott, B.M., Ward, L.S. and Sulakvelidze, A. (2009) Bacteriophage therapy of venous leg ulcers in humans: results of a phase I safety trial. *Journal of Wound Care*. 18 (6), pp. 237–243.
- Ripp, S. and Miller, R. V. (1997) The role of pseudolysogeny in bacteriophage-host interactions in a natural freshwater environment. *Microbiology*. 143 (6), pp. 2065–2070.
- Roach, D.R. and Donovan, D.M. (2015) Antimicrobial bacteriophage-derived proteins and therapeutic applications. *Bacteriophage*. 5 (3), pp. e1062590.
- Rocha, E.P., Danchin, A. and Viari, A. (2001) Evolutionary role of restriction/modification systems as revealed by comparative genome analysis. *Genome research*. 11 (6), pp. 946–958.
- Rocha, S.P.D., Pelayo, J.S. and Elias, W.P. (2007) Fimbriae of uropathogenic *Proteus mirabilis*. *FEMS Immunology and Medical Microbiology*. 51 (1), pp. 1–7.

- Rodríguez-Rubio, L., Martínez, B., Donovan, D.M., Rodríguez, A. and García, P. (2013) Bacteriophage virion-associated peptidoglycan hydrolases: potential new enzybiotics. *Critical reviews in microbiology*. 39 (4), pp. 427–434.
- Roessner, C.A. and Ihler, G.M. (1984) Proteinase sensitivity of bacteriophage lambda tail proteins gpJ and pH in complexes with the lambda receptor. *Journal of bacteriology*. 157 (1), pp. 165–170.
- Rohwer, F., Prangishvili, D. and Lindell, D. (2009) Roles of viruses in the environment. *Environmental Microbiology*. 11 (11), pp. 2771–2774.
- Rutherford, K., Parkhill, J., Crook, J., Horsnell, T., Rice, P., Rajandream, M.A. and Barrell, B. (2000) Artemis: sequence visualization and annotation. *Bioinformatics (Oxford, England)*. 16 (10), pp. 944–945.
- Sabat, A.J., Budimir, A., Nashe, D., Sá-Leão, R., Dijk, J.M. van, Laurent, F., Grundmann, H. and Friedrich, A.W. (2013) *Overview of molecular typing methods for outbreak detection and epidemiological surveillance*. Available from: <http://www.eurosurveillance.org/ViewArticle.aspx?ArticleId=20380>
- Sabbuba, N.A., Mahenthiralingam, E. and Stickler, D.J. (2003) Molecular epidemiology of *Proteus mirabilis* infections of the catheterized urinary tract. *Journal of clinical microbiology*. 41 (11), pp. 4961–4965.
- Salipante, S.J., SenGupta, D.J., Cummings, L.A., Land, T.A., Hoogestraat, D.R. and Cookson, B.T. (2015) Application of whole-genome sequencing for bacterial strain typing in molecular epidemiology. *Journal of clinical microbiology*. 53 (4), pp. 1072–1079.
- Salmond, G.P.C. and Fineran, P.C. (2015) A century of the phage: past, present and future. *Nature Reviews Microbiology*. 13 (12), pp. 777–786.
- Sambrook, J. and Russell, D.W. (2001) Purification of Bacteriophage λ particles by Isopycnic Centrifugation through CsCl Gradients. *Molecular Cloning: A Laboratory Manual*. (1). pii: pdb.prot3968.
- Sathaliyawala, T., Rao, M., Maclean, D.M., Birx, D.L., Alving, C.R. and Rao, V.B. (2006) Assembly of human immunodeficiency virus (HIV) antigens on bacteriophage T4: a novel in vitro approach to construct multicomponent HIV vaccines. *Journal of virology*. 80 (15), pp. 7688–7698.
- Sauer, R.T., Krovatin, W., DeAnda, J., Youderian, P. and Susskind, M.M. (1983) Primary structure of the imm1 immunity region of bacteriophage P22. *Journal of molecular biology*. 168 (4), pp. 699–713.
- Scandella, D. and Arber, W. (1976) Phage lambda DNA injection into *Escherichia coli* pel- mutants is restored by mutations in phage genes V or H. *Virology*. 69 (1), pp. 206–215.
- Scavone, P., Iribarnegaray, V., Caetano, A.L., Schlapp, G., Härtel, S. and Zunino, P. (2016) Fimbriae have distinguishable roles in *Proteus mirabilis* biofilm formation Filip Ruzicka (ed.). *Pathogens and Disease*. 74 (5), pp. ftw033.

- Schatten, H. and Eisenstark, A. (2007) *Salmonella : methods and protocols*. Humana Press.
- Schattner, P., Brooks, A.N. and Lowe, T.M. (2005) The tRNAscan-SE, snoscan and snoGPS web servers for the detection of tRNAs and snoRNAs. *Nucleic acids research*. 33 (Web Server issue), pp. W686-9.
- Schmidt, H. (2001) Shiga-toxin-converting bacteriophages. *Research in microbiology*. 152 (8), pp. 687–695.
- Schumm, K. and Lam, T.B.L. (2008) Types of urethral catheters for management of short-term voiding problems in hospitalized adults: A short version cochrane review. *Neurourology and Urodynamics*. 27 (8), pp. 738–746.
- Senior, B.W. (1977) Typing of Proteus Strains by Proticine Production and Sensitivity. *Journal of Medical Microbiology*. 10 (1), pp. 7–17.
- Serwer, P., Hayes, S.J., Thomas, J.A. and Hardies, S.C. (2007) Propagating the missing bacteriophages: a large bacteriophage in a new class. *Virology Journal*. 4 (1), pp. 21.
- Shenot, P., Rivas, D.A., Kalman, D.D., Staas, W.E. and Chancellor, M.B. (1994) Latex allergy manifested in urological surgery and care of adult spinal cord injured patients. *Archives of physical medicine and rehabilitation*. 75 (11), pp. 1263–1265.
- Siddiq, D.M. and Darouiche, R.O. (2012) New strategies to prevent catheter-associated urinary tract infections. *Nature reviews. Urology*. 9 (6), pp. 305–314.
- Silver, L.L. (2011) Challenges of antibacterial discovery. *Clinical microbiology reviews*. 24 (1), pp. 71–109.
- Skurnik, M., Pajunen, M. and Kiljunen, S. (2007) Biotechnological challenges of phage therapy. *Biotechnology Letters*. 29 (7), pp. 995–1003.
- Skurnik, M. and Strauch, E. (2006) Phage therapy: Facts and fiction. *International Journal of Medical Microbiology*. 296 (1), pp. 5–14.
- Slopek, S., Weber-Dabrowska, B., Dabrowski, M., and Kucharewicz-Krukowska, A. (1987) Results of bacteriophage treatment of suppurative bacterial infections in the years 1981-1986. *Arch Immunol The Exp*. 35pp. 569–583.
- Smith, H.W. and Huggins, M.B. (1982) Successful Treatment of Experimental Escherichia coli Infections in Mice Using Phage: its General Superiority over Antibiotics. *Microbiology*. 128 (2), pp. 307–318.
- Söding, J., Biegert, A. and Lupas, A.N. (2005) The HHpred interactive server for protein homology detection and structure prediction. *Nucleic acids research*. 33 (Web Server issue), pp. W244-8.
- Solano, C., Echeverz, M. and Lasa, I. (2014) Biofilm dispersion and quorum sensing. *Current Opinion in Microbiology*. 18pp. 96–104.

- Son, J.-S., Lee, S.-J., Jun, S.Y., Yoon, S.J., Kang, S.H., Paik, H.R., Kang, J.O. and Choi, Y.-J. (2010) Antibacterial and biofilm removal activity of a podoviridae Staphylococcus aureus bacteriophage SAP-2 and a derived recombinant cell-wall-degrading enzyme. *Applied Microbiology and Biotechnology*. 86 (5), pp. 1439–1449.
- Stahl, S.J., Stewart, K.R. and Williams, F.D. (1983) Extracellular slime associated with *Proteus mirabilis* during swarming. *Journal of bacteriology*. 154 (2), pp. 930–937.
- Stamm, W.E. (1991) Catheter-associated urinary tract infections: Epidemiology, pathogenesis, and prevention. *The American Journal of Medicine*. 91 (3), pp. S65–S71.
- Steinbacher, S., Miller, S., Baxa, U., Budisa, N., Weintraub, A., Seckler, R. and Huber, R. (1997) Phage P22 tailspike protein: crystal structure of the head-binding domain at 2.3 Å, fully refined structure of the endorhamnosidase at 1.56 Å resolution, and the molecular basis of O-antigen recognition and cleavage. *Journal of Molecular Biology*. 267 (4), pp. 865–880.
- Stewart, P.S. and William Costerton, J. (2001) Antibiotic resistance of bacteria in biofilms. *The Lancet*. 358 (9276), pp. 135–138.
- Stickler, D. J., Morris, N. S., Winters, C. (1999) Simple physical model to study formation and physiology of biofilms on urethral catheters. *Methods in enzymology*. 310pp. 494–501.
- Stickler, D., Ganderton, L., King, J., Nettleton, J. and Winters, C. (1993) *Proteus mirabilis* biofilms and the encrustation of urethral catheters. *Urological research*. 21 (6), pp. 407–411.
- Stickler, D. and Hughes, G. (1999) Ability of *Proteus mirabilis* to Swarm over Urethral Catheters. *European Journal of Clinical Microbiology and Infectious Diseases*. 18 (3), pp. 206–208.
- Stickler, D., Morris, N., Moreno, M.-C. and Sabbuba, N. (1998a) Studies on the formation of crystalline bacterial biofilms on urethral catheters. *European Journal of Clinical Microbiology and Infectious Diseases*. 17 (9), pp. 649–652.
- Stickler, D., Young, R., Jones, G., Sabbuba, N. and Morris, N. (2003) Why are Foley catheters so vulnerable to encrustation and blockage by crystalline bacterial biofilm? *Urological Research*. 31 (5), pp. 306–311.
- Stickler, D.J. (2008) Bacterial biofilms in patients with indwelling urinary catheters. *Nature Clinical Practice Urology*. 5 (11), pp. 598–608.
- Stickler, D.J. and Feneley, R.C.L. (2010) The encrustation and blockage of long-term indwelling bladder catheters: a way forward in prevention and control. *Spinal Cord*. 48 (11), pp. 784–790.

- Stickler, D.J. and Morgan, S.D. (2006) Modulation of crystalline *Proteus mirabilis* biofilm development on urinary catheters. *Journal of Medical Microbiology*. 55 (5), pp. 489–494.
- Stickler, D.J. and Morgan, S.D. (2008) Observations on the development of the crystalline bacterial biofilms that encrust and block Foley catheters. *Journal of Hospital Infection*. 69 (4), pp. 350–360.
- Stickler, D.J., Morris, N.S., McLean, R.J. and Fuqua, C. (1998b) Biofilms on indwelling urethral catheters produce quorum-sensing signal molecules in situ and in vitro. *Applied and environmental microbiology*. 64 (9), pp. 3486–3490.
- Stickler, D.J. and Zimakoff, J. (1994) Complications of urinary tract infections associated with devices used for long-term bladder management. *The Journal of hospital infection*. 28 (3), pp. 177–194.
- Stratton, C.W. (2003) Dead Bugs Don't Mutate: Susceptibility Issues in the Emergence of Bacterial Resistance. *Emerging Infectious Diseases*. 9 (1), pp. 10–16.
- Strauss, H. and King, J. (1984) Steps in the stabilization of newly packaged DNA during phage P22 morphogenesis. *Journal of molecular biology*. 172 (4), pp. 523–543.
- Suller, M.T.E., Anthony, V.J., Mathur, S., Feneley, R.C.L., Greenman, J. and Stickler, D.J. (2005) Factors modulating the pH at which calcium and magnesium phosphates precipitate from human urine. *Urological Research*. 33 (4), pp. 254–260.
- Sun, Y., Parker, M.H., Weigele, P., Casjens, S., Prevelige Jr, P.E. and Krishna, N.R. (2000) Structure of the coat protein-binding domain of the scaffolding protein from a double-stranded DNA virus. *Journal of Molecular Biology*. 297 (5), pp. 1195–1202.
- Susskind, M.M. and Botstein, D. (1978) Molecular genetics of bacteriophage P22. *Microbiological reviews*. 42 (2), pp. 385–413.
- Sybesma, W., Zbinden, R., Chanishvili, N., Kutateladze, M., Chkhotua, A., Ujmajuridze, A., Mehnert, U. and Kessler, T.M. (2016) Bacteriophages as Potential Treatment for Urinary Tract Infections. *Frontiers in microbiology*. 7, pp. 465.
- Tack, K.J. and Sabath, L.D. (1985) Increased minimum inhibitory concentrations with anaerobiasis for tobramycin, gentamicin, and amikacin, compared to latamoxef, piperacillin, chloramphenicol, and clindamycin. *Chemotherapy*. 31 (3), pp. 204–210.
- Tambyah, P.A., Halvorson, K.T. and Maki, D.G. (1999) A Prospective Study of Pathogenesis of Catheter-Associated Urinary Tract Infections. *Mayo Clinic Proceedings*. 74 (2), pp. 131–136.

- Tambyah, P.A. and Maki, D.G. (2000) Catheter-associated urinary tract infection is rarely symptomatic: a prospective study of 1,497 catheterized patients. *Archives of internal medicine*. 160 (5), pp. 678–682.
- Tan, I.-K. and Gajra, B. (2006) Plasma and urine amino acid profiles in a healthy adult population of Singapore. *Annals of the Academy of Medicine, Singapore*. 35 (7), pp. 468–475.
- Tarkowski, T.A., Mooney, D., Thomason, L.C. and Stahl, F.W. (2002) Gene products encoded in the ninR region of phage lambda participate in Red-mediated recombination. *Genes to cells : devoted to molecular and cellular mechanisms*. 7 (4), pp. 351–363.
- Tavares, P., Lurz, R., Stiege, A., Rückert, B. and Trautner, T. (1996) Sequential headful packaging and fate of the cleaved DNA ends in bacteriophage SPP1. *J Mol Biol*. pp. 954–967.
- Tenke, P., Riedl, C.R., Jones, G.L., Williams, G.J., Stickler, D. and Nagy, E. (2004) Bacterial biofilm formation on urologic devices and heparin coating as preventive strategy. *International Journal of Antimicrobial Agents*. 23pp. 67–74.
- Tenover, F.C., Arbeit, R.D., Goering, R. V, Mickelsen, P.A., Murray, B.E., Persing, D.H. and Swaminathan, B. (1995) GUEST COMMENTARY Interpreting Chromosomal DNA Restriction Patterns Produced by Pulsed-Field Gel Electrophoresis : Criteria for Bacterial Strain Typing. *Journal of clinical microbiology*. 33 (9), pp. 2233–2239.
- Teschke, C.M. and Parent, K.N. (2010) ‘Let the phage do the work’: Using the phage P22 coat protein structures as a framework to understand its folding and assembly mutants. *Virology*. 401 (2), pp. 119–130.
- Thiel, K. (2004) Old dogma, new tricks--21st Century phage therapy. *Nature biotechnology*. 22 (1), pp. 31–36.
- Thingstad, T. and Lignell, R. (1997) Theoretical models for the control of bacterial growth rate, abundance, diversity and carbon demand. *Aquatic Microbial Ecology*. 13 (1), pp. 19–27.
- Toothman, P. (1981) Restriction alleviation by bacteriophages lambda and lambda reverse. *Journal of virology*. 38 (2), pp. 621–631.
- Torres-Barceló, C. and Hochberg, M.E. (2016) Evolutionary Rationale for Phages as Complements of Antibiotics. *Trends in Microbiology*. 24 (4), pp. 249–256.
- Torzewska, A. and Rozalski, A. (2014) Inhibition of crystallization caused by *Proteus mirabilis* during the development of infectious urolithiasis by various phenolic substances. *Microbiological Research*. 169 (7), pp. 579–584.

- Tóthová, L., Celec, P., Bábíčková, J., Gajdošová, J., Al-Alami, H., Kamodyova, N., Drahovská, H., Liptáková, A., Turňa, J. and Hodosy, J. (2011) Phage therapy of Cronobacter-induced urinary tract infection in mice. *Medical science monitor : international medical journal of experimental and clinical research*. 17 (7), pp. BR173-8.
- Trautner, B.W., Hull, R.A. and Darouiche, R.O. (2003) Escherichia coli 83972 inhibits catheter adherence by a broad spectrum of uropathogens. *Urology*. 61 (5), pp. 1059–1062.
- Trautner, B.W., Hull, R.A., Thornby, J.I. and Darouiche, R.O. (2007) Coating urinary catheters with an avirulent strain of Escherichia coli as a means to establish asymptomatic colonization. *Infection control and hospital epidemiology*. 28 (1), pp. 92–94.
- Tsiskarishvili, L.D. (1957) Phage Therapy of Closed Purulent Cites. *Bacteriophage Research*. pp. 387–396.
- Tsulukidze, A.P. (1938) Application of phages in urology. *Urologia*. 15, pp. 10–13.
- Tunney, M.M. and Gorman, S.P. (2002) Evaluation of a poly(vinyl pyrrolidone)-coated biomaterial for urological use. *Biomaterials*. 23 (23), pp. 4601–4608.
- Van Twest, R. and Kropinski, A.M. (2009) Bacteriophage Enrichment from Water and Soil. *Methods in molecular biology (Clifton, N.J.)*. pp. 15–22.
- Vapnek, J.M., Maynard, F.M. and Kim, J. (2003) A Prospective Randomized Trial Of The Lofric Hydrophilic Coated Catheter Versus Conventional Plastic Catheter For Clean Intermittent Catheterization. *The Journal of Urology*. 169 (3), pp. 994–998.
- Veesler, D. and Cambillau, C. (2011) A common evolutionary origin for tailed-bacteriophage functional modules and bacterial machineries. *Microbiology and molecular biology reviews : MMBR*. 75 (3), pp. 423–33, first page of table of contents.
- Verbeken, G., Pirnay, J.-P., De Vos, D., Jennes, S., Zizi, M., Lavigne, R., Casteels, M. and Huys, I. (2012) Optimizing the European Regulatory Framework for Sustainable Bacteriophage Therapy in Human Medicine. *Archivum Immunologiae et Therapiae Experimentalis*. 60 (3), pp. 161–172.
- Verma, V., Harjai, K. and Chhibber, S. (2009) Characterization of a T7-like lytic bacteriophage of Klebsiella pneumoniae B5055: a potential therapeutic agent. *Current microbiology*. 59 (3), pp. 274–281.
- Verma, V., Harjai, K. and Chhibber, S. (2010) Structural changes induced by a lytic bacteriophage make ciprofloxacin effective against older biofilm of *Klebsiella pneumoniae*. *Biofouling*. 26 (6), pp. 729–737.

- Voegele, P., Badiola, J., Schmidt-Malan, S.M., Karau, M.J., Greenwood-Quaintance, K.E., Mandrekar, J.N. and Patel, R. (2015) Antibiofilm Activity of Electrical Current in a Catheter Model. *Antimicrobial agents and chemotherapy*. 60 (3), pp. 1476–1480.
- Voroshilova, N.N., Bogovazova, G.G., Kazakova, T.B., Alferova, E. V, Fattakhov, B.T., Pushkarev, A.E., Bulgakova, A.I., Perepanova, T.S., Derbeeva, O.S., Lazareva, E.B., Yatsik, G. V, Samsygina, G.A. and Ankarskaya, A.S. (2000) *Contemporary Issues of Elaboration, Manufacturing, and Application of Immunobiological and Pharmaceutical Preparations*. In: 2000 pp. pp. 87–93.
- Waldor, M.K. and Mekalanos, J.J. (1996) Lysogenic conversion by a filamentous phage encoding cholera toxin. *Science (New York, N.Y.)*. 272 (5270), pp. 1910–1914.
- Walker, K.E., Moghaddame-Jafari, S., Lockatell, C. V, Johnson, D. and Belas, R. (1999) ZapA, the IgA-degrading metalloprotease of *Proteus mirabilis*, is a virulence factor expressed specifically in swarmer cells. *Molecular microbiology*. 32 (4), pp. 825–836.
- Wang, J.-T., Chen, P.-C., Chang, S.-C., Shiau, Y.-R., Wang, H.-Y., Lai, J.-F., Huang, I.-W., Tan, M.-C., Lauderdale, T.-L.Y. and TSAR Hospitals, T. (2014) Antimicrobial susceptibilities of *Proteus mirabilis*: a longitudinal nationwide study from the Taiwan surveillance of antimicrobial resistance (TSAR) program. *BMC infectious diseases*. 14, pp. 486.
- Warren, J.W. (1997) Catheter-associated urinary tract infections. *Infectious disease clinics of North America*. 11 (3), pp. 609–622.
- Warren, R.A.J. (1980) Modified Bases in Bacteriophage DNAs. *Annual Review of Microbiology*. 34 (1), pp. 137–158.
- Waters, E.M., Rowe, S.E., O’Gara, J.P., Conlon, B.P., Wood, T. and Su, F. (2016) Convergence of *Staphylococcus aureus* Persister and Biofilm Research: Can Biofilms Be Defined as Communities of Adherent Persister Cells? Kimberly A. Kline (ed.). *PLOS Pathogens*. 12 (12), pp. e1006012.
- Wenner, J.J. and Rettger, L.F. (1919) A Systematic Study of the *Proteus* Group of Bacteria. *Journal of bacteriology*. 4 (4), pp. 331–353.
- Westall, F., de Wit, M.J., Dann, J., van der Gaast, S., de Ronde, C.E. and Gerneke, D. (2001) Early Archean fossil bacteria and biofilms in hydrothermally-influenced sediments from the Barberton greenstone belt, South Africa. *Precambrian Research*. 106 (1), pp. 93–116.
- Whitman, W.B., Coleman, D.C. and Wiebe, W.J. (1998) Prokaryotes: the unseen majority. *Proceedings of the National Academy of Sciences of the United States of America*. 95 (12), pp. 6578–6583.
- Wikoff, W.R., Liljas, L., Duda, R.L., Tsuruta, H., Hendrix, R.W. and Johnson, J.E. (2000) Topologically linked protein rings in the bacteriophage HK97 capsid. *Science (New York, N.Y.)*. 289 (5487), pp. 2129–2133.

- Wilhelm, S.W., Suttle, C.A. (1999) Viruses and Nutrient Cycles in the Sea. *BioScience*. 49 (10), pp. 781.
- Willette, P. and Coffield, S. (2012) Current Trends in the Management of Difficult Urinary Catheterizations. *Western Journal of Emergency Medicine*. 13 (6), pp. 472–478.
- Wilson, M.L. and Gaido, L. (2004) Laboratory Diagnosis of Urinary Tract Infections in Adult Patients. *Clinical Infectious Diseases*. 38 (8), pp. 1150–1158.
- Yacoby, I., Bar, H. and Benhar, I. (2007) Targeted drug-carrying bacteriophages as antibacterial nanomedicines. *Antimicrobial agents and chemotherapy*. 51 (6), pp. 2156–2163.
- Yakubu, D.E., Old, D.C. and Senior, B.W. (1989) The haemagglutinins and fimbriae of *Proteus penneri*. *Journal of Medical Microbiology*. 30 (4), pp. 279–284.
- Yarnell, W.S. and Roberts, J.W. (1992) The phage lambda gene Q transcription antiterminator binds DNA in the late gene promoter as it modifies RNA polymerase. *Cell*. 69 (7), pp. 1181–1189.
- Young, R. (2002) Bacteriophage holins: deadly diversity. *Journal of molecular microbiology and biotechnology*. 4 (1), pp. 21–36.
- Young, R. (2014) Phage lysis: Three steps, three choices, one outcome. *Journal of Microbiology*. 52 (3), pp. 243–258.
- Zhu, H., Sun, X., Lu, J., Wang, M., Fang, Y. and Ge, W. (2012) The effect of plum juice on the prevention of struvite calculus formation *in vitro*. *BJU International*. 110 (8b), pp. E362–E367.
- Zowawi, H.M., Harris, P.N.A., Roberts, M.J., Tambyah, P.A., Schembri, M.A., Pezzani, M.D., Williamson, D.A. and Paterson, D.L. (2015) The emerging threat of multidrug-resistant Gram-negative bacteria in urology. *Nature reviews. Urology*. 12 (10), pp. 570–584.
- Zuker, M. (2003) Mfold web server for nucleic acid folding and hybridization prediction. *Nucleic Acids Research*. 31 (13), pp. 3406–3415.
- Zunino, P., Geymonat, L., Allen, A.G., Legnani-Fajardo, C. and Maskell, D.J. (2000) Virulence of a *Proteus mirabilis* ATF isogenic mutant is not impaired in a mouse model of ascending urinary tract infection. *FEMS immunology and medical microbiology*. 29 (2), pp. 137–143.
- Zylicz, M., Gorska, I., Taylor, K. and Georgopoulos, C. (1984) Bacteriophage lambda replication proteins: formation of a mixed oligomer and binding to the origin of lambda DNA. *Molecular and general genetics : MGG*. 196 (3), pp. 401–406.

Appendix: Supplementary Material

Table 8. Functional annotation of the predicted coding sequences of phage vB_PmiS_NSM6

| Gene | Coordinates | Strand | Length (nt) | Length (aa) | pI | MW | Putative Product | Best homologue | E-value |
|------|--------------|--------|----------------|----------------|-------|---------|-------------------------------|--|---------|
| 1 | 1..426 | + | 426 | 141 | 4.95 | 15205.1 | terminase, small subunit | Acinetobacter phage YMC-13-01-C62 YP_009055422 | 3e-45 |
| 2 | 410..1660 | + | 1251 | 416 | 8.03 | 47915.7 | terminase, large subunit | Enterobacteria phage ES18 YP_224140 | 0.0 |
| 3 | 1660..3015 | + | 1356 | 451 | 4.9 | 50499.8 | portal vertex protein | Salmonella phage vB_SosS_Oslo YP_006560809 | 0.0 |
| 4 | 2966..3895 | + | 930 | 309 | 9.39 | 35183.2 | minor capsid protein | Salmonella phage vB_SosS_Oslo YP_006560810 | 4e-124 |
| 5 | 3899..5173 | + | 1275 | 424 | 4.99 | 45948 | prohead protease | Cronobacter phage ES2 AEM24695 | 0.0 |
| 6 | 5173.. 5610 | + | 438 | 145 | 5.84 | 15344.3 | DUF2190 domain protein | Salmonella phage vB_SosS_Oslo YP_006560812 | 1e-61 |
| 7 | 5627.. 6721 | + | 1095 | 364 | 5.77 | 39674.8 | major capsid protein | Cronobacter phage ES2 AEM24696 | 0.0 |
| 8 | 6731.. 6904 | + | 174 | 57 | 6.72 | 6342.28 | - | Cronobacter phage ES2 AEM24717 | 8e-16 |
| 9 | 6961..7359 | + | 399 | 132 | 6.81 | 14277.4 | - | Salmonella phage vB_SosS_Oslo YP_006560815 | 2e-73 |
| 10 | 7359..7700 | + | 342 | 113 | 5.27 | 12624.3 | head-tail joining protein | Mannheimia phage vB_MhS_587AP2 YP_009193561 | 4e-28 |
| 11 | 7702..8073 | + | 372 | 123 | 10.18 | 13699.9 | tail component | Cronobacter phage ES2 AEM24713 | 1e-55 |
| 12 | 8070..8438 | + | 369 | 122 | 4.46 | 13871.6 | head-tail connector protein | Cronobacter phage ENT47670 YP_007237612 | 5e-14 |
| 13 | 8503..9258 | + | 756 | 251 | 4.47 | 26878.1 | major tail protein | Cronobacter phage ES2 AEM24699 | 1e-46 |
| 14 | 9308..10000 | + | 693 | 230 | 8.98 | 26534.8 | tail assembly chaperone | Cronobacter phage ES2 AEM24701 | 8e-76 |
| 15 | 10070..10450 | + | 381 | 126 | 7.91 | 14365.4 | lipoprotein | No significant database matches | |
| 16 | 10514..13921 | + | 3408 | 1135 | 7.59 | 121863 | tape-measure protein | Enterobacteria phage ES18 YP_224159 | 0.0 |
| 17 | 13925..14401 | + | 477 | 158 | 4.58 | 18258.7 | minor tail protein | Cronobacter phage ENT47670 YP_007237618 | 9e-75 |
| 18 | 14401..14871 | + | 471 | 156 | 9.16 | 18256.9 | DUF1833 domain protein | Cronobacter phage ENT47670 YP_007237619 | 7e-55 |
| 19 | 14868..15260 | + | 393 | 130 | 6.51 | 15048.2 | tail associated peptidoglycan | Cronobacter phage ENT47670 YP_007237620 | 9e-58 |

| Gene | Coordinates | Strand | Length (nt) | Length (aa) | pI | MW | Putative Product | Best homologue | E-value |
|------|--------------|--------|----------------|----------------|------|---------|---------------------------------------|--|---------|
| 20 | 15247..17715 | + | 2469 | 822 | 4.91 | 93446.8 | tail tip protein/baseplate structural | Cronobacter phage ENT47670 YP_007237575 | 0.0 |
| 21 | 17834..20461 | + | 2628 | 875 | 5.72 | 95941.3 | tail spike protein | No significant database matches | |
| 22 | 20495..22339 | - | 1845 | 614 | 9.12 | 70439.3 | acetyl transferase | Enterobacter phage Tyrion ANN86195 | 0.0 |
| 23 | 22410..22640 | - | 231 | 76 | 8.01 | 8769.91 | DNA polymerase small subunit | Escherichia phage HK639 YP_004934090 | 3e-28 |
| 24 | 23027..24202 | + | 1176 | 391 | 9.53 | 45261.4 | integrase | Stx2-converting phage 86 YP_794083 | 0.0 |
| 25 | 24180..24371 | - | 192 | 63 | 9.78 | 7232.44 | excisionase | Stx2 converting phage vB_EcoP_24B YP_009168094 | 6e-16 |
| 26 | 24381..24575 | - | 195 | 64 | 6.03 | 7155.02 | zinc-finger domain protein | No significant database matches | |
| 27 | 24660..25205 | - | 546 | 181 | 5.92 | 20552.4 | DNA N-6-adenine-methyltransferase | Enterobacteria phage HK97 NP_037744 | 1e-70 |
| 28 | 25195..25527 | - | 333 | 110 | 4.13 | 12530.3 | NinX-like protein | Enterobacteria phage P22 NP_059615 | 2e-11 |
| 29 | 25520..25693 | - | 174 | 57 | 4.42 | 6740.69 | - | No significant database matches | |
| 30 | 25753..26781 | - | 1029 | 342 | 9.16 | 40009.7 | DNA N-6-adenine-methyltransferase | Enterobacteria phage phi50 B47029 | 5e-70 |
| 31 | 26913..27167 | - | 255 | 84 | 7.82 | 9820.51 | - | No significant database matches | |
| 32 | 27160..27414 | - | 255 | 84 | 9.39 | 9794.98 | - | Enterobacteria phage Phi1 YP_001469347 | 4e-07 |
| 33 | 27449..28168 | - | 720 | 239 | 5.46 | 27646.9 | - | No significant database matches | |
| 34 | 2823128509 | - | 279 | 92 | 9.3 | 10055.5 | - | No significant database matches | |
| 35 | 28572..29027 | - | 456 | 151 | 4.6 | 16970.2 | ASCH domain | Enterobacteria phage P7 AAQ07560 | 5e-14 |
| 36 | 29030..29203 | - | 174 | 57 | 4.13 | 6670.35 | antitermination protein | No significant database matches | |
| 37 | 29254..29793 | - | 540 | 179 | 6.83 | 19750.2 | single-strand DNA binding protein | Enterobacteria phage IME_EC2 AGZ17812 | 7e-76 |

| Gene | Coordinates | Strand | Length (nt) | Length (aa) | pI | MW | Putative Product | Best homologue | E-value |
|------|--------------|--------|----------------|----------------|-------|---------|-------------------------------------|--|---------|
| 38 | 29793..30347 | - | 555 | 184 | 7.89 | 20795.7 | - | Salmonella phage SEN22 YP_009191483 | 2e-83 |
| 39 | 30347..31171 | - | 825 | 274 | 4.9 | 31616.9 | exodeoxyribonuclease VIII | Salmonella phage SEN22 YP_009191484 | 7e-138 |
| 40 | 31168..31422 | - | 255 | 84 | 4.38 | 9500.79 | - | No significant database matches | |
| 41 | 31419..31694 | - | 276 | 91 | 5.31 | 10553.8 | - | No significant database matches | |
| 42 | 31685..31861 | - | 177 | 58 | 10.3 | 6649.94 | - | No significant database matches | |
| 43 | 31917..32858 | - | 942 | 313 | 5.61 | 36441 | - | Edwardsiella phage GF-2 YP_009126656 | 4e-49 |
| 44 | 32922..33209 | - | 288 | 95 | 4.64 | 10604 | - | Enterobacterial phage mEp213 YP_007112392 | 1e-25 |
| 45 | 33936..34109 | - | 174 | 57 | 4.73 | 6288.16 | - | No significant database matches | |
| 46 | 34119..34391 | - | 273 | 90 | 10.13 | 10163.8 | antitermination peptide-RNA-complex | No significant database matches | |
| 47 | 34890..35585 | - | 696 | 231 | 6.34 | 25551.4 | repressor; like phage lambda CI | Escherichia phage 434 S32822 | 1e-73 |
| 48 | 35646..35873 | + | 228 | 75 | 9.52 | 8291.75 | Cro-like regulatory protein | Enterobacteria phage 933W NP_049486 | 5e-32 |
| 49 | 36003..36329 | + | 327 | 108 | 7.89 | 12390.2 | transcriptional regulator | No significant database matches | |
| 50 | 36447..36623 | + | 177 | 58 | 10.08 | 6973.99 | DUF2740 domain protein | No significant database matches | |
| 51 | 36616..37452 | + | 837 | 278 | 9.61 | 31344.6 | O-like transcriptional regulator | Enterobacteria phage HK97 NP_037739 | 2e-89 |
| 52 | 37453..38823 | + | 1371 | 456 | 5.55 | 49862.6 | DnaB-like replicative DNA helicase | Salmonella phage vB_SemP_Emek YP_006560600 | 0.0 |
| 53 | 38843..39046 | + | 204 | 67 | 4.89 | 7639.54 | - | No significant database matches | |
| 54 | 39030..39344 | + | 315 | 104 | 6.75 | 12194.9 | - | Enterobacteria phage N15 NP_046939 | 2e-08 |
| 55 | 39344..39577 | + | 234 | 77 | 9.51 | 9144.62 | - | No significant database matches | |
| 56 | 39603..39884 | + | 282 | 93 | 9.74 | 10957.6 | - | No significant database matches | |

| Gene | Coordinates | Strand | Length (nt) | Length (aa) | pI | MW | Putative Product | Best homologue | E-value |
|------|--------------|--------|----------------|----------------|-------|---------|---------------------------------|---|---------|
| 57 | 39871..40119 | + | 249 | 82 | 4.39 | 9881.05 | DUF551 domain protein | Stx2-converting phage Stx2a_1447 BAT32382 | 0.001 |
| 58 | 40119..40328 | + | 210 | 69 | 9.99 | 8459.33 | - | No significant database matches | |
| 59 | 40330..40512 | + | 183 | 60 | 7.56 | 6809.64 | Lar-like protein | Escherichia phage Rac-SA53 ALP46925 | 2e-05 |
| 60 | 40505..40726 | + | 222 | 73 | 9.91 | 8895.35 | - | No significant database matches | |
| 61 | 40728..41174 | + | 447 | 148 | 9.24 | 17094.6 | NinB-like recombinase | Escherichia phage HK639 YP_004934092 | 4e-52 |
| 62 | 41195..41554 | + | 360 | 119 | 8.39 | 14126 | - | Edwardsiella phage GF-2 YP_009126670 | 9e-12 |
| 63 | 41551..41775 | + | 225 | 74 | 6.57 | 8748.05 | DUF3310 domain protein | Enterobacter phage phiKDA1 AFE86127 | 8e-35 |
| 64 | 41772..41900 | + | 129 | 42 | 7.9 | 5279.04 | - | Klebsiella phage JD001 YP_007392874 | 2e-04 |
| 65 | 41897..42355 | + | 459 | 152 | 9.73 | 17552.4 | DNA-binding protein | No significant database matches | |
| 66 | 42333..42449 | + | 117 | 38 | 5.05 | 4337.96 | NinF-like protein | No significant database matches | |
| 67 | 42449..43069 | + | 621 | 206 | 10.05 | 24161.9 | NinG-like recombination protein | Salmonella phage FSL SP-016 AGF88105 | 2e-59 |
| 68 | 43069..43284 | + | 216 | 71 | 9.44 | 8244.58 | - | No significant database matches | |
| 69 | 43281..43784 | + | 504 | 167 | 9.56 | 19493.5 | antiterminator Q protein | Enterobacteria phage Sfl YP_009147507 | 9e-72 |
| 70 | 44437..44826 | + | 390 | 129 | 6.54 | 13235.4 | antiholin | Salmonella phage FSL SP-076 YP_008240201 | 2e-16 |
| 71 | 44823..45116 | + | 294 | 97 | 9.44 | 11153.3 | holin | Escherichia phage TL-2011b YP_007002002 | 2e-10 |
| 72 | 45103..45435 | + | 333 | 110 | 6.91 | 12451.9 | endolysin | Cronobacter phage ESSI-2 ADX32406 | 2e-46 |
| 73 | 45422..45889 | + | 468 | 155 | 5.06 | 17745.9 | RZ lysis protein | Enterobacteria phage P21 P27358 | 2e-16 |
| 74 | 45645..45821 | + | 177 | 58 | 10.02 | 6547.9 | RZ1 lysis protein | No significant database matches | |
| 75 | 45864..46217 | - | 354 | 117 | 6.57 | 13045 | - | No significant database matches | |
| 76 | 46238..46801 | + | 564 | 187 | 8.8 | 21148.3 | DNA-binding protein | Acinetobacter bacteriophage AP22 YP_006383824 | 4e-27 |
| 77 | 46791..47210 | + | 420 | 139 | 5.91 | 15928.1 | - | No significant database matches | |
| 78 | 47372..47554 | + | 183 | 60 | 8.9 | 7133.52 | - | No significant database matches | |

| Gene | Coordinates | Strand | Length (nt) | Length (aa) | pI | MW | Putative Product | Best homologue | E-value |
|------|--------------|--------|----------------|----------------|------|---------|------------------|---------------------------------|---------|
| 79 | 47547..47729 | + | 183 | 60 | 5.09 | 6659.59 | - | No significant database matches | |

Table 9. Functional annotation of the predicted coding sequences of phage vB_PmiP_#3

| Gene | Coordinates | Strand | Length (nt) | Length (aa) | pI | MW | Putative Product | Best homologue | E-value |
|------|--------------|--------|----------------|----------------|------|---------|--------------------------------|--|---------|
| 1 | 1..492 | + | 492 | 163 | 6.18 | 18841.3 | terminase, small subunit | Salmonella phage vB_SemP_Emek YP_006560551 | 2e-95 |
| 2 | 467..1963 | + | 1497 | 498 | 5.69 | 57968.1 | terminase, large subunit | Salmonella phage ST64T NP_720326 | 0.0 |
| 3 | 1966..4056 | + | 2091 | 696 | 4.78 | 79386.7 | portal vertex protein | Enterobacteria phage P22 YP_063735 | 0.0 |
| 4 | 4071..4985 | + | 915 | 304 | 4.89 | 33421 | scaffolding protein | Enterobacteria phage P22 YP_063736 | 1e-117 |
| 5 | 4985..6268 | + | 1284 | 427 | 5.01 | 46382.3 | capsid protein | Enterobacteria phage IME10 YP_007004324 | 0.0 |
| 6 | 6320..6520 | + | 201 | 66 | 4.77 | 7314.4 | - | No significant database matches | |
| 7 | 6517..6720 | + | 204 | 67 | 7.81 | 7683.73 | - | Salmonella phage SPN9CC YP_006383892 | 3e-08 |
| 8 | 6698..7195 | + | 498 | 165 | 6.59 | 18316.7 | tail connector protein | Enterobacteria phage IME10 YP_007004325 | 8e-64 |
| 9 | 7167..8948 | + | 1782 | 593 | 6.09 | 66484.2 | DNA stabilisation protein | Endosymbiont phage APSE-1 NP_050989 | 0.0 |
| 10 | 8945..9646 | + | 702 | 233 | 4.72 | 25596.5 | tail needle protein | Enterobacteria phage Sf101 YP_009153083 | 1e-75 |
| 11 | 9646..10107 | + | 462 | 153 | 6.07 | 17533.2 | acetyltransferase | Sodalis phage phiSG1 YP_516196 | 3e-79 |
| 12 | 10101..10760 | + | 660 | 219 | 4.83 | 22597.2 | DNA injection protein | Enterobacteria phage Sf6 NP_958187 | 3e-72 |
| 13 | 10770..12215 | + | 1446 | 481 | 5.41 | 51800.3 | translocase | Enterobacteria phage ST104 YP_006416 | 7e-120 |
| 14 | 12215..14236 | + | 2022 | 673 | 8.53 | 72453.3 | DNA injection protein | Enterobacteria phage Sf6 NP_958189 | 0.0 |
| 15 | 14259..14735 | - | 477 | 158 | 7.56 | 17809.3 | - | No significant database matches | |
| 16 | 14753..15004 | - | 252 | 83 | 9.19 | 9756.24 | Mnt-like repressor protein | Enterobacteria phage P22 NP_059641 | 6e-35 |
| 17 | 15092..15256 | + | 165 | 54 | 9.7 | 6374.36 | ARC-like repressor protein | Salmonella phage epsilon34 YP_002533476 | 4e-10 |
| 18 | 15323..15514 | + | 192 | 63 | 9.04 | 7023.19 | Ant-like antirepressor protein | Enterobacteria phage CUS-3 ABQ88384 | 7e-27 |
| 19 | 15516..16067 | + | 552 | 183 | 9.72 | 21559.2 | HNH homing endonuclease | Pseudomonas phage PpW-3 YP_008873228 | 3e-25 |
| 20 | 16128..18005 | + | 1878 | 625 | 5.51 | 68808.5 | tail spike protein | Enterobacteria phage Sf101 YP_009153089 | 1e-61 |
| 21 | 17944..18237 | - | 294 | 97 | 9.07 | 11466.2 | DNA polymerase III theta | Escherichia phage HK639 YP_004934090 | 6e-28 |

| Gene | Coordinates | Strand | Length (nt) | Length (aa) | pI | MW | Putative Product | Best homologue | E-value |
|------|--------------|--------|----------------|----------------|-------|----------|--|--|---------|
| | | | | | | | subunit | | |
| 22 | 18629..19813 | + | 1185 | 394 | 9.53 | 45907.9 | integrase | Erwinia phage phiEt88 YP_004327334 | 2e-135 |
| 23 | 19817..20023 | - | 207 | 68 | 6.25 | 8137.24 | excisionase | Enterobacteria phage P4 2211375A | 1e-11 |
| 24 | 20033..20227 | - | 195 | 64 | 5.53 | 7314.17 | - | No significant database matches | |
| 25 | 20235..20780 | - | 546 | 181 | 6.73 | 20530.4 | DNA N-6-adenine- methyltransferase | Enterobacteria phage Lahn2 CAJ26400 | 9e-72 |
| 26 | 20770..21084 | - | 315 | 104 | 4.59 | 11828.3 | NinX-like protein | Serratia phage Eta YP_008130327 | 8e-13 |
| 27 | 21081..21290 | - | 210 | 69 | 4.39 | 8066.94 | - | No significant database matches | |
| 28 | 21280..21444 | - | 165 | 54 | 7.77 | 6074.24 | - | No significant database matches | |
| 29 | 21447..21683 | - | 237 | 78 | 7.82 | 9096.62 | - | No significant database matches | |
| 30 | 21676..21867 | - | 192 | 63 | 6.71 | 7243.13 | - | Enterobacteria phage Phi1 YP_001469347 | 9e-08 |
| 31 | 21990..22184 | - | 195 | 64 | 10.07 | 7703.08 | - | No significant database matches | |
| 32 | 22189..22605 | - | 417 | 138 | 5.70 | 15343.84 | - | No significant database matches | |
| 33 | 22652..22930 | - | 279 | 92 | 4.36 | 10488 | - | No significant database matches | |
| 34 | 22946..23482 | - | 537 | 178 | 7.9 | 19733 | single-stranded DNA binding protein | Enterobacteria phage CP-1639 CAC83134 | 5e-67 |
| 35 | 23475..24035 | - | 561 | 186 | 9.05 | 20698.6 | - | Salmonella phage SEN22 YP_009191483 | 6e-79 |
| 36 | 24035..24859 | - | 825 | 274 | 5.08 | 31309.7 | exodeoxyribonuclease VIII | Salmonella phage SEN22 YP_009191484 | 3e-139 |
| 37 | 24856..25110 | - | 255 | 84 | 4.25 | 9583.88 | - | No significant database matches | |
| 38 | 25107..25382 | - | 276 | 91 | 5.31 | 10539.8 | - | No significant database matches | |
| 39 | 25373..25549 | - | 177 | 58 | 10.38 | 6721.92 | - | No significant database matches | |
| 40 | 25603..25863 | - | 261 | 86 | 9.94 | 9999.58 | - | No significant database matches | |
| 41 | 25926..26090 | - | 165 | 54 | 4.72 | 6234.18 | - | Enterobacteria phage CUS-3 ABQ88443 | 1e-08 |

| Gene | Coordinates | Strand | Length (nt) | Length (aa) | pI | MW | Putative Product | Best homologue | E-value |
|------|--------------|--------|----------------|----------------|-------|---------|---|---|---------|
| 42 | 26125..26715 | - | 591 | 196 | 6.34 | 22310.4 | - | Enterobacteria phage P22 YP_063720 | 1e-30 |
| 43 | 26880..27065 | + | 186 | 61 | 5.66 | 6794.8 | - | No significant database matches | |
| 44 | 27062..27214 | - | 153 | 50 | 4.56 | 5651.45 | - | No significant database matches | |
| 45 | 27400..27615 | + | 216 | 71 | 5.32 | 7959.34 | - | No significant database matches | |
| 46 | 27612..27827 | - | 216 | 71 | 7.87 | 8363.85 | - | No significant database matches | |
| 47 | 27836..28108 | - | 273 | 90 | 10.06 | 10134.8 | N-like antitermination protein | No significant database matches | |
| 48 | 28615..28920 | - | 306 | 101 | 4.86 | 11431 | - | No significant database matches | |
| 49 | 28951..29652 | - | 702 | 233 | 5.25 | 26658.4 | CI-like repressor protein | Escherichia phage HK75 YP_004934144 | 3e-62 |
| 50 | 29760..29945 | + | 186 | 61 | 9.9 | 6886.08 | - | No significant database matches | |
| 51 | 30077..30415 | + | 339 | 112 | 9.25 | 12670.5 | CII-like transcriptional activator | Cronobacter phage phiES15 YP_006590017 | 2e-18 |
| 52 | 30437..31120 | + | 684 | 227 | 9.02 | 25868.1 | Roi-like DNA-binding protein | Cronobacter phage ENT47670 YP_007237602 | 1e-75 |
| 53 | 31117..32202 | + | 1086 | 361 | 9.29 | 41531.6 | O-like transcriptional regulatory protein | Erwinia phage phiEt88 YP_004327353 | 9e-105 |
| 54 | 32202..33578 | + | 1377 | 458 | 5.39 | 50390.3 | DnaB-like replicative helicase | Erwinia phage phiEt88 YP_004327354 | 0.0 |
| 55 | 33598..33801 | + | 204 | 67 | 4.89 | 7600.5 | - | No significant database matches | |
| 56 | 33812..34099 | + | 288 | 95 | 7.97 | 11188.8 | - | No significant database matches | |
| 57 | 34099..34416 | + | 318 | 105 | 10.85 | 12292.3 | - | No significant database matches | |
| 58 | 34403..34651 | + | 249 | 82 | 4.39 | 9840.97 | DUF551-like protein | No significant database matches | |
| 59 | 34651..34743 | + | 93 | 30 | 9.52 | 3829.52 | - | No significant database matches | |
| 60 | 34869..35132 | + | 237 | 78 | 10.19 | 8937.75 | - | No significant database matches | |
| 61 | 35142..35585 | + | 444 | 147 | 8.98 | 17455.1 | NinB-like protein | Cronobacter phage phiES15 YP_006590021 | 1e-40 |

| Gene | Coordinates | Strand | Length (nt) | Length (aa) | pI | MW | Putative Product | Best homologue | E-value |
|------|--------------|--------|----------------|----------------|-------|---------|--------------------------------|---------------------------------------|---------|
| 62 | 35578..35784 | + | 207 | 68 | 7.71 | 7627.92 | - | Klebsiella phage JD001 YP_007392845 | 4e-28 |
| 63 | 35781..36230 | + | 450 | 149 | 9.96 | 16855.7 | - | No significant database matches | |
| 64 | 36208..36351 | + | 144 | 47 | 4.45 | 5211.83 | NinF-like protein | No significant database matches | |
| 65 | 36323..36916 | + | 594 | 197 | 9.43 | 23709.9 | NinG-like protein | Edwardsiella phage GF-2 YP_009126676 | 5e-86 |
| 66 | 36906..37079 | + | 174 | 57 | 10.54 | 7008.3 | - | No significant database matches | |
| 67 | 37069..37269 | + | 201 | 66 | 9.05 | 7580.76 | - | No significant database matches | |
| 68 | 37266..37904 | + | 639 | 212 | 9.22 | 24713.3 | - | Salmonella phage ST64B NP_700422 | 4e-40 |
| 69 | 38622..38927 | + | 306 | 101 | 8.82 | 11183.9 | holin | Salmonella phage ST64T NP_720319 | 2e-26 |
| 70 | 38924..39328 | + | 405 | 134 | 8.72 | 14941.8 | Endolysin / structural protein | Escherichia phage Seurat YP_009152030 | 7e-35 |
| 71 | 39325..39726 | + | 402 | 133 | 9 | 14993.2 | RZ lysis protein | No significant database matches | |
| 72 | 39641..39868 | + | 228 | 75 | 5.55 | 8503.93 | RZ1 lysis protein | Bacteriophage APSE-7 ACJ10113 | 1e-18 |
| 73 | 39910..40302 | + | 393 | 130 | 4.68 | 14791.8 | GP63 like protein | Klebsiella phage phiKO2 YP_006643 | 1e-29 |
| 74 | 40535..40762 | + | 228 | 75 | 4.76 | 8455.64 | - | Salmonella phage SPN9CC YP_006383885 | 3e-17 |
| 75 | 40817..41176 | + | 360 | 119 | 5.8 | 13298.2 | - | Serratia phage Eta YP_008130342 | 9e-27 |